IAEA-BIOMASS-3

Modelling the environmental transport of tritium in the vicinity of long term atmospheric and sub-surface sources

Report of the Tritium Working Group of the Biosphere Modelling and Assessment (BIOMASS) Programme, Theme 3

INTERNATIONAL ATOMIC ENERGY AGENCY

The originating Section of this publication in the IAEA was:

Waste Safety Section
International Atomic Energy Agency
Wagramer Strasse 5
P.O. Box 100
A-1400 Vienna, Austria

MODELLING THE ENVIRONMENTAL TRANSPORT OF TRITIUM IN THE VICINITY OF
LONG TERM ATMOSPHERIC AND SUB-SURFACE SOURCES
IAEA, VIENNA, 2003
ISBN 92–0–102303–0

Printed by the IAEA in Austria
March 2003

FOREWORD

The IAEA Programme on *BIO*sphere *M*odelling and *ASS*essment (BIOMASS) was launched in Vienna in October 1996. The programme was concerned with developing and improving capabilities to predict the transfer of radionuclides in the environment. The programme had three themes:

Theme 1: Radioactive Waste Disposal. The objective was to develop the concept of a standard or reference biosphere for application to the assessment of the long term safety of repositories for radioactive waste. Under the general heading of "Reference Biospheres", six Task Groups were established:

Task Group 1: Principles for the Definition of Critical and Other Exposure Groups.

Task Group 2: Principles for the Application of Data to Assessment Models.

Task Group 3: Consideration of Alternative Assessment Contexts.

Task Group 4: Biosphere System Identification and Justification.

Task Group 5: Biosphere System Descriptions.

Task Group 6: Model Development.

Theme 2: Environmental Releases. BIOMASS provided an international forum for activities aimed at increasing the confidence in methods and models for the assessment of radiation exposure related to environmental releases. Two Working Groups addressed issues concerned with the reconstruction of radiation doses received by people from past releases of radionuclides to the environment and the evaluation of the efficacy of remedial measures.

Theme 3: Biosphere Processes. The aim of this Theme was to improve capabilities for modelling the transfer of radionuclides in particular parts of the biosphere identified as being of potential radiological significance and where there were gaps in modelling approaches. This topic was explored using a range of methods including reviews of the literature, model inter-comparison exercises and, where possible, model testing against independent sources of data. Three Working Groups were established to examine the modelling of: (1) long term tritium dispersion in the environment; (2) radionuclide uptake by fruits; and (3) radionuclide migration and accumulation in forest ecosystems.

This report describes results of the studies undertaken by the Tritium Working Group under Theme 3. It discusses the six model test exercises (three model-model intercomparisons and three model-data exercises) and the twenty-month field sampling programme undertaken to investigate the environmental transport of tritium in the vicinity of long term atmospheric and sub-surface sources. It has been produced with valuable contributions from all the participants in the Tritium Working Group. The IAEA Scientific Secretary was initially Mr. Y. Inoue and subsequently Mr. M. Balonov of the Waste Safety Section, Division of Radiation and Waste Safety. The IAEA wishes to acknowledge the contribution of the Working Group Leader, Mr. Yves Belot of France, and of Ms. Barbara Watkins of the United Kingdom, to the preparation of this report. Additional financial support was provided to this group by the Commissariat a L'Énergie Atomique, Direction des Applications Militaires, Direction de la Qualité et de la Sécurité.

CONTENTS

PART A: MODELLING THE ENVIRONMENTAL TRANSPORT OF TRITIUM IN THE VICINITY OF PERMANENT ATMOSPHERIC SOURCES:
Model-model inter-comparison exercise based on Scenario 1

PART B: MODELLING THE ENVIRONMENTAL TRANSPORT OF TRITIUM IN THE VICINITY OF PERMANENT ATMOSPHERIC SOURCES:
A test of chronic atmospheric release models using Canadian data

PART C: MODELLING THE ENVIRONMENTAL TRANSPORT OF TRITIUM IN THE VICINITY OF PERMANENT ATMOSPHERIC SOURCES:
A test of chronic atmospheric release models using Russian data

PART D: MODELLING THE ENVIRONMENTAL TRANSPORT OF TRITIUM IN THE VICINITY OF PERMANENT ATMOSPHERIC SOURCES:
A test of chronic atmospheric release models using French data

PART E: MODELLING THE ENVIRONMENTAL TRANSPORT OF TRITIUM IN THE VICINITY OF PERMANENT ATMOSPHERIC SOURCES:
Model inter-comparison exercise on sub-surface infiltration pathways following long term atmospheric releases

PART F: MODELLING THE ENVIRONMENTAL TRANSPORT OF TRITIUM IN THE VICINITY OF PERMANENT ATMOSPHERIC SOURCES:
Model-model intercomparison exercise on predicting the rise of tritium from contaminated groundwaters

PART G: MODELLING THE ENVIRONMENTAL TRANSPORT OF TRITIUM IN THE VICINITY OF PERMANENT ATMOSPHERIC SOURCES:
Field data for wet and dry deposition of tritium

ANNEX I: MODEL DESCRIPTIONS

ANNEX II: TRITIUM WORKING GROUP SCENARIO DESCRIPTIONS

SUMMARY

In 1996, in the framework of the IAEA Co-ordinated Research Project on Biosphere Modelling and Assessment (BIOMASS), a Tritium Working Group (TWG) of participants from twelve different organisations was established with the objective of improving our ability to model situations where tritium is released in a nearly continuous way from primary or secondary sources. These situations had not been widely considered before, and at that time there was a need for an international forum in which models of long term release of tritium could be discussed, intercompared and improved.

From December 1996 until December 2000, the TWG developed and analysed six model test exercises and carried out a specifically commissioned field sampling and analysis programme in order to study and understand more fully the behaviour of long term releases of tritium in the environment. Four of the scenarios were concerned with atmospheric pathways (Parts A to D). Both model-model inter-comparison tests and model-data exercises were undertaken. Two further scenarios were devoted to sub-surface pathways (Parts E and F), both involving model-model intercomparisons. A field sampling programme was specifically designed to investigate wet and dry deposition of tritium following atmospheric releases (Part G). As a result of the work undertaken in the modelling exercises and field sampling programme a number of recommendations are made for modelling tritium behaviour in the environment, data acquisition methods and further work.

PART A

The first task of the TWG was devoted to a model-model intercomparison exercise on the transport of tritium in the vicinity of permanent atmospheric sources. Eleven institutions participated in this exercise and to an exchange of results and ideas. The work was carried out over three years in parallel to the other TWG scheduled tasks.

Determination of tritium concentration in air humidity was approached by classical models of atmospheric dispersion, and also by specially developed models that consider both primary emission from main sources and secondary emission from the contaminated soil surface. The results obtained in assessing the impact of HTO releases were not very dependent on the way in which the secondary emission was treated, since the contribution of the latter process is generally relatively small. In contrast, for HT releases, the results are highly dependent on the method used to estimate the secondary emission, because this process is the only one that brings tritiated water into the atmosphere. It is recommended that air concentrations from a groundlevel source should be calculated using the wind speed at a height related to the height of the centre of mass of the plume, which is not fixed but increases with downwind distance. Alternatively, air concentrations of HTO following deposition of HT can be estimated as a first approximation by using empirical results drawn from the HT chronic release controlled field experiments carried out in 1994 at the Chalk River Laboratories of Atomic Energy Canada Limited, Canada.

The estimation of average tritium concentrations in soil moisture following HTO releases is more difficult and this was modelled by several approaches based on different assumptions that involve either a balance of tritium activity in the soil, or semi-empirical approximations. The differences between the modelling approaches led to a factor of nearly seven between the extreme calculated values obtained by different participants. As a result, the TWG participants recommended that further investigations be carried out into the contribution of dry and/or wet

deposition to the tritium concentration in the soil, with the objective of improving modelling methods. Following this recommendation, a 20-month experimental programme was undertaken and results are summarised below (Part G). For HT releases, the concentrations of tritium in near-surface soil moisture, calculated using the balance of activity in the near-surface soil, or alternatively empirical ratios drawn from field experiments, were spread over a factor of ten. Modellers considered that the second modelling approach was presently more reliable. For plants rooted in the soil, the estimations of tritium concentrations in leaves, either as tritiated water or as organically bound tritium, are much less variable than the corresponding tritium concentrations in soil water. The reason is that a large fraction of the tritium is taken up by the plant leaves by exchange with the atmosphere, and only a small fraction by transport from the soil.

PART B

The third scenario of the TWG (the second scenario was concerned with sub-surface pathways, see Part F) was devoted to a model-data test exercise concerning the transport of tritium in the vicinity of long term atmospheric sources at the Chalk River Laboratories (CRL) site of AECL in Canada. Participants were given hourly meteorological data and the observed HTO concentrations in air at three sampling sites. From this information they were asked to predict long term average tritium concentrations in rainfall, soil water, plant water and plant organic material. Seven institutions participated in this exercise and others also contributed to the exchange of information and ideas. The work was carried out in parallel with other model test exercises developed by the TWG and was completed over a two-year period.

The models used by most participants were similar, but predictions for a given endpoint typically varied over a factor of 2 or 3 among the models. This was due both to the way in which the models were applied and to the different values of the parameters used in them. Differences between predictions and observations were also commonly about a factor of 2 to 3. The predictions for soil generally overestimated the observed values but were able to reproduce the main features of the spatial variability, which is driven by differences in the joint frequency of wind direction and rainfall occurrence. The results indicate that a substantial part of the permanent tritium inventory in soil arises from dry deposition, although more work is needed to quantify this. The predictions for HTO concentration in plant water were systematically high, suggesting that the plant model used by the participants or the parameter values input to it may be biased. The models were not generally able to reproduce the strong diurnal variation observed in the grass/air ratio, although this variation may be due simply to differences in morning and afternoon relative humidities. The predictions for rainwater all substantially underestimated the observations.

The observations on which Scenario 3 are based suggested that, at CRL, the long term average soil concentration is typically one-fifth to one-third the average air moisture concentration. This ratio will depend on soil properties and on the joint frequency of wind direction and rainfall occurrence and may be quite different at other sites. The long term plant water/air moisture concentration ratio had a best estimate of 0.65 and a range between 0.50 and 0.85. This ratio was obtained for grass and likely applies to the foliar parts of other plant types but may be different for fruit or root crops. It probably shows less variability from site to site than the soil/air ratio because plant concentrations are driven primarily by air concentrations.

PART C

The fourth of the six scenarios developed by the TWG was based on environmental sampling data collated at the Russian Federal Nuclear Centre – VNIIEF. The unique feature of this fourth scenario was the significant decrease in the amounts of tritium released to atmosphere over the 20 years of observation and modellers were asked to investigate the possible consequent retention of tritium in the biosphere.

The experimental data on which the scenario was based included tritium concentrations in air, vegetation, soil and the overlying snow cover. Scenario 4 is the only one of the TWG set of scenarios which provides data for a snow compartment. To test the models against this observational data, the requested scenario endpoints were predictions of average annual HTO concentrations in atmospheric humidity, plant tissue free water, soil water and snow water for 5, 10, 15 and 20 years after the beginning of the releases at given sampling locations. Seven participants submitted results.

Most participants used traditional assessment models to generate their predictions. Predicted and observed values of HTO concentrations in air due to atmospheric dispersion of the primary plume at Sampling Points 2 and 6 were within a factor of 4. Most of the predicted values agreed with observations within experimental uncertainties, which were a factor of 2. However, observed HTO concentrations in the atmosphere at Sampling Point 4 were significantly greater than predicted values. Predicted and observed values for tissue free water and soil moisture were in good agreement at Sampling Points 2 and 6, and in less good agreement at Sampling Point 4. The largest difference between predicted and observed data was for the snow compartment. The reason for the large discrepancy between observed and predicted values at Sampling Point 4 was subsequently shown to be a low-intensity ground source that had previously been unknown to the scenario developer and therefore information on this source was not provided in the scenario description and so was not taken into account in the models.

The experimental data showed that tritium retention may occur in biosphere media when there is a significant decrease of emission rates (in this case, over 2 orders of magnitude during 20 years of releases). The observed tritium air concentrations showed a slight increase in time when normalized by the release rates. However, the magnitude of the increase is comparable to the experimental uncertainties and firm conclusions regarding retention cannot be made. There is a need for further study to determine if retention really does occur and, if necessary, to determine those processes responsible for it so that it can be taken into account in long term assessment models. This scenario has also demonstrated that model predictions can be used to check sampling data and where predictions and observations are found to be different then both modelling approaches and experimental data need to be reviewed to ascertain the reasons.

PART D

The objective of the fifth scenario was to use environmental data collated at a French site to further test and improve models of long term atmospheric releases of tritium. Modellers were asked to calculate concentrations of tritium in air, rain, and plant tissue water at four stations around the site. They also had to develop a map of OBT concentrations in oak tree leaves for one particular year and utilise information on historic releases at the site in order to calculate OBT concentrations in beech tree rings for specific years. This scenario was interesting because it allowed participants to model two aspects that had not previously been addressed: topographic effects on dispersion; and calculation of OBT concentrations in the leaves and growth rings of trees. Six institutions participated in this modelling exercise, which was carried out over two years in parallel to other Tritium Working Group activities.

The conclusion of this scenario was that modellers were able to calculate tritium concentrations in air, rain and in plant free water and organic material that are in reasonable agreement with measurements arising from long term atmospheric releases. Discrepancies between model results and site data varied by a factor of 4 at most. It was also found that the topographic effect is not of paramount importance when the relief is moderate and tritium concentrations are calculated at medium or long distances from the source.

PART E

This model-model intercomparison exercise was developed early in the work programme (as a separate part of Scenario 1) to investigate modelling approaches to the assessment of impacts on groundwaters arising from chronic atmospheric tritium releases. The estimation of the vertical profiles of tritium concentration in groundwaters following infiltration from the overlying contaminated unsaturated layer was required for simplified, yet realistic conditions. Eight participants undertook calculations using either numerical, or analytical hydraulic transport models, in the latter case with some simplifying assumptions. The analytical models can be used more easily than the relatively complex numerical models but are less adapted to real situations where the characteristics of the aquifer are more complicated than those taken in the present exercise.

Most of the results obtained for both low and high vertical dispersivity of the aquifer agreed within a factor of two and were not dependent on the modelling approach. It was shown that the groundwater vertical concentration profiles depend on the formulation of boundary conditions that describe the transport of tritium through the watertable, and to a much greater extent on the values given to the dispersive properties of the aquifer. It was agreed that it was preferable to simulate the transfer of tritium into the aquifer by setting a prescribed-flux condition at the watertable in the model rather than the prescribed-concentration condition that is sometimes used by modellers. Moreover, it was shown that the shape of the vertical profile of tritium in the aquifer is very sensitive to the value of the vertical dispersivity parameter used in the model. Reliable predictions of vertical mixing can only be made if the dispersivity parameter has been determined by independent tracer experiments. Approximate indications can nevertheless be drawn from dispersivity values found in the literature.

PART F

The second sub-surface model-model inter-comparison exercise was research-oriented. It addressed the problem of the movement of tritium from a contaminated perched aquifer to the soil surface, that is either vegetated or not. Participants were provided with information on water table level, soil characteristics, and hourly meteorological and evapotranspiration data. Modellers were asked to predict the vertical profiles of tritium concentration in soil water at specified times after the start of tritium migration, and also the monthly values of the tritiated water vapour flux from the soil surface to the atmosphere. Nine institutions participated in this modelling exercise (called Scenario 2), which was carried out over three years in parallel to other TWG activities.

For this specific application, some participants adapted multipurpose models that are available commercially. Other participants developed their own codes based on process models and techniques published by others. For most of these models, the equations of moisture movement and tritium transport in the soil were solved numerically. Only one modeller tried to approximate tritium transport by an analytical formula that had been derived from the transport equation assuming constant coefficients and a constant concentration at the water table. All the modellers agreed and/or showed that the balance of precipitation and evaporation and the mechanical dispersion processes were the key factors in the transport of tritium through the unsaturated soil layer situated above a contaminated water table. The results obtained by the different participants for the specific configuration of conditions in the scenario were typically within a factor of about two. When using numerical models, it is necessary to pay attention to time and space discretisation, since inappropriate increments could lead to large numerical errors. The convergence of the results that were derived from the different models was only obtained at the expense of using very small time and space increments.

The model-model inter-comparison exercise has shown that the upward transport of tritium from a contaminated aquifer can be predicted best, especially in research exercises, by using numerical models that are relatively sophisticated. However, these models need detailed input information on meteorological conditions and soil characteristics, and need to be operated at small time and space scales. It was shown that very simple models are not always suitable, due to the fact that tritium concentrations vary sharply over short distances and are very sensitive to many interacting factors. Nevertheless, there are occasions when more simple models are adequate for the assessment purpose.

PART G

Motivated by a recommendation arising from work on Scenario 1 (see Part A), researchers from CEA/DAM/DASE, France, in collaboration with German colleagues from the ZSR institute of the University of Hannover, undertook an experimental program to clarify the importance of wet and dry deposition of tritium to the consequent concentrations of HTO in soil water. Data on air and rain concentrations in sectors around an emission point which received either mainly dry or mainly wet deposition were obtained from monthly averaged samples. At the end of each sampling interval soil samples were also taken in the two areas.

It is clear from the data that soil concentrations are correlated not only to rain concentrations but also to air concentrations. Averaged over 20 months, the ratio of soil to air concentrations was approximately 0.2 and the ratio of soil to rain concentrations was approximately 1 in the case of the East sampling point, which lies in the sector affected mainly by wet deposition. The second sector, the West sampling point, is affected mainly by dry deposition. Here, on average, the concentration in soil was twice the concentration in rain and 0.08 times the concentration in air.

The experimental program has proved that dry deposition is important and that this process should be included in models for those times or sites with low effective wet deposition.

RECOMMENDATIONS

As a result of the six model test exercises and the field sampling programme undertaken by the TWG during the four-year international collaborative programme, a number of recommendations can be made concerning: (a) modelling tritium behaviour due to chronic atmospheric and sub-surface sources; (b) field sampling and data acquisition methods; and (c) future studies.

Modelling

Dry deposition is an important process that contributes to long term average soil moisture concentrations of HTO and should be included in models.

Secondary sources of HTO due to re-emission from soil can be ignored for ground level atmospheric sources and at distances >500 m from elevated sources but must be considered if the source is sub-surface.

To calculate near-surface soil moisture concentrations due to an atmospheric source, a more accurate estimate is made if soil moisture concentrations are related to air rather than rain concentrations.

In the absence of a suitable model, the assumption that the soil moisture concentration (Bq l^{-1}) is 0.3 times the air concentration (Bq l^{-1}) can be used. In screening assessments, a conservative value of 0.5 can be adopted.

For HT releases, air and near-surface soil concentrations of HTO can be obtained from empirical data obtained in the CRL chronic HT release experiment.

For tritium transport down through deeper soil layers, and up from contaminated aquifers, the division of the model soil compartment into a large number of thin layers is likely to give more accurate results than if a small number of thick layers is used.

Data acquisition methods

It is essential to have good source data and accurate measurements for model inputs (e.g. well-defined meteorological data statistics, soil properties) in order to achieve good assessment predictions and for developing, testing and applying models.

One of the reasons for the differences between predictions and observations in the atmospheric scenarios may lie in a mismatch between the assumptions of the models and the realities of the data. Most of the models assume equilibrium conditions when in fact the air concentrations over a given sampling site fluctuate continually in response to changing atmospheric conditions. Moreover, the observed soil and grass concentrations are normally determined from samples taken irregularly throughout the growing season. Averages of these samples may not reflect true mean values, which are what the models are designed to predict. Sampling programmes should be planned to yield mean concentrations, which are the quantities of primary interest in dose assessments.

Models can be used to highlight problems with observational data and it should not be automatically assumed that model predictions are inaccurate if they do not agree with the observations.

Future studies

We have adequate models for assessing air moisture, soil moisture and plant TFWT concentrations of HTO resulting from both short term and chronic releases of HTO. Work is now required to develop and test models for OBT formation and translocation in food crops, animals and aquatic systems. More work is also needed to understand and model tritium deposition to snow and the fate of the tritium when the snowpack melts.

Further experimental work is needed to confirm the concentration ratios determined in the CRL HT chronic release study and to extend the ratios obtained to sites with climate, soil and plant properties different than those at CRL.

Data sets are required to test models for sub-surface processes and pathways involved in tritium transport in saturated and unsaturated media due to chronic atmospheric or sub-surface sources of tritium.

Data are required to improve modelling of wet and dry deposition to soil.

Further work is needed to determine if tritium can be retained in the environment to a significant extent if a previously constant source of tritium is reduced or cut off.

Tracer experiments are required to provide information on tritium dispersivity in the saturated and unsaturated zones.

GENERAL INTRODUCTION

(1) In the recent past, the assessment of the potential impact of tritium emissions has focused on accidental releases to the atmosphere from future fusion power plants. Accident-oriented models and related computer codes were actively developed in parallel to the progress made in the knowledge of tritium behaviour in the environment. Inter-comparison and validation of such models was carried out in the framework of a working group of the second phase of the international Biosphere Model Validation Study (BIOMOVS II) from 1991 to 1996 (BIOMOVS II, 1996 a, b; Barry et al., 1999). It gave rise to substantial progress in modelling accidental releases of tritium and predicting the subsequent radiological consequences.

(2) In addition to models for accidental releases, there is a need for models that are suitable to assess the impacts of long term chronic releases of tritium. Testing of such models has not been widely considered until now. Long term continuous releases arise from discharges to the atmosphere from tritium installations, or releases to the sub-surface from contaminated land or waste disposal facilities. The modelling of these situations is justified by the need for predicting the levels of contamination in food and water resources and for planning the future land use of contaminated areas. A *Tritium Working Group* (TWG) was approved by IAEA in the framework of its Biosphere Modelling and Assessment (BIOMASS) co-ordinated research programme during the first BIOMASS Plenary meeting in October 1996. It was proposed that the TWG should concentrate its activities on the development of models and use of data to understand and assess the behaviour of tritium released over long periods from both atmospheric sources and sub-surface sources.

(3) Four main objectives were agreed upon in discussions between organisers and participants:

- Testing whether the existing models for calculating long term air concentrations are suitable for assessing concentrations of HTO and HT in air following chronic atmospheric releases.
- Testing and modifying appropriate models for calculating HTO concentrations in near-surface soil moisture and plants, and OBT concentrations in plants, following chronic atmospheric releases.
- Modifying or developing models for processes involved in tritium transport down through deeper soil layers to groundwater and up through unsaturated media to the soil surface as a result of long term atmospheric or sub-surface sources respectively.
- Identifying a key modelling problem for which observational data were lacking so that experimentalists and modellers could collaborate in the development of a suitable sampling programme to provide the required data.

(4) Two main approaches were used to meet these objectives. First, work was initiated by defining three scenarios that served as a basis for model inter-comparison exercises. Secondly, it was stressed that there should be interactions between modellers and experimentalists to obtain data for model validation exercises and to help obtain information on important tritium transport processes. This resulted in the development of three model-data test scenarios, based on environmental sampling data, plus an experimental programme.

(5) Technical work on defining the scope of the programme and drafting scenarios for model calculations began in December 1996 following the first BIOMASS Plenary meeting. Over the next four years, six model test exercises were developed and refined. Moreover, a specially commissioned experimental programme was planned and carried out at Bruyeres le Chatel in France in parallel to the modelling exercises. A sampling survey and analysis programme carried out over a twenty-month period was specifically dedicated to deriving information and data for a key issue on tritium behaviour. Results from modelling exercises and the experimental programme were discussed at meetings and models were tested, developed and refined through individual work and multi-lateral exchanges between participants. Regular meetings were held twice each year – in the autumn, in the framework of the BIOMASS Plenary Meetings organised by the IAEA at its headquarters in Vienna, and in the spring, at different locations at the invitation of individual participants on behalf of their institution. TWG spring meetings were held in Cadarache, France (April 1997), Deep River, Canada (May 1998), Sarov, Russia (May 1999) and Toki, Japan (May 2000). In some cases, these spring meetings were associated with special Tritium Workshops and visits to technical installations which enabled scientific exchanges between the TWG members and other scientists working on tritium in the country where the meeting was held. Seventeen participants from thirteen different organisations and nine countries formed the core members of the TWG, although many others attended meetings and contributed to discussions. All these exchanges helped to advance an understanding of tritium transport processes in the environment.

(6) Four of the scenarios dealt with the atmospheric pathways following long term releases of tritium. All of these exercises centred on modelling the primary dispersion of tritium from either a single or multiple chronic atmospheric sources, its subsequent deposition to soil and vegetation and its secondary emission from the contaminated soil surface.

(7) Two further scenarios were devised to help with the development of models for the transport of tritium to and from shallow aquifers. The objective of the first of these sub-surface scenarios was to predict the transport of tritium down through an unsaturated soil layer and the penetration of tritium through a watertable into a previously uncontaminated aquifer. The second exercise considered the upward movement of tritium from a contaminated aquifer to the soil surface. These test exercises gave the opportunity to adapt commercially available generic models and to develop new, original models. Unfortunately, despite concerted efforts by participants no observational data sets could be found during the study to test the models against actual data.

(8) This report presents the results from the six model test scenarios and from the field sampling programme as follows:

Atmospheric pathways:

- A model-model inter-comparison exercise involving the steady state behaviour of tritium in the environment when atmospheric releases are assumed to be nearly constant (Part A).
- Three model-data test exercises based on monitoring data for long term releases at Canadian (Part B), Russian (Part C) and French (Part D) sites.

Sub-surface pathways:

- A model-model intercomparison exercise based on an atmospheric source of tritium and the consequences of tritium transport down through the soil profile to a previously uncontaminated aquifer (Part E).
- A model-model intercomparison exercise based on a contaminated aquifer and the consequences of tritium transport up through the unsaturated soil profile to the soil surface either with or without vegetation (Part F).

Commissioned field sampling survey:

- Results from a specially designed experimental programme to obtain data on the relative importance of wet and dry deposition of tritium (Part G).

(9) Information on the models used by participants for the atmospheric, soil and groundwater pathways is provided in Annex I. The six scenarios used as the basis for the model test exercises are given in full in Annex II.

REFERENCES

[1] BARRY, P.J., WATKINS, B.M., BELOT, Y., DAVIS, P.A., EDLUND, O., GALERIU, D., RASKOB, W., RUSSELL, S., TOGAWA, O., Intercomparison of model predictions of tritium concentrations in soil and foods following acute airborne HTO exposure, Journal of Environmental Radioactivity **42** (1999) 191–207.

[2] BIOMOVS II, Tritium in the Food Chain: Intercomparison of model predictions of contamination in soil, crops, milk and beef, after a short exposure to tritiated water vapour in air, Published on behalf of the BIOMOVS II Steering Committee by the Swedish Radiation Protection Institute, Sweden ISBN 91-972134-7-0 (1996a).

[3] BIOMOVS II, Tritium in the Food Chain: Comparison of Predicted and Observed Behaviour; A: Re-emission from soil and vegetation, B: Formation of organically bound tritium in grain of Spring Wheat; Published on behalf of the BIOMOVS II Steering Committee by the Swedish Radiation Protection Institute, Sweden ISBN 91-972958-2-5 (1996b).

PART A

MODELLING THE ENVIRONMENTAL TRANSPORT OF TRITIUM IN THE VICINITY OF PERMANENT ATMOSPHERIC SOURCES:

Model-model inter-comparison exercise based on Scenario 1

A1. BACKGROUND AND OBJECTIVES

(A1) Dispersion of atmospheric radioactive pollutants following accidental or continuous release has been intensively studied for a very long period of time and, in parallel, models of atmospheric transport have been developed that have been tested in many circumstances. These models are applicable to the dispersion of any trace substance and can be used to predict the atmospheric transport of tritium. But, if interest extends to the understanding of environmental impacts in a general sense, and to the delayed consequences of exposure from water and food consumption, many other processes need to be considered and modelled appropriately, taking into account the properties and behaviour of the radionuclide under consideration.

(A2) The first BIOMASS atmospheric tritium release scenario was developed with the general aim of modelling the transport of tritium in the environment when atmospheric releases from a stack are assumed to be on average nearly constant and a steady state equilibrium is approached. The environment was considered to encompass air, vegetation and soil water (impacts on groundwater following atmospheric deposition are considered in Part E). Long term atmospheric releases have not been considered very much in the past, despite their importance in assessing the radiological impact of tritium released from nuclear installations. Particular aims of the task were as follows.

- To model tritium transport over the whole chain of processes from the release at the stack to the buildup of tritium in environmental media in order to investigate if existing models can also be applied to long term, near continuous releases.
- Point out the difficulties that were encountered in some specific components of the transport chain.
- To try to solve any problems encountered through the exchange of ideas, experience and information between members of the group.

(A3) A total of eleven organisations participated in the study by submitting results, and others contributed to ideas and the discussion. The models employed were either existing codes that had been developed and used in previous assessment studies (often for accidental or short term releases), or newly developed codes, or sometimes a mixture of sub-programs of different origins and status.

A2. SCENARIO DESCRIPTION

(A4) An outline description of the first scenario (called Scenario 1.0) was proposed to the TWG in December 1996. From this initial description, three modified versions of the scenario were subsequently developed to account for requests for additional information and to facilitate further intercomparisons of results. Scenario 1.3 is given in full in Annex II–A. This version of the scenario served as a basis for the requested calculations and the corresponding results presented here.

(A5) The scenario considers an idealised tritium facility that releases tritium in the form of either HTO or HT through a stack at a constant average rate (1 g y^{-1}), under meteorological conditions typical of a temperate climate. The scenario is a relatively simple one in which local characteristics and time–variations are omitted. Moreover, most of the variable parameters were supplied to the modellers to limit difficulties in interpreting results obtained with different modelling assumptions. The modellers were provided with the description of meteorological conditions and vertical profiles of wind speed, and also with the vertical dispersion parameters, the washout coefficient and the dry deposition rate of HT and HTO. These data are based on well established, and generally accepted, values drawn from the literature.

(A6) The end points to be calculated by modellers were annual concentrations of tritium in air humidity, soil moisture, vegetation water and vegetation organic matter, after 20 years of release.

A3. DESCRIPTION OF TRANSPORT PROCESSES AND MODELLING APPROACHES

A3.1. TRANSPORT OF TRITIUM IN THE ATMOSPHERE

(A7) The stack that releases tritium is called the primary source. It induces average concentrations of tritium in the atmosphere at ground level which are referred to as primary concentrations (χ_1, Bq m^{-3}). These concentrations are generally calculated by the statistical Gaussian formula, otherwise called the sector-averaged Gaussian formula, based on the consideration of sectors of wind direction centred at the source. The dispersion formula is based on the assumption that the wind blows with equal probability in any direction of the sector concerned. This leads to an average concentration that is independent of lateral position in the sector. The basic formula is:

$$\chi_1(X,0) = \sqrt{\frac{2}{\pi}}\frac{Q}{X\theta}\sum_{ij}\left[\frac{f_{ijk}}{u_j\sigma_i(X)}\exp\left(-\frac{H^2}{2\sigma_i^2(X)}\right)\right] \tag{1}$$

where:

χ_1	is the primary plume concentration.
f_{ijk}	is the joint frequency of wind blowing from the source into sector k containing the sampling point, for stability class i and wind speed class j.
u_j	is the nominal wind speed for wind speed class j, adjusted to the release height H, (m s^{-1}).
θ	is the angular width of sectors, depending on the meteorological data available, (radians).
X	is the distance from the source to the sampling point, (m).
σ_i	is the vertical dispersion parameter for stability class i, (m).
Q	is the release rate, (Bq s^{-1}).

(A8) The HTO secondary air concentrations (χ_2, Bq m^{-3}) at ground level are due to re-emission of HTO to the atmosphere from the contaminated soil surface. They are determined by summing the contribution at the sampling point *(x,y,0)* of each secondary ground level source situated at *(ξ,η,0)*:

$$\chi_2(x,y,0) = \sqrt{\frac{2}{\pi}}\int_{-\infty}^{\infty}\int_{-\infty}^{\infty}\frac{F(\xi,\eta,0)}{\rho(x,y;\xi,\eta)\theta}\sum_{ij}\left[\frac{f_{ijk}(x,y;\xi,\eta)}{u_j(\rho)\sigma_i(\rho)}\right]d\xi d\eta \tag{2}$$

where:

f_{ijk} is the joint frequency of wind blowing from the ground level source $(\xi,\eta,0)$ into the sector k of the sampling point $(x,y,0)$ for stability class i and wind velocity class j. The joint frequency distribution is the same as the one used for primary dispersion.

u_j is the nominal wind speed for wind speed class j, adjusted to a specified height above ground level (see paragraph below).

ρ is the radial distance from the ground level source $(\xi,\eta,0)$ to the sampling point $(x,y,0)$, (m).

The upward flux, F, is calculated from the concentration of tritium in the water of the top layer of soil (C_s) by using the formula (2 bis):

$$F = (v_e \rho_s + T_r)C_s \qquad \text{(2 bis)}$$

where:

v_e is the exchange velocity of HTO from soil to atmosphere (m s^{-1}).

ρ_s is the water concentration in air saturated at the soil surface temperature (kg m^{-3}).

T_r is the transpiration rate of the plants rooted in the soil.

The total air concentration at the sampling point is $\chi = \chi_1 + \chi_2$.

(A9) The main problem encountered in predicting the primary and secondary concentrations of tritium by using the equations above, concerns the estimation of the wind speed, $u_j(\rho)$, that appears in the two equations. This parameter is in fact the average advection velocity of the diffusing plume, i.e. the average horizontal velocity of the HTO molecules in the plume. Classically, one assumes that the average advection velocity of the plume is equal to the average wind speed at the height of the source. This is easy to manage in the case of an elevated primary source such as a stack, but not so evident in the case of ground level secondary area-sources. In the latter case the advection velocity is taken to be significantly lower than for the elevated primary source. The advection velocity of the plume originating from the ground can be determined, either by assuming that the plume is emitted at some virtual height to be estimated through an empirical approach, or by assuming that the advection velocity which is very low close to the source increases as the vertical extension of the plume increases. This second approach was proposed by Smith and Singer (1966) and Horst (1979). These authors showed that the average advection velocity of the plume is equal to the wind velocity at a height 0.6 $\sigma_i(\rho)$ above ground level. The advection velocity thus increases with the vertical extension of the plume and with the distance between the source and the sampling point. This variable advection velocity is derived from the wind velocity measured at some defined reference height by using well known vertical profiles of wind speed that have been established for different roughness lengths and different indices of atmospheric stability.

(A10) In the case of an HT release, the prediction of HTO concentrations in air due to the secondary re-emission from the contaminated soil surface, can be based on results of field experiments, assuming that the re-emission is only very moderately sensitive to local soil and weather conditions, and that the results obtained for the particular experimental situation can be generalised to other situations. The ratio of the HTO concentration to the HT concentration in air, as empirically determined in the 1994 chronic HT release experiment at Chalk River was independent of downwind distance (Davis et al., 1995; Davis and Bickel, 2000).

A3.2. WET DEPOSITION OF TRITIATED WATER

(A11) Tritium in the form of HT is not appreciably scavenged by precipitation because of its extremely low solubility in water. On the contrary, HTO is easily dissolved in raindrops and transported to the soil that constitutes a reservoir for further transport of tritium to the terrestrial components of the biosphere and to groundwaters (see Part E).

(A12) Most of the modellers adopted the classical formula that is based on the use of an apparent washout coefficient Λ (s^{-1}). Using the model of Hales et al. (1973), it has been shown by Belot (1998) that the washout coefficient depends mainly on source height and precipitation intensity and varies only moderately with distance from the source. The proposed coefficient is $\Lambda_0 = 5.5 \times 10^{-5}\ s^{-1}$ for an average precipitation rate $I_0 = 1$ mm hr^{-1} during the rain episodes and a 60 m-stack. For an actual average precipitation rate I, the apparent washout coefficient is $\Lambda = \Lambda_0\ (I / I_0)^{0.7}$. The coefficient is almost constant between 0.1 and 10 km from the stack. The coefficient would be larger for a lower stack.

(A13) The long term time-averaged downward, wet deposition flux F_w (Bq $m^{-2}\ s^{-1}$) at the sampling point *(X,0)* is most often calculated by the following sector-averaged formula:

$$F_w(X\ ,0) = \frac{\Lambda Q}{X\theta}\sum_{ij}\frac{\Phi_{ijk}}{u_j} \tag{3}$$

where:

u_j	is the average wind speed during rain at source height, (m s^{-1}).
Λ	is the apparent washout coefficient as given above, (s^{-1}).
Q	is the average emission rate of the source, (Bq s^{-1}).
ϕ_{ij}	is the joint frequency of rain and wind into the sector containing the sampling point for stability class *i* and wind speed class *j.*
θ	is the sector angle, (radians).

(A14) In the case of high stacks, the use of other parameters, such as wet deposition velocity or washout ratio, is not recommended, since the rapid increase of these parameter values when distance from the stack decreases leads to large uncertainties in F_W.

A3.3. BUILDUP OF TRITIUM IN SOIL AND PLANTS

(A15) In the case of both HTO and HT releases, the steady state concentration of tritium in the water of the root layer can be estimated from a balance equation between average inputs and outputs to and from the root layer. The tritium inputs are attributable to dry and wet deposition, and the tritium outputs to infiltration, plant uptake and re-emission from soil surface; losses due to radioactive decay being negligible. The concentration of tritium so obtained is independent of the thickness of the root layer, but depends only on the relative magnitude of the inputs and outputs. This yields the following formula:

$$C_s(x,y) = \frac{v_t \chi(x,y) + F_w(x,y)}{v_e \rho_s + T_r + I_r} \qquad (4)$$

where:

v_e	is the exchange velocity of HTO from soil to atmosphere (m s^{-1}).
v_t	is the transfer velocity of HT or HTO from atmosphere to soil (m s^{-1}).
C_s	is the tritium concentration in soil water (Bq kg^{-1})
F_w	is the average flux density of tritium wet deposition [Eq.(3)] (Bq m^{-2} s^{-1}).
I_r	is the infiltration rate of water through the soil layer (kg m^{-2} s^{-1}).
T_r	is the transpiration rate of the plants rooted in the soil (kg m^{-2} s^{-1}).
χ	is the average air concentration of tritium (Bq m^{-3}).
ρ_s	is the water concentration in air saturated at the soil surface temperature (kg m^{-3}).

Evaporation from the soil is implicitly accounted for in the terms v_e and ρ_s. It is assumed that $I_r + T_r$ is equal to the precipitation flux. This approximation is true only when precipitation is greater than evaporation.

(A16) In the case of an HTO release, as an alternative to the tentative physical approach developed above, several participants used a semi-empirical approach. Three different modelling options are possible. A first option is to consider the contribution of wet deposition only. The argument in favour of this approach is based on observations of short term releases, namely that a major part of the dry deposited tritium is rapidly re-emitted to the atmosphere and does not remain appreciably in the soil. A second option is to consider the contribution of dry deposition only, assuming that the deposited tritium is not appreciably re-emitted to the atmosphere. Finally, a third option is to consider both wet and dry deposition and assume that the concentration in soil is a linear function of the concentrations in rainwater and air humidity, in this case using coefficients drawn from observations in the field. Details of the different conceptual models are given in the model descriptions in Annex I–A.

(A17) In the case of an HT release, one assumption is that the ratio of HTO concentration in soil water to HT concentration in air is the same as determined in long term field experiments at Chalk River (Davis et al., 1995; Davis and Bickel, 2000). This ratio is 6 Bq L^{-1} per Bq m^{-3}. In a different conceptual model, the tritium inventory in the soil is assumed to be 20% of the dry deposition determined from the given deposition velocity of HT. Another alternative is to attempt to linearly relate the concentration of tritium in soil water to the concentrations of tritium in air humidity and rainwater, using empirical coefficients that were derived from observational data.

(A18) To determine the average tritium concentration in plant leaf tissue water (C_p, Bq L^{-1}), participants used the classical formula derived for plants exposed to constant levels of tritiated water in the atmosphere and/or the soil:

$$C_p(x,y) = \alpha_E \left[\left(\frac{\rho_a}{\rho_s} \right) C_a(x,y) + \alpha_K \left(1 - \frac{\rho_a}{\rho_s} \right) C_s(x,y) \right] \qquad (5)$$

where:

C_a	is the tritium concentration in air humidity (Bq L^{-1}).
C_s	is the tritium concentration in the root zone water (Bq L^{-1}).

α_E is the equilibrium isotopic ratio (1.1).
α_K is the kinetic isotopic ratio, or diffusion coefficient ratio, (1.05).
ρ_a is the water vapour density in the air (kg m^{-3}).
ρ_s is the water vapour density in the air saturated at the leaf temperature (kg m^{-3}).

When the temperature of leaves is identical to that of surrounding air, the ratio ρ_a / ρ_s is the relative humidity of the atmosphere. Expression (5) can be roughly interpreted by saying that a fraction of leaf water derives from atmospheric water; the remainder derives from the soil via the root and the vascular system.

(A19) The non-exchangeable organically bound tritium concentration (OBT) in leaves is expressed as the concentration of tritium in the water obtained by combustion of a sample of dry leaves, after having removed the exchangeable tritium of the sample. The combustion water is sometimes termed ‘equivalent water’. Some modellers assume that the ratio of tritium in the equivalent water of leaves to tritium in the tissue free water of leaves is 0.6, other modellers assume that the ratio is 0.8 or 1.0. The deficit of tritium in the organic matter of leaves represents the true biological fractionation by isotope effect. The most recent experiments are in favour of the lower fractionation value (Kim and Baumgärtner, 1994).

A4. RESULTS AND DISCUSSION

(A20) The calculations related to the atmospheric pathway and presented below have been made by eleven participants on the basis of Scenario 1.3. The transport processes and general modelling approaches have been described in Sections A3.1 to A3.3. A brief comparison of the modelling approaches used by the participants can be seen in Table A1. Detailed descriptions of individual models are given in Annex I–A.

A4.1. TRITIUM CONCENTRATION IN AIR HUMIDITY

(A21) Figure A1 shows the total concentration of HTO in atmospheric water as a function of distance from the stack, as obtained by each of the eleven modellers, for the assumed HTO release. As fixed in Scenario 1.3, the distance of interest for calculations extends from 0.2 km to 10 km, because of the difficulty of predicting the concentrations at distances smaller than 0.2 km, and because the concentrations at distances larger than 10 km are outside the scope of the study. The majority of the eleven different curves are relatively well grouped and lie together within a factor of two, in spite of the fact that some modellers have not considered the secondary emission from the soil. If we exclude the BEAK curve that has been obtained for a different set of vertical dispersion parameters, we observe that the curves obtained from primary dispersion only are generally lower than those obtained for primary and secondary dispersion by a factor 1.5 to 2. The difference tends to increase at small distances from the source (less than 0.5 km), because the primary concentration becomes smaller and smaller as the elevated primary source is approached. The influence of the secondary dispersion is not so marked for the JAERI results. This is probably due to the fact that in the JAERI model, the dispersion from ground level area sources is calculated with the same advection velocity as for the primary elevated source, while in the CEA and FZK models, the dispersion from ground level is determined with a much reduced advection velocity in order to deal with the effect of reduced ventilation at ground level (cf. Table A1).

TABLE A1. COMPARISON OF MODELLING APPROACHES USED IN THE TWG MODEL-MODEL INTERCOMPARISON EXERCISE BASED ON SCENARIO 1.3

Institution (Modeller)	Primary HTO Concentration in Air Humidity determined from:	Secondary HTO Concentration in Air Humidity determined from:	HTO Concentration in Soil Moisture determined from:
AECL (P.A. Davis)	Sector-averaged plume model	– *Considered implicitly by not depleting the primary plume* (HTO release) – Empirical results (HT release)	– Wet deposition (HTO release) – Empirical results (HT release)
ANDRA (C. Meurville)	Sector-averaged plume model	*Not considered*	– I / O balance (HTO release) – *Not considered* (HT release)
BEAK (D. Lush)	IMPACT code Sector-averaged model	*Not considered*	– I / O balance (HTO release) – *Not considered* (HT release)
Consultant (Y. Belot)	TRIMASS code Sector-averaged model (Rectangular grid system)	Area-sources contribution with correction of advection velocity	I / O activity balance (HTO and HT releases)
CEA (G. Guinois)	TRIMASS code Sector-averaged model (Rectangular grid system)	Area-sources contribution with correction of advection velocity	I / O activity balance (HTO and HT releases)
FZK (W. Raskob)	NORMTRI code Sector-averaged model (Polar grid system)	Area-sources contribution with correction of advection velocity	– Wet deposition (HTO release) – 20% of dry deposition (HT release)
JAERI (H. Amano)	ETDOSE code Sector-averaged model (Rectangular grid system)	Area-sources contribution **without** correction of advection velocity	Dry deposition (HTO and HT releases)
NIPNE (D. Galeriu)	Sector-averaged plume model	– *Not considered* (HTO release) – Empirical results (HT release)	– Dry plus wet deposition (HTO release) – Empirical results (HT release)
STUDSVIK (O. Edlund)	Sector-averaged plume model	*Not considered*	– Dry deposition (HTO release) – Dry deposition (HT release)
VNIIEF (A. Golubev)	Sector-averaged plume model	– *Not considered* (HTO release) – Area-sources contribution (HT release)	Dry deposition (HTO and HT releases)
ZSR (M. Täschner)	Sector-averaged plume model	– *Not considered* (HTO release) – Empirical results (HT release)	– Concentrations in air humidity and rainwater (HTO release) – Dry deposition (HT release)

(A22) Figure A2 represents the concentrations of tritium in air humidity for a HT release, with the same release rate as assumed in the HTO case. As expected, the HTO concentrations are much lower, since HTO is formed in the soil and brought only indirectly to the atmosphere by re-emission. The curves are not so well grouped as in the HTO release, because of appreciable differences in modelling approaches and because the environmental behaviour of HT is not as well known as that of HTO. As can be seen in Table A1, four curves are based on a secondary re-emission model that allows for the contribution of ground level area sources and three curves are based on the use of empirical constants derived from Canadian field experiments (Davis et al., 1995). The results obtained by six of the participants differ only by a factor 2 to 3, which is acceptable for the simulation of such a complex process in which certain models use an empirical approach and others a theoretical approach. The much lower values obtained from the JAERI model could be explained, in part, as indicated in the paragraph above, by the use of a high advection velocity in the formula describing dispersion from ground level sources. No explanation has been found for the divergence of the RFNC-VNIIEF curve at large distances from the source.

(A23) The HTO concentration in air humidity obtained for a release in the form of HTO approaches 200 Bq L^{-1} for a release rate of 1 g y^{-1} whereas an equal release of HT results in a concentration of only a few Bq L^{-1}, that is a few percent of the result obtained in the first case.

The absolute values of the concentrations might be appreciably different if the average weather conditions were very different, and particularly if the windrose was strongly anisotropic, but the ratio of the two values probably should not be extremely different. This ratio is of importance in radiation protection assessment, if sources are emitting tritium in both forms.

A4.2. TRITIUM CONCENTRATION IN SOIL AND PLANTS

(A24) Figure A3 shows the relative concentrations of HTO in soil water, for the HTO release. The following analysis of results concentrates separately on those obtained at distances greater than 1 km and those obtained at distances less than 1 km.

- For distances greater than 1 km, two groups of curves can be seen on the graph depending on whether or not dry deposition is included in the model. The average difference between the two groups of curves is appreciable and amounts to an average factor of nearly five. The upper group of curves corresponds to the models that consider dry deposition without re-emission; the lower group to the models that consider only wet deposition without re-emission.
- At less than 1 km from the source, some curves of the upper group decrease rapidly toward much lower concentrations. These curves are those which correspond to the consideration of dry deposition only. In this case, as one approaches the source, the tritium in soil moisture decreases in parallel to the concentration in air. The curves which correspond to consideration of wet deposition only do not decline when approaching the source, but on the contrary rise to higher concentrations, since wet deposition results in more and more tritium deposition as distance from the source decreases.

(A25) As already indicated in the general description of models, the question of whether to model wet deposition or dry deposition, or both is a matter of debate. The choice between approaches is not irrelevant since it may lead to important differences, as reported above. The difference would be even more important in sectors where the joint frequency of wind and rain is nearly zero, and where the only possible input of tritium to the soil, if any, is dry deposition. Hence, there is a necessity to examine existing survey data or to carry out new field measurements in order to investigate whether or not the concentration of tritium in soil water is related both to wet and dry deposition, or only to one of the two processes. Some of the data that were collected in the past at a few sites have been compared to the predictions obtained from different models. Moreover, experimentalists who participated in the TWG carried out a field sampling programme to identify the main process(es) that contribute to tritium buildup in the soil due to wet and dry deposition. The results of this 20 month field sampling programme are reported in Part G.

(A26) Figure A4 refers to the concentration of HTO in soil water for an HT release. The levels of HTO are, as expected, much lower than in the preceding case. The variation in the results can be explained by the fact that different methods are used, including the use of an input-output balance, and the use of empirical relationships drawn from a field experiment (see Table A1). The input-output balance tends to give high concentrations whilst the empirical relationship gives lower results. Some of the variation is also due to the calculation of different air concentrations. It is not possible to decide from this model intercomparison alone which of the approaches is the best.

(A27) Figures A5 and A6 relate to the concentration of tritium in leaves, in the form of HTO and OBT (organically bound tritium) respectively. The concentration of HTO in the free water (TFWT) of leaves depends directly on the concentrations of HTO in air humidity and soil moisture and can be determined by the classical Eq.5 given above in Section A3.3. All the modellers have used the same formula with only minor differences in numerical coefficients. The variability in the calculated results for HTO concentrations in plant water is relatively low, this is because HTO concentrations in plant water depend mainly on HTO concentrations in air humidity and these showed only a relatively low variation between results. With respect to the concentration of tritium in the combustion water (or water equivalent) of dry leaves, termed the OBT concentration, the range of results is also relatively small. The reason is because this concentration is obtained by multiplying the concentration of tritium in leaf free water by a discrimination factor that was taken by the different modellers to be between 0.6 and 1.0.

A5. CONCLUSIONS

(A28) Modelling the environmental transport of tritium in the vicinity of permanent atmospheric sources was the first task of the TWG. The determination of average values of tritium concentration as HTO in air humidity is more complicated than for other radionuclides since it requires firstly, the consideration of the transport and dispersion of tritium from primary source(s) (generally one or several stacks), and secondly the consideration of the re-emission to the atmosphere of some of the tritium deposited to the soil surface. The prediction of the primary concentrations of tritium in air humidity was approached in the same way by all the participants. However, the prediction of the secondary concentration due to re-emission was approached in different ways and by a few participants only. The results of tritium concentration in air humidity, in the case of an HTO release, were very similar, even though some participants considered only the primary emission. This was explained by the low importance of the secondary emission process compared to primary emission. In contrast, the predictions of tritium concentration in air humidity, in the case of an HT release, were much more dispersed, because of the unique importance of the secondary emission, and because of the different ways to estimate the consequences of such a release.

(A29) The prediction of average values of HTO concentration in soil moisture was made using different approaches. Some of the modellers derived the concentration from a balance of tritium inputs and outputs to and from the soil surface. Others based their calculations on semi-empirical considerations. The diversity of approaches led to results that were spread over a factor of nearly seven. This raised the questions of how to explain the reasons for such a spread, and how to determine which type of approach is the most convenient and suitable. It was decided to try to find answers by undertaking model-data comparisons, using either a series of survey data that were acquired in the past at different sites, or using a series of new data specially collated for this purpose at a few conveniently placed monitoring stations. Both approaches were adopted in subsequent work undertaken by the TWG.

(A30) The results of tritium concentrations in leaf water are much less variable than those in soil water, but show the same variability as those in air humidity, to which they are more strongly related. As the fractionation coefficient is taken to be between 0.6 and 1, the results of tritium concentrations in the combustion water of leaves are understandably more variable than those obtained for tissue water.

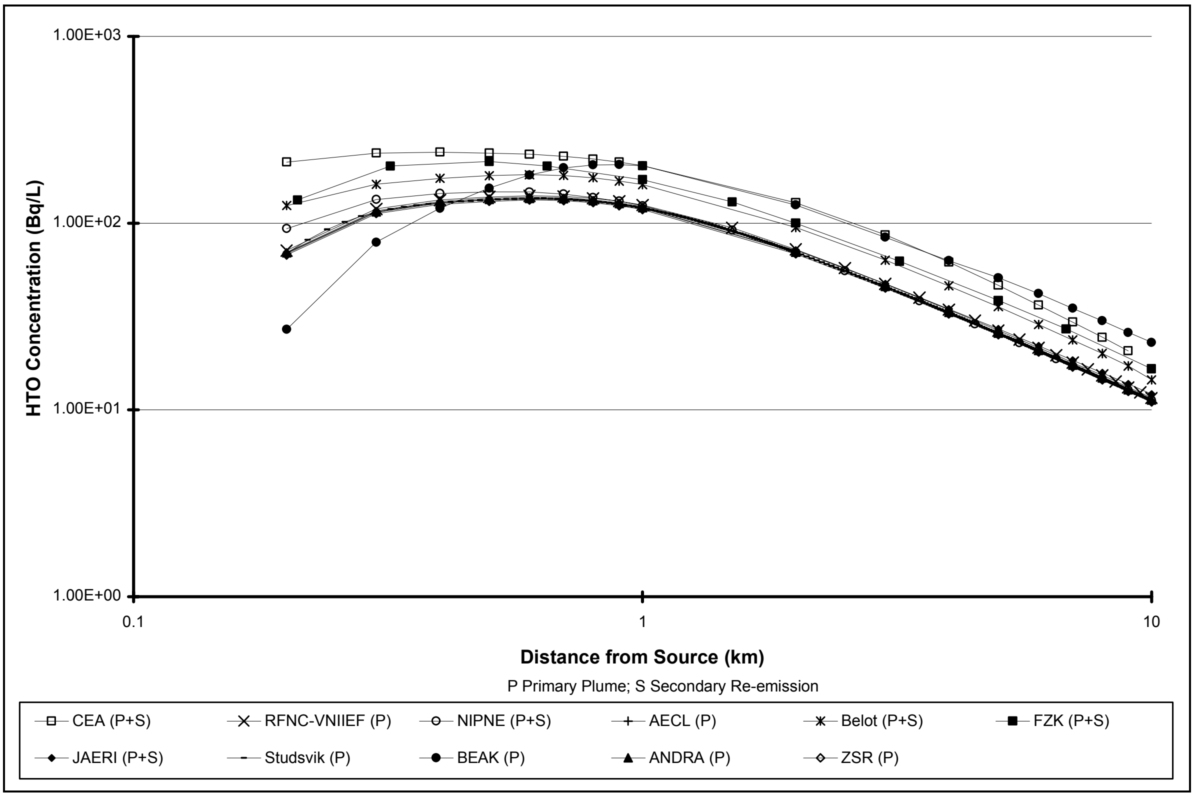

FIG. A1. HTO Release – HTO concentration in air humidity.

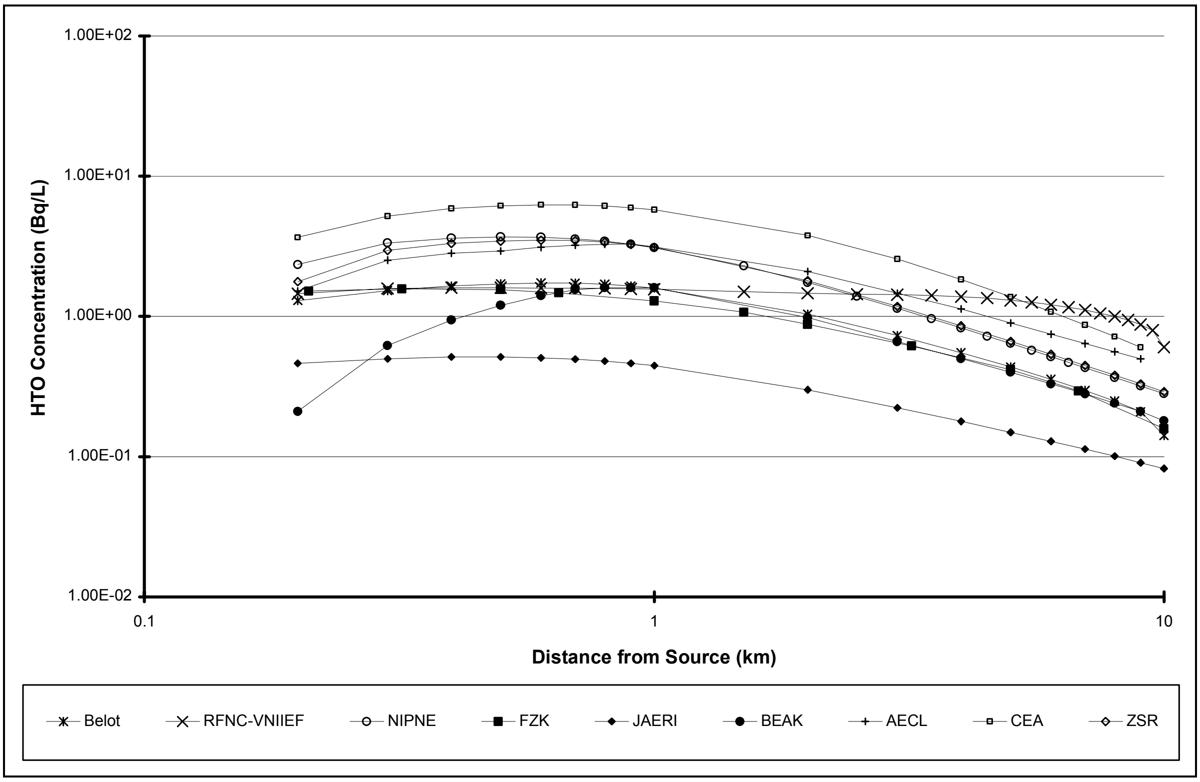

FIG. A2. HT Release – HTO concentration in air humidity.

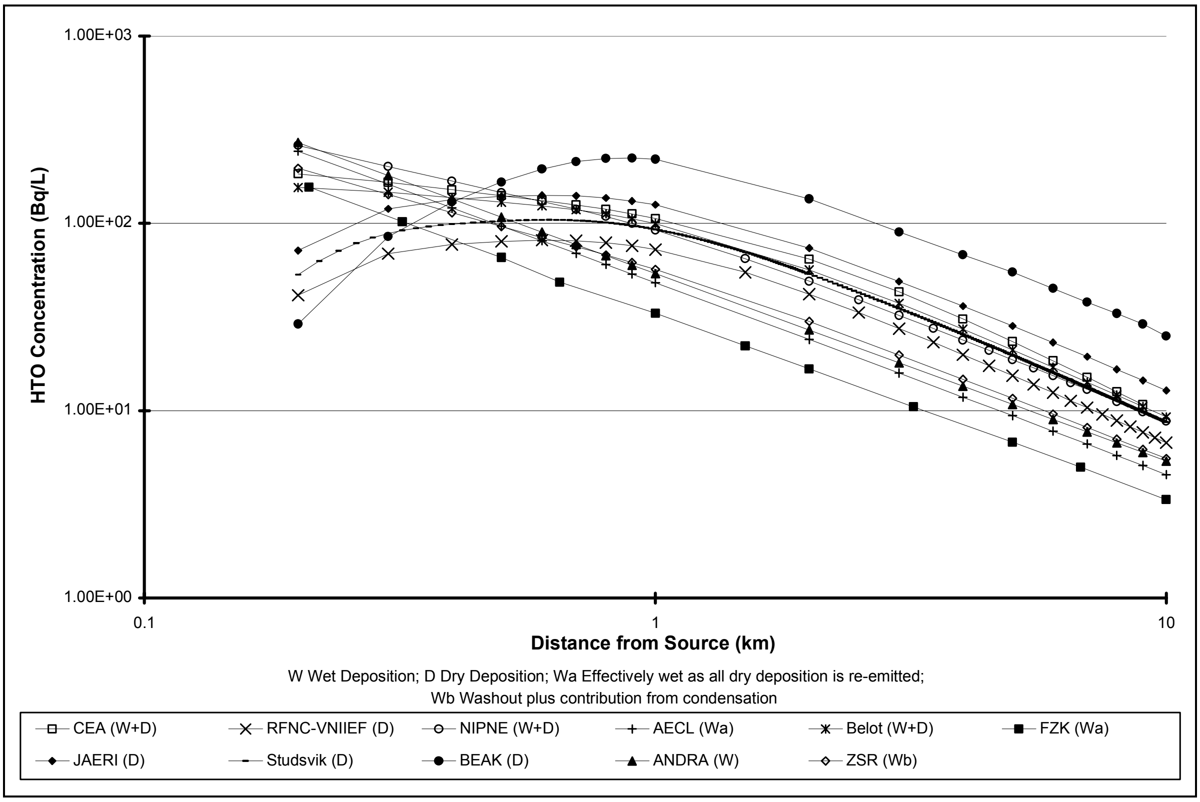

FIG. A3. HTO Release–- HTO concentration in soil water.

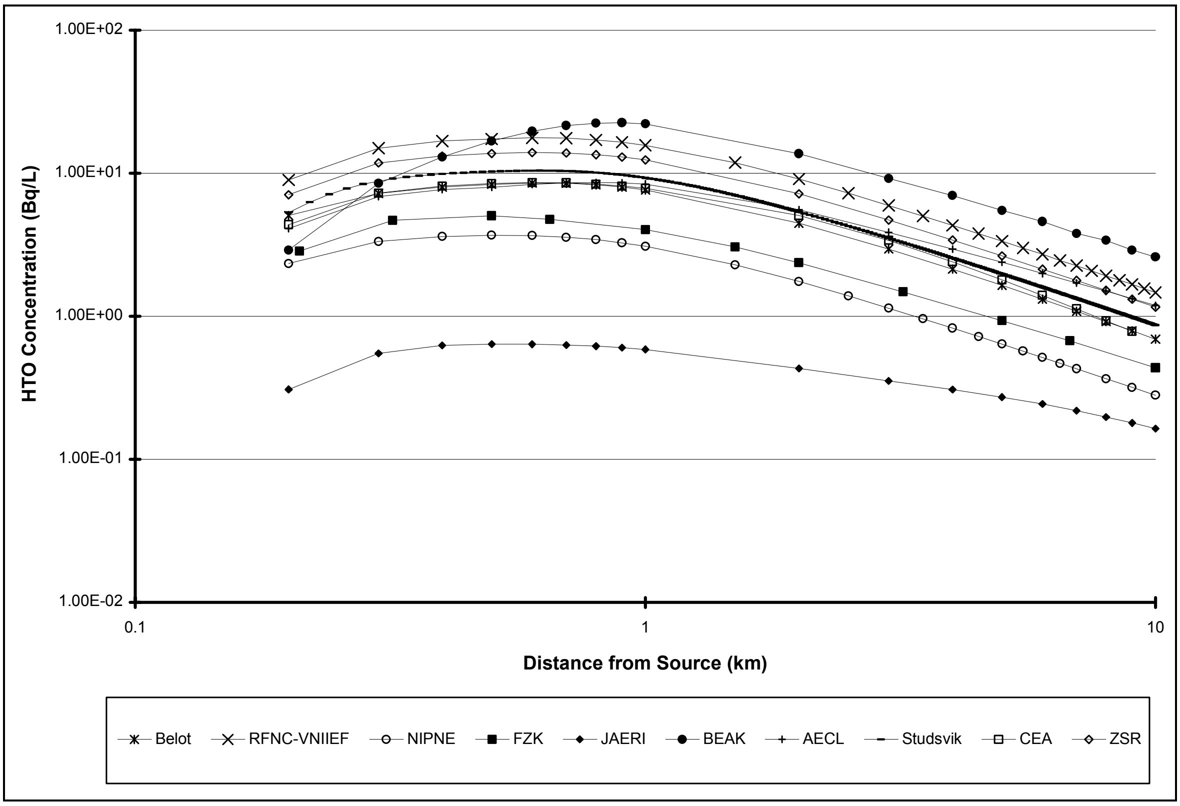

FIG. A4. HT Release – HTO concentration in soil water.

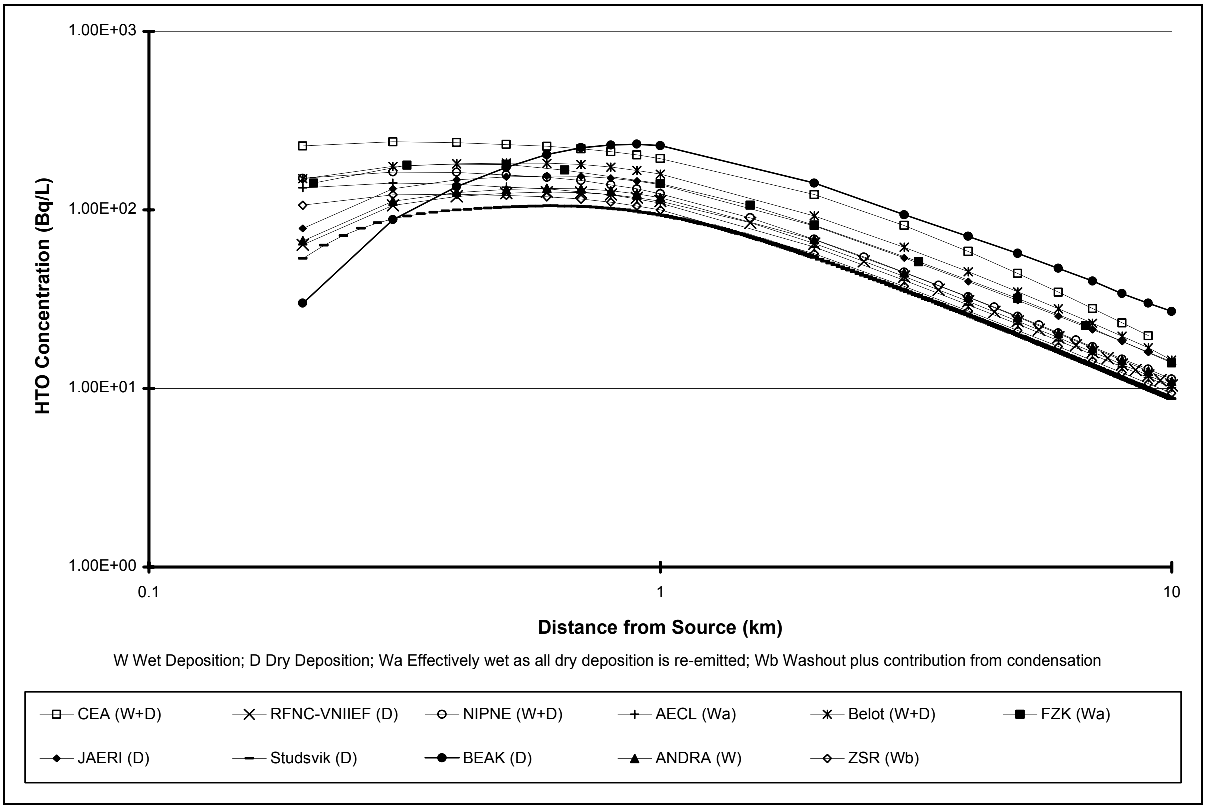

FIG. A5. HTO Release – HTO concentration in plant water.

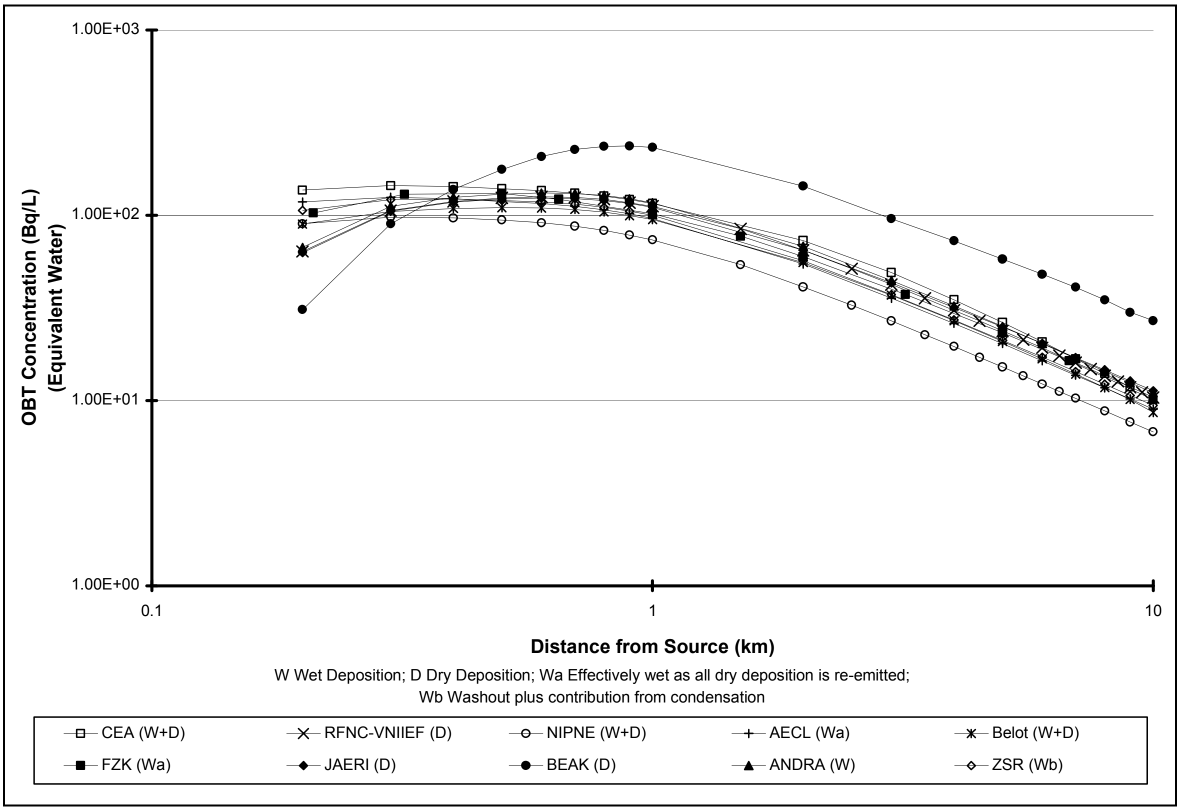

FIG. A6. HTO Release – Plant OBT concentration.

REFERENCES TO PART A

[1] BARRY, P.J., WATKINS, B.M., BELOT, Y., DAVIS, P.D., EDLUND, O., GALERIU, D., RASKOB, W., RUSSELL, S., TOGAWA, O., Intercomparison of Model Predictions of Tritium Concentrations in Soil and Foods Following Acute Airborne HTO Exposure, Journal of Environmental Radioactivity **42** (1999) 191–207.

[2] BELOT, Y., Predicting the washout of tritiated water from atmospheric plumes, Presented at the Workshop of the IEA Task Group on Tritium Safety and Environmental Effects, held at AECL, Chalk River, Canada, on May 11–12 (1998).

[3] BIOMOVS II, Tritium in the Food Chain: Intercomparison of model predictions of contamination in soil, crops, milk and beef after a short exposure to tritiated water vapour in air, Published on behalf of the BIOMOVS II Steering Committee by SSI, Sweden, ISBN 91-972134-7-0 (1996a).

[4] BIOMOVS II, Tritium in the Food Chain: Comparison of predicted and observed behaviour; A. Re-emission from soil and Vegetation; B. Formation of organically bound tritium in grain of Spring Wheat, Published on behalf of the BIOMOVS II Steering Committee by SSI, Sweden, ISBN 91-972958-2-5 (1996b).

[5] DAVIS, P.A., BICKEL, P.A., Transfer parameters for environmental pathway models for chronic emissions of tritiated hydrogen gas, Atomic Energy of Canada Limited Report Rc-2501, Chalk River Laboratories, Chalk River, Ontario (2000).

[6] DAVIS, P.A., GALERIU, D.C., SPENCER, F.S., AMIRO, B.D., Evolution of HTO concentration in soil, vegetation and air during an experimental HT release, Fusion Technology **28** (1995) 833–839.

[7] HALES, J.M., WOLF, M.A., DANA, M.T., A linear model for predicting the washout of pollutant gases from industrial plumes, AIChe. Journal **19** (1973) 292–297.

[8] HORST, T.W., Lagrangian similarity modelling of vertical diffusion from a ground level source, J. Appl. Meteor. **18** (1979) 733–740.

[9] KIM, M.A., BAUMGÄRTNER, F., Equilibrium and non-equilibrium partition of tritium between organics and tissue water of different biological systems. Appl. Radiat. Isotopes **45** (1994) 353–360.

[10] SMITH, M.E., SINGER, I.A., An improved method of estimating concentrations and related phenomena from a point source emission, J. Appl. Meteor. **5** (1966) 631–639.

PART B

MODELLING THE ENVIRONMENTAL TRANSPORT OF TRITIUM IN THE VICINITY OF PERMANENT ATMOSPHERIC SOURCES:

A test of chronic atmospheric release models using Canadian data

B1. BACKGROUND AND OBJECTIVES

(B1) Scenario 3 provided a test of models that predict long term average tritium concentrations in the environment (excluding groundwaters) due to chronic atmospheric releases. Such models are essential for estimating doses to the public near tritium-handling facilities but they have undergone little formal testing in the past. Scenario 3 treats essentially the same processes and endpoints as Scenario 1.3 (see Part A) but is based on field observations rather than hypothetical data. Conclusions from Scenario 3 therefore address the quantitative performance of the models and the best way to simulate particular processes whereas Scenario 1.3 was restricted to a comparison of modelling approaches and model results. Scenario 3 was proposed at the 1998 spring meeting of the Tritium Working Group (TWG). A scenario description was prepared for the Plenary Meeting in October 1998 and distributed to participants shortly thereafter. Results were discussed at the spring and autumn meetings in 1999 and conclusions were finalised at the spring meeting in 2000.

B2. SCENARIO DESCRIPTION

(B2) The full Scenario 3 description is given in Annex II–B. Briefly, the scenario is based on data collected at the Chalk River Laboratories (CRL) of AECL, where small amounts of tritium have been released continuously to the atmosphere over many years during normal operation of three facilities: the NRU reactor building, the 46-m reactor exhaust stack, and a waste management area beneath a lake and wetland. Tritium concentrations in air, vegetation and soil were measured twice daily on selected days over a 2-month period in the summer of 1995. HTO concentrations in air were measured over the time intervals 0900–1500 and 1500–0900 each day and represent averages over these periods. Grass samples were collected at 0900 and 1500. Because tritium concentrations in vegetation change rapidly in response to environmental conditions, the grass concentrations reflect conditions in the hour or so prior to sampling. A few grass samples were analysed for their non-exchangeable OBT concentrations. Soil samples were collected at 0900 each day. Soil concentrations, which change fairly slowly over time, reflect conditions in the few hours or days prior to sampling. The 0900 and 1500 sampling times will be referred to as the morning and afternoon samples, respectively.

(B3) The measurements were made at three locations on CRL property. The Acid Rain Monitoring Site (ARS) is located 2 km northwest of the reactor stack in a 100 m wide tract of land cut through the surrounding forest. Releases from NRU and the reactor stack contribute about equally to air concentrations at this location. The second sampling site (B600) is located just north of Building 600 in the laboratory complex, 500 m southeast of NRU. The terrain is open for the first 150 m from B600 toward NRU but buildings occupy the remaining distance. Air concentrations at B600 are dominated by releases from the reactor building. The third sampling site (PL) is located in a meadow about 100 m in diameter on the east shore of Perch Lake, which adjoins the waste management area. It receives most of its airborne tritium through evapotranspiration from the lake and wetland, which represent a finite-area source at ground level. The local vegetation at ARS and PL is a mixture of natural grasses. At B600, the grass is tended but was left uncut in the sampling area itself.

(B4) Estimates of the ratio of HTO concentration in rain to HTO concentration in air at ARS were available from measurements made at site MR, located colinearly with ARS and NRU but 3 km farther downwind. Hourly measurements of various meteorological parameters (wind speed, wind direction, standard deviation in wind direction, relative humidity, air temperature, net radiation, leaf temperature, soil temperature and rainfall rate) were made throughout the study.

(B5) Participants in the scenario were provided with the hourly meteorological data and the observed HTO concentrations in air at the three sampling sites. From this information, they were asked to predict:

(i) HTO concentrations in rainfall (Bq L^{-1}) averaged over the study period at ARS;

(ii) HTO concentrations in soil water (Bq L^{-1}) averaged over the study period at each of the 3 sampling sites, broken down into morning and afternoon averages;

(iii) HTO concentrations in the free water of grass (Bq L^{-1}) averaged over the study period at each of the 3 sampling sites, broken down into morning and afternoon averages;

(iv) non-exchangeable OBT concentrations in grass (Bq L^{-1} water equivalent) at the 3 sampling sites on June 28, July 12 and August 9;

(v) HTO concentrations in soil water and free water of grass (Bq L^{-1}) at ARS at specific times when meteorological conditions had been steady for several hours; and

(vi) 95% confidence intervals on all predictions in (i)–(v).

B3. OBSERVATIONS

(B6) The observed values corresponding to the requested predictions are shown in Tables B1 and B2. Each of the observations has an associated uncertainty that arises for several reasons. Uncertainties in the air concentrations are due to counting errors and to uncertainty in determining the volume of air sampled. The total uncertainty in these concentrations is estimated to be less than 10% in most cases but could reach 20% for some of the lower concentrations. Counting errors for grass and soil HTO concentrations were relatively low (5% and 10% respectively) but concentrations in replicate samples differed by 20–30% because of natural variability. The uncertainties in the OBT concentrations are estimated to be about 10%. The uncertainty in the rain/air ratio at site MR was about 30% but this increases when the value is applied to ARS because the sampling interval at MR did not coincide precisely with the study period.

(B7) Tritium concentrations in all compartments are highest for B600, which is closest to NRU and the reactor stack, and lowest for ARS, which is farthest away. PL is relatively far from these sources but is close to the waste management area and shows concentrations between those of B600 and ARS. Morning air concentrations at all three sites were slightly lower than afternoon values. Atmospheric conditions tend to be stable at night and concentrations in the airborne plume relatively high. However, stable plumes are fairly narrow and the frequency with which the plume was present over the sampling sites would have been lower during the night than during the day, resulting in the lower overnight concentrations.

(B8) The observations show two noteworthy features that a successful model should be able to reproduce:

— site-to-site variations in the soil/air and plant water/air ratios; and

— the low afternoon plant water/air concentration ratios relative to the morning values at all 3 sites.

TABLE B1. OBSERVED TRITIUM CONCENTRATIONS IN AIR, RAIN, SOIL AND PLANTS AT EACH OF THE THREE CRL STUDY SITES

		ARS	B600	PL
Air (Bq m^{-3}) -	Morning	3.4	18.4	7.7
	Afternoon	4.1	21.9	11.7
	24h	3.6	19.3	8.7
Air (Bq L^{-1}) -	Morning	264	1581	627
	Afternoon	285	1862	980
	24h	269	1651	715
Rain (Bq L^{-1}) -	24h	(0.81)	–	–
Soil (Bq L^{-1}) -	Morning	81 (0.31)	405 (0.26)	136 (0.22)
Grass (Bq L^{-1}) -	Morning	218 (0.83)	1322 (0.84)	445 (0.71)
	Afternoon	92 (0.32)	1048 (0.56)	501 (0.51)
	24h	155 (0.58)	1185 (0.72)	473 (0.66)
OBT (Bq L^{-1}) -	Jun 28	83 (0.86; 0.46)	841 (0.52; 0.53)	262 (0.34; 0.38)
	Jul 12	126 (1.36; 0.63)	–	254 (0.42; 0.48)
	Aug 9	163 (1.82; 0.90)	1359 (1.26; 1.08)	322 (0.64; 0.70)

Note: Values in Brackets for Rain, Soil and Grass are Concentrations Divided by the Corresponding Air Concentration in Bq L^{-1}. Values in Brackets for OBT are Concentrations Divided by the Corresponding Plant Water Concentration, Time-Averaged up to the Time of the OBT Sample. The First Value in Brackets was Obtained by Dividing by the Afternoon Plant Water Concentration and the Second by the 24-Hour Concentration.

TABLE B2. SOIL AND PLANT WATER CONCENTRATIONS AT ARS AT SPECIFIC TIMES DURING THE CRL STUDY

Time and Date		Plume status	Air (Bq L^{-1})	Soil (Bq L^{-1})	Plant Water (Bq L^{-1})
0900	Jun 8	Absent	149	35 (0.23)	66 (0.44)
	Jun 29	Present	171	90 (0.53)	91 (0.53)
	Jul 12	Absent	124	72 (0.58)	64 (0.52)
1500	Jun 15	Absent	172	70 (0.41)	84 (0.49)
	Jun 28	Present	251	28 (0.11)	107 (0.43)
	Jul 5	Present	420	98 (0.23)	97 (0.23)
	Jul 19	Absent	120	75 (0.63)	47 (0.39)

Note: Values in Brackets are Concentrations Divided by the Air Concentration Observed at the Time of Sampling.

B4. COMPARISON OF PREDICTIONS AND OBSERVATIONS

(B9) The seven participants who submitted predictions for Scenario 3 are listed in Table B3. Full descriptions of the models they used to carry out their calculations are given in Annex I–A. Details of the models will be introduced in this Section as needed to explain the results. Some participants used the same model for Scenario 3 as they did for Scenario 1.3 but others used different models.

(B10) All participants submitted results for ARS and B600 but only three carried out calculations for PL, since most models are unable to handle the distributed nature of the PL tritium source. The emphasis in the discussion will therefore be on ARS and B600, with results for PL introduced only to provide insight into specific questions.

TABLE B3. PARTICIPANTS IN SCENARIO 3

Participant	Affiliation	Designation used in text
Y. Belot	Consultant, France	Belot
O. Edlund*	Studsvik EcoSafe, Sweden	SES
D. Galeriu*	NIPNE, Romania	NIPNE
G. Guinois*	CEA, France	CEA
S-R. Peterson	LLNL, United States	LLNL
W. Raskob	FZK, Germany	FZK
M. Taeschner*	ZSR, Germany	ZSR

* These participants submitted some results after the observations had been released.

Some participants treated the scenario as a blind test of their models and submitted results before the observed tritium concentrations were made known to them. However, others submitted some results after the observations had been released (Table B3).

(B11) Five of the seven participants submitted uncertainty estimates with their model predictions. On the basis of expert judgement, the users of the NIPNE and FZK models estimated their 95% confidence intervals on concentrations in a given compartment to span an order of magnitude. However, both reduced their confidence intervals for endpoints involving ratios of compartmental concentrations to air concentrations. The ZSR participant also used expert judgement and took account of the long averaging time of the predictions to deduce an uncertainty of a factor 1.5 above and below his best estimates. The uncertainty estimates for the SES and LLNL models were both obtained through the method of parameter perturbation, but the number and nature of the parameters considered in the analyses were quite different in the two cases. The LLNL participant used a semi-empirical model in her calculations and varied all the parameters in it (air concentration, tritium release rate, wind speed, rainfall amount, relative and absolute humidity, washout coefficient, deposition velocity, fraction of dry deposition retained in the soil and isotopic discrimination factor), choosing high and low values for each of these parameters on the basis of expert judgement to lie one standard deviation above and below their respective means. This defines a 68% confidence interval for the individual parameters but the resulting uncertainty range in the model endpoints is likely larger because parameter perturbation accords equal weight to all combinations of parameter values when in fact the combination of extreme values is relatively unlikely. On the other hand, the SES participant used a time-dependent, process-oriented model in his calculations and had a different set of parameters to deal with. He varied only a limited number of these (leaf area index, minimum stomatal resistance, soil depth and isotopic discrimination factor) and so likely underestimated the 95% confidence interval in his predictions.

B4.1. AIR CONCENTRATIONS

(B12) Observed air concentrations were provided as part of the scenario description. The LLNL participant used the data as given to drive her model. The SES participant determined 24-hour air concentrations by first interpolating values for days on which no measurements were made and then averaging over all days in the study period. This resulted in concentrations slightly different than the observed values shown in Table B1, which were averaged over only those days on which measurements were made.

(B13) The remaining five participants modelled the air concentrations. Their predictions for the average concentrations at ARS and B600 over the entire study period are shown in Table B4, together with the predicted/observed (P/O) ratios. The NRU reactor is the main source of tritium for both sites, with the reactor stack contributing substantially to ARS but less so to

B600. PL makes little contribution to the tritium concentration at either site and was not considered by any of the participants in making their estimates. Most of the predictions lie within 25% of the observations, a good result for this type of calculation. The two predictions showing poorer agreement (FZK at ARS and NIPNE at B600) still lay within a factor of 3 of the observations.

TABLE B4. PREDICTED AIR CONCENTRATIONS AVERAGED OVER THE STUDY PERIOD

Participant	ARS		B600	
	Prediction (Bq m^{-3})	P/O	Prediction (Bq m^{-3})	P/O
Belot	3.5	0.97	19.5	1.01
NIPNE	3.3	0.92	11.3	0.59
CEA	3.1	0.86	20.0	1.04
FZK	1.1	0.30	14.6	0.76
ZSR	2.9	0.80	17.7	0.92

TABLE B5. ASSUMPTIONS MADE BY THE VARIOUS PARTICIPANTS IN CALCULATING AIR CONCENTRATIONS

Participant	σ_z Scheme	Height for NRU release and wind speed extrapolation (m)	Depletion/Re-emission
Belot	Briggs	15	Not explicitly considered
NIPNE	KfK 50-m	15	Not explicitly considered
CEA	Briggs	15	Not explicitly considered
FZK	Mol	20	Considered during study period
ZSR	Briggs	30 for ARS, 15 for B600	Considered

(B14) All of the participants used a form of the long term average Gaussian plume model to carry out their calculations. Three participants used the sector-average approach and the others, FZK and NIPNE, the straight-line model. All participants used the meteorological data as given in the scenario description with the exception of FZK, who deduced his own stability classes from the data before stability information had been included in the scenario description.

(B15) All participants treated the reactor stack as an isolated point source with an effective release height of 46 m and extrapolated the observed wind speeds to this height. Only one participant (NIPNE) considered plume broadening due to building-induced turbulence. The modellers made different assumptions in other areas: in the scheme used to calculate the vertical dispersion parameter σ_Z; in the effective release height adopted for the NRU source (and the height to which the wind speed was extrapolated for this source); and in the treatment of plume depletion / re-emission. The approaches taken by the modelers in these areas are shown in Table B5.

(B16) The three models that performed best (Belot, CEA and ZSR) were all very similar except in their approach to depletion and re-emission. Belot and CEA did not deplete the primary plume and so implicitly accounted for re-emission. ZSR on the other hand modeled re-emission explicitly but produced the lowest concentrations among the three models. This suggests that the model may underestimate the magnitude of re-emission, an interpretation supported by the fact that it underpredicts air concentrations on days when the airborne plume is not present. The NIPNE and FZK models both underestimated the observed air concentrations, by a small amount at one site and by a substantial amount at the other. This suggests that the Mol and KfK schemes for calculating σ_z may not be as suitable for the CRL site as Briggs' scheme. Similarly, the stability classes deduced by the FZK participant may not have been as appropriate as the classes supplied in the scenario description.

(B17) Since the focus of the scenario is concentration in rain, soil and plants rather than in air, most remaining results will be normalized to the air concentrations predicted by each participant to remove the variability introduced by differences in air concentrations.

B4.2. RAIN CONCENTRATIONS

(B18) All participants calculated the wet deposition flux of HTO from air to soil using an equation similar to:

$$F_w = Q \Lambda \Phi / (x u \theta) \tag{1}$$

where:

F_w	is the HTO flux from air to soil due to rain (Bq m^{-2} s^{-1});
Q	is the release rate (Bq s^{-1});
Λ	is the washout coefficient (s^{-1});
Φ	is the joint frequency of occurrence of wind direction and rainfall in the sector containing the receptor;
x	is the distance from source to receptor (m);
u	is the mean wind speed (m s^{-1}); and
θ	is the angular width of the sector (radians).

(B19) The concentration of HTO in rainwater (C_r, Bq L^{-1}) was then found from:

$$C_r = F_w T / (1000 P) \tag{2}$$

where T is the duration of the study period (s); P is the total amount of rain that fell during the study period (m); and the factor 1000 converts the units of C_r from Bq m^{-3} to Bq L^{-1}.

(B20) Values for Q, x and P were given in the scenario description and all participants set $u \sim 3$ m s^{-1}. The values for Λ showed greater variability, ranging from 6×10^{-5} s^{-1} (Belot, CEA, SES, FZK and ZSR) to 1.56×10^{-4} s^{-1} (LLNL). Values of $\Phi T/\theta$ also varied since the participants deduced this parameter in different ways from the data provided. As a result, the predictions for the rainwater concentrations ranged over a factor of 3, from 28 Bq L^{-1} to 87 Bq L^{-1} (Figure B1). All the predictions were substantially lower than the observed value of 218 Bq L^{-1}, which, at 81% of the air moisture concentration, seems unusually high. As noted in Section B2, the uncertainty in this value is probably greater than 30%. The uncertainty in the predictions is also large, due in part to the uncertainty in the parameter values but also to flaws in the model itself. The model assumes that material in the plume has a Gaussian distribution in the vertical, which is not necessarily the case, especially for a source near ground level. In addition, the model may not work well for heavy rains or for a plume that fluctuates in direction. Figure B1 shows that the lower confidence limit of the observation overlaps with the upper confidence limit for some models. In these cases, predictions and observations are in agreement when uncertainties are taken into account.

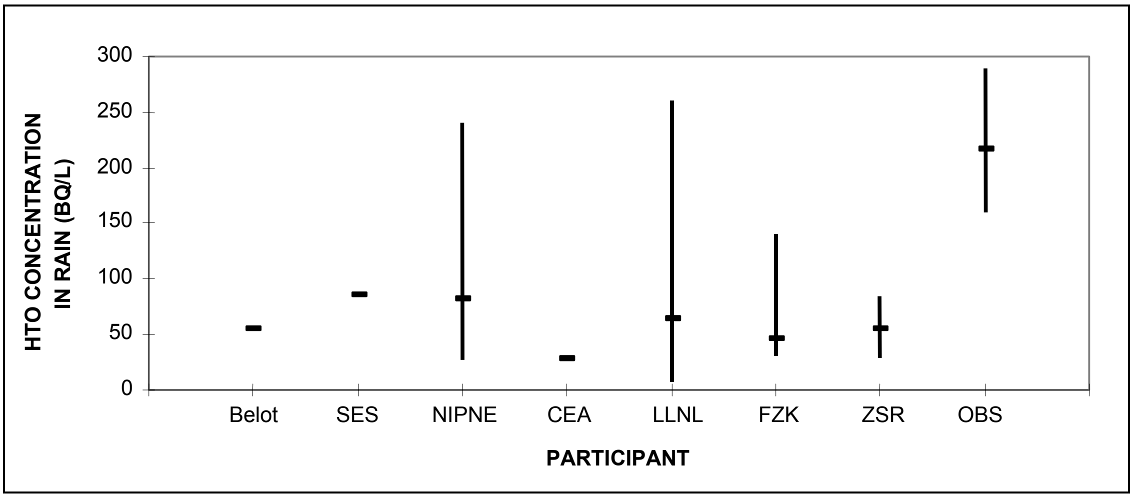

FIG. B1. Predicted and observed HTO concentrations in rain averaged over the entire study period. The horizontal bars mark the best estimate predictions and the vertical lines span the nominal 95% confidence intervals.

B4.3. SOIL CONCENTRATIONS

(B21) The methods used by the participants to calculate soil concentrations can be broken down into three main types:

(i) Activity balance approach: The models of Belot and CEA are based on an activity balance equation for the flux of HTO into and out of the soil, taking into account wet and dry deposition, re-emission and infiltration. This leads to the following equation for the HTO concentration in soil water (C_s, Bq L^{-1}):

$$C_s = (v_d\, C_a + F_w) / (v_e\, \rho_s + 1000\, R) \tag{3}$$

where:

v_d is the transfer velocity of HTO from air to soil (m s^{-1});
C_a is the HTO concentration in air (Bq m^{-3});
v_e is the transfer velocity of HTO from soil to air (m s^{-1});
ρ_s is the water concentration in air saturated at the soil surface temperature (kg m^{-3}); and
R is the rainfall intensity (m s^{-1}).

In practice, the air temperature was used in place of the soil surface temperature in calculating ρ_s and v_d was set equal to v_e.

(ii) Semi-empirical approach: In the models of NIPNE, LLNL and FZK, C_s is calculated by considering the contributions of wet and dry deposition. Each model assumes that the soil concentration due to wet deposition equals the concentration in rain, but treats dry deposition in different ways. FZK assumes that all dry-deposited HTO is eventually re-emitted to the atmosphere so that $C_s = C_r$. LLNL assumes that a fraction 0.08 of the dry-deposited HTO is retained in the soil, and sets $C_s = C_r + 0.08\ v_d\ C_a\ T\ /\ (1000\ P)$. In contrast, NIPNE assumes that the soil concentration due to dry deposition is equal to a fraction 0.2 of the concentration in air moisture (C_{am}, Bq L^{-1}), so that $C_s = C_r + 0.2\ C_{am}$.

(iii) Time-dependent approach: SES and ZSR simulate the soil compartment using process-oriented, multi-layer, time-dependent models in which soil water and tritium contents are calculated on a 1-hour time step. SES uses Richards' equation to model soil water transport, with inputs from precipitation and condensation and losses from evapotranspiration, calculated using the Monteith/Penman relation. In the model, water is allowed to drain down to deeper soil layers if the water content of the upper layer exceeds field capacity. Tritium enters the soil with precipitation and by dry deposition and is re-emitted to the atmosphere from soil and plants. Exchange between air and the soil/plant system is diffusion driven and modeled using the exchange velocity approach. Tritium movement within the soil is by advection with water and by diffusion along the tritium vapour pressure gradient. HTO concentrations in soil water are calculated at any time from the current water and tritium contents of the layer in question. Mean values over any time period are obtained as the average over all hours in that period. ZSR uses a similar model with two main differences: soil water contents are determined from a water balance approach rather than from Richards' equation; and the mean concentrations at 0900 and 1500 are averages at those times rather than averages over the intervals 1500–0900 and 0900–1500. Note that the soil concentrations predicted by the activity balance and empirical models are long term averages for the entire study period.

(B22) In addition to the semi-empirical model described above, the NIPNE participant also used a time-dependent model to calculate soil concentrations. This model assumes constant water content and uniform tritium concentration in the soil column, piston flow of tritiated rainwater and a simplified description of the dry deposition/re-emission process. The tritium inventory in the soil at time t was found from:

$$A_s(t) = A_s(t - \Delta t) + v_e\, f_r\, [C_{am} - C_s(t - \Delta t)] + D_w - P_d\, C_s\, (t - \Delta t) \qquad (4)$$

where:

A_s	is the total tritium activity in the soil column (Bq m^{-2}),
f_r	is the retention factor for dry deposition,
D_w	is the activity deposited daily through wet deposition (Bq m^{-2}), and
P_d	is the daily rainfall (m).

(B23) The soil concentration was then found by dividing A_s by the water content of the soil. The time step Δt was taken as one day and the tritium concentration in air moisture appearing in Equation (4) was the daily average. The values of v_e and f_r were set to 0.002 m s^{-1} (170 m d^{-1}) and 0.05 respectively.

(B24) Predicted and observed soil concentrations are shown in Figure B2 for ARS and Figure B3 for B600. The NIPNE results in these figures are from the semi-empirical model. Predictions from Equation (4) are a factor of 2 larger and do not agree as well with the observations. Most predictions exceed the observations at both sites. The variation among models is due to differences in model structure, in the predicted rainwater concentrations and in the values chosen for the parameters. For example, the exchange velocity used to describe the transfer of HTO from air to soil ranged from 0.002 m s^{-1} to 0.0041 m s^{-1} among participants. The confidence intervals on the predictions varied substantially from modeller to modeller but were generally quite large.

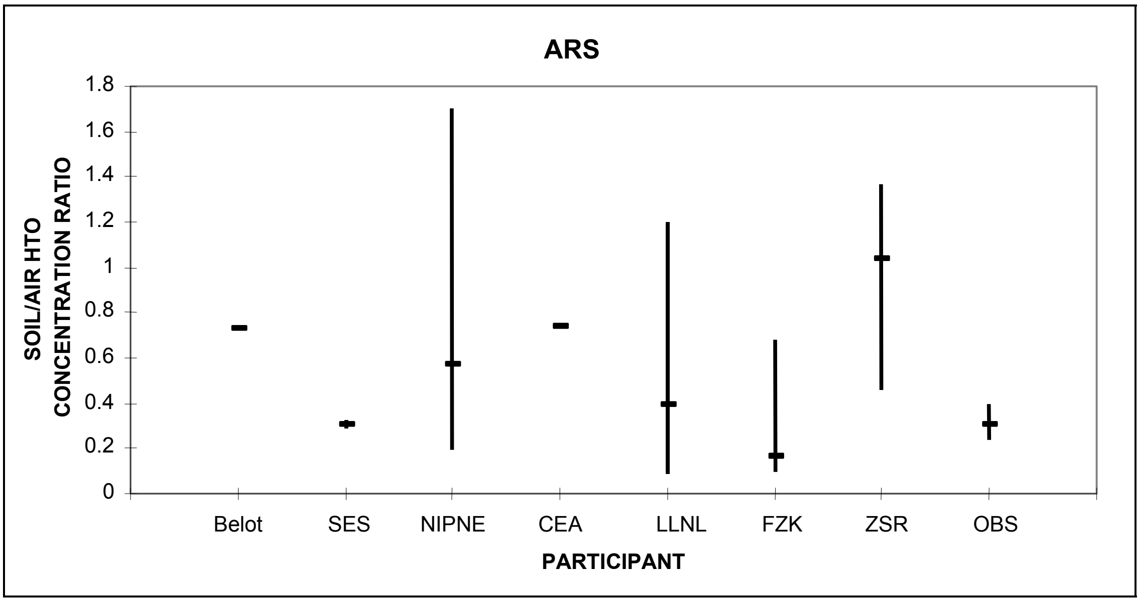

FIG. B2. Predicted and observed HTO concentrations in soil at ARS averaged over the entire study period. The soil concentration predicted by a given participant has been normalized by the air moisture concentration used to drive his/her model.

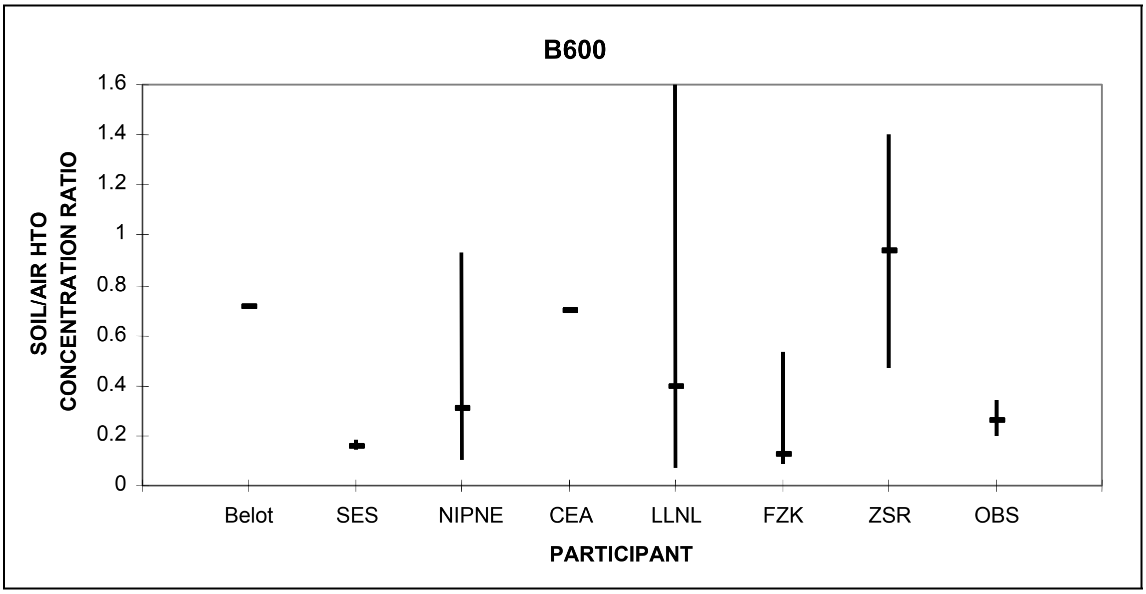

FIG. B3. Predicted and observed HTO concentrations in soil at B600 averaged over the entire study period. The soil concentration predicted by a given participant has been normalized by the air moisture concentration used to drive his/her model.

(B25) The predictions of the activity balance models of Belot and CEA lie a factor 2–3 above the observations. These models attribute about 75% of the soil tritium inventory to dry deposition, which appears to be too much. They underestimate the amount of tritium re-emitted from the soil to the atmosphere and so overestimate the soil concentration. In addition, the exchange velocities used in these models ($v_d = v_e = 0.003\ ms^{-1}$) may have been too high. The published empirical and theoretical values on which they are based were obtained under windy conditions and may not apply during the periods of low wind speed, stable conditions that occurred frequently during the study. Moreover, the exchange velocity decreases substantially as the soil dries out, as it did during the early part of the study. An exchange velocity of about 0.001 ms^{-1} would bring the predictions of the activity balance models into agreement with the observations.

(B26) The FZK model, which sets the soil concentration equal to the rain concentration, underpredicts at both sites, suggesting that dry deposition must be considered in estimating soil concentrations. The semi-empirical model of LLNL performs well, with predictions lying within about 50% of the observations at both sites. This model assumes that dry and wet deposition contribute about equally to the soil tritium inventory. The semi-empirical model of NIPNE overpredicts by a factor of 2 at ARS but is only slightly high at B600. The time-dependent model of SES performs well for ARS but underpredicts at B600 by almost a factor of 2. In contrast, the predictions of the ZSR model for the two sites lie a factor of 3 above the observed soil concentrations, and just slightly below the corresponding air concentrations. This is further evidence that the ZSR model underestimates the magnitude of re-emission.

(B27) The observed ratio of soil water to air moisture concentrations decreased from 0.31 at ARS to 0.26 at B600 to 0.22 at PL. Given the uncertainties in the measurements, it is not clear if these differences are real. But all participants with the exception of ZSR predicted a lower soil/air ratio at B600 than at ARS because of the lower amount of tritium that enters the soil through wet deposition at B600. The joint frequency of occurrence of wind direction and rainfall (the parameter Φ in Equation 1) is a factor 3 lower for B600 and PL than for ARS. This is more than enough to explain the spatial variation in the soil/air ratio if it is assumed that wet and dry deposition contribute equally to the soil concentration at ARS. The FZK model correctly predicts the magnitude of the observed decrease between ARS and B600 whereas the SES and NIPNE models predict a greater decrease than is observed. On the other hand, the activity balance models of Belot and CEA, in which wet deposition plays a relatively small role in determining soil concentrations, underestimate the decrease, as does the LLNL model. Spatial variability in the soil/air ratio may also arise from other causes that the models do not treat. For example, differences in soil properties at the three sites may result in differences in the rates at which tritium is transferred from air to soil through dry deposition, from soil and plants to air through evapotranspiration, or from surface soil to deeper layers through drainage.

B4.4. PLANT WATER CONCENTRATIONS

(B28) All of the participants except SES based their predictions of HTO concentrations in plant water (C_{pw}, Bq L^{-1}) on the following equation (Raney and Vaadia 1965; Murphy 1984):

$$C_{pw} = [RH\ C_{am} + (1 - RH)\ C_s] / \gamma \qquad (5)$$

where RH is the relative humidity. The parameter γ is the ratio of HTO vapour pressure to H_2O vapour pressure. It has a value of 0.91 but was set equal to 1 in the Belot, NIPNE and

ZSR models. Equation (5) can be modified to account for the effects of leaf-air temperature differences on tritium exchange but none of the modelers did this.

(B29) Most modelers calculated C_{am} in Equation (5) as the average over the relevant air sampling period (0900–1500, 1500–0900 or 0900–0900). In contrast, the participant from NIPNE based his afternoon value of C_{am} on the average of the air moisture concentrations predicted for the 3 hours prior to 1500. The morning value was assumed equal to:

$$C_{am} = [C_{am}(1500\text{–}0900) + C_{am}(0900)] / 2 \tag{6}$$

where $C_{am}(1500\text{–}0900)$ is the mean air moisture concentration predicted over the night time period and $C_{am}(0900)$ is the concentration at 0900. The 24-hour NIPNE prediction of C_{pw} was calculated as the average of the morning and afternoon values.

(B30) The ZSR model applied Equation (5) in a time-dependent manner, calculating the plant water concentration at a given hour from the predictions of Equation (5) for that hour and for the previous hour:

$$C_{pw} = \alpha\, C_{pw}(t - \Delta t) + (1 - \alpha)\, C_{pw}(t) \tag{7}$$

(B31) The weighting factor α was chosen to reflect the rate at which the plant concentration comes into equilibrium with the current air and soil concentrations. For daytime conditions (net radiation $R_N > 0$), when exchange between the plant and its surroundings is rapid, α was chosen to be 0.5. For $R_N < 0$, α was set to 0.94, implying much slower exchange.

(B32) In the SES model, tritium enters the plant in the transpiration stream and via diffusion from the atmosphere at a rate driven by the HTO gradient between air and plant. The tritium activity and water content of the plant for a given hour are calculated from the values in the previous hour taking into account any changes in activity or water content due to these processes. C_{pw} is then determined by dividing the activity by the water content.

(B33) The predictions of the various models for plant water concentration averaged over the entire study period are compared with the observations in Figures B4 and B5. All the models overestimate the observed value at ARS and all but two overestimate at B600. Most of the predictions cluster about 1 with relatively little scatter because Equation (5) predicts that plant concentrations are dominated by air concentrations. The predictions of the FZK model are within 10% of the observations at both sites. The good performance of this model is due to the fact it predicts relatively low soil concentrations. In this case, an underprediction in one part of the model appears to compensate for the tendency of another part of the model to overpredict. The uncertainties associated with the predictions of most of the models remain high.

(B34) If the observed values of the soil water and air moisture concentrations are used in Equation (5), the resulting C_{pw}/C_{am} ratio is 0.94 for ARS and 0.93 for B600. These values are both substantially larger than the observations, suggesting that Equation (5) itself is biased toward higher concentrations. There could be several reasons for this:

- as written, Equation (5) does not account for air-leaf temperature differences;
- Equation (5) assumes that all water is accessible to exchange when this may not be the case;

— Equation (5) is meant to apply to steady state conditions when in fact air concentrations fluctuate continually at a given site in response to variations in meteorological conditions; and

— the plants were very dry during part of the study period and tritium uptake and loss may have occurred differently than assumed by Eq (5).

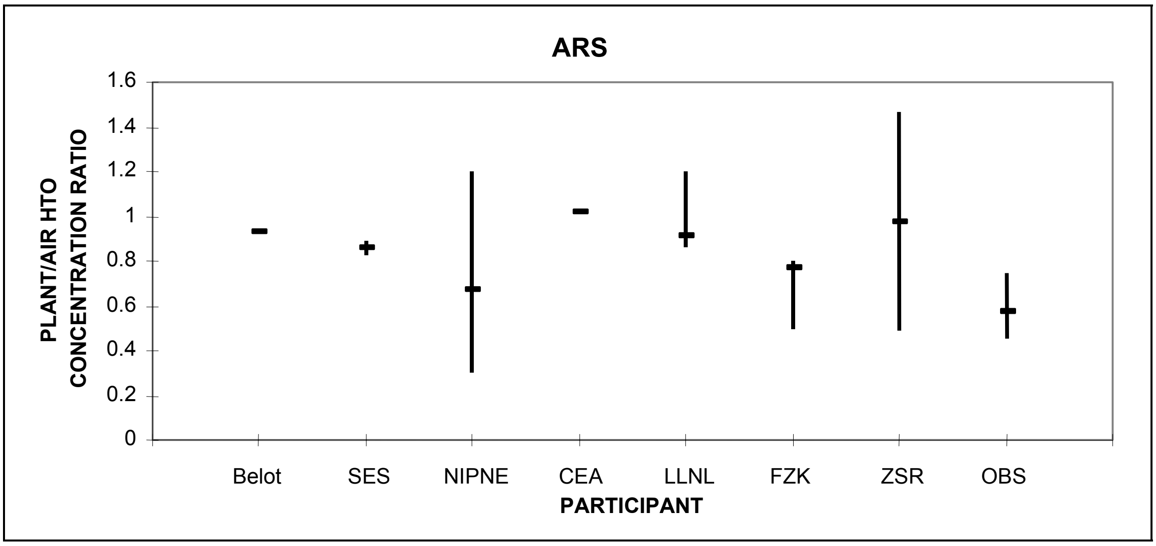

FIG. B4. Predicted and observed HTO concentrations in plant water at ARS averaged over the entire study period. The plant water concentration predicted by a given participant has been normalized by the air moisture concentration used to drive his/her model.

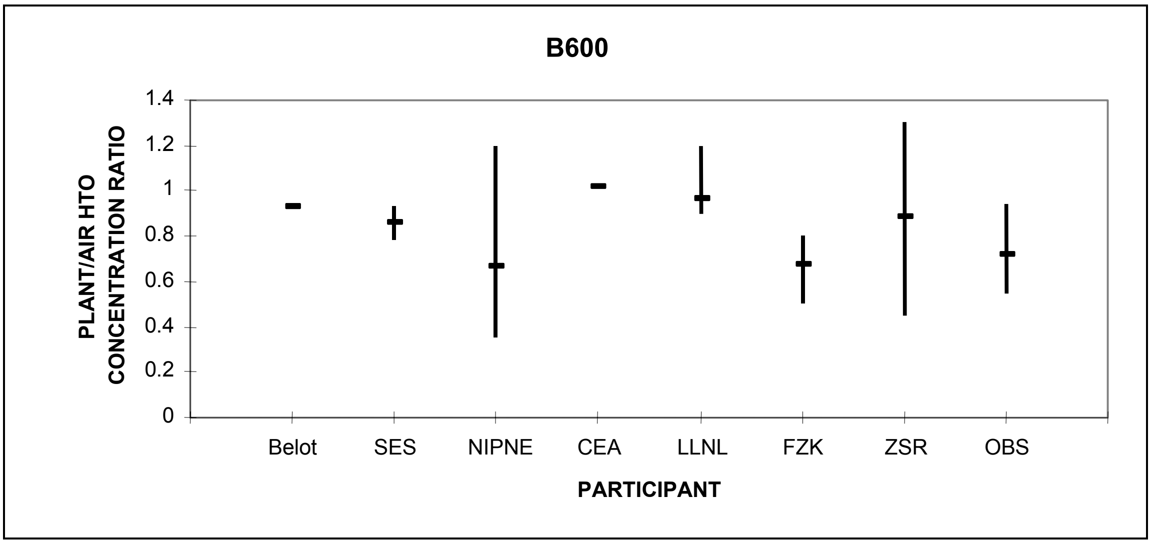

FIG. B5. Predicted and observed HTO concentrations in plant water at B600 averaged over the entire study period. The plant water concentration predicted by a given participant has been normalized by the air moisture concentration used to drive his/her model.

(B35) Alternatively, the parameter values used in Equation (5) may not be suitable. The averaging time for RH may be inappropriate, or the values, which were measured at PL, may not be representative of conditions at ARS and B600. Similarly, the air concentrations measured from 0900–1500 and from 1500–0900 may have been different than the concentrations in the 2 or 3 hours prior to the 0900 and 1500 samplings, the hours important in determining plant concentrations. In fact, the NIPNE model, which calculates plant water concentrations from the air concentrations immediately before the sampling times, predicts C_{pw} values that are lower than the other models and that agree well with the observations.

(B36) Equation (5) predicts that C_{pw}/C_{am} decreases as C_s/C_{am} decreases. Therefore, if RH is constant in space, C_{pw}/C_{am} should be higher at ARS than at B600 and this is what all the models predict. However, the observations show the opposite tendency, with $C_{pw}/C_{am} = 0.58$ at ARS and 0.72 at B600. A physical explanation for this behaviour is difficult to find, which suggests that the observed trend is not real. In fact, the difference between the observations at the two sites is much less than the associated uncertainties and the trend could just as easily be the other way around. The observed value of C_{pw}/C_{am} at PL was 0.66, which lies between the ARS and B600 observations.

(B37) At all three sites, the C_{pw}/C_{am} observations derived from the 0900 measurements were substantially higher than the 1500 values (Table B6). There are several reasons to expect a diurnal variation in C_{pw}/C_{am}, since many factors affect the rate at which tritium is exchanged between the plant and its environment. The exchange proceeds faster during the day than at night, when transpiration rates are low and stomata are closed. Nevertheless, plant leaves are able to take up tritium from the air at night and the absence of significant transpiration at this time means concentrations in the plant may increase. This may not have been a major factor in the present case because the morning measurements were made at 0900, when the sun had been up for several hours. The grass species at the sampling sites had low leaf area indices and high minimum stomatal resistances, which would have hindered exchange during the day. Similarly, the plants were under considerable water stress early in the study period and would have been relatively slow at reaching equilibrium with air and soil concentrations. Another factor affecting the morning/afternoon ratios would have been the different prevailing humidity conditions. The average RH at 0900 was 0.885 and the average at 1500 was 0.585. If these values are used in Equation (5) with the observed soil/air concentration ratios, the predictions for $(C_{pw}/C_{am})_{afternoon} / (C_{pw}/C_{am})_{morning}$ become 0.77 for ARS, 0.76 for B600 and 0.74 for PL. The B600 and PL results are similar to the observed values (Table B6), although the agreement at ARS is not as good.

TABLE B6. PREDICTED AND OBSERVED VALUES OF THE RATIO

$(C_{pw}/C_{am})_{afternoon} / (C_{pw}/C_{am})_{morning}$

Participant	ARS	B600	PL
SES	0.83	0.83	0.85
NIPNE	0.96	1.44	-
LLNL	0.84	0.82	0.93
FZK	1.26	1.45	-
ZSR	1.31	2.20	-
Observation	0.39	0.67	0.72

(B38) The participants modelled day/night effects in different ways. The LLNL approach was similar to that discussed above: Equation (5) was used with different values of RH for the different sampling intervals. The values used were those averaged over the 0900–1500 and 1500–0900 periods (0.65 and 0.85, respectively) rather than the values occurring at the sampling times themselves. The predicted difference between the morning and afternoon results is therefore not as great as in the calculations above or in the observations, but the trend to lower daytime values is present (Table B6). The only other model to predict $(C_{pw}/C_{am})_{afternoon}$ / $(C_{pw}/C_{am})_{morning}$ ratios less than one was SES. Here results are based on averages of hourly estimates of plant concentrations.

(B39) The remaining models all predicted afternoon/morning ratios greater than one. Results for the ZSR model are based on averages of the hourly values calculated with Equations (5) and (7). The weighting factor α is used to force a slower rate of exchange between the plant and its surroundings during the night than during the day. This appears to have the effect of freezing night time concentrations at relatively low values. The FZK model uses the same idea although applied in a different way. The morning C_{pw} values calculated from Equation (5) were reduced by factors of 0.38 and 0.34 for ARS and B600, in accordance with data obtained from a recent experiment at FZK in which winter wheat was exposed to atmospheric tritium. The reduction factors account for the observation that the plant is slower to reach equilibrium during the night than during the day. The FZK modeller speculates that the concentrations occurring at 1500, which are often low because the plume is seldom over the sampling site, are carried through the night, even when the plume is present at night. These arguments may be correct even though the ZSR and FZK models do not reproduce the observed afternoon/morning ratio. The models assume that the 0900 measurements reflect conditions over the entire 1500–0900 period. As noted above, they more likely reflect only the previous hour or two because at 0900 the plant stomata are probably open and exchange with the atmosphere is rapid.

B4.5. OBT CONCENTRATIONS

(B40) In the CEA and NIPNE models, the concentration of non-exchangeable OBT in plants (C_{OBT}, Bq L^{-1} water equivalent) was calculated from the equation

$$C_{OBT} = D_f \, [C_{pw}]_t \tag{8}$$

where D_f is an isotopic discrimination factor (taken to be 0.6) and $[C_{pw}]_t$ is the HTO concentration in plant water averaged up to the time of OBT sampling. The FZK model also followed Equation (8) except that the average air moisture concentration was used to approximate $[C_{pw}]_t$. The LLNL model was also similar to Equation (8) except that D_f was taken to be 0.8 and the averaging was done over the 30 days prior to sampling. In the SES model, OBT concentrations at time t were calculated from:

$$C_{OBT}(t) = 0.6 \, C_{pw}(t) \, t/T \tag{9}$$

where $C_{pw}(t)$ is the tritium concentration in plant water at time t (measured from the start of the study) and T is the duration of the study. In the ZSR model, the OBT concentration was calculated hourly from:

$$C_{OBT}(t) = \beta \, C_{OBT}(t - \Delta t) + (1 - \beta) \, C_{pw}(t) \tag{10}$$

where β = 0.993 and $C_{OBT}(t = 0) = 94$ Bq L^{-1}. This describes an organic compartment in which the OBT is metabolized slowly with a 100-hour half-life and newly-formed OBT has the same concentration as plant water. The ZSR model does not account for isotopic discrimination in OBT formation. Belot did not predict OBT concentrations and CEA supplied results only for the August 9 sampling date.

(B41) The observed values of $[C_{pw}]_t$ were fairly constant over time at ARS and decreased gradually at B600 (Table B1). OBT predictions from models based on Equation (8) (LLNL, NIPNE and FZK) followed the same pattern (Figures B6 and B7). So do the predictions of the SES model, which is based on a different theory. The ZSR model shows the same time-dependence as the other models at ARS but exhibits a peak in the middle of the study period at B600. Taken together, the models show a range of about a factor of 2 in the predicted OBT concentrations. The normalized predictions of the CEA model (not shown on Figures B6 and B7) for August 9 were 0.61 for both ARS and B600.

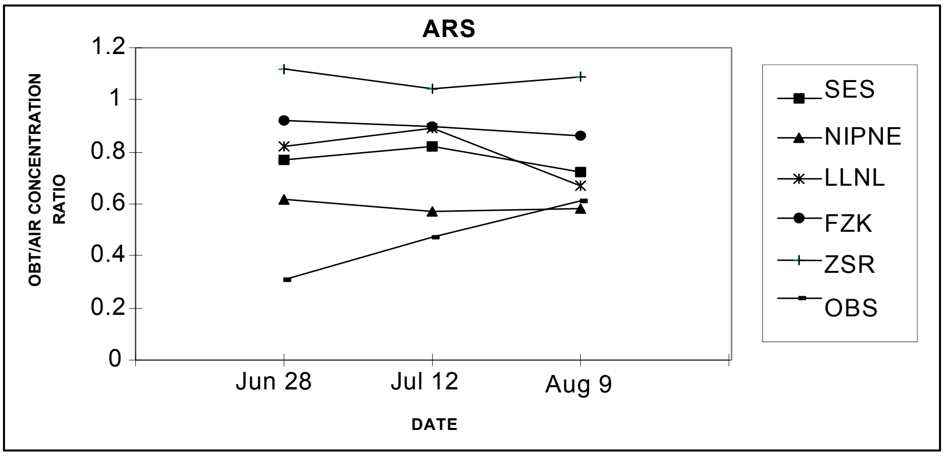

FIG. B6. Predicted and observed OBT concentrations at ARS at three times during the study period. The OBT concentration predicted by a given participant has been normalized by the average air moisture concentration used to drive his/her model.

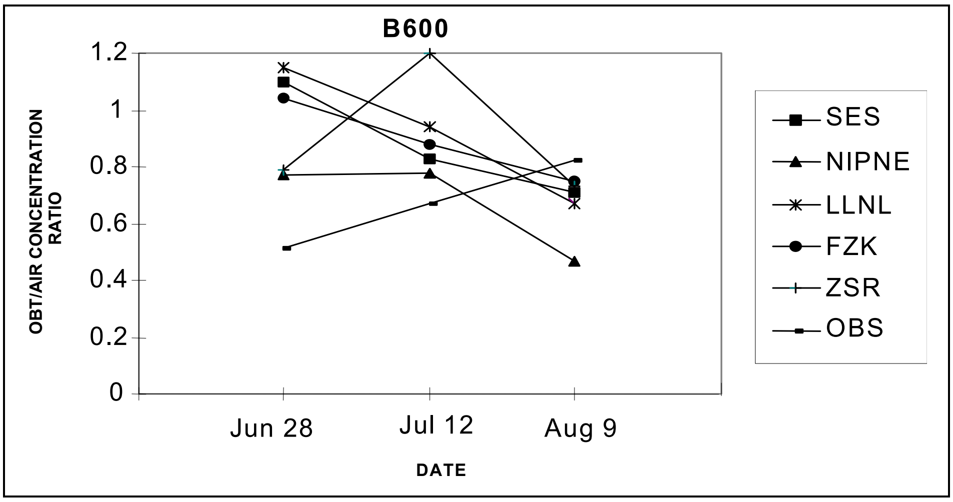

FIG. B7. Predicted and observed OBT concentrations at B600 at three times during the study period. The OBT concentration predicted by a given participant has been normalized by the average air moisture concentration used to drive his/her model.

(B42) The observed OBT concentrations increased steadily throughout the study period at all three sampling sites (Figures B6 and B7). This was unexpected since Equation (8) reflects the current theory of OBT formation and $[C_{pw}]_t$ remained constant or decreased during the study period. There are a number of possible explanations for the difference between theory and observation:

- the OBT measurements may have been subject to a systematic error larger than the 10% uncertainty assigned to them. In fact, OBT concentrations measured in grass throughout the 1999 growing season at B600 followed the time-integrated HTO concentrations in water very closely, suggesting that the 1995 data are in error;
- OBT concentrations may not follow Equation (8) if the plants were directly exposed to tritiated organic compounds such as tritiated volatile carboxylic acids. However, there is no information on whether such compounds were released at CRL in the latter part of the study period;
- the conceptual model of OBT formation may need to be rethought for sites that are subject to a fluctuating airborne plume.

(B43) Because the data do not support Equation (8), they cannot be used to address issues such as the value of the discrimination factor D_f, or whether $[C_{pw}]_t$ should be averaged over the full day or over daylight hours only.

B4.6. SOIL AND PLANT HTO CONCENTRATIONS AT SPECIFIC TIMES

(B44) The specific times at which HTO concentrations were requested were times when the wind blew steadily toward or away from ARS over the preceding air sampling period. The expectation was that the grass concentrations would be in equilibrium with the air concentrations at these times and that the models would return reasonable predictions even though they are designed to estimate long term average concentrations rather than short term ones. But equilibrium does not seem to have occurred. In the absence of the airborne plume, the soil concentration should have been higher than the grass concentration, which is turn should have been higher than air. But of the four instances when the wind blew away from ARS, the HTO concentration in air always exceeded that in grass and soil and in half the instances the grass concentration was higher than the soil concentration (Table B2). The air concentration always exceeded the grass concentration when the wind blew toward ARS, as expected, but grass was significantly higher than soil in only one case out of three. Moreover, the grass/air ratio was essentially the same whether the plume was present over the site or not. The explanation for these observations may lie in the fact that the air concentration was known only as an average over the 6 or 18 hours before the grass and soil samples were taken, when in reality the plant concentration reflects the air concentration in the hour or two immediately preceding sampling. Although the attempt was made to choose times for these calculations when the meteorological conditions were steady, the 6- and 18-hour averages may have differed substantially from the shorter period averages.

(B45) Five of the seven participants (SES, NIPNE, LLNL, FZK and ZSR) submitted predictions for these endpoints. For the time-dependent codes of SES and ZSR, concentrations at specific times are part of the normal model output. For these calculations, the ZSR code was driven by the average of predicted and observed air concentrations. The FZK results assumed very simply that the grass concentrations equalled the observed air concentrations in the period before the sample was taken, without considering the role of the soil. In the LLNL model, soil concentrations were determined from the long term average rainfall concentration plus a dry deposition term calculated from the air concentration averaged over the 3-hour period preceding the time of sampling. Grass concentrations were then calculated from Equation (5) using a combination of predicted and observed air concentrations. In the NIPNE model, soil concentrations were calculated from a consideration of wet and dry deposition and dilution with clean rain in the hours prior to sampling. Grass concentrations were then calculated from Equations (5) and (6).

(B46) None of the models, with the exception of ZSR, performed well in predicting the soil and grass concentrations at specific times. The models tended to overestimate the observations, and the correlation between predictions and observations was poor, with correlation coefficients (r) based on linear regression varying between -0.04 and 0.4 for grass. In contrast, the ZSR predictions (Table B7), although also tending to overpredict, showed a strong correlation with r = 0.92 for grass. The success of this model for these endpoints is likely due to its ability to resolve the hourly time scale on which plants respond to changes in air concentrations, to the fact that it considers re-emission and to the fact that the air concentrations it uses are based in part on measured values.

TABLE B7. GRASS CONCENTRATIONS PREDICTED BY THE ZSR MODEL AT SPECIFIC TIMES AND THE CORRESPONDING OBSERVATIONS

Time and Date		Air Concentration (Bq L^{-1})		Grass Concentration (Bq L^{-1})	
		Predicted	Observed	Predicted	Observed
0900	Jun 8	85	149	106	66
	Jun 29	268	171	223	91
	Jul 12	66	124	90	64
1500	Jun 15	87	172	205	84
	Jun 28	215	251	266	107
	Jul 5	261	420	312	97
	Jul 19	61	120	95	47

Note: The observed air concentrations and the concentrations used to drive the model are also shown.

B5. CONCLUSIONS

(B47) Scenario 3 was fairly simple and air concentrations, which drive the models for an atmospheric release, were given. The scenario addressed the type of calculations that must be performed by most tritium-handling facilities. Traditional models are available for these calculations and variations of them were used by most participants. But despite the simplicity of the scenario and the similarity of approaches, predictions for a given endpoint typically varied over a factor of 2 or 3 among the models. This was due both to the way in which the models were applied and to the different values of the parameters used in them. Confidence intervals on the predictions varied from model to model but were generally large. Because of the different ways in which these uncertainties were obtained, it is hard to compare one with another or to know which is most realistic. Differences between predictions and observations were also commonly about a factor of 2 to 3. None of the models performed consistently better than the others, although the equilibrium models as a group did better than the time-dependent models. This is not unexpected since the equilibrium models are designed for the types of endpoints requested in this scenario. The time-dependent models provided valuable insights into the processes responsible for tritium transport through the system.

(B48) With two exceptions, the predicted air concentrations agreed with the observations to within 25%, a very acceptable result. The predictions for the HTO concentration in rainwater all substantially underestimated the observed concentration, although in this case there is reason to question the observation. The predictions for soil generally overestimated the observed values but were able to reproduce the main features of the spatial variability, which is driven by differences in the joint frequency of wind direction and rainfall occurrence. The results indicate that a substantial part of the permanent tritium inventory in soil arises from dry deposition, although more work is needed to quantify this. The dynamic soil models require thin layers near the surface to simulate re-emission realistically. The predictions for HTO concentration in plant water were systematically high, suggesting that Equation (5) or the parameter values input to it may be biased. The models were not generally able to reproduce the strong diurnal variation observed in the grass/air ratio, although this variation may be due simply to differences in morning and afternoon relative humidities. None of the models was able to simulate the observed increase in plant OBT concentration with time. This increase was unexpected on theoretical grounds and may not be real. Replicate measurements made in the summer of 1999 indicate that OBT concentrations are proportional to the HTO concentration in plant water integrated up to the time of sampling. Since this is the theory on which the models are based, the predictions for Scenario 3 may be reasonable despite their disagreement with the observations. The models were unable to predict concentrations in grass and soil at specific times, but these types of predictions are beyond expectations for the long term average models used here. The specific activity concepts on which the models are based do not apply to short averaging times or short term releases.

(B49) Another reason for the differences between predictions and observations may lie in a mismatch between the assumptions of the models and the realities of the data. Most of the models assume equilibrium conditions when in fact the air concentrations over the sampling sites fluctuated continually in response to changing atmospheric conditions. Moreover, the observed long term average concentrations for soil and grass were calculated from samples taken once or twice per day on selected days during part of the growing season. These averages may not reflect true mean values, which are what the models are designed to predict. Finally, several of the participants modelled the morning endpoints using parameter values and assumptions representative of night time conditions when in fact plants are likely to be almost fully active at 0900 in midsummer.

(B50) This discussion has pointed out some of the deficiencies in the models that are used to calculate long term average tritium concentrations in the environment due to chronic atmospheric releases and has opened the way for improvements to them. It has also identified the need for additional experimental data to verify the possibility of high rain/air ratios and increases in OBT concentration with time. Moreover, the findings can be used to help design environmental monitoring programs for tritium to ensure representative results.

(B51) The observations on which Scenario 3 are based provide useful parameter values for assessing environmental concentrations at a site subject to a chronic fluctuating airborne plume. At CRL, the long term average soil concentration is typically one-fifth to one-third the average air moisture concentration. This ratio will depend on soil properties and on the joint frequency of wind direction and rainfall occurrence and may be quite different at other sites (see Part G). The long term plant water/air moisture concentration ratio lies between 0.50 and 0.85. This ratio was obtained for grass and likely applies to the foliar parts of other plant types but may be different for fruit or root crops. It probably shows less variability from site to site than the soil/air ratio because plant concentrations are driven primarily by air concentrations.

The plant water/air ratio is a key parameter in several regulatory models (CSA 1987, USNRC 1977) and in this regard is the most important endpoint of the scenario. The models predict this ratio reasonably well, tending to overestimate it and so erring on the side of conservatism. The uncertainties associated with the predictions are large but are immaterial in the sense that the ratio has a maximum value of 1.1 when the plant water is in specific activity equilibrium with air moisture. The uncertainties in the experimental data and in the model predictions can be avoided by setting the plant water/air ratio equal to this maximum value, ensuring that concentrations will not be underestimated without being overly conservative.

REFERENCES TO PART B

[1] CANADIAN STANDARDS ASSOCIATION, Guidelines for Calculating Derived Release Limits for Radioactive Material in Airborne and Liquid Effluents for Normal Operation of Nuclear Facilities, CSA Guide CAN/CSA-N288.1-M87 (1987).

[2] MURPHY, C.E., Jr., The Relationship Between Tritiated Water Activities in Air, Vegetation and Soil Under Steady state Conditions, Health Physics **47** (1984) 635–639.

[3] RANEY, R., VAADIA, Y., Movement and Distribution of THO in Tissue Water and Vapor Transpired by Shoots of Helianthus and Nicotiana, Plant Physiology **40** (1965) 383–388.

[4] U.S. NUCLEAR REGULATORY COMMISSION, Calculation of Annual Doses to Man from Routine Releases of Reactor Effluents for the Purpose of Evaluating Compliance with 10 CFR, Part 50, Appendix 1 (Revision 1), U.S. NRC Regulatory Guide 1,109 (1977).

PART C

MODELLING THE ENVIRONMENTAL TRANSPORT OF TRITIUM IN THE VICINITY OF PERMANENT ATMOSPHERIC SOURCES:

A test of chronic atmospheric release models using Russian data

C1. BACKGROUND AND OBJECTIVES

(C1) Part C presents the results of a model-data type test exercise based on field sampling data collated by RFNC-VNIIEF (Russia) following long term tritium releases at the site. Two other model-data test exercises that were developed by the TWG based on Canadian and French data are reported in Part B and D respectively.

(C2) The goal of the fourth scenario described here is to test, and hence improve, models that are used to predict tritium concentrations in environmental media as a consequence of long term atmospheric releases and to investigate whether tritium is retained in various biosphere media as a consequence of the releases. The environmental processes involved and the environmental compartments represented in the participating models are similar to those studied in the first scenario (Part A). However, the main difference between Scenario 1 and Scenario 4 is that the latter is based on experimental data. Scenario 4 is also unique in that it investigates the consequences of significant decreases in the chronic tritium releases over the 20 years of observation.

(C3) The feasibility of a model test exercise based on data collated by RFNC-VNIIEF was discussed at the BIOMASS TWG meeting in October 1997 in Vienna, Austria, when an outline draft of the scenario was presented. At the meeting, modellers requested that meteorological information should be provided to complement the scenario description. Consequently, such information was extracted from the RFNC-VNIIEF records and presented at the BIOMASS TWG Meeting in May 1998 in Deep River, Canada. Scenario 4.0, supplemented by additional meteorological information was presented at the BIOMASS Tritium Working Group Meeting in October 1998 in Vienna and was distributed to the participants after that meeting. Initial modelling results were presented at the BIOMASS TWG Spring Meeting in May 1999 in Sarov, Russia. However, modellers asked for additional information to clarify certain aspects of the scenario description and they also requested data on atmospheric absolute humidity. Version 4.1 of the Scenario was then distributed for calculation in July 1999. Comparison of modelling results with the actual experimental data was first presented at the TWG Meeting in October 1999 in Vienna, Austria. Additional material was then provided following discussions at the meeting and Version 4.2 was distributed for final calculation. Draft versions of the report were prepared for discussion at the BIOMASS TWG Spring and Plenary 2000 meetings, and at a subsequent consultants' meeting in January 2001. It is the results of the latest version of the scenario calculations and associated documentation that are reported here.

C2. SCENARIO DESCRIPTION

(C4) Scenario 4.2 was developed on the basis of environmental sampling data collected in the vicinity of long term tritium emission sources at RFNC-VNIIEF. The full scenario description is provided in Annex II–C. The distinctive feature of the Scenario is that during 20 years of observations the tritium release strength decreased by more than two orders of magnitude. The dynamics of the annual releases are presented in Table II–C.5 of the scenario description (see Annex II–C). Such a reduction of the emission source provides an opportunity to study processes involved in both tritium transport and retention in the environment and the effects of past releases on current concentrations in the biosphere. Similar situations may occur following the closure of any tritium facility or nuclear reactor, and in such cases a very important issue is to know how quickly the tritium levels in the environment around the emission source will reduce to background levels.

(C5) The specific objectives of this scenario were therefore to:

- validate models used to predict tritium concentrations in environmental media following long term releases;
- investigate whether process of tritium retention occur in the biosphere; and
- evaluate the effect of past releases on current levels of contamination.

(C6) The area around the emission source has a relatively simple relief with no observable slope; there is an average variation of elevation of ±20m. This means that the topography does not affect the dispersion of the primary plume. The area to the South of the emission source is wooded with trees about 25m high; to the North of the emission source is a city. The specific features of relief and climate (including the wind rose, well-defined seasons, long snow cover period), infiltration processes and groundwater characteristics may affect tritium retention in soil, vegetation and ground water. These environmental compartments may also be sources of secondary contamination of the atmosphere.

(C7) In the first version of the Scenario, seven sampling points (SPs) were considered (see Figure II–C.2, Annex II–C). In the final version of the Scenario, Sampling Point 1 was excluded because it is in the same direction as Sampling Point 2 and the distance between the two locations is only 1 km. More experimental data were available for Sampling Points 2, 4 and 6 so modelling calculations concentrated on these SPs. Two SPs are in the city area (SP2 and 6) whilst SP4 is located in the forest area (for information about the sampling locations see in Table II–C.6 of Annex II–C).

(C8) Modellers were asked to calculate tritium concentrations at Sampling Points 2, 4 and 6 in a number of different environmental media based on either average or yearly averaged meteorological data. The term “average” means that the data for *5 years* of observations that had been provided to the modellers were used to obtain the required weather statistics, whilst the term “yearly averaged” means that only data for *1 specific year* were used.

The requested endpoints for each of years 5, 10, 15 and 20 after the beginning of the release **using average meteorological data** were:

- average annual tritium concentrations (Bq/l) of HTO in atmospheric humidity;
- tritium concentrations (Bq/l) in plant tissue free water (TFW) on 15 September; and
- tritium concentrations (Bq/l) in soil water on 15 September and snow water on 31 March.

(C9) Additional endpoints were originally requested in the Scenario description but as not all of the modellers submitted results, these results are not discussed here.

C3. MONITORING TECHNIQUES

(C10) The sampling and analysis techniques used to obtain the experimental data are described briefly below and more fully in the cited references.

C3.1. TRITIUM ON-SITE SAMPLING AND ANALYSIS

Tritium monitoring in environmental media included:

- HT and HTO monitoring in the atmosphere – every 2 weeks;
- HTO monitoring of vegetation and soil – once a year at the end of the vegetation period;
- HTO monitoring of in snow cover – once a year at the end of snow cover period.

C3.2. SAMPLING TECHNIQUE

(Belovodsky et al., 1985)

- Air sampling was carried out by active and passive samplers containing a synthetic zeolite NaA both with a catalyst of HT oxidation and without a catalyst. HTO is adsorbed only by an active sampler. HT and HTO are adsorbed by a passive (diffusion type) sampler. The HT concentration was determined as the difference between the HTO content in water extracted from passive and active samplers.
- Water samples (precipitation, surface water, drinking water) were collected in glass vials.
- Snow samples were collected in plastic bags by an “envelop” method at a flat, open plot of 10 × 10 m^2 size without bushes and trees. Snow samples were taken as far as the underlying surface using precautions in order to exclude sampling the surface soil. The volume of melted water was ~3 litres.
- Soil samples were collected in plastic bags using a "triangle" method with sides of ~ 5 m and a depth of 1 cm from an area 10 × 10 m^2. The water content of the soil was 2–25%.
- Vegetation was sampled from the same triangle as the soil sample and packed in plastic bags. The amount of fresh vegetation taken as a sample was 1 kg. Vegetation with shallow roots (<20 cm) was used for sampling. The water content in grass vegetation was 10–15 %. Soil and vegetation sampling was performed at the same time.

C3.3. SAMPLE PROCESSING

Water was extracted from the zeolytes, vegetation and soil samples by a thermal vacuum desorption technique (Belovodsky et al., 1997). Samples of drinking water were analysed without treatment. Samples of snow and water were filtered or distilled before analysis.

C3.4. MEASURING TRITIUM CONTENT

(Vedeneev et al., 1997)

Measurement of HT activity in stack gases was carried out by an on-line ionization chamber; HTO content was measured with an active sampler. Measurement of tritium activity in the water extracted from the environmental media was obtained by liquid scintillation counting. The overall standard deviation of HTO measured values in atmospheric humidity was 100–200% due to a number of factors including: counting errors; variation in atmospheric humidity with the seasons; and variations of HTO concentrations per volume of air. The standard deviation of HTO measured values due to counting errors in snow, soil and vegetation samples was estimated to be 10–100%.

C3.5. METEOROLOGY

Meteorological data presented in the scenario description were measured in the following way. Wind speed and wind direction were both measured by meteorological equipment installed at a reference height of 10 m on the roof of a building near the stack. Air temperature and air humidity were measured at a reference height of 1.5 m by sensors installed in a shelter. All signals were recorded manually once per hour. Shielding effects of buildings and trees cause systematic error in wind speed measurements. For this reason, measured values were corrected using meteorological data from a nearby station provided by the Russian meteorological service. The meteorological data given in the Scenario description were not in the standard format normally used in models. Some of the data for wind direction were given as a sector, in some cases the given wind direction is for calm conditions. Information was only provided on whether a rain event had occurred or not; data on actual precipitation amount were not provided. Consequently, modellers had to process the data to obtain the meteorological statistics required by the models. This processing is probably a source of some of the uncertainty in model predictions for atmospheric concentrations. The consequences of processing the meteorological data are discussed in Section C5.1.

C4. MODELS AND PARTICPANTS

(C11) Six organisations submitted results for Scenario 4 (see Table C1).

(C12) Models used in this model-data comparison study were generally similar to those used for the atmospheric part of Scenario 1. A summary of the general characteristics of each of the models is given in Annex I–A. A list of parameters and associated parameter values used in the models is provided in Table C2. A number of different conceptual models were used. For example, the LLNL modeller took into account the non-continuous nature of the release source (i.e. releases only occurred during working hours on Monday to Friday, see description of release source in Annex II–C, Section II–C.4). Some modellers included a representation of tritium retention processes (ZSR, RFNC-VNIIEF).

TABLE C1. MODELS AND PARTICIPANTS

Participant	Organization	Model	Designation used in the text
D. Galeriu	NIPNE, Romania	DISPT	NIPNE
G. Guinois, E. Pili	CEA/DIF/DASE, France	TRIMASS2	CEA
A. Golubev	RFNC-VNIIEF, Russia	TRIEF	VNIIEF
S-R. Peterson	LLNL, USA	DCART	LLNL
W. Raskob	FZK, Germany	NORMTRI	FZK
M. Taschner, C. Bunnenberg	ZSR, Germany	ZSR Model	ZSR

C5. COMPARISON OF PREDICTIONS AND OBSERVATIONS

(C13) Modelling results and observed data for HTO content in atmospheric humidity, soil moisture, tissue free water, and snow water at each SP and for each requested year after the beginning of the release are presented as normalised values in the report. Normalised values (s/l) were determined by the relationship of HTO concentration (Bq/l) to release rate (Bq/s): C_{HTO}/Q_{HTO}. Such a representation of the data was chosen because the data on actual release rates were not provided in the scenario description and information was presented only in relative units (see Annex II–C). Participants used the Scenario information to calculate their own virtual release rates for the purpose of subsequent calculations (see Table C3).

(C14) Release rate values used in VNIIEF calculations are mean values calculated from the previous five years of release; release rates in parenthesis were used to produce normalized values of HTO concentration. The LLNL participant took into account the operational cycle of the release source by using higher release rates (values in parenthesis) for the daytime operation hours on working days. Mean values of yearly release rates used by the LLNL participant are also given in Table C3.

(C15) Normalized values make it possible to compare modelling results and experimental data irrespective of the release rate units used. The above mentioned ratio is proportional to the meteorological dilution coefficient. One of the objectives of Scenario 4 is to determine whether or not tritium retention occurs in the environment as a consequence of long term atmospheric releases. This ratio is very useful for such a determination. Stability of the ratio indicates that tritium retention in the environment does not occur. An increase in the ratio indicates additional sources of tritium release, whilst a decrease in the ratio demonstrates that accelerated removal of tritium from the environment occurs.

(C16) The ratio of HTO concentration in TFW, soil and snow water to HTO concentration in atmospheric humidity is used for comparison of the predicted and observed data. However, it should be borne in mind that requested HTO concentrations in atmospheric humidity are for average HTO concentrations over the year, while HTO concentrations in TFW, soil and snow water are concentrations for the specific dates requested. Therefore the ratio of HTO concentration in TFW (soil and snow water) to HTO concentration in atmospheric humidity is used here only as a tool for comparing modelling results with observations and should not be interpreted in any other way.

(C17) As noted in Section C3, experimental error is 10–100% depending on the measured value of HTO concentration. A measurement error of 100%, at a confidence level of 0.95, is found when the HTO concentration is measured at minimum detectable activity (MDA) level. A measurement error of 10% occurred when HTO concentrations are measured at the levels >10 × MDA.

TABLE C2. LIST OF MODEL PARAMETERS AND ASSOCIATED VALUES

Parameter	DCART	NORMTRI	TRIMASS	DISPT Model	ZSR Model	TRIEF
Atmospheric Dispersion	Canadian standard, “Hotspot”, HOSKER parameters	Gaussian type, Mol parameters	Gaussian type, BRIGGS parameters	Gaussian type, Mol parameters	Gaussian type, BRIGGS parameters	Gaussian type, BRIGGS parameters
HTO Wash-out coefficient	8.51 10^{-5}s^{-1}	6 10^{-5}s^{-1}	6 10^{-5} s^{-1}	6.5 10^{-5}s^{-1}	6 10^{-5} s^{-1}	1 10^{-5} s^{-1}
HTO Snow-out coefficient	2.41 10^{-5}s^{-1}	No snow-out	1.46 10^{-5} s^{-1}	1.46 10^{-5} s^{-1}	1.46 10^{-5} s^{-1}	1.46 10^{-5} s^{-1}
HT dry deposition on soil	2.68 10^{-4} m s^{-1}	3 10^{-4}m s^{-1}	3 10^{-4}m s^{-1}		3 10^{-4} s^{-1}	3 10^{-4} m s^{-1}
HTO dry deposition on soil	4.44 10^{-3}m s^{-1}	3 10^{-3}m s^{-1}	3 10^{-3} m s^{-1}	–	3 10^{-3} m s^{-1}	1.7 10^{-3} m s^{-1}
HTO dry deposition on snow	2.3 10^{-3} m s^{-1}	–	1.6 10^{-3} m s^{-1}	1.6 10^{-3} m s^{-1}	1.6 10^{-3} m s^{-1}	Equilibrium by Henry law
HT dry deposition on snow	2 10^{-6} m s^{-1}	–	No	No	No	No
Amount of precipitation winter/summer	242/303 mm	Variable year to year	160/560 mm	170/390 mm	160/400 mm	160/400 mm
Humidity winter/summer	4/13 g m^{-3}	5/15 g m^{-3}	3/15 g m^{-3}	3.7/12.3 g m^{-3}	2.97/10.35 g m^{-3}	3/11 g m^{-3}
‘Memory’ to past releases	No	No	No	No	Yes, by adding “old” soil water	Yes, by averaging strength of source
Infiltration	–	–	–	–	100 mm	–

TABLE C3. VIRTUAL RELEASE RATES USED BY MODELLERS

Participant	Release Rate a 5^{th} year, Bq/s	Release Rate at 10^{th} year, Bq/s	Release Rate at 15^{th} year, Bq/s	Release Rate a 20^{th} year, Bq/s
NIPNE	120	12	4	1
CEA	$3.8\ 10^{6}$	$1.58\ 10^{5}$	$1.27\ 10^{5}$	$3.17\ 10^{4}$
VNIIEF	72	33	2	1
	(120)	(12)	(4)	(1)
LLNL	$3.8\ 10^{6}$	$1.58\ 10^{5}$	$1.27\ 10^{5}$	$3.17\ 10^{4}$
	($9.12\ 10^{6}$)	($3.8\ 10^{5}$)	($3.04\ 10^{5}$)	($7.6\ 10^{4}$)
FZK	$1.4\ 10^{9}$	$5.86\ 10^{7}$	$4.69\ 10^{7}$	$1.17\ 10^{7}$
ZSR	120	12	4	1

C5.1. ATMOSPHERIC HUMIDITY

(C18) Normalised values of predicted and observed data for atmospheric moisture are presented in Figures C1 to C4 for Sampling Points 2, 4 and 6. Figure C1 presents normalised values of the observed data for HTO concentration in atmospheric humidity for Sampling Points 2, 4, and 6 for the selected time periods after the start of the release. HTO concentrations in atmospheric humidity are the initial values used for subsequent calculations of HTO concentrations in other environmental media. It can be seen from Figures C2 to C4 that most of the modellers did not take into account tritium retention in the biosphere. In these cases the factor C_{HTO}/Q was taken to be constant. Tritium retention was taken into account only in two models (ZSR and RFNC-VNIIEF). The ZSR modeller assumed the tritium retention was due to “old” soil water contaminated by washout and snow-out processes in previous years when the release rates were higher. The RFNC-VNIIEF model took into account tritium retention by correcting the real release rate by averaging it over the previous 5 years of release (see Table C3).

(C19) It can be seen from Figure C1 that the observed value of C_{HTO}/Q is not constant with time. For instance, at Sampling Point 2, the ratio varies and slightly increases with time. The equation of the linear trend in semi-logarithmic scale is:

$$\ln R = 4\ 10^{-6} * t + 2\ 10^{-5} \qquad (1)$$

where $R = C_{HTO}/Q$; and t is time after start of release in years.

(C20) At Sampling Point 6, the ratio shows more variation but also increases with time. The variation at this Sampling Point at the 9th and 16th years after the start of the release is due to spike releases at specific dates. The equation of the linear trend in semi-logarithmic scale is:

$$\ln R = 9\ 10^{-7} * t + 4\ 10^{-5} \qquad (2)$$

(C21) At SP4 the ratio has a negative trend. This is due to an additional, separate but irregular source of emission near the SP. Unfortunately it is not possible to provide a more definite analysis for this SP because of the lack of observational data. If the R value is ~$4\ 10^{-5}$ at SP2 and ~$1\ 10^{-5}$ at SP6 for the first years of release, this gives an increase of the relative HTO concentration of roughly 10% per year due to retention of tritium compared with the HTO concentrations in atmospheric moisture due to the primary source.

(C22) It can be seen from Figures C2 to C4 that modelling results for SP2 and 6 are in reasonable agreement with the observed data. Predicted and observed values of HTO concentrations in the atmospheric humidity due to atmospheric dispersion of primary plume at SP 2 and 6 are within factor of 4. Most of the predicted values are within the experimental uncertainty, which is 100%. It can be seen from the results obtained by one model (RFNC-VNIIEF), that accounting for tritium retention by averaging the previous 5 years of releases gives an over-prediction compared to the experimental trend. However, it can be seen from the observations that tritium retention should be taken into account if the release strength decreases by more than order of magnitude.

(C23) Modelling results for SP4 are not in such good agreement when compared with the observed data. The discrepancy is greater than an order of magnitude. Models gave values of HTO concentration at SP4 that are an order of magnitude less than at SP 2 and 6. Observed values for these three sampling points are much closer to each other – normalised values are $\sim 10^{-4}$. Taking into account the fact that SP4 is further from the source than the others and is in the sector with low frequency of winds blowing from the source, the models apparently make reasonable predictions of HTO concentrations at this sampling point. This suggests that at this SP there may be either additional sources of release or secondary contamination of the atmosphere from contaminated soil water. These hypotheses were studied after examining the model results. It was discovered that there is a low intensity aboveground source of emission near SP4, which impacts on HTO concentrations at this SP but not at the other two SPs. In addition, increased concentrations of HTO in soil water were found at various depths below the surface near SP4. These two reasons explain the difference between model predictions and observations.

(C24) Most of the participants used long term average Gaussian type models (see Annex I–A for full model descriptions). Five modellers, CEA, FZK, LLNL, VNIIEF and ZSR, used the sector-average approach, one other modeller, NIPNE, used the straight line approach. The LLNL participant used the Canadian standard 288.1 Gaussian model and HOTSPOT Gaussian puff model for calculating time dependent concentrations on specific dates. The participants used different dispersion parameters (see Table C2) and roughness height. The release was considered to be a point source; plume rise and building wake effects were not taken into account. The effective height of the source was 30 m; wind speed was extrapolated at this height using the power function relationship.

(C25) The participants processed the meteorological information presented in the Scenario description in a different ways. The ZSR participant reduced the meteorological data (27277 records) to frequencies. Two seasons were identified with different kinds of precipitation: Snow (Nov–Mar) and Rain (Apr–Oct). Sector width was 30 degrees. The FZK participant produced four sets of weather statistics using data for four years (1985–1988). Only one set of weather statistics (1985) was used to predict concentrations in snow water. The LLNL participant used the windrose given in Table II–C.2 of the Scenario description and produced weather frequencies using daytime meteorological data. The NIPNE participant used 27295 records for summer and winter statistics for the operation (week day, daylight hours); separate statistics were produced to obtain humidity and precipitation intensity for winter and summer time. Plume rise was tentatively included in the atmospheric part. The VNIIEF modeller produced separate weather frequencies, atmospheric humidity and precipitation information by using separately the meteorological data for winter and summer time.

C5.2. TFWT CONCENTRATION

(C26) Normalized values of tissue free water tritium (TFWT) concentrations are presented in Figures C5 to C7. Observations are available only for 15th–20th years after the beginning of the release. The amount of data does not allow a definite conclusion to be made about the retention of HTO in TFW since the variation of experimental data over time is not significant. Comparison of experimental data and model predictions shows that there is a reasonable agreement at SP2 and 6, but again there is a discrepancy between observations and predictions at SP4, which is explained by the additional source of emission (see above). Taking into account that TFWT concentration is determined largely by HTO concentration in atmospheric humidity it is important to consider the relationship between the two. As mentioned above, this relationship is not a ratio in a usual sense. The main difference is that TFWT concentration is determined at specific dates (15th of September) while HTO concentration in atmospheric humidity is determined as an average over the whole year. Table C4 gives the values of the ratio of HTO concentration in TFW to HTO concentration in atmospheric humidity. The observed ratios were determined as mean values of corresponding HTO concentrations for 15th and 20th year after beginning of release. It can be seen that there are two groups of models, which give different values of this ratio. Models of FZK, ZSR and RFNC-VNIIEF give ratio values close to 0.5 (0.295 to 0.592), LLNL, NIPNE and CEA models give values close to 1 (0.825 to 1.46). The variation between observed values is 0.131 to 0.349 for the three SPs. It can be seen that the values obtained by the first group of models are closer to the experimental values.

TABLE C4. RATIO OF HTO CONCENTRATION IN TFW AND ATMOSPHERIC MOISTURE

Participant	Sampling Point 2	Sampling Point 4	Sampling Point 6
FZK	0.498	0.295	0.366
LLNL	1.25	1.46	1.14
NIPNE	0.872	0.825	1.05
CEA	0.957	0.961	0.942
RFNC-VNIIEF	0.592	0.51	0.488
ZSR	0.388	0.43	0.388
Observed (mean value for 15th and 20th year)	0.259	0.131	0.349

(C27) The modelling approach of LLNL, CEA and NIPNE used to calculate HTO concentrations in plant water was similar to the classical formula (Murphy, 1984):

$$C_{pw} = 1/\gamma * \ [R_H\, C_a / H_a + (1 - R_H)\, C_{sw}] \tag{3}$$

where:

C_{pw} is the tritium activity in the plant water (Bq L^{-1});
γ is 0.909, the ratio of vapour pressure HTO/H_2O at 20°C;
R_H is the relative humidity;
C_a is the concentration of tritium in air (Bq m^{-3});
H_a is the absolute humidity (kg m^{-3}); and
C_{sw} is the concentration of tritium in soil moisture (Bq L^{-1}).

The CEA participant used two different values of γ parameter for atmospheric humidity and soil water: 0.909 and 0.855. The LLNL participant used higher values of release rates to account for day time facility operation – this may be the reason for the highest values of ratios predicted by LLNL. The ZSR, FZK and VNIIEF participants calculated plant concentrations using average summer concentrations in soil moisture and in atmospheric humidity. The ZSR modeller used the so-called 'specific activity' approach. In contrast, the VNIIEF participant used the following formula to calculate tritium activity in plant water:

$$C_{pw} = 0.75\ C_{aw} + 0.25\ C_{sw} \tag{4}$$

where C_{aw} is average summer concentration in atmospheric humidity (Bq/l).

The difference resulting from use of the two formulae is as follows. Use of a mean value of relative humidity in summer of about 0.8 in formula [3] means that 90% of HTO concentration in TFWT is derived from atmospheric humidity and 10% is from soil water. In contrast, use of formula [4] (by VNIIEF) results in 75% of HTO concentration arising from atmospheric humidity and 25% coming from soil water. An additional source of discrepancy in predicted TWFT concentrations is due to the use of different absolute humidity values in summer time, which vary from 11 to 15 g/m^3 (see Table C2).

C5.3. SOIL MOISTURE

(C28) Normalised values of soil moisture concentrations are presented in Figures C8 to C10. The general picture is the same as for air humidity and TFWT – there is reasonable agreement between predicted and observed values at SP 2 and 6, and obviously there is a discrepancy at SP4 for reasons discussed above. Four models (LLNL, CEA, ZSR and RFNC-VNIIEF) give good predictions for SP2 (Figure C8) – predicted values are within the range of uncertainty of observed data ±50%. Two other models (FZK, NIPNE) underestimate HTO concentrations; the NIPNE model predicts a lower value of ~ 4 times and the FZK model gives a lower value of 7 times. Thus, the overall variation between predictions and observations is within order of magnitude at SP2. The dispersion of the model predictions at SP6 (Figure C10) is slightly greater, however all predictions are within one order of magnitude of the observed data. One model (ZSR) gives predictions in close agreement with observed data. Two models (LLNL, RFNC-VNIIEF) are within a factor of 2–3 times of the experimental data. Two other models (CEA, NIPNE) underestimate experimental results by 4–6 times and one model (FZK) underestimates the experimental results by one order of magnitude.

(C29) Ratios of HTO concentration in soil moisture to HTO concentration in atmospheric humidity are given in Table C5. The best predicted ratios at SP2 are given by the ZSR and NIPNE models. The best predicted ratios at SP6 are given by the LLNL and ZSR models.

(C30) The participants assumed that HTO concentrations in soil water is determined by HTO dry and wet deposition and that deposited HTO is diluted by precipitation. Two main modelling approaches were used for the soil water compartment: an activity balance approach (used by CEA model), and the empirical approach (all others). The CEA participant calculated HTO concentration in soil water using formula:

$$C_{sw} = (F_d + F_w)/(v_e\rho_s + R) \tag{5}$$

where:

F_d is the dry deposition flux, Bq/m^2 s;
F_w is the wet deposition flux, Bq/m^2 s;
v_e is the exchange velocity, m/s;

ρ_s is the soil specific water content, kg/m^3;
R is the re-emission flux, Bq/m^2 s.

The FZK participant calculated HTO concentrations in soil water due to wet deposition only.

The LLNL participant assumed HTO concentrations in soil water are a fraction retained, f_r, after deposition, using 75% of the values of f_r = 20% for HTO deposition, and f_r = 6% for HT deposition as determined from a previous release experiment at Chalk River Laboratories (CRL). The amount of precipitation in summer used by the LLNL participant was 303 mm, which is lower that given in the Scenario description (400 mm; see also Table C2).

The NIPNE participant did not consider HT dry deposition on soil directly, but took into account the HT to HTO soil conversion factor determined at CRL. For HTO dry deposition, the NIPNE participant used the empirical formula $C_{sw} = 0.15\ C_{aw}$.

The ZSR participant used the 'specific activity' approach. To model retention of HTO in soil water, it was assumed that snow/soil water in spring comprises: 18% of soil water from the previous year; 23% of the average moisture during winter; and 9% of the average HTO concentration in snow according to the snow-out factor given in the scenario. Soil water in autumn was assumed to be composed of 13% of the spring soil water, 51% of average air moisture during summer and 36% of the average HTO concentration in rain according to a wash-out factor of 6 10^{-5} s^{-1}. The contributions of dry deposited HTO to the soil water was calculated by allocating an effective water volume for the exchange between atmosphere and soil, determined by three factors: (1) the average absolute humidity of the air; (2) the HTO dry deposition velocity; and (3) the exposure time for the respective season.

The VNIIEF participant considered that HTO concentrations in soil water consist of 0.2 dry deposited HTO and 0.8 of wet deposited HTO. Dry deposited HTO was determined from the HTO concentration in atmospheric humidity. Wet deposited HTO was assumed to include half of the amount in snow, with the HTO concentration determined by a snow-out coefficient and the total amount of rainwater (see Table C2) with a HTO concentration of $0.4C_{aw}$.

(C31) It can be seen that the activity balance approach used by CEA over-predicts ratios by a factor of 1.5–2. A possible reason may be the non-continuous nature of the release source, which results in increased re-emission and exchange. The LLNL approach, based on CRL field data, corrected to take into account the non-continuous nature of release source, gives a better agreement with observed data at SP 2 and 6. The large amount of precipitation used by the FZK participant (784, 1044, 1021, 608 mm) gives low ratios and low concentrations of HTO in soil water for SP2 and 6. The VNIIEF empirical approach overpredicts the ratios whilst the ZSR approach gives good predictions for ratios at SP 2 and 6.

TABLE C5. RATIO OF HTO CONCENTRATION IN SOIL MOISTURE AND ATMOSPHERIC HUMIDITY

Participant	Sampling Point 2	Sampling Point 4	Sampling Point 6
FZK	0.11	0.098	0.115
LLNL	0.394	0.455	0.35
NIPNE	0.334	0.596	0.961
CEA	0.514	0.532	0.468
RFNC-VNIIEF	0.506	0.55	0.52
ZSR	0.326	0.393	0.312
Observed average	0.261	0.131	0.344

C5.4. SNOW WATER

(C32) Differences between predicted values and observed data are greater for HTO concentrations in snow water than for other environmental media (Figures C11 to C13). A possible reason is lack of specific models for HTO deposition with snow and consequently different approaches were used by modellers to calculate HTO deposition in winter. It is also interesting that the observed values of HTO concentrations vary by 6 times at different sampling points and in different years (see Tables C6 and C7), while variation of the observed ratios is 3 times higher ~ 0.09 to 1.88. In addition, the observed ratios can be divided into three categories: about 0.1; close to 0.5; and close to 2. This may mean that the process of HTO deposition with snow depends more on the meteorological conditions than deposition with rain. Despite the fact that concentrations in snow water are measured on March 31st, the HTO concentration itself results from HTO wet and dry deposition during winter. However, the ratios presented are still not real ratios because the mean values of absolute humidity for the winter and the whole year differ by a factor of ~2. The variation of the predicted ratios is much higher than the observed ones – from 0.006 to 31.8. The FZK model predicts ratios from 0.5 to 31.8. Predicted ratios from the VNIIEF model are 2.1 – 2.4. Predicted ratios of the LLNL, NIPNE and ZSR models are ~ 0.45–0.84. The CEA model gives ratios less than 0.01. Three models (FZK, LLNL, ZSR) give good predictions of HTO concentrations in snow water for the 20th year at SP2, but overpredicts them by ~3–4 times for the 15th year. In contrast, the NIPNE model gives the best predictions of HTO concentration for the15th year. The VNIIEF model gives good predictions of HTO concentration in snow water at SP6 in the 20th year. The CEA model underestimates both concentrations and ratios at all sites. It seems that data for SP4 should be considered separately due to the additional source of release.

(C33) As mentioned above, no new models were developed specifically to model HTO deposition with snow as required for the Scenario 4 calculations.

TABLE C6. RATIO OF HTO CONCENTRATION IN SNOW WATER AND ATMOSPHERIC HUMIDITY

Participant	Sampling Point 2	Sampling Point 4	Sampling Point 6
FZK	1.24	31.8	0.523
LLNL	0.69	0.646	0.739
NIPNE	0.615	0.679	0.838
CEA	0.0076	0.0058	0.0103
RFNC-VNIIEF	2.06	2.16	2.44
ZSR	0.452	0.468	0.448
Observed (Mean value)	0.294	0.1041	1.16

TABLE C7. RATIO OF HTO CONCENTRATION IN PLANT TISSUE FREE WATER, SNOW WATER AND SOIL MOISTURE TO HTO CONCENTRATION IN ATMOSPHERIC HUMIDITY

	TFWT SP 2	TFWT SP 4	TFWT SP 6	Snow SP 2	Snow SP 4	Snow SP 6	Soil SP 2	Soil SP 4	Soil SP 6
Observed (15th year)	0.247	0.135	0.218	0.134	0.0921	0.439	0.252	0.135	0.21
Observed (20th year)	0.271	0.128	0.479	0.454	0.116	1.88	0.271	0.128	0.479
FZK	0.498	0.295	0.366	1.24	31.8	0.523	0.11	0.098	0.115
LLNL	1.25	1.46	1.14	0.69	0.646	0.739	0.394	0.455	0.35
NIPNE	0.872	0.825	1.05	0.615	0.679	0.838	0.334	0.596	0.961
CEA	0.957	0.961	0.942	0.0076	0.0058	0.0103	0.514	0.532	0.468
VNIIEF	0.592	0.51	0.488	2.06	2.16	2.44	0.506	0.55	0.52
ZSR	0.388	0.43	0.388	0.452	0.468	0.448	0.326	0.393	0.312

The approach of CEA, NIPNE, ZSR and FZK was to calculate HTO concentration in snow water C_{snw} (Bq l^{-1}) due to wet deposition of HTO with snow (rain) using the formula:

$$C_{snw}\ (\mathrm{Bq}\ l^{-1}) = Q\ \Lambda\ \Phi\ T/(x\ u\ \theta\ 1000{*}V_{precip}) \tag{6}$$

The LLNL participant used a similar formula:

$$C_{snw}\ (\mathrm{Bq}\ l^{-1}) = \Lambda\ Q\ \exp(-\Lambda\ x\ /u)\ \Delta T/\ (\ x\ u\ \theta\ 1000{*}V_{precip}) \tag{7}$$

where:

Λ is the washout coefficient (s^{-1});
Q is the release rate (Bq s^{-1});
X is the downwind distance (m) from the source;
U is the mean windspeed (m s^{-1}) for the stability class for snow;
Φ is the joint frequency of occurrence of wind direction and rainfall;
T is the duration of studied period (s);
ΔT is the duration of rainfall when plume is present (s);
θ is the sector width (radians); and
V_{precip} is the precipitation (m) occurring in winter.

The participants used different values of washout coefficients and precipitation intensity (see Table C2). The NIPNE and CEA modellers used the Λ value given in the Scenario description. The LLNL modeller used a value 1.65 times higher, and the FZK modeller used a value 4.1 times higher than given in the Scenario description. This latter was the highest value used and was equal to the washout coefficient for rain. This participant calculated HTO concentrations in snow water as HTO concentrations in rainwater using meteorological conditions for the first winter. The same approach was used to model HTO washout by rain. The VNIIEF participant used the washout approach for wet deposited HTO and the 'specific activity' approach for dry deposited HTO in accordance with the formula:

$$C_{snw}\ (\mathrm{Bq/l}) = \Lambda\ Q/(\gamma\ 2\ \pi\ x\ u\ I) + C_{am}/\gamma \tag{8}$$

Where I is snow intensity (m/s) and other parameters have the same meaning as in formulae [3, 6]. It can be seen from the observed ratios that the specific activity approach overpredicts ratios in most of cases.

The FZK participant did not take into account HTO dry deposition. The LLNL, CEA and NIPNE participants considered HTO dry deposition on snow using a flux deposition approach. Dry deposition was calculated for both HT and HTO as follows:

$$F_d = f_r * C_a * v_g \tag{9}$$

where:

F_d is the dry deposition flux (Bq m^{-2});
C_a is the time-integrated concentration of HT or HTO in air at the location of interest (Bq s m^{-3});
v_g is the deposition velocity (m s^{-1}); and
f_r is the fraction retained.

C6. CONCLUSIONS

(C34) As noted in the Introduction, Scenario 4 was developed on the basis of experimental data collated at RFNC-VNIIEF for monitoring the impacts of a long term tritium emission source. Although Scenario 4 is similar to Scenario 1 (which is a model-model intercomparison exercise), it demonstrates how the different models performed for an actual case of long term tritium release. The features of the release source make it possible to study the process of tritium retention in the environment, as well as the effects of past releases on the current contamination of the environment. The specific goals of this Scenario were to:

- validate models used to predict tritium concentrations in environmental media at long term releases;
- investigate the process of tritium retention in biosphere; and
- evaluate the effect of past releases on current level of contamination.

(C35) A comparison of modelling results against the observed data shows that in many cases existing long term assessment models have the following specific features. Predicted and observed values of HTO concentrations in atmospheric humidity due to atmospheric dispersion of primary plume at SP 2 and 6 are within a factor of 4. Most of predicted values are within the range of experimental uncertainties, which are within a factor of 2. It can be seen from the results of one model (RFNC-VNIIEF) that accounting for tritium retention by averaging the previous 5 years of releases results in an over-prediction compared to the observational trend. However, it follows from the observations that tritium retention should be taken into account if the release strength decreases by more than order of magnitude. Observed HTO concentrations in the atmospheric moisture at SP4 are significantly greater than predicted values. Upon further investigation, it was found that there is a low intensity aboveground source of emission near SP4, which impacts on the HTO concentrations at the SP that does not occur at SP 2 and 6. Besides, increased concentrations of HTO in soil water were found at various depths below the surface at SP4. These two reasons explain the difference between model predictions and observations.

(C36) Both classical and empirical approaches were used to predict HTO concentration in plant TFW. Use of the classical formula predicts that 90% of HTO concentration in TFW is from atmospheric humidity and 10% is from soil water. This method results in an over prediction compared to observed ratios. The empirical approach appears to predict the ratios better. An additional source of discrepancy in the predicted TWFT concentrations is due to the absolute humidity values, which vary from 10.35 to 15 g/m^3 (see Table C2).

(C37) Modelling HTO concentrations in soil water using the activity balance approach over-predicts ratios by 1.5 – 2 times. A possible reason may be the non-continuous nature of the release source. Empirical approaches used by different participants gave reasonable predictions for tritium concentrations in the soil compartment.

(C38) Discrepancies in model predictions for HTO concentrations in snow water are higher than for the other environmental media considered in the scenario (atmospheric humidity, soil water, plant TFWT). Indeed, the spatial variation of the actual observational data is also higher for snow water than for the other sampling data. There are number of reasons: use of different values for the washout coefficients, different precipitation volumes, and variation in joint frequencies. The ‘specific activity’ approach used by the VNIIEF modeller overpredicts ratios in most of cases. It seems that the process of HTO deposition by snow is strongly dependent on the meteorological conditions at the time and requires additional efforts if appropriate models are to be developed.

(C39) One of the conclusions from the model test exercise is that lack of reliable meteorological information results in additional sources of discrepancy between the models used as well as between predictions and observations. This includes variation in such parameters as frequencies, air humidity, precipitation, etc. Many of these parameters have a strong impact on calculation of HTO concentrations in soil water and TFWT. Availability of reliable meteorological information should result in an agreement between predictions and observations within a factor of 2.

(C40) It would appear from the results presented that the ratio of measured HTO concentrations to the tritium release rate increase slightly over the 15 years of observation. This may mean that tritium retention takes place if there are significant decreases of emission rates. Therefore one important conclusion from this model test exercise is that tritium retention should be taken into account if tritium release values decrease by more than an order of magnitude over a period of several years. The modelling approaches to HTO retention that were included in the ZSR and RFNC-VNIIEF models were not entirely successful. In the former case the model underestimated retention, whilst the latter approach over-predicted the observational trend. The problem of tritium retention in the environment should be considered in the future.

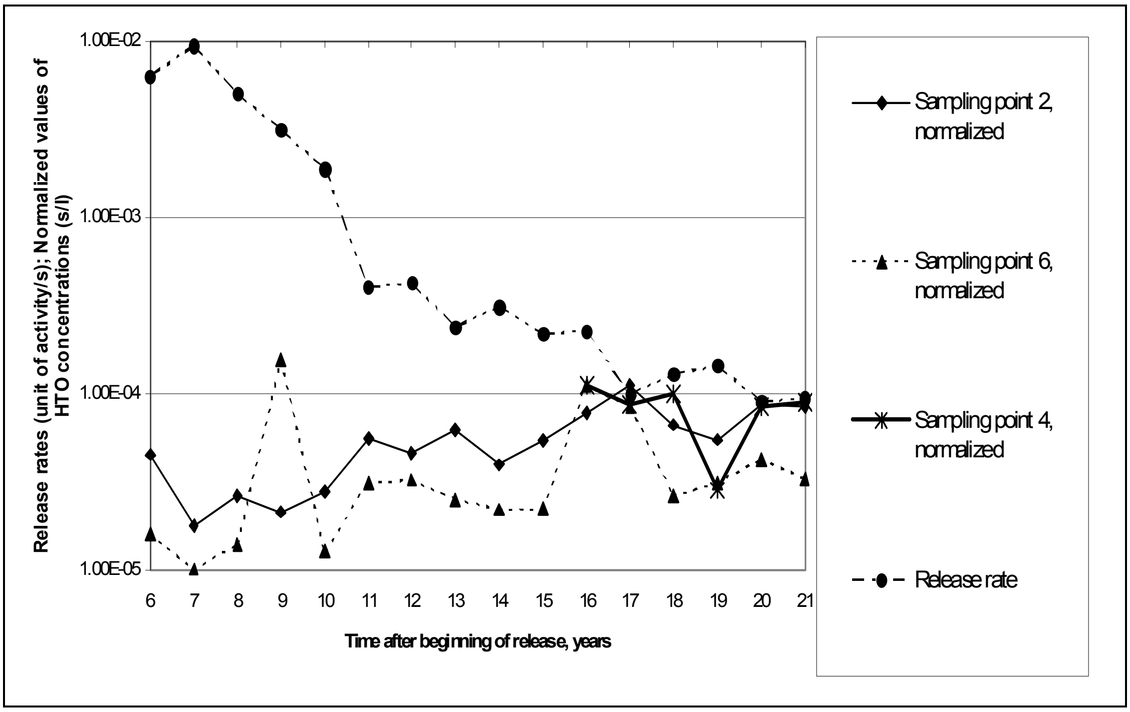

FIG. C1. Release rate (Q) and observed normalised values of HTO concentration in atmospheric humidity (Ca/Q).

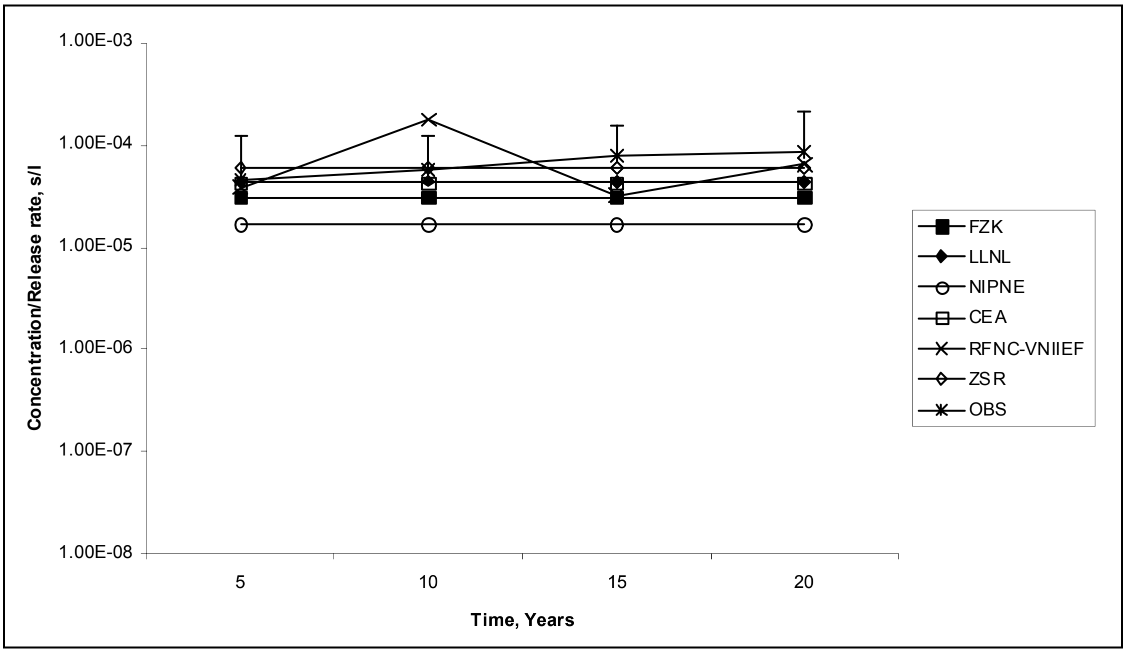

FIG. C2. Predicted and observed normalised tritium concentrations in atmospheric humidity. Sampling Point 2.

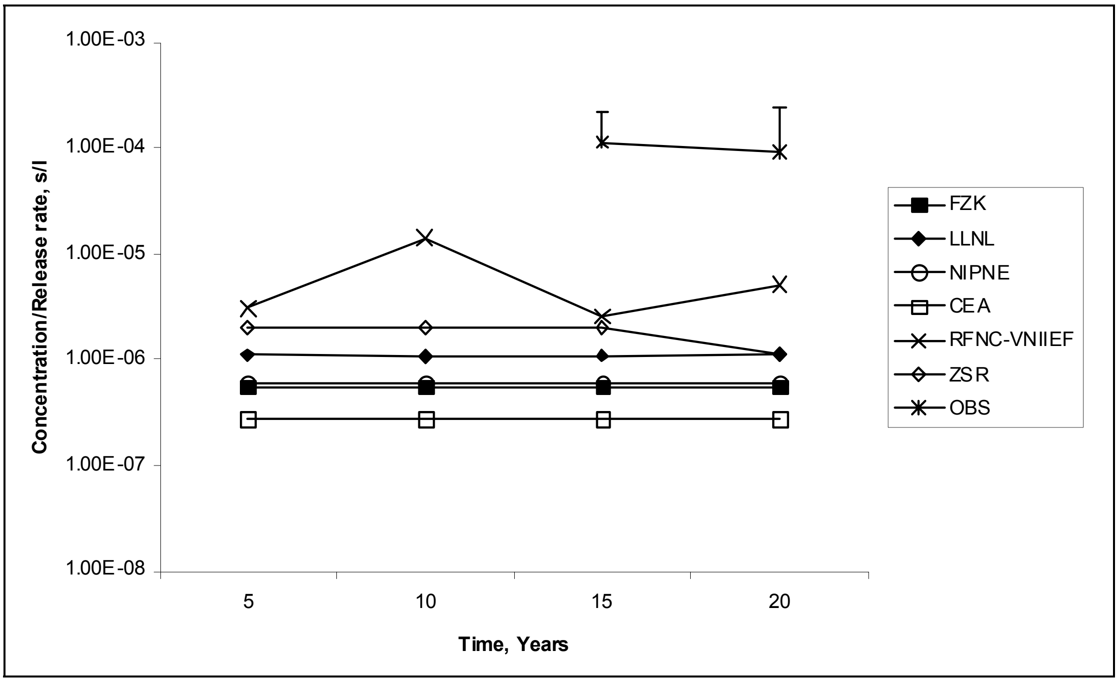

FIG. C3. Predicted and observed normalised tritium concentrations in atmospheric humidity. Sampling Point 4.

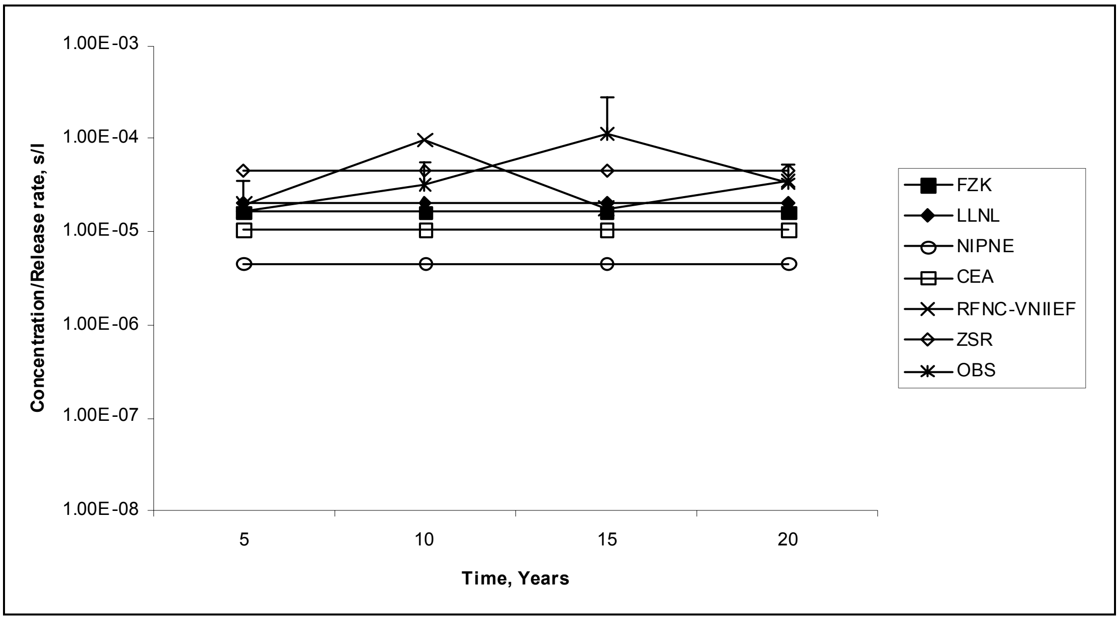

FIG. C4. Predicted and observed normalised tritium concentrations in atmospheric humidity, Sampling Point 6.

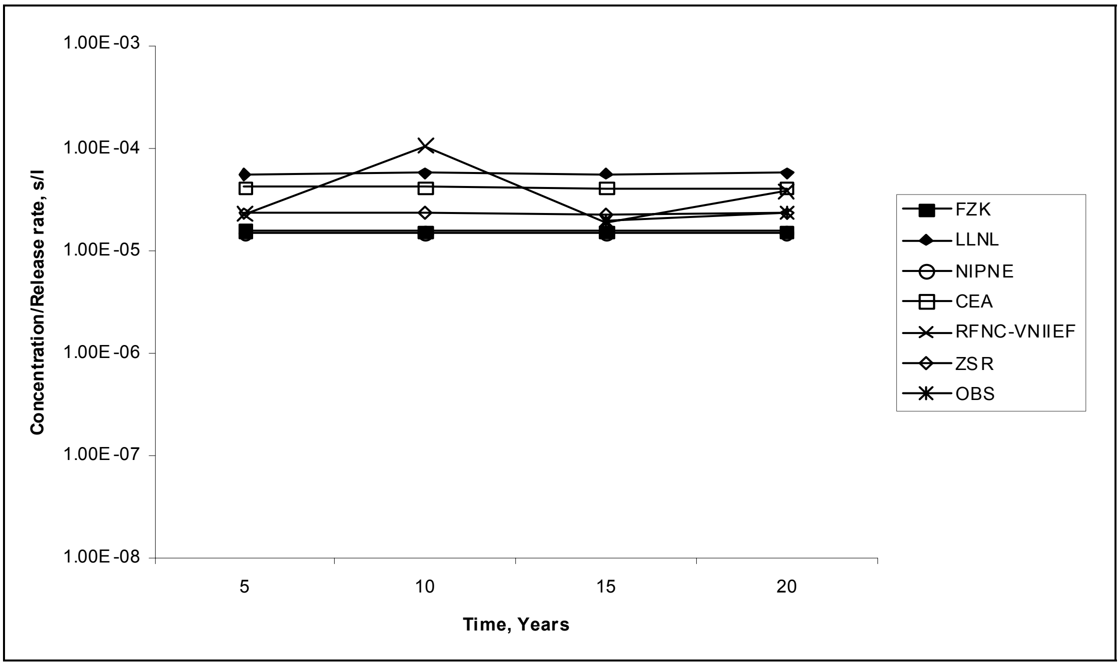

FIG. C5. Predicted and observed normalised tritium concentrations in TFW, Sampling Point 2.

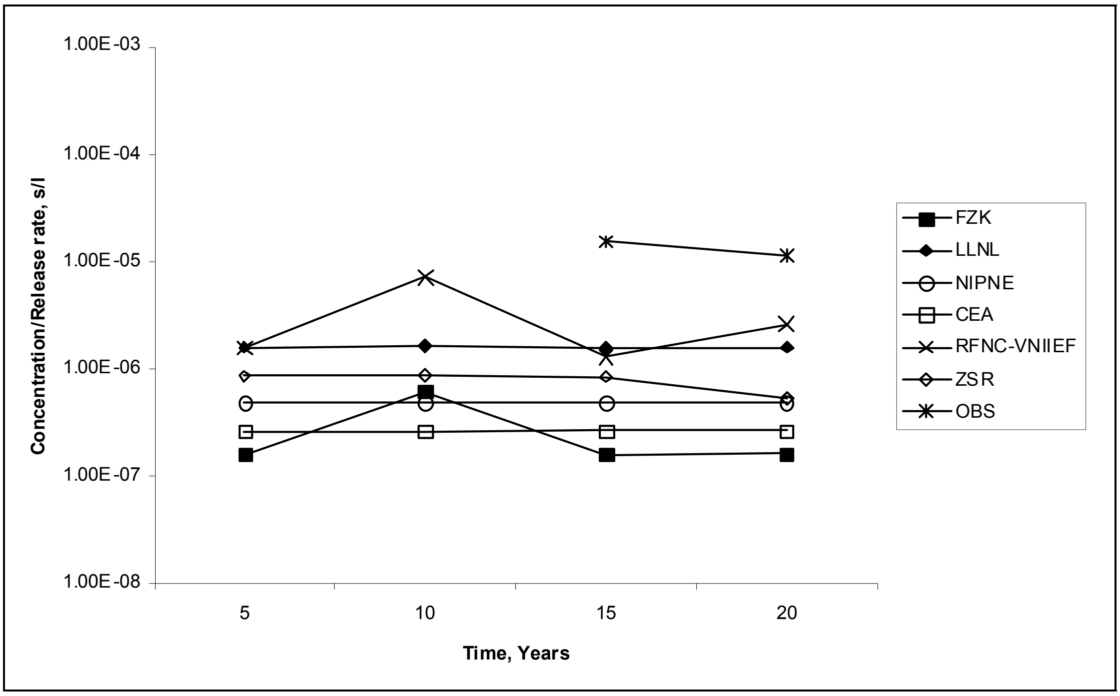

FIG. C6. Predicted and observed normalised tritium concentrations in TFW, Sampling Point 4.

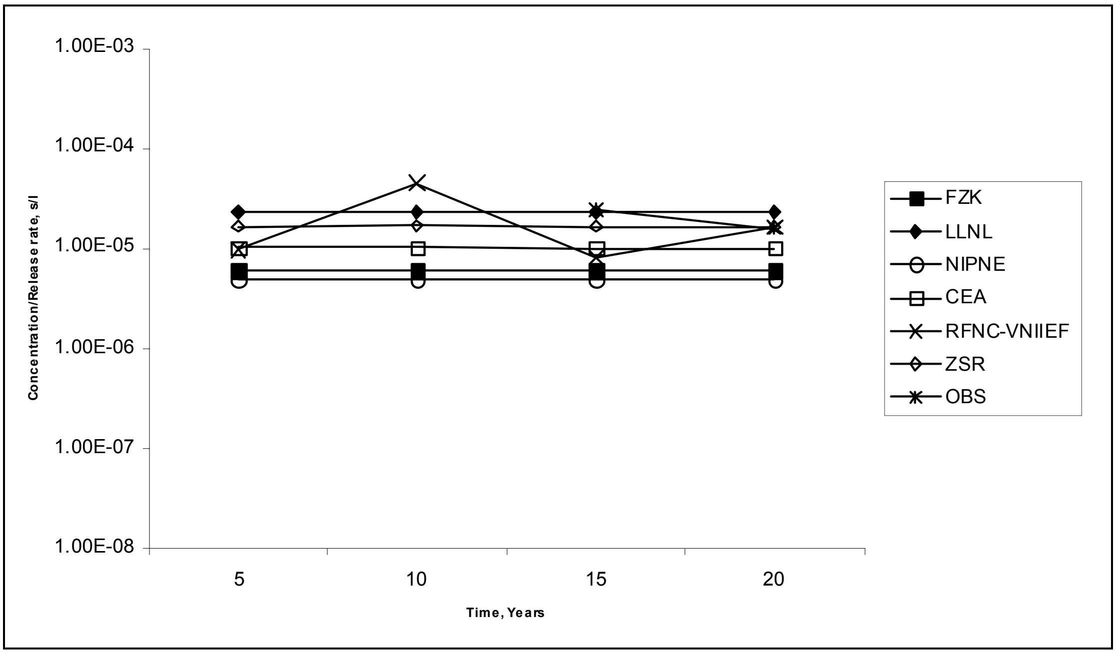

FIG. C7. Predicted and observed normalised tritium concentrations in TFW, Sampling Point 6.

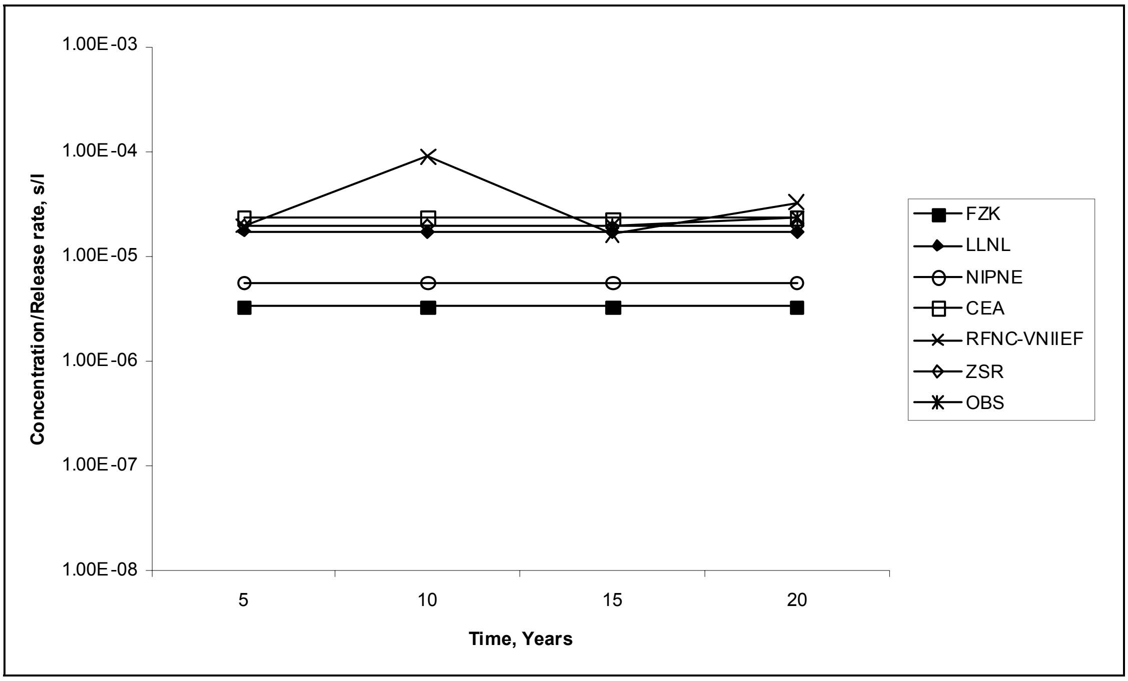

FIG. C8. Predicted and observed normalised tritium concentrations in soil water, Sampling Point 2.

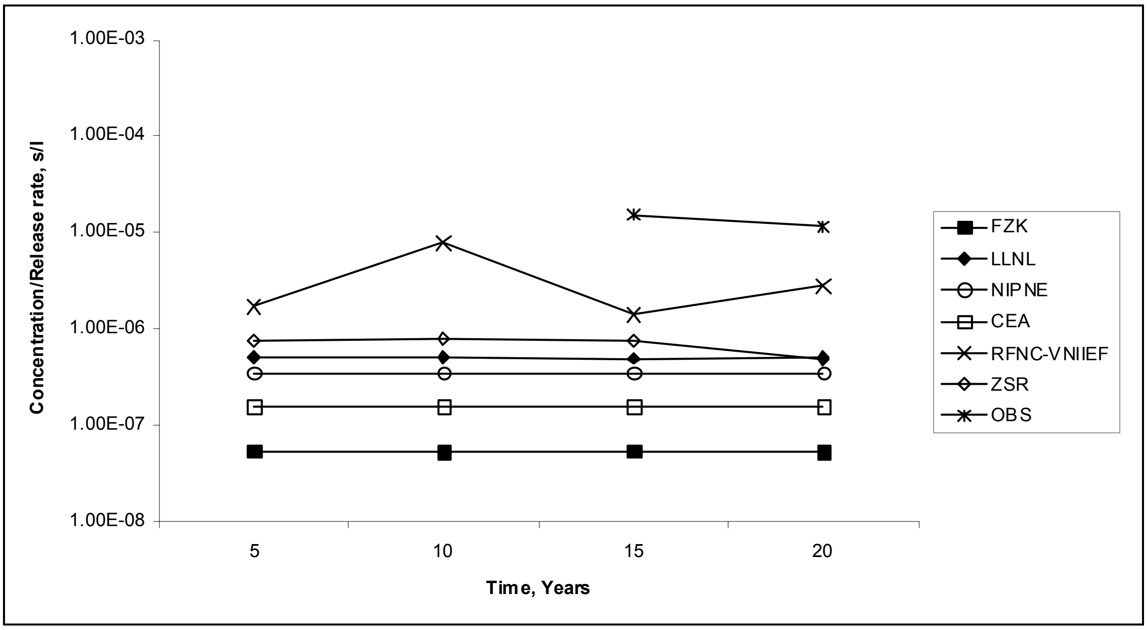

FIG. C9. Predicted and observed normalised tritium concentrations in soil water, Sampling Point 4.

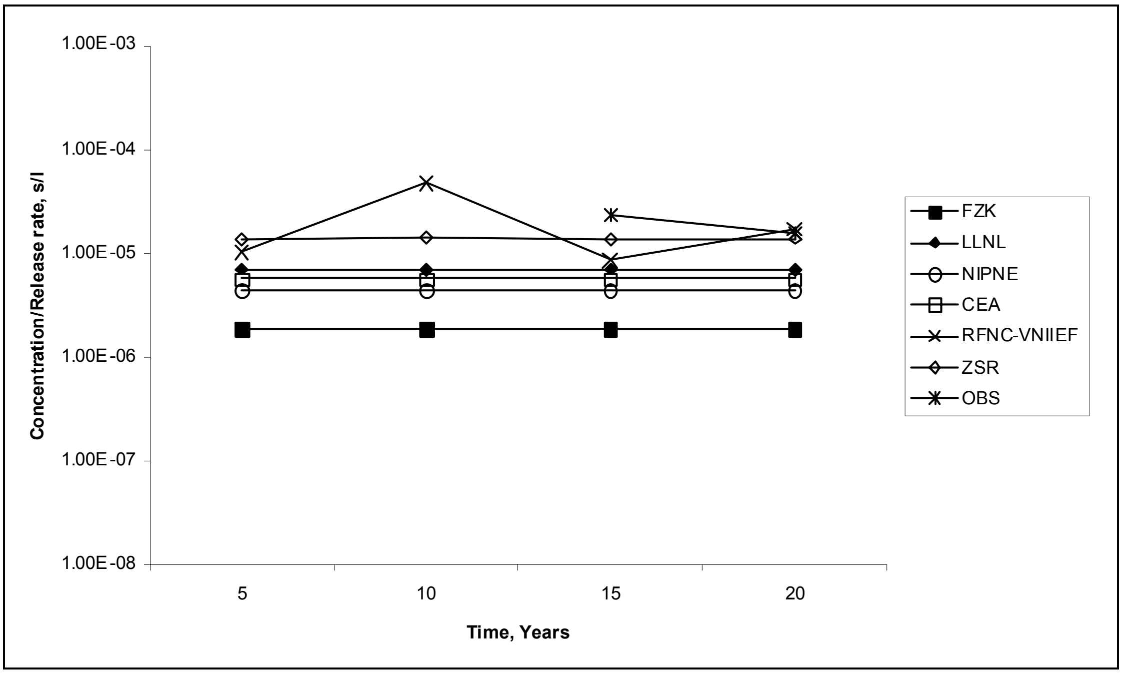

FIG. C10. Predicted and observed normalised tritium concentrations in soil water, Sampling Point 6.

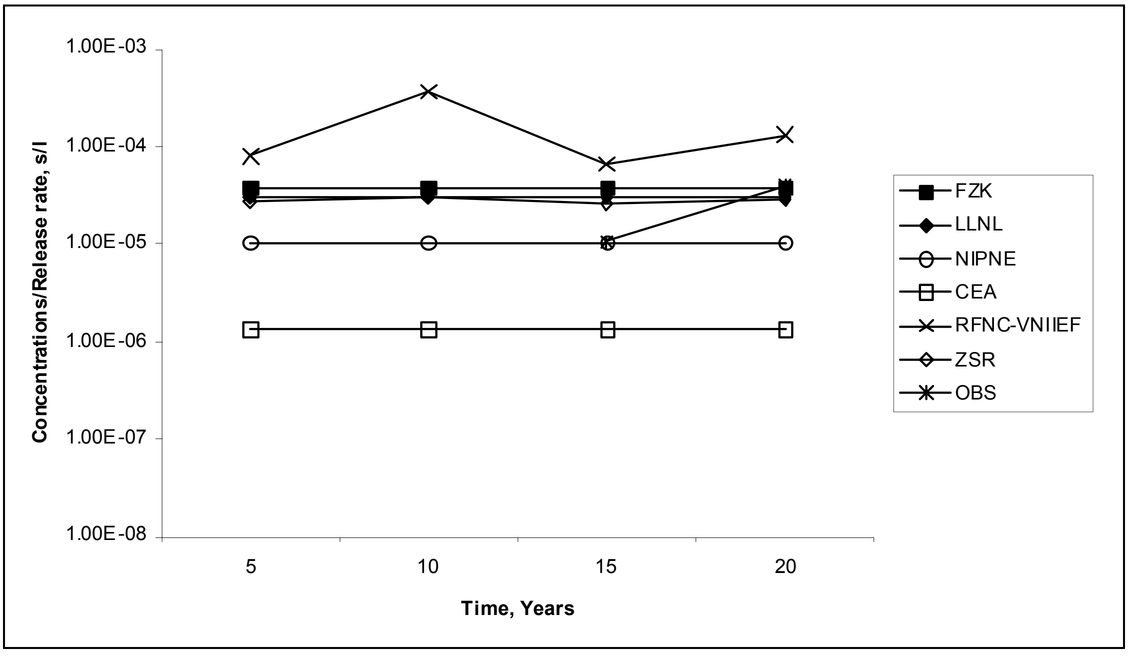

FIG. C11. Predicted and observed normalised tritium concentrations in snow water, Sampling Point 2.

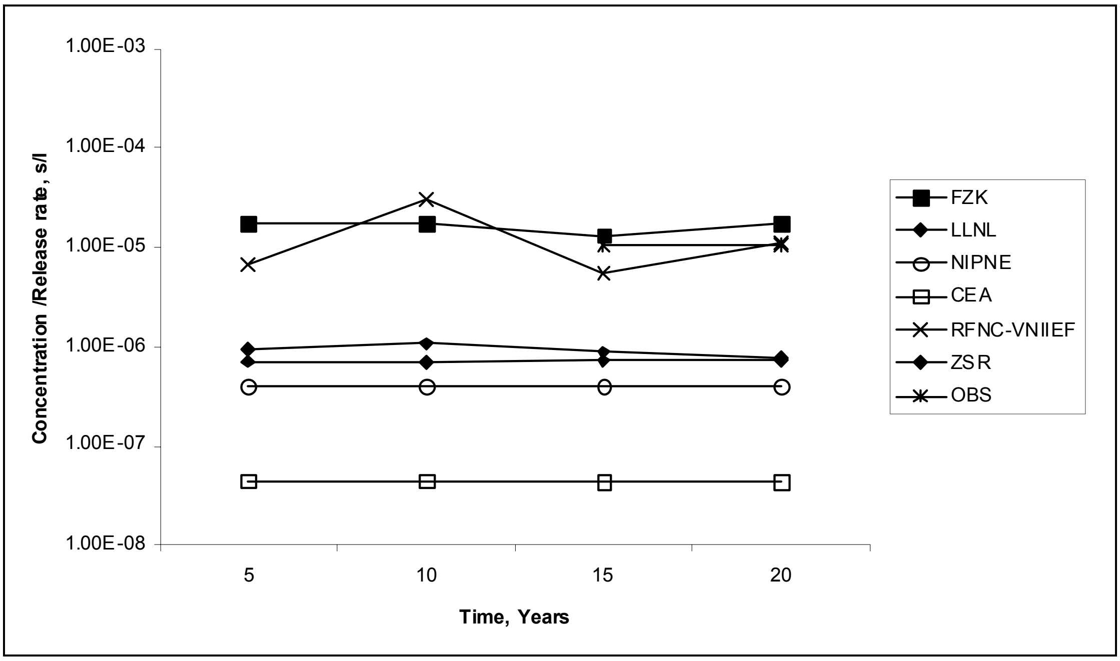

FIG. C12. Predicted and observed normalised tritium concentrations in snow water, Sampling Point 4.

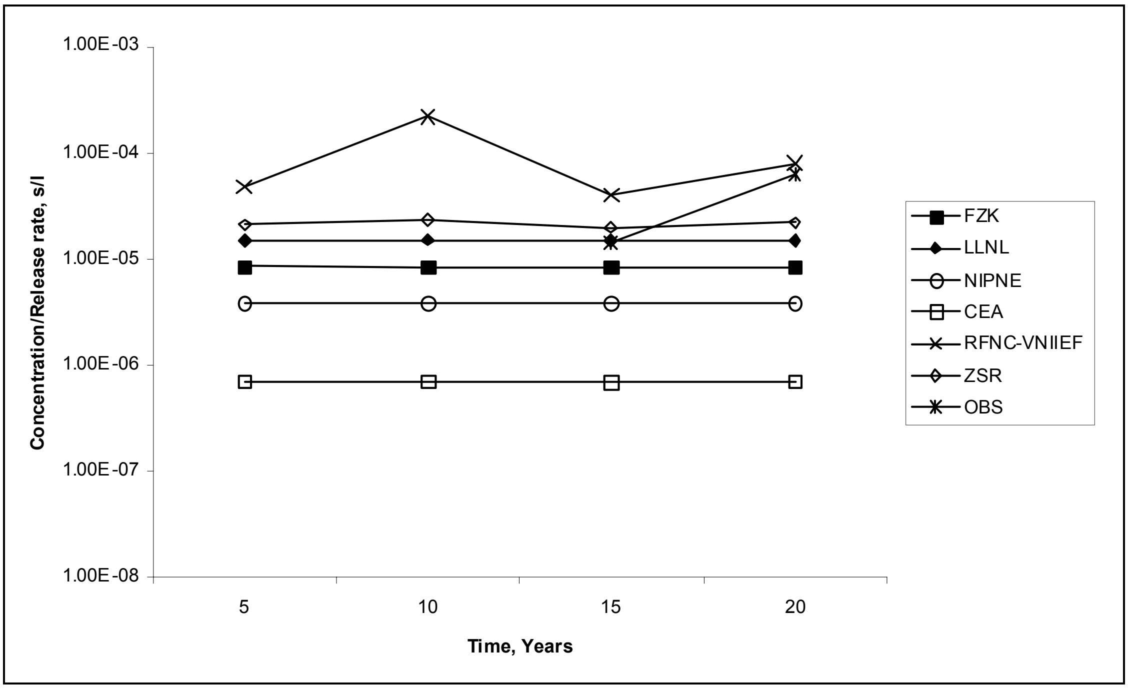

FIG. C13. Predicted and observed normalised tritium concentrations in snow water, Sampling Point 6.

REFERENCES TO PART C

[1] BELOVODSKY, L., GAEVOY L., GRISHMANOVSKY, V., Tritium, M: Energoatomizdat, 248 pages (1985).

[2] BELOVODSKY, L., FAILOR, R., GAEVOY, V., GOLUBEV, A., Method for rapid, high-sensitivity tritiated water extraction, IV Conference of Methods and Applications of Radioanalytical Chemistry, Hawaii, April 6–11 (1997).

[3] BIOMASS, Modelling Environmental Transport of Tritium in the Vicinity of Permanent Sources, Atmospheric Sources: Model-Model Intercomparison, BIOMASS Theme 3 Tritium Working Group, Working Document 1, IAEA Limited Distribution Report BIOMASS/T3TM/WD01, IAEA, Vienna (1999).

[4] VEDENEEV, A.I., GOLUBKOV, A.N., KLEVTSOV, V.G., et al., Experimental Closed Loop for Dynamic Modelling of Fusion Reactors Vacuum-Tritium System. Pre-print RFNC-VNIIEF 57–97 (1997).

PART D

MODELLING THE ENVIRONMENTAL TRANSPORT OF TRITIUM IN THE VICINITY OF PERMANENT ATMOSPHERIC SOURCES:

A test of chronic atmospheric release models using French data

D1. BACKGROUND AND OBJECTIVES

(D1) This report presents the results of a model test exercise based on field sampling data obtained following long term tritium releases at the Valduc site in France. The objective of the modelling exercise was to test and hence improve tritium models through comparison of results with sampling data for concentrations of tritium in air, rain and plant tissue free water (TFWT), and concentration of organically bound tritium (OBT) in trees. The scenario for the model test exercise (called Scenario 5) was one of a set of scenarios developed by the Tritium Working Group (TWG) within the framework of the IAEA Biosphere Modelling and Assessment (BIOMASS) co-ordinated research programme. It is an interesting scenario because it allowed modellers to address two different topics that were not considered in the other two model test exercises that were based on experimental data (Scenario 3, Part B, and Scenario 4, Part C). First, the site that is represented in this scenario is not a flat site and modellers had to consider how to address topographic effects. Secondly, modellers were asked to develop a map of OBT concentrations in tree leaves around the site for one particular year and also to utilise historic releases at the site to calculate OBT concentrations in tree rings for specific years. Like the scenario based on Canadian data (Part B), the modellers also had to consider multiple atmospheric sources of tritium.

(D2) The outline of Scenario 5.0 was first presented in May 1999 at the BIOMASS TWG spring working group meeting in Sarov (Russia). The scenario description was then developed and distributed to the participants after the meeting. Comparison of modelling results was first presented at the TWG meeting in October 1999 in Vienna. Further clarification of the scenario description was provided and subsequently some of the modellers submitted new results. Final results and the first version of the draft report were presented at the TWG spring meeting in Toki (Japan) in May 2000. At this time modellers were asked to provide more information on how they approached the calculations to take account of topographic effects. The report was then finalised for distribution.

D2. SCENARIO DESCRIPTION

(D3) Scenario 5 provides a test for models that predict long term average tritium concentrations in the environment due to chronic atmospheric releases. It is based on data obtained from an actual site (Valduc) in France. The scenario description is given in full in Annex II–D. This scenario aims to help verify the consistency and the capability of the different models when it comes to reproducing measurements at the Valduc site.

(D4) The Valduc area consists of rolling terrain where the differences in elevation reach 150 m or so over several km. This terrain has only moderate slopes and shallow valleys. It is unevenly covered with patchy associations of forest trees. The atmospheric tritium sources are situated close to the tritium facility buildings at the most elevated part of the area. These releases come from 3 different sources: a 50 m stack; and two storage buildings. The stacks of these two buildings are 20 and 11.5 meters high. Information on the chronic releases of tritiated water and tritiated hydrogen gas was provided for the years 1983 to 1998. The release values for each tritium source were provided for the years 1988 to 1998, whilst the total release of the three sources was provided for the years 1983 to 1987. Characteristics and positions of the sources and sampling stations were also given. The effect of topography could be important in this scenario because two of the sampling points are at about 150 metres lower elevation than the sources (Table D1).

TABLE D1. ELEVATION ABOVE SEA LEVEL OF SOURCES AND SAMPLING STATIONS

Location	Source 1	Source 2	Source 3	Station 1	Station 2	Station 3	Station4
Z(m)	495	482	477	325	460	440	370

(D5) Some meteorological data were measured by the Valduc sodar. Every ten minutes, the date and hour of the measurement, height of measurement, wind direction, wind speed, stability mark and standard deviation of the wind speed were recorded. The general wind rose and the rain wind rose were obtained for 6 wind classes, 18 sectors and each of the Pasquill classes. These roses were calculated from sodar meteorological data at a height of 150 m for the years 1993 to 1997.

(D6) The tritium measurements were made at four stations at about 2 to 5 km from the Valduc site and in the four principal wind directions. The team in charge of the environmental survey took periodic samples. Air and rain sampling were made at the end of each week. Air was collected by a bubbler system and rain was collected in a container throughout the week. Grass was sampled monthly but only during the April–September period prior to 1993. Since 1993, it was sampled monthly.

(D7) At the end of October 1988, a measurement campaign was carried out to assess OBT concentrations in oak leaves. These measurements gave a map of the impact of the releases for 1988 for an area of 30 km × 30 km centred on Valduc, with a 4 km resolution. OBT in beech tree rings for the same year (1988) was also measured at one point 9 km to the East of Valduc.

(D8) Modellers were asked to calculate:

- Tritium concentrations in air (Bq/m^3), in grass tissue free water (TFWT) (Bq/l), and in rain (Bq/l) at the four sampling stations for the years 1988 to 1998.
- OBT concentrations in beech tree rings (Bq/l) for the years 1983 to 1988.
- OBT concentrations in oak leaves for the year 1988 (Bq/l) on a map grid of 30x30 km^2 centred on the Valduc 50 m stack, at 4 km intervals.

D3. MEASUREMENTS

(D9) Grass was sampled only during the April–September growing period before 1993, but has been sampled monthly since 1993. Sampling of air and rain occurred weekly. Air was sampled via a dynamic system (bubbler). Rain was collected in a container; water was not isolated from the surrounding air. The quantity of rain was not reported. The TFWT in grass leaves was determined by extracting the water with azeotropic distillation and counting it with a liquid scintillation technique. The OBT in oak leaves and beech tree-rings was obtained by desiccating the sample, removing any exchangeable tritium by prolonged contact of the sample with tritium-free water vapour, combusting the dry matter so obtained under a flow of oxygen, distilling the combustion water and finally counting it as usual.

(D10) Uncertainties on the measurements of tritium concentrations in air, rain and TFWT are a minimum of 5% for values over 100 Bq/l and reach a maximum of 50% for values of less than 10 Bq/l. Uncertainties on measurements of OBT concentrations are between 5 and 10% for values over 10 Bq/l and reach 40% for lower values.

D4. COMPARISON OF PREDICTIONS WITH OBSERVATIONS

(D11) Six modellers submitted results for Scenario 5 (see Table D2). Model descriptions are given in Annex I–A. Participants used the same models, with appropriate adaptations, as those used for Scenario 1, Scenario 3 and Scenario 4 (see Parts A, B and C respectively). Some modellers submitted new results following the first presentation of results in October 1999 in Vienna.

TABLE D2. DETAILS OF PARTICIPANTS AND MODELS USED FOR SCENARIO 5

Participant	Affiliation	Model name	Designation used in the text
Y. Belot	Consultant, France	TRIMASS1	Belot
D. Galeriu	NIPNE, Romania	DISPT	NIPNE
A. Golubev	RFNC-VNIIEF, Russia	TRIEF	RFNC-VNIIEF
G. Guinois	CEA, France	TRIMASS2	CEA
S-R. Peterson	LLNL, USA	DCART	LLNL
D. Lush	BEAK, Canada	IMPACT	BEAK

D4.1. TRITIUM CONCENTRATIONS IN AIR

(D12) Figures D1 to D4 show comparisons between modelling results and observed values for sampling Stations 1 to 4 respectively. The modelling results for the four stations are in a good agreement with each other and compared with the measurements. The predictions range from a factor of 3 below the observations to a factor of 2 above. RFNC-VNIIEF obtained low values for Station 1 and Station 4 which can be attributed to an overestimation of the topographic effect correction (see Section D5 for further details).

(D13) The ratios of calculated to observed tritium concentrations in air for the ten years 1988–1998 are given in Table D3.

TABLE D3. RATIOS OF CALCULATED TO OBSERVED TRITIUM CONCENTRATIONS IN AIR

Participant	Station 1	Station 2	Station 3	Station 4
Belot	1.07	1.1	1.52	1.29
Beak	0.8	0.76	1.15	1.01
CEA	0.72	0.79	0.96	1.06
NIPNE(with topo. effect)	0.42	0.66	0.82	0.8
NIPNE (no topo. effect)	0.81	0.74	1.07	1.71
LLNL	1.11	0.78	1.04	0.92
RFNC-VNIIEF	0.31	1.56	1.96	0.48

(D14) All the participants used a formulation of the long term Gaussian plume model to carry out their calculations.

(D15) Participants took into account sodar wind speeds at 150 m height and made corrections for different elevations of the sources. The site is not flat; the stack is located at a higher topographic elevation than the sodar which is located in a valley. Parameter values used by the modellers are given in Table D4.

(D16) All participants used a wind speed correction as given in Table D4. Some of the participants did not take into account any topographical effect and treated the dispersion over the Valduc area as if the terrain was flat (see Table D4). By doing so, they assumed that the airflow remained parallel to the underlying surface, and that the height of the plume centreline above the terrain was then always equal to the initial effective plume height H. Other participants introduced a topographical effect by varying the height of the plume centreline in the Gaussian expression, and expressing it as H+ F DZ, where H is the initial plume height, DZ the difference of topographic elevation between the base of the source and the receptor, and F is a deflection coefficient that depends on the stability of the atmosphere. The plume centreline heights adopted in the different models are shown in Table D4. Wind speeds were corrected to these heights using the profiles down in the table.

(D17) Observed air concentrations do not show the same tendencies as the actual long term releases. Incidental releases could have contributed to the measured values and so caused high annual averages in one wind direction (i.e. at one station) which cannot be modelled by a steady state model. Figure D5 gives the average annual tritium concentrations in air observed at the four stations. For the same releases, differences in tritium concentration in air measured at the 4 stations are the result of variations in the wind directions, speeds and stabilities. The wind rose used in modelling is a statistical average over a 5 year period, therefore it smoothes values for which wind direction has a great influence. But year to year differences in the wind rose are likely to be small.

(D18) As we can see in Table D4, all modellers have used different parameter values to simulate this scenario. Each of the parameters and parameter values used has an influence on the calculated results. We can try to understand the difference between modelling results by looking at the consequences of selecting different parameter values. It can be seen that the spread of results is much lower for Stations 2 and 3, than at Stations 1 and 4. This can be understood by observing that the topographic effect correction is negligible for Stations 2 and 3 because they are situated at nearly the same level as the sources. However, the effect is appreciable for the two others stations that are situated at a much lower elevation. This interpretation was further substantiated by the NIPNE results, which showed predicted concentrations with and without topographic effects (the difference is as large as 50%). The modelling approaches of Belot, Beak and LLNL models did not include a topographic effect so they have high values for stations 1 and 4. Therefore the plume central height is always at the same height above the ground. RFNC-VNIIEF uses a strong correction of elevation (H+DZ) for neutral, stable and unstable Pasquill classes and therefore calculates a very low concentration. This approach assumes that the plume central height is always at a constant elevation above sea level. The inclusion or omission of re-emission from the soil and the use of different sets of dispersion parameters can explain part of the remaining spread in the results (the differences are up to 30%). The modelling approaches of Beak, LLNL, RFNC-VNIIEF, NIPNE did not take into account the reemission of HTO, whereas Belot and CEA did. The correction of wind speed seems to have a less important effect (a difference of less than 10%) than topographic effects and re-emission.

TABLE D4. PARAMETER VALUES USED BY THE DIFFERENT MODELLERS

Parameters	Belot	Beak	CEA	NIPNE	LLNL	VNIIEF
Number of sources	3	3	3	3	3	3
Reference height of wind measurement (m), (1)	150		85	85, 98, 103	85,98,103	150
HTO deposition velocity (m/s)	$3\ 10^{-3}$	10^{-3}	$3\ 10^{-3}$	–	$3.92\ 10^{-3}$	$1.6\ 10^{-3}$
HT deposition velocity (m/s)	$3\ 10^{-4}$	10^{-4}	$3\ 10^{-4}$		$2.53\ 10^{-4}$	
Washout coefficient (s^{-1})	$6\ 10^{-5}$		$6\ \ 10^{-5}$	$6.\ 10^{-5}$	$1.3\ 10^{-4}$	10^{-5}
Roughness length (m)	1.0	0.4	0.3	0.8	0.4	0.3
Air humidity (kg/m3)	0.0072		0.0088	0.0093	0.0087	0.0076
Relative humidity (%)	81%		81%	70%	75.6%	
Re-emission:						
HTO	yes	no	yes	no	no	no
HT	yes	no	yes	yes	yes	yes
Topographic effect	no	no	yes	yes	no	yes
Plume centreline height, (2):						
Unstable	H	H	H+0.5DZ	H	H	H+DZ
Neutral	H	H	H+0.5DZ	H+0.6DZ	H	H+DZ
Stable	H	H	H+DZ	H+DZ	H	H+DZ
Wind speed correction Formula	Van Ulden profile	Power law profile	Power law profile	Van Ulden profile	Power law profile	Power law profile
Vertical dispersion parameters	Hosker-Smith's		Brigg's	Karsruhe-Jülich	Hosker-Smith's	Brigg's
OBT / HTO ratio in oak leaf	0.6	0.61	0.6	0.6	0.8	1.0
OBT / HTO ratio in beech rings	0.6	0.61	0.6	0.6	0.4	1.0

Notes:

(1) This reference height is the height above the stack base at which the wind speed is the same as the wind speed measured at 150m above the sodar emplacement. There is some divergence in the estimation of this reference height. Some modellers take the same value for all the stacks. Others calculate the correct value for each stack (Source1 : 85m ; Source2 : 98m ; and Source3 : 103m).

(2) The plume centreline height is the height of the centreline above the underlying terrain. H is the initial effective plume height above stack base; DZ is the difference in the topographic elevation between the base of the stack and the receptor.

D4.2. TRITIUM CONCENTRATIONS IN PLANT WATER

(D19) Comparisons between model results and measurements of tritium concentrations in grass (TFWT) are shown in Figures D6 to D9 for Stations 1 to 4 respectively. The ratios between calculated and measured concentrations are given in Table D5. All models overestimated the observations by up to a factor 4. In order to assess the impacts of tritium releases, it is important to be able to estimate as accurately as possible the concentrations of tritium in plants. The results presented here are considered to be satisfactory. The differences between model results are similar to the differences obtained for Scenario 1 (see Part A).

TABLE D5. RATIOS OF CALCULATED TO MEASURED TRITIUM CONCENTRATIONS IN GRASS (TFWT)

Participants	Station 1	Station2	Station 3	Station 4
Belot	2.3	2.8	3.97	3.5
Beak	1.4	1.34	2.2	2.
CEA	1.3	1.56	2	2.32
NIPNE (with topo. effect)	0.9	2.04	1.7	1.63
NIPNE (no topo. effect)	1.5	2.18	2.13	3.33
LLNL	2.14	1.34	2.02	2.35
RFNC-VNIIEF	0.43	2.7	3.34	0.83

D20. The ratio of calculated values of tritium concentrations in grass to in air humidity is about 0.9, whereas the same ratio for measured values is about 0.5 (see Table D6). The concentration in air humidity was obtained by dividing the concentration in air by the quantity of water contained per unit volume of air.

TABLE D6. RATIOS OF CONCENTRATIONS IN GRASS TFWT TO AIR HUMIDITY AND COMPARISON WITH MEASURED RATIOS

Participants	Station 1	Station2	Station 3	Station 4
Measured	0.55	0.49	0.48	0.43
Belot	0.97	0.99	0.97	0.97
Beak	1.	0.89	0.89	0.89
CEA	0.99	0.99	0.97	0.97
NIPNE (with topo. effect)	1.24	1.59	0.95	0.92
NIPNE (no topo. effect)	1.04	1.5	0.92	0.87
LLNL	0.9	0.9	0.9	0.9
RFNC-VNIIEF	0.68	0.74	0.68	0.66

(D21) As for tritium concentrations in air, it is not possible to differentiate between tritium concentrations due to the incidental releases from those due to routine, steady state releases. Tritium concentrations in plants depend greatly on the release rates and wind directions in the days and hours before sampling. There is only one sample each month and before 1993 samples have been obtained only during the growing period. There are too few samples to derive a reliable long term average. This may explain the strange dynamics in Figure D10. The curves for tritium concentrations in grass do not show the same variations as the release curve when annual release averages are used. This can also explain part of the difference between predictions and observations.

(D22) Modelling leads to an overestimation of tritium concentrations in plants by a factor of two. Variations in monthly measurements are readily caused by changes in the wind direction. Also, relative and absolute humidity values used in modelling are based on an annual average of parameter values that show great variations during the year (see Table II–D.1 in Annex II–D). This may explain the differences between calculated and observed values. As far as tritium uptake by plants is concerned, it is suggested that the models should be refined in order to take into account, at least, seasonal variations.

(D23) Again, we can try to understand the difference between modelling results by looking at the influence of the parameters and parameter values used by the modellers. The parameters that have the major influence on model results are dry deposition velocity, topographic effect, sigma parameters and reemission. There may be up to 50% variation between model results if topographic effects are considered or not. A variation of 75% results from the use of a dry deposition velocity of 10^{-4} m/s compared to 4.10^{-3}m/s, whilst calculations are about 30% lower if reemission is not taken into account. Wind speed correction has less of an effect since lower concentrations (10%) are obtained if there is no correction for wind speed.

(D24) From Figures D6 to D9, we see that much of the difference between model results can be explained by the differences in air concentrations. The modelling approaches used by Belot, CEA, LLNL and NIPNE to calculate HTO concentrations in plant water were similar to the classical formula of Murphy (1984):

$$C_p = \frac{1}{\gamma}\left(\frac{H_r}{H_a}Ca + (1 - H_r)Cs\right) \tag{1}$$

where:

Cp	is the plant water concentration (Bq/l);
Hr	is the relative humidity (%);
Ha	is the absolute humidity (kg/m^3);
Ca	is the tritium concentration in air (Bq/m^3);
Cs	is the tritium concentration in soil moisture (Bq/l); and
γ	= 0.909.

The VNIIEF model uses a formula with a constant coefficient for air and soil contribution as follows:

$$C_p = 0.75\frac{C_a}{H_a} + 0.25C_s \tag{2}$$

where:

Ca	is the tritium concentration (Bq/m^3);
Cs	is the tritium concentration in soil moisture (Bq/l); and
Ha	is the absolute humidity in air (kg/m^3).

As can be seen in Table D4, modellers used different values for relative and absolute humidity. As a consequence, air and soil coefficient in formula (1) and (2) varied. NIPNE used a low relative humidity (compared with other modellers) and a high absolute humidity. In this case the contribution for the air is higher than obtained by Belot who used a high relative humidity and low absolute humidity. For example, if the absolute humidity is changed from 0.0072 to 0.0093, plant concentrations are reduced by up to 30% and if the relative humidity is changed from 70% to 81%, plant concentrations are changed by +10%.

D4.3. TRITIUM CONCENTRATIONS IN RAIN

(D25) Figures D11 to D14 show the comparisons between modelling results and measurements of tritium concentrations in rain for 10 years from 1988 to 1998 for Stations 1 to 4 respectively. Table D7 shows the ratio between calculated and measured values. This ratio ranges from 0.12 to 3.9. RFNC-VNIIEF systematically calculates low values for stations 1 and 4 for grass and air, this pattern conforms to that for rain. Most of the calculated values are either lower than or equal to the observed values (ratios from 0.12 to 1.01) except for NIPNE (all sampling stations, ratios 1.42 to 3.9). The NIPNE participant obtained a higher value because he uses a formula to calculate rain concentration that divides the wet flux by the intensity of the rain with an exponent of 0.7 ($F_w/I^{0.7}$). Other participants just divide the wet flux by the intensity of the rain (F_w/I), C_{rain} (Bq/l) = F_w/I (see model descriptions in Annex I–A).

TABLE D7. RATIOS OF CALCULATED TO MEASURED TRITIUM CONCENTRATIONS IN RAIN

Participants	Station 1	Station 2	Station 3	Station 4
Belot	0.74	1.01	0.71	0.7
Beak	1.5	0.32	1.7	0.32
CEA	0.4	0.59	0.16	0.43
NIPNE (with topo. effect)	2.22	3.9	1.42	1.51
LLNL	0.97	0.97	0.59	0.66
RFNC-VNIIEF	0.12	0.32	0.39	0.18

(D26) Table D8 gives the ratios of the calculated tritium concentrations in rain to that in air moisture as obtained by the different modellers. The measured ratio ranges from 0.44 for Station 2 to 0.17 for Station 4. The concentration in air humidity has been obtained by dividing concentrations in air by the quantity of water contained per unit volume of air. The factor of 2 difference between the modelling results (except for NIPNE) and the actual data are considered to be satisfactory. Similar differences were found between modellers in Scenario 1. As the NIPNE modeller uses a different formula, as explained above, the ratio between tritium concentrations in rain and tritium concentrations in air humidity must be higher than for other modellers. However, he used the same model as other modellers, therefore the lower ratio for Station 3 and 4 cannot be explained at the present time.

(D27) Unfortunately the quantity of rain sampled each week at the four stations was not reported. Therefore tritium concentrations in rain have been estimated from measured tritium activities at the sampling stations but using the amount of rain measured each month at another nearby station. Some high tritium concentrations in rain that do not correspond to simultaneous high tritium concentrations in air have been reported. Such high values could come from larger tritium releases during rain periods with a given wind direction. It is difficult to remove these meaningless values from the annual average. The steady state models cannot deal with this phenomenon and there is not enough information to take it into account.

(D28) The modellers' results are in good agreement with the frequencies of wind direction when it rains. As can be see in Annex II–D, Section IID-3, the rain wind rose has most of the direction coming from Southwest. Calculation of the ratio between rain and air gives high values for Station 2 in the Northeast and low values for Station 4 in the Southwest. The measurement ratio has a high value in the Northeast but the other ratio are similar. There could be problems with the samples if they were not isolated from the air. The concentrations could have been enhanced by dry deposition on the measurement equipment. This may be an explanation for a ratio of rain to air measurement higher than for rain to air calculation.

(D29) Again we can try to understand the differences in model results by looking at the effect of certain parameters. The parameter values that have the major influence on rain concentrations are those for the washout coefficient and the intensity of precipitation. Results may be multiplied by a factor 10 if a coefficient of 1.3 10^{-4} is used instead of 10^{-5} s^{-1}. If we look at Figures D11 to D14, it can be seen that VNIIEF has calculated the lowest concentration because the modeller uses a low value for the washout coefficient.

TABLE D8. RATIOS OF TRITIUM CONCENTRATIONS IN RAIN TO CONCENTRATIONS IN AIR HUMIDITY

Participants	Station 1	Station 2	Station 3	Station 4
Measured	0.27	0.44	0.24	0.17
Belot	0.14	0.3	0.09	0.07
Beak	0.49	0.19	0.34	0.05
CEA	0.14	0.31	0.04	0.06
NIPNE (with topo. effect)	1.36	2.52	0.38	0.3
LLNL	0.2	0.50	0.13	0.11
RFNC-VNIIEF	0.09	0.07	0.04	0.05

LLNL should have calculated the highest concentration as the modeller uses the highest value for the washout coefficient (see Table D3). But in fact the intensity of rain was estimated by assuming that it rained 0.048 of the time. This was based on the rainfall duration given in Table II–D.1 of the scenario description (Annex II–D) for the period April – October (214 days) that was assumed to be the growing period and rainfall season. This results in lower rain concentrations being calculated. The difference in results between Belot, CEA and NIPNE is due to assumptions about the intensity of rain; NIPNE uses a different formula with rain intensity raised to a power 0.7.

D4.4. OBT CONCENTRATIONS

D4.4.1. OBT concentrations in beech tree rings

(D30) The tree ring samples came from a beech tree located 9 km east of the Valduc site (Station 5). Figure D15 shows the calculated and measured OBT concentrations in tree rings and Table D9 gives the ratio between calculated and measured values.

(D31) Except for LLNL, the results show a difference of a factor of about 3 between calculated and measured values. LLNL obtained lower concentrations than other participants because a lower OBT to HTO ratio was used (0.4 compared with 0.6).

TABLE D9. RATIOS OF CALCULATED TO MEASURED OBT CONCENTRATIONS IN BEECH TREE RINGS

Participants	Station 5
Belot	3.26
Beak	1.95
CEA	2.8
NIPNE (with topographic effect)	3.33
LLNL	1.76
RFNC-VNIIEF	2.4

D4.4.2. OBT concentrations in oak leaves

(D32) A map of OBT concentrations in oak leaves in the Valduc surroundings was drawn after a sampling and measurement campaign carried out in 1988. It gives insight into the geographical impact of tritium release upon the environment. Modellers were requested to calculate OBT concentrations for oak leaves for the year 1988 on a map grid of 30 km × 30 km (see Section D2).

(D33) Figure D16 shows the comparison between calculated and measured OBT concentrations in oak leaves and Table D10 gives the ratio of calculated to measured values obtained by the participants. The given value is the average of the ratio of the calculated concentrations over measured OBT concentrations at each point of the map grid. For all the participants, there is a good agreement between calculated and measured values, although there is a tendency to overpredict.

TABLE D10. RATIOS OF CALCULATED TO MEASURED OBT CONCENTRATIONS IN OAK LEAVES

Participants	Oak leaves
Belot	2.2
Beak	0.95
CEA	1.31
NIPNE (with topographic effect)	1.37
NIPNE (without topographic effect)	1.53
LLNL	0.92
RFNC-VNIIEF	1.57

D4.4.3. Discussion

(D34) For the year 1988, measured OBT concentrations in oak leaves are about 2 times higher than the OBT concentration in beech tree rings. The reasons for the differences have not been studied but may be due to species differences or different physiological processes occurring in beech tree rings compared with oak leaves. Modelling of OBT concentrations in oak leaves gives satisfactory results as calculated values are close to the measured values (Table D10). The oak leaf concentrations obtained by Belot are higher than those obtained for other participants even though the OBT/HTO ratio used was the same as, or lower than, the value used by other modellers (Tables D10 and D3). This is because Belot calculated higher concentrations of tritium in air because topographic effects were not taken into account, and a lower absolute humidity value and a roughness value of 1 m were used. These factors resulted in higher concentrations of HTO and OBT being calculated for the leaves.

(D35) A comparison between calculated and measured values for OBT concentrations in beech tree-rings (Table D9) shows that the calculated values are greater than the observed values by a factor of up to about 2.5. The overestimation is not very different from the overestimation of the HTO concentrations in leaf TFWT observed in grass. This seems to indicate that the overestimation of OBT in tree rings is probably due to the overestimation of HTO in the leaves of the trees. As OBT concentrations in oak leaves and in beech tree rings are both derived from tritium concentrations in plant TFWT by using the same coefficient (except for LLNL), (see Table D3), it would appear that the models give a better estimation of OBT in beech tree rings than OBT in oak leaves. However, the difference is only a factor of 1.5 to 2.5.

D5. CONCLUSIONS

(D36) The Valduc site is different from many other sites because of its topography. The Valduc area consists of a rolling terrain with moderate slopes and shallow valleys, and where elevational differences reach about 150 metres over several kilometres. The problem was to know if these elevational differences are to be taken into account in models by applying appropriate corrections or if they can be neglected. Some modellers have considered that the plume centre-lines were at constant elevation above the sea level and this resulted in relatively low air concentrations. In contrast, some modellers assumed that the centre-lines were at a constant height above ground level and the calculated concentrations were relatively high. The remaining modellers considered some intermediary deflection of the plumes and obtained intermediary results. From a comparison of the predicted with the observed values, it appears that the influence of topography is not very important for this site. Hence, a model for flat terrain that corresponds to a constant height of the plume above ground level can be applied with a resulting error of less than a factor of two. Nevertheless, it would be appropriate to apply a moderate correction of the plume height above ground level for such rolling terrain.

(D37) The main discrepancies in the results were for free plant tissue water concentrations and rain concentrations. Ratios of calculated air tritium concentration to free plant tissue water tritium concentration are very similar to observations (0.9 to 1.6); there is a factor of two difference compared to the measurement ratio. This difference could be attributed to the fact that only one sample was taken during a month and so there are too few values to be fully representative of a routine release. Concerning tritium concentrations in rain, results are in good agreement with observation for Station 2 that is in the main direction of the wind when it rains. For the other stations, there was a difference of up to factor of 6 between measured and calculated values. All the models calculated low values for concentrations in rain. One possible explanation could be due to the value for rain intensity used by the modellers. However, errors in sampling may also have contributed to the apparent discrepancies. For example, dry deposition on the rain collector equipment or the lack of isolation of the rainwater from the surrounding air could have resulted in sampling errors. In view of this, it is recommend that care is taken when sampling rain water. It is important to add a small amount of mineral oil to the collector to prevent exchange between the collected water and subsequent atmosphere vapour. The rain collector funnel should made of hydrophobic materials to prevent the formation of a film of water and dry deposition of tritium on its surface.

(D38) The OBT results show that concentrations in leaves are in quite good agreement with measurements (ratio from 0.92 to 1.5). The ratios of calculated to measured values of OBT concentrations in tree rings are between 1.8 to 3.3. Calculated values are 2 times higher than measurements. It is impossible to know if this difference is due to a lower contribution from the air.

(D39) It is difficult to deal with short term non-routine releases that result in high amounts of tritium being liberated as batches to the environment. These releases are usually detected and reported as releases from the various stacks, but there may also be releases under limit of detection. These releases cannot be modelled using steady state models. Such releases may lead to particular ‘spots’ of high tritium concentrations in some environmental media depending on the wind direction at the time of the release, the other meteorological parameters, and the duration of the event. Unlike steady state releases, a non-planned release detected at the stack may not have an effect on all the media compartments and therefore should not be taken into account in modelling. It is possible to remove high values due to a non-planned release on a case by case basis and so deal with the smoothed releases. In the present scenario, possible effects of the non-planned release on one or more of the compartments in some localities cannot be ruled out and this would account for an underestimation of modelling calculations for some tritium concentrations compared with the measurements.

(D40) The present exercise dealt with the prediction of tritium dispersion over a terrain of moderate relief. The problem was to know if, under such conditions, it was necessary or not to modify the classical Gaussian model to take into account topographic effects. The comparison of calculated results with observed data has shown that the topographic effect is not of paramount importance when the relief is only moderate and when concentrations are to be calculated at medium or long distances from the source(s). However, the model test exercise does not tell us if this conclusion is also valid at short distances from the source(s) or for more hilly terrain where the topographic effect might be more important.

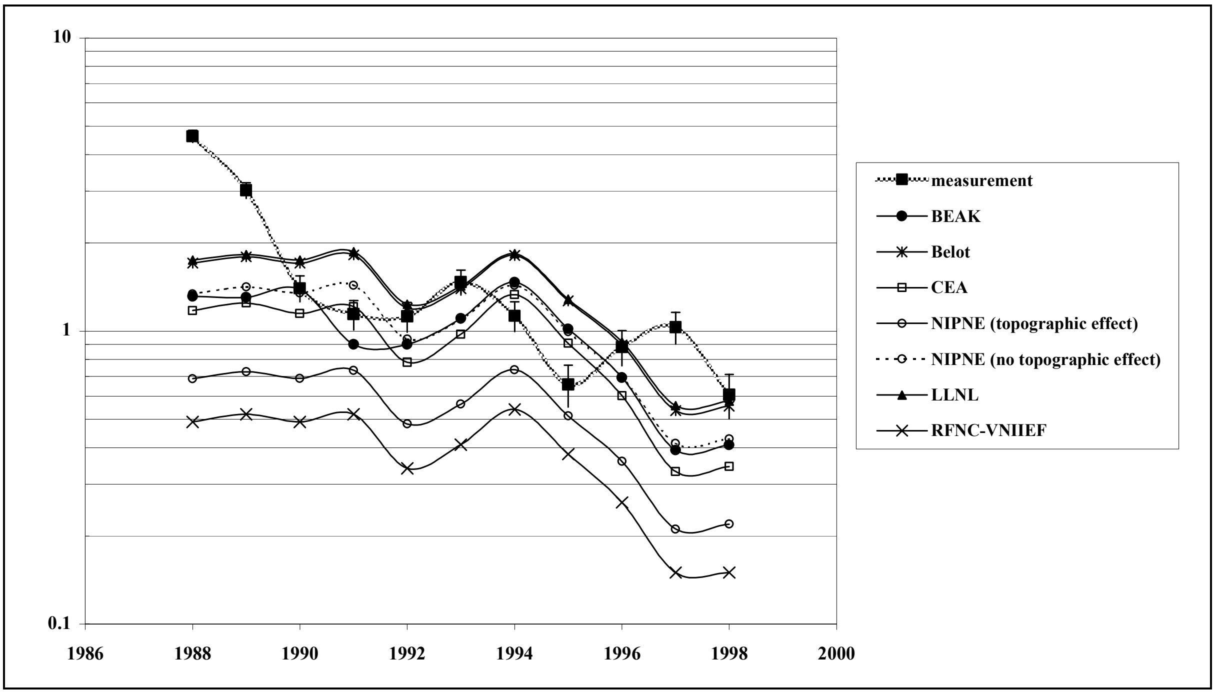

FIG. D1. Annual average tritium concentration in air (Bq m^{-3}) at Sampling Station 1.

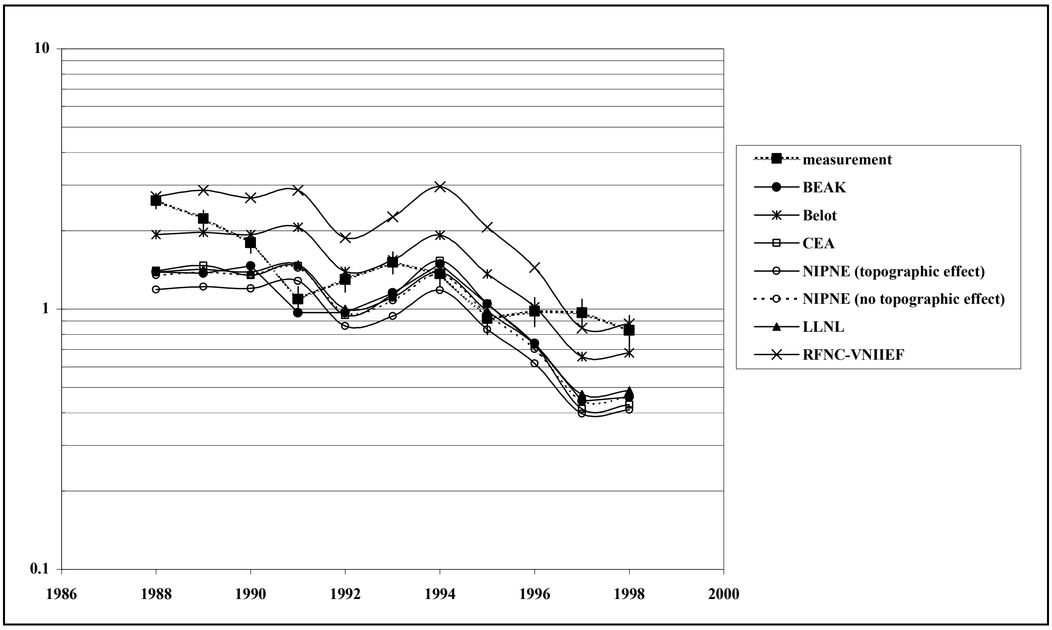

FIG. D2. Annual average tritium concentrations in air (Bq/m^3) at Sampling Station 2.

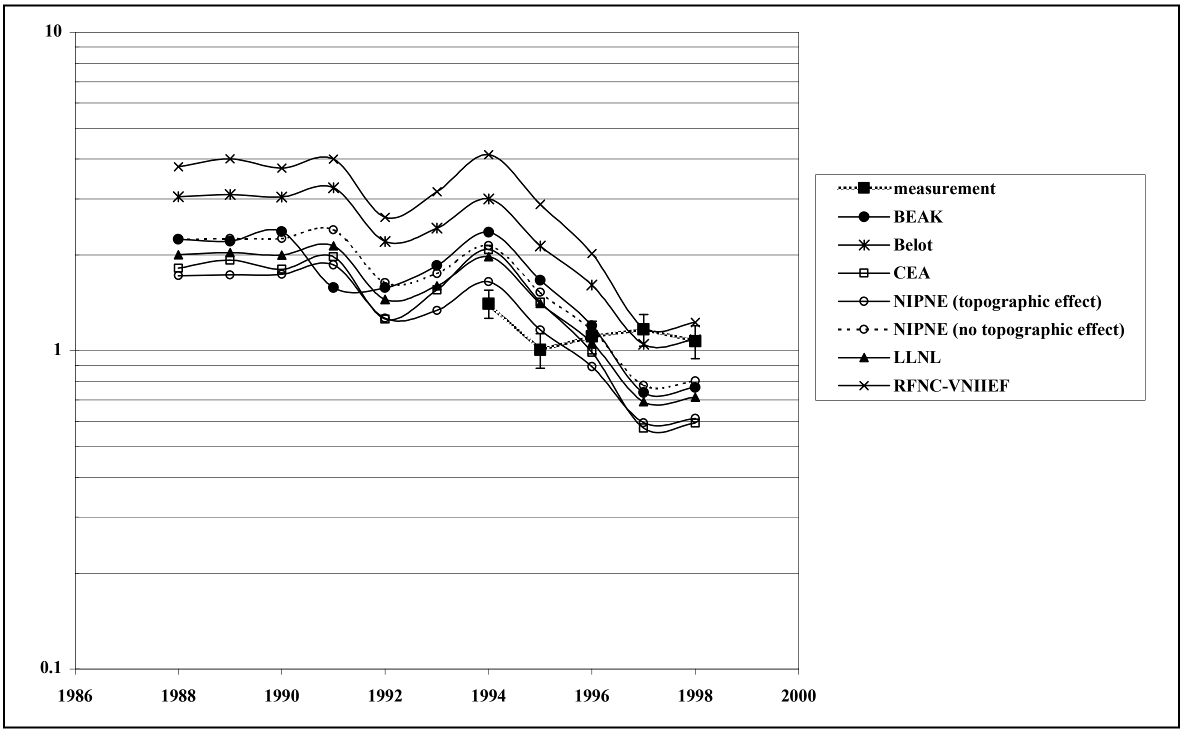

FIG. D3. Annual average tritium concentrations in air (Bq m^{-3}) at Sampling Station 3.

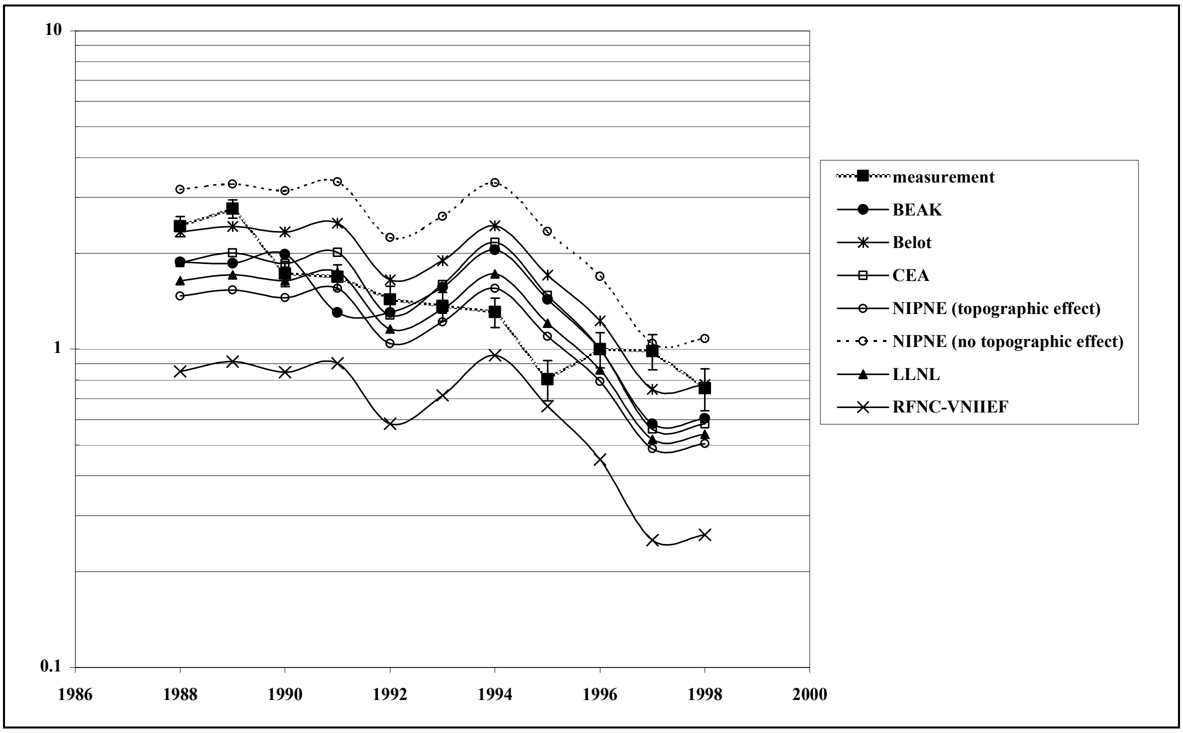

FIG. D4. Annual average tritium concentrations in air (Bq m^{-3}) at Sampling Station 4.

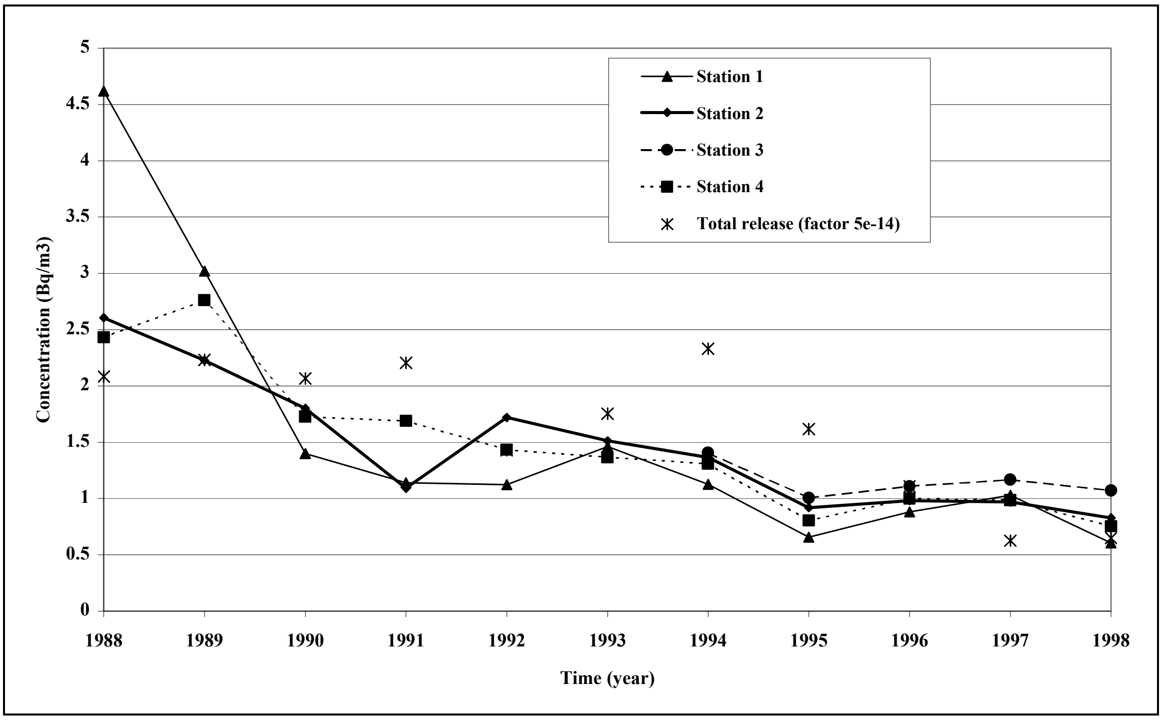

FIG. D5. Average annual tritium concentrations in air (Bq/m^3).

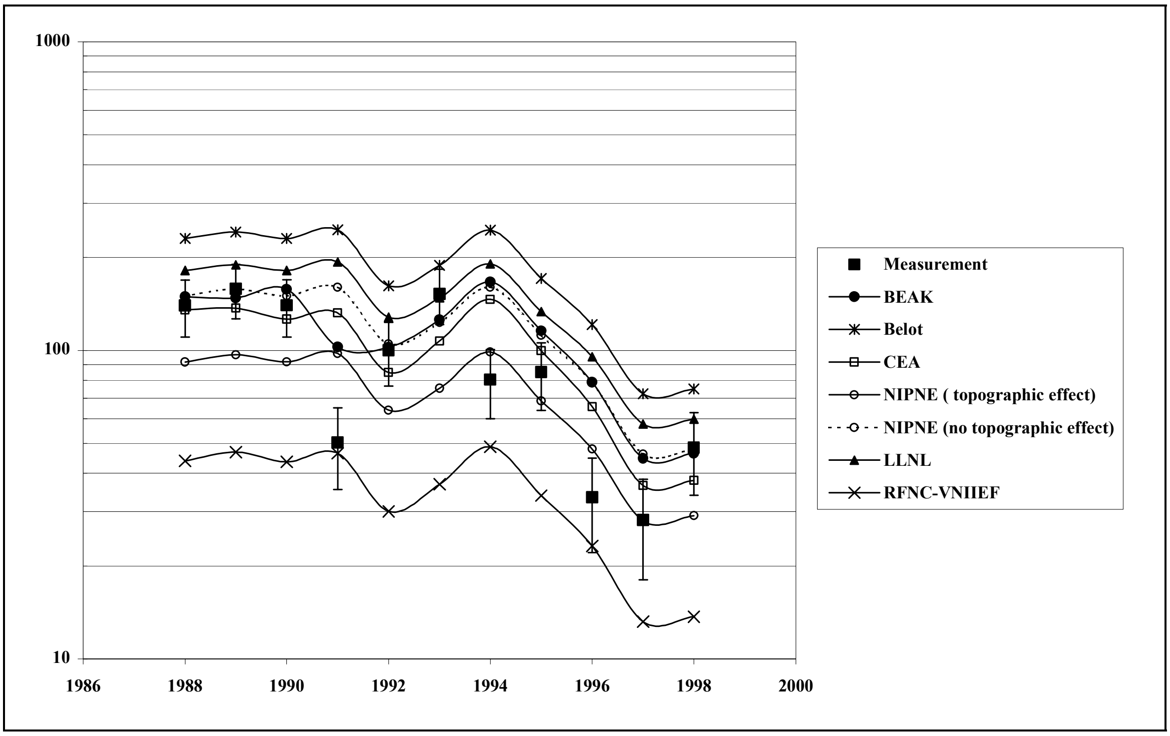

FIG. D6. Annual average tritium concentrations (Bq/l) in plant tissue free water at Sampling Station 1.

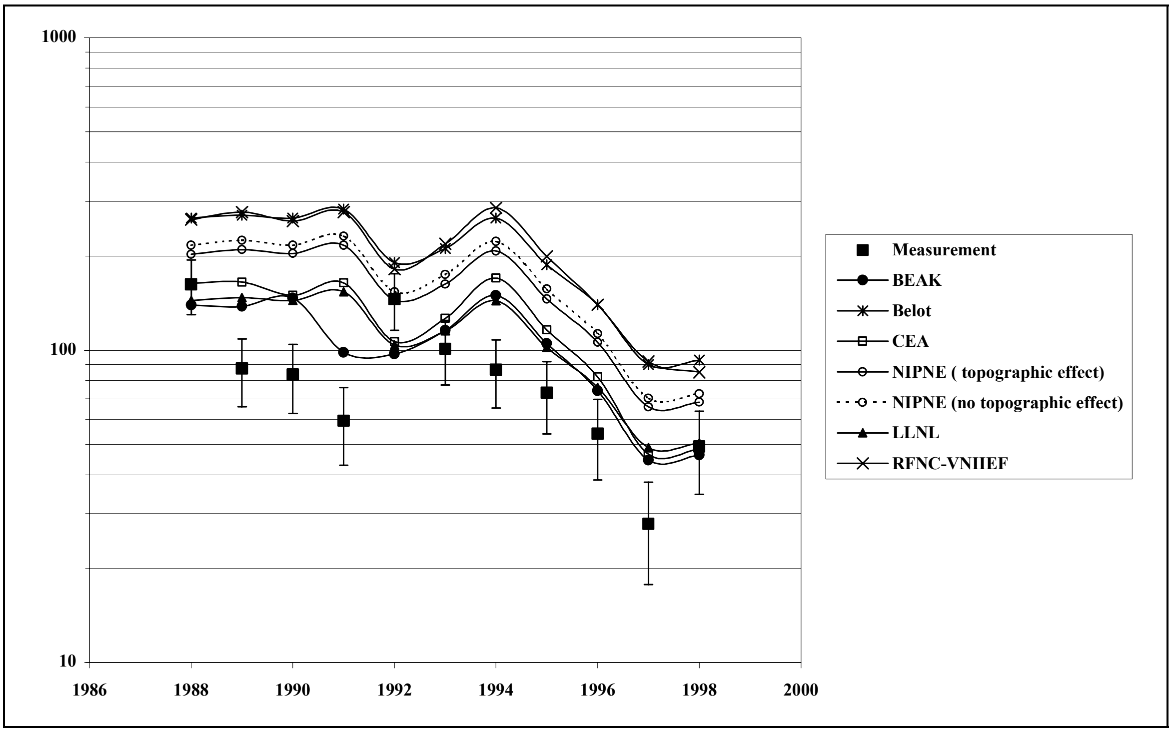

FIG. D7. Annual average tritium concentrations (Bq/l) in plant tissue free water at Sampling Station 2.

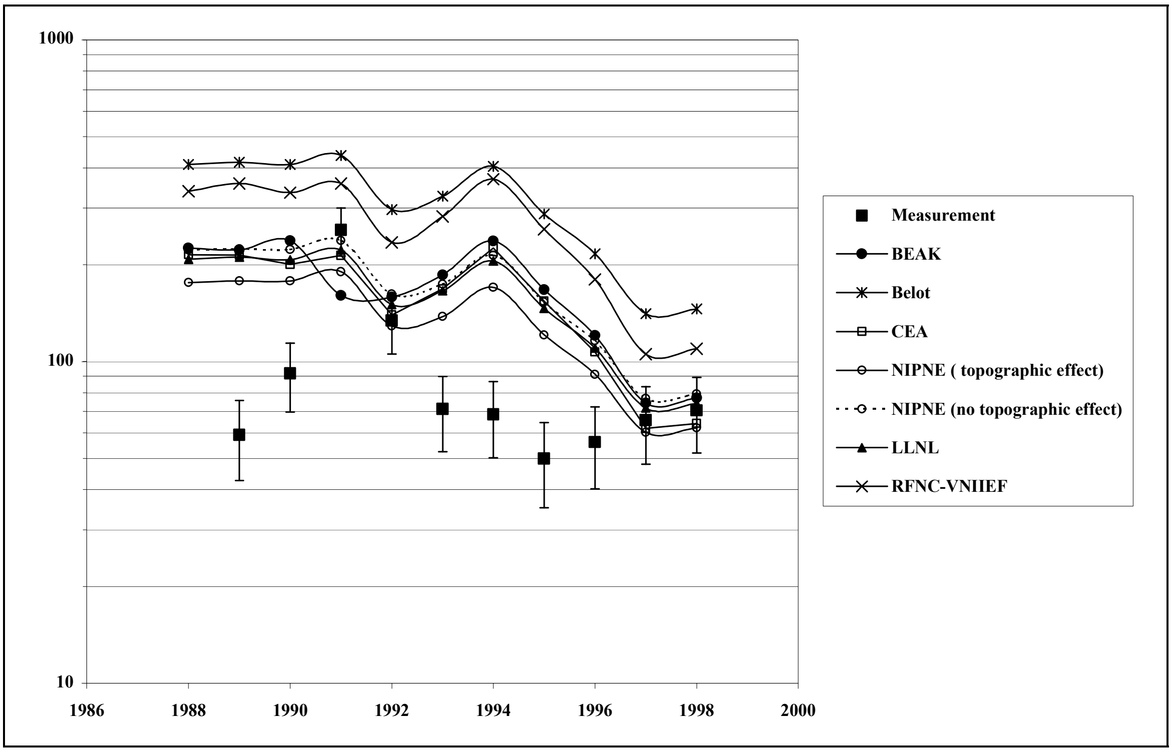

FIG. D8. Annual average tritium concentrations (Bq/l) in plant tissue free water at Sampling Station 3.

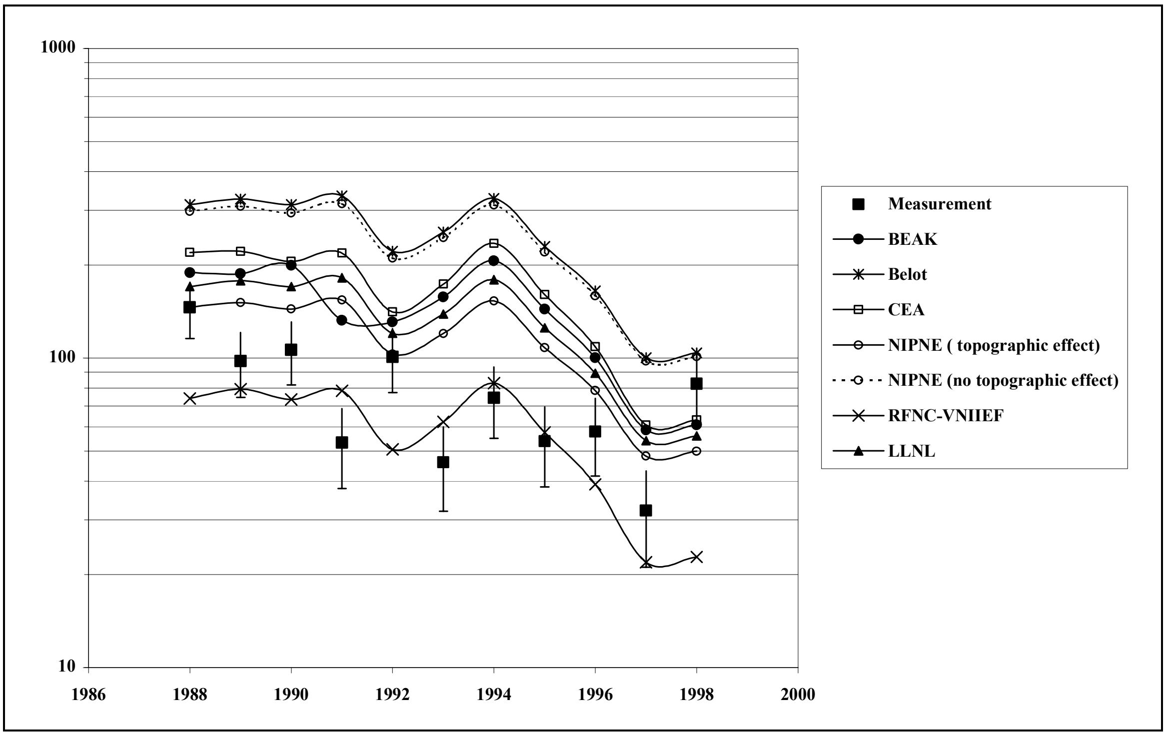

FIG. D9. Annual average tritium concentrations (Bq/l) in plant tissue free water at Sampling Station 4.

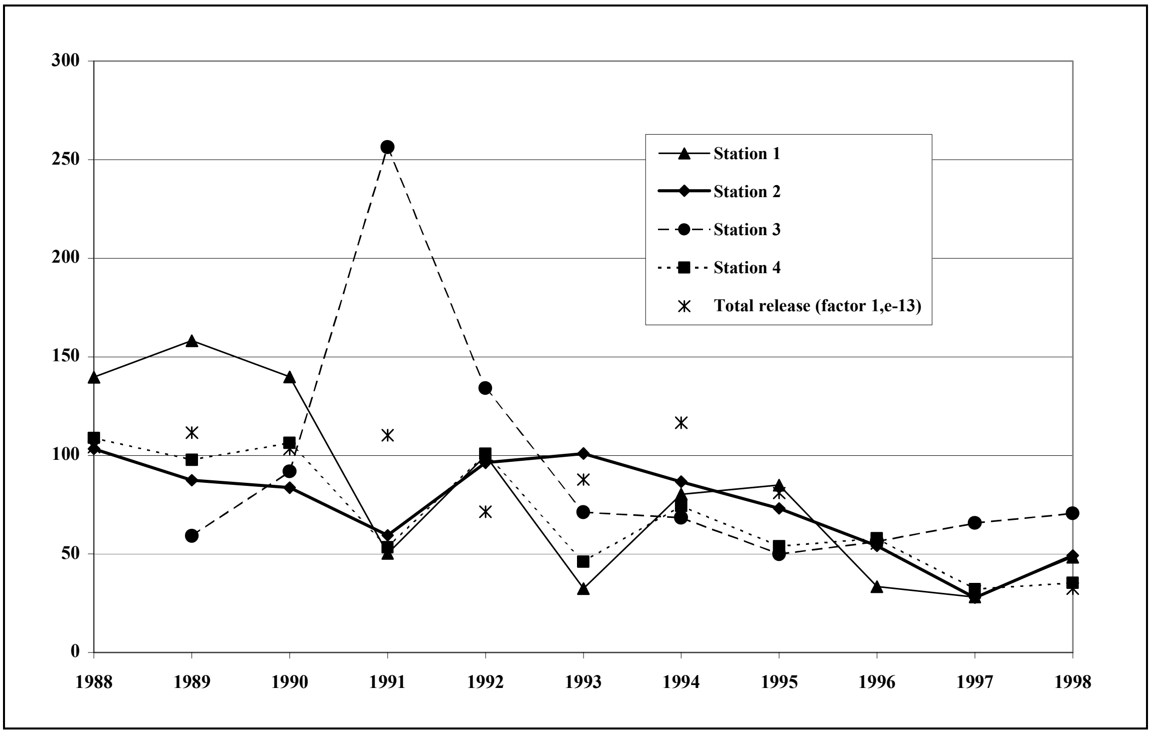

FIG. D10. Plant tissue free water tritium concentrations compared to release curve.

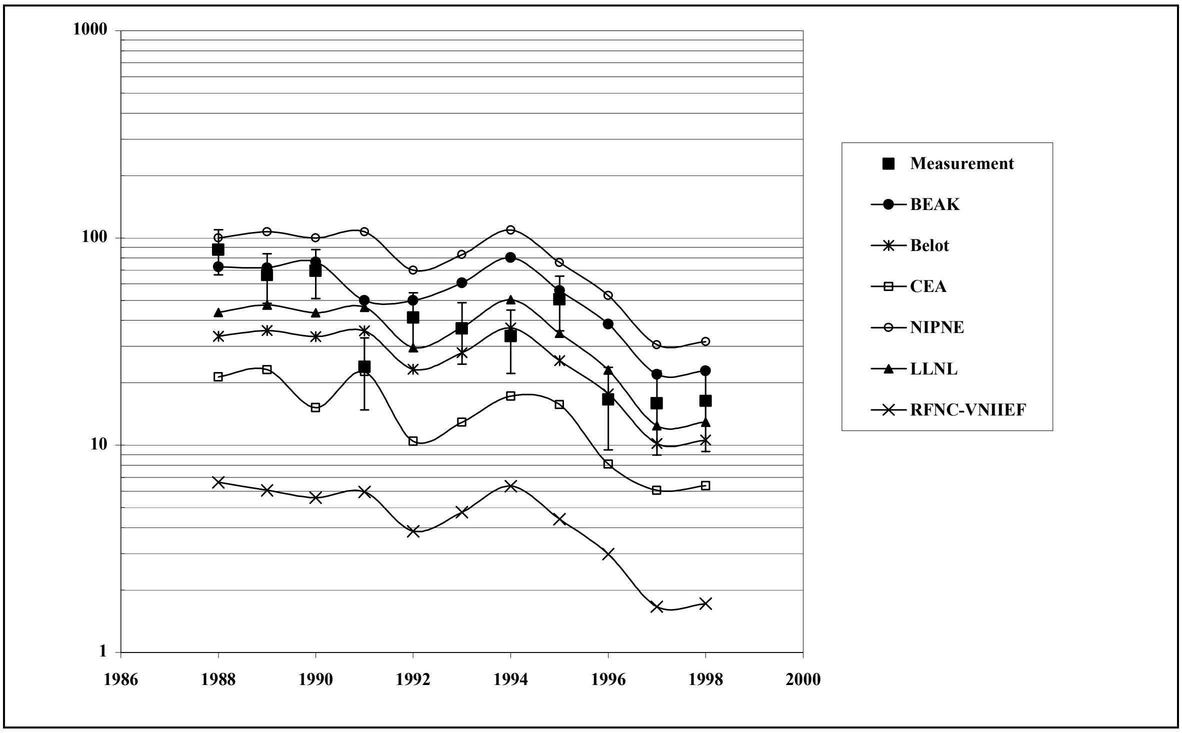

FIG. D11. Annual average tritium concentrations (Bq/l) in rainwater at Sampling Station 1.

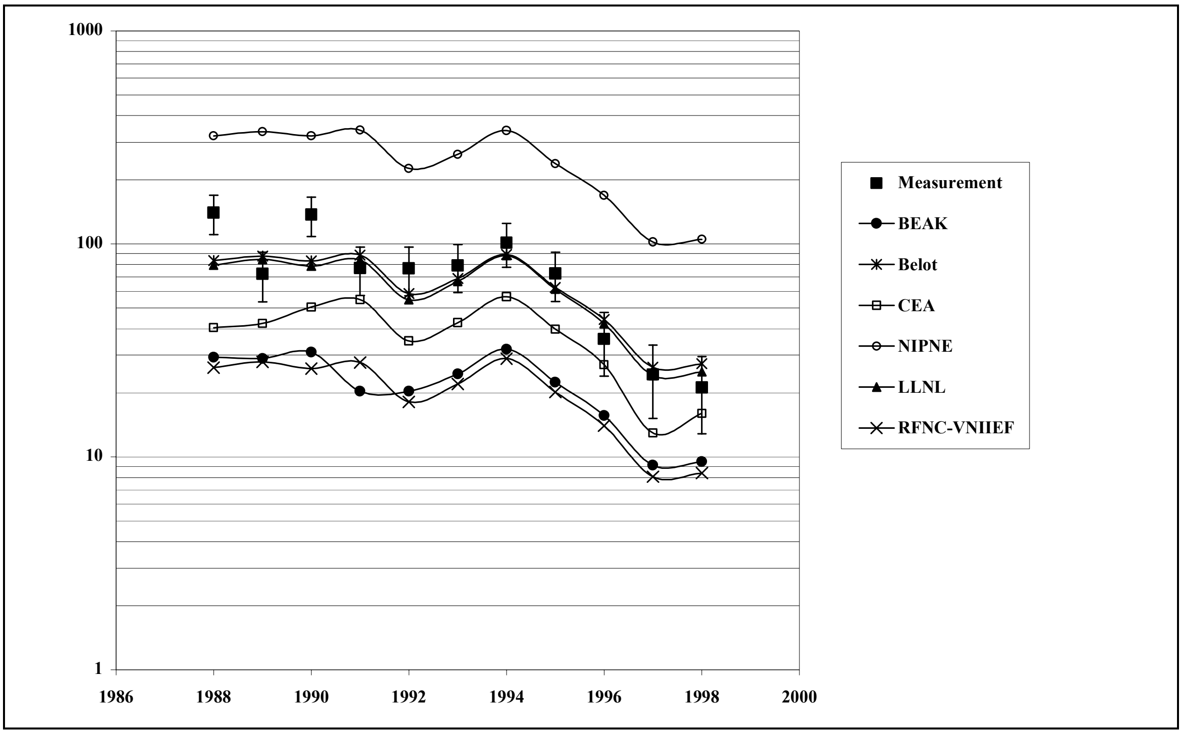

FIG. D12. Annual average tritium concentrations (Bq/l) in rainwater at Sampling Station 2.

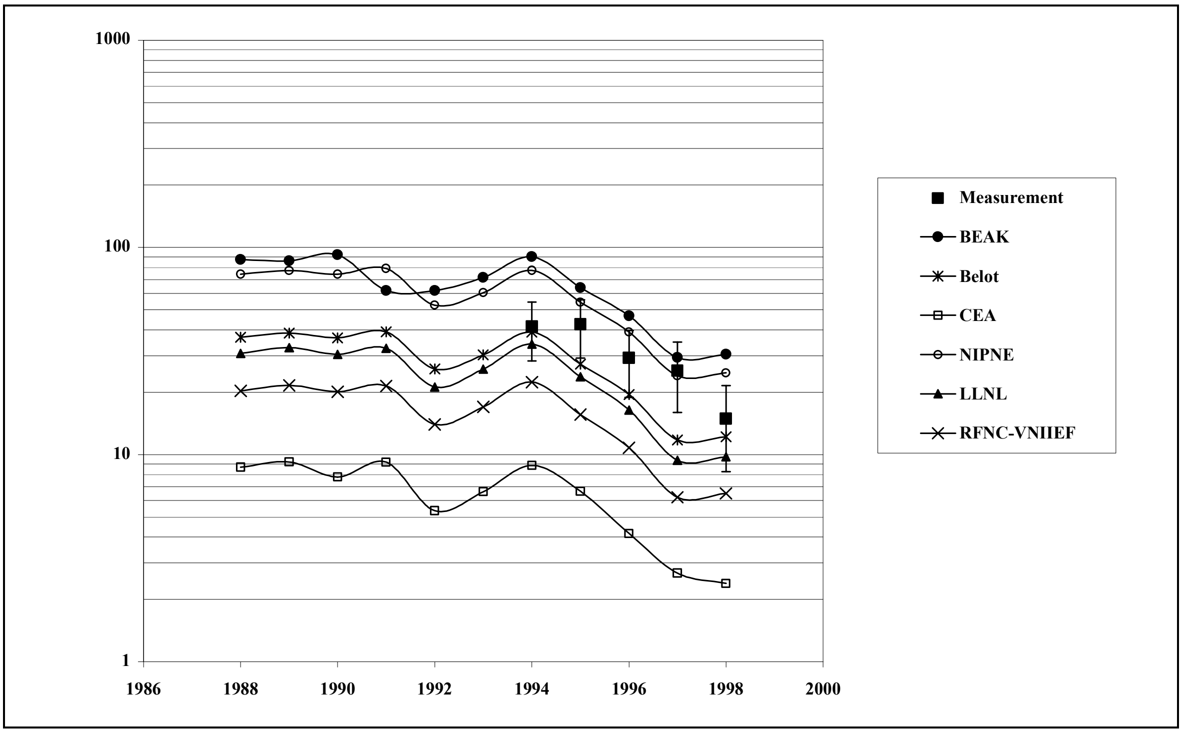

FIG. D13. Annual average tritium concentrations (Bq/l) in rainwater at Sampling Station 3.

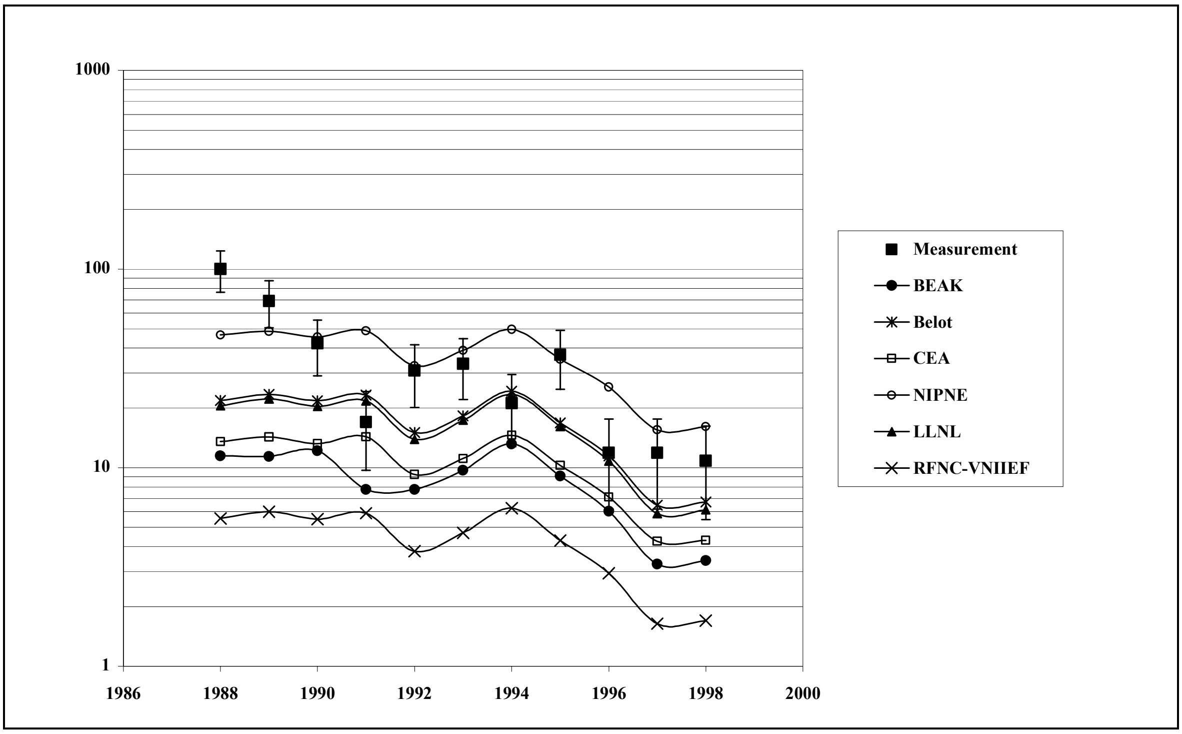

FIG. D14. Annual average tritium concentrations (Bq/l) in rainwater at Sampling Station 4.

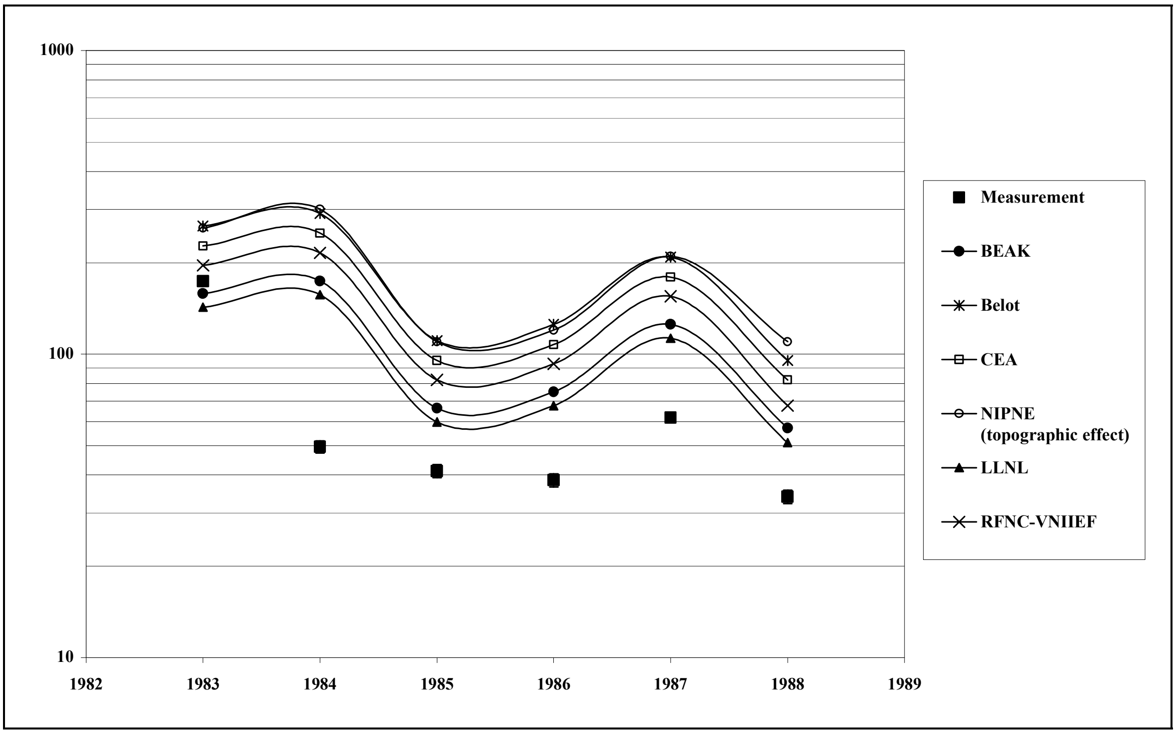

FIG. D15. Annual average tritium concentrations (Bq/l) in OBT in birch trees at Sampling Station 5.

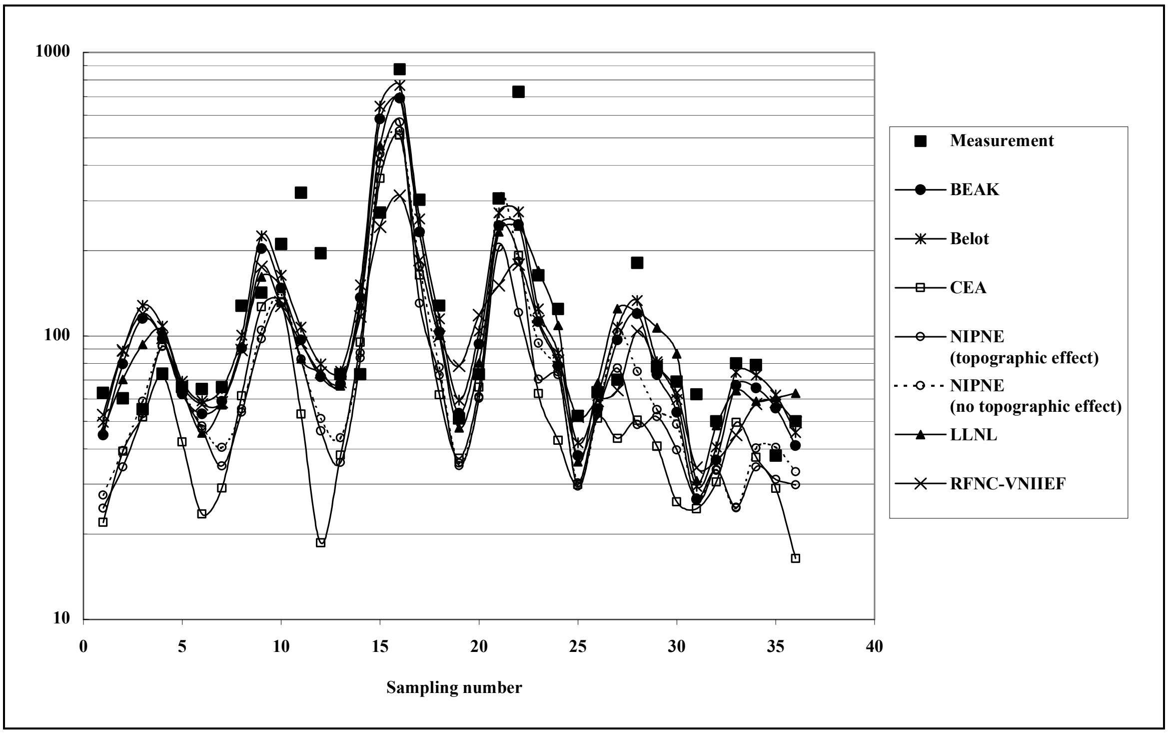

FIG. D16. Average OBT concentrations (Bq/l) in oak leaves for 1988.

PART E

MODELLING THE ENVIRONMENTAL TRANSPORT OF TRITIUM IN THE VICINITY OF PERMANENT ATMOSPHERIC SOURCES:

Model inter-comparison exercise on sub-surface infiltration pathways following long term atmospheric releases

E1. BACKGROUND AND OBJECTIVES

(E1) In the past, the modelling of atmospheric releases of tritium addressed mainly the determination of the doses that were delivered either to the workers on the site, or to the people living beyond the facility fence. Consequently, the endpoints of the dispersion models were generally the concentrations of tritium in air and plants that could be used as input to the dose calculations to assess impacts to humans. The concentration of tritium in groundwaters was rarely estimated because it was assumed that that the water below the site was not used for consumption. Nowadays, even though atmospheric releases have generally greatly decreased, the interest of the public and regulatory authorities has extended beyond the above ground environment to include the sub-surface media. In particular groundwaters are of interest because such water bodies may have become contaminated through previous releases at much higher levels either from atmospheric or sub-surface sources. Hence, groundwaters are considered as a potential source of delayed contamination for the above ground environment or those living in the vicinity. Consequently, there is a growing interest in estimating the concentration of tritium in groundwaters that have been exposed to contamination over a long period of time.

(E2) An early objective of the Tritium Working Group (TWG) was to develop modelling approaches in order to be able to predict vertical profiles of tritium concentrations in groundwaters arising from either atmospheric or sub-surface sources of tritium. The work reported in this part concerns tritium transport pathways arising from atmospheric sources; sub-surface sources are addressed in Part F.

(E3) A total of nine organisations participated in the study by submitting results, and others contributed to ideas and the discussion. The models employed were either existing codes that were adapted to address the requirements of the scenario, or newly developed codes. The range of models used encompassed a wide degree of complexity, from complex numerical models to simplified analytical formulae, all of them based on more or less simple representations of the physical processes involved in tritium transport.

E2. SCENARIO DESCRIPTION

(E4) An outline description of the first modelling test exercise was proposed to the TWG in December 1996 and part of this scenario (called Scenario 1.4) was concerned with the infiltration of contaminated water down through soil layers to the underlying aquifer. Scenario 1.4 is given in full in Annex II–E. This version of the scenario served as a basis for the requested calculations and the corresponding results presented here.

(E5) The scenario considers an idealised tritium facility that releases tritium in the form of HTO through a stack at a constant average rate (1 g y^{-1}), under meteorological conditions typical of a temperate climate. The part of the scenario concerned with atmospheric pathways has been described in Part A. For sub-surface pathways, it was agreed to consider the problem of an unconfined aquifer situated just below the emitting stack that extends from a flow divide to a surface stream. The scenario conditions were deliberately chosen to reduce the variations arising from scenario interpretation in order to be able to easily understand the modelling results. Nevertheless, realistic values were assigned to the vertical extent, the recharge rate and the permeability of the aquifer. Two sets of dispersivity coefficients, respectively high and low, depending on the nature of the terrain, were imposed for use by the modellers. The coefficients were taken from a review of experimentally determined field dispersivities (Gelhar et al., 1992).

(E6) The end-points to be calculated by modellers were vertical tritium concentration profiles in the aquifer using either low or high dispersivity values and with two different boundary conditions, after 20 years of atmospheric releases.

E3. DESCRIPTION OF TRANSPORT PROCESSES AND MODELLING APPROACHES

E3.1. TRANSPORT OF TRITIUM TO THE WATERTABLE

(E7) The vertical migration of tritiated water through the unsaturated layer is treated either in a simple way assuming that tritium moves by pure convection, or in a more realistic way assuming that tritium moves down by convection-dispersion with a certain dispersivity that depends on the structure of the permeable unsaturated layer. In the first treatment, the breakthrough of tritiated water through the watertable is a step function of time; in the second treatment the breakthrough can be represented by a sigmoid function whose slope is related to the dispersivity of the permeable layer.

(E8) In the present intercomparison exercise, most of the modellers considered only convection (piston-type flow). They determined the steady state flux of tritium at the watertable by a simple exponential function that expresses the decay of tritium during the time necessary for the infiltration water to percolate through the unsaturated layer down to the watertable.

(E9) Some modellers used a time-dependent analytical solution of the one dimensional convective-dispersive system that represents the movement of tritium in a real unsaturated layer where the dispersion is appreciable compared to the convection (Bear 1972):

$$\frac{S(h_s,t)}{S_0}=\frac{1}{2}\exp\left[\frac{v_r h_s}{2D}\left(1-\sqrt{1+\frac{4\lambda D}{v_r^2}}\right)\right]erfc\left[\frac{h_s-v_r t\sqrt{1+\frac{4\lambda D}{v_r^2}}}{\sqrt{4Dt}}\right]$$

$$+\frac{1}{2}\exp\left[\frac{v_r h_s}{2D}\left(1+\sqrt{1+\frac{4\lambda D}{v_r^2}}\right)\right]erfc\left[\frac{h_s+v_r t\sqrt{1+\frac{4\lambda D}{v_r^2}}}{\sqrt{4Dt}}\right] \qquad (1)$$

where:

$S(h_S,t)$ is the flux of tritium that passes through the watertable at a depth h_S and time t after the beginning of the release (Bq m^{-2} s^{-1}); and

D is the dispersion coefficient that represents all effects of random nature due to diffusion and fluctuations of the convection velocity and can be expressed by the formula $D=D^{*}+A_W v_r$, ($m^2\ s^{-1}$).

where:

D^{*} is the coefficient of molecular diffusion in the porous medium ($m^2\ s^{-1}$);
A_W is the dispersivity of the medium (m); and
v_r is the average pore water velocity determined from infiltration rate and porosity ($m\ s^{-1}$).

E3.2. TRANSPORT AND DECAY OF TRITIUM IN GROUNDWATER

E3.2.1. Numerical modelling approach

(E10) Figure 1 in Scenario 1.4 (i.e. Figure II–E.1, Annex II–E) shows an idealised representation of the unsaturated-saturated subsurface flow system to be modelled herein. It shows a section of the unconfined aquifer extending from a groundwater divide to a stream. The aquifer is specified in Scenario 1.4 as an unconfined aquifer resting on a horizontal impervious surface, with a distance L = 10 km between the flow divide and the stream, a Darcy recharge rate $V_r = 0.15\ m\ y^{-1}$, and a uniform hydraulic conductivity $K = 3154\ m\ y^{-1}$ ($10^{-4}\ m\ s^{-1}$). The aquifer is considered to be in steady state hydraulic conditions, assuming a 20-year simulation time and small negligible seasonal watertable fluctuations.

(E11) The steady state groundwater flow is simulated either as two dimensional in the vertical plane, or as three dimensional, allowing for water velocity determination at each point of the aquifer. The formulation is expressed as:

$$\frac{\partial}{\partial x_i}\left(K_i \frac{\partial h}{\partial x}\right) = 0 \qquad (2)$$

where:

x_i are the horizontal and vertical coordinate directions (m);
K_i is the uniform hydraulic conductivity ($m\ y^{-1}$); and
h is the hydraulic head (m).

This simulation approach assumes a saturated, steady state flow field, and a non-deforming porous medium. Boundary conditions consist of an average recharge rate V_r ($m\ s^{-1}$) across the upper watertable boundary, a no-flow condition at the upstream groundwater divide and along the bottom impervious layer, and a constant head h_0 at the downstream boundary.

(E12) The governing equation for transient advective-dispersive mass transport of a dilute species undergoing first-order decay within the porous saturated medium of the aquifer can be classically written as:

$$\frac{\partial c}{\partial t} = D_i \frac{\partial^2 c}{\partial x_i^2} - \frac{\partial}{\partial x_i}(v_i c) - \lambda c \qquad (3)$$

where:

x_i are the spatial coordinates (m);

v_i is the average pore water velocity (m s^{-1});
D_i is the hydrodynamic dispersion coefficient (m^2 s^{-1});
λ is the decay rate (s^{-1});
t is the time (s); and
c is the concentration of tritium in the groundwater (Bq m^{-3}).

The hydrodynamic dispersion coefficient D_i is assumed to be $D_i = \alpha_i v_i$, where α_i is the field macrodispersivity (Gelhar et al., 1992). The velocity v_i in (8) is obtained from the Darcy relationship $v_i = (K/p)\partial h/\partial x_i$ where p is the effective porosity and h is the solution of (7).

(E13) The tritium transport simulation uses either a Dirichlet's or Cauchy's boundary condition, depending on whether a prescribed concentration or a prescribed flux is used at the watertable boundary. Cauchy's boundary condition represents continuity of mass flux across an external boundary and is written:

$$V_r C_0 = v_n c - D_n \frac{\partial c}{\partial \underline{n}} \tag{4}$$

where:

$V_r C_0$ is a known mass flux term at the boundary; and
$\underline{n}$ is the unit normal vector at the boundary.

The condition expresses the fact that the rate at which tritium is transported into the groundwater is equal to the rate at which it crosses the watertable by combined flow and diffusion. At all remaining transport boundaries, including the outflow, a zero-concentration gradient condition is generally applied. The initial background tritium concentration at the beginning of the 20-year release period is assumed to be zero.

(E14) The groundwater flow and tritium transport simulations are generally made using a finite difference or finite element model capable of simulating steady state groundwater flow and transient advective-dispersive mass transport with linear decay. The numerical implementation of the above equations is detailed in the model descriptions (Annex I–B).

E3.2.2. Tentative analytical modelling approach

(E15) Some participants have been attracted by the advantages of using analytical dispersion models similar to those currently used in atmospheric dispersion predictions. As this approach is not often used in hydrogeology, there was a need to examine if this treatment was feasible and could give rise to satisfactory results, at least in certain cases, compared to the more classical but more complex method described above. It was felt that an analytical solution, even if restrictive regarding the conditions of application, would possess a greater flexibility and would not suffer from some of the difficulties that may be associated with numerical solutions.

(E16) The method tentatively used herein to derive an analytical expression of the transient dispersion of tritium in the steady flow of an aquifer is based on solving the advective-dispersive partial differential equation by the use of 'Green's functions', otherwise called 'impulse responses' in the terminology of signal theory. A Green's function is simply the concentration as a function of time and space arising from a unit instantaneous source.

(E17) The current problem can be reduced to the estimation of dispersion in a vertical 2D-plane. The concentration of tritium at horizontal distance x from the flow divide, at depth z below the watertable, at time t after beginning of release, is:

$$c(x,z,t)=\int_0^t\int_{l_1}^{l_2} g_1(\xi,\tau;x)g_3(\xi,\tau;z)\exp(-\lambda\tau)d\xi d\tau \tag{5}$$

where:

g_1 and g_3 are the Green's functions for the transport of tritium in the x and z-directions;
l_1 and l_2 are empirical limits of integration along the x-axis;
τ is the time of an elemental release of duration $d\tau$. ;
ξ is the distance of the flow divide to the watertable source-element of width $d\xi$.

(E18) Function g_1 refers to the transport of tritium in the horizontal x-direction which is practically unbounded. This function is known to be Gaussian with a shift to account for main water flow in the x-direction:

$$g_1(\xi,\tau;x)=\frac{1}{\sqrt{4\pi D_x\tau}}\exp\left[-\frac{(x-\xi-u\tau)^2}{4D_x\tau}\right] \tag{6}$$

where:

u is the main horizontal component of the pore water velocity (m s^{-1}); and
$D_x=\alpha_x u$ is the dispersion coefficient in the x-direction, defined as above (m^2 s^{-1}).

In the central part of the aquifer, the horizontal velocity u varies only moderately with x and can be assumed here to be constant in the field of interest.

(E19) Function g_3 which refers to the transport of tritium in the vertical z-direction is more complicated because of the watertable boundary condition. Function g_3 is the solution obtained for the instantaneous injection of a tracer at the boundary of a semi-infinite bed. The following solutions were reported by Kreft and Zuber (1978) for a prescribed-flux condition or a prescribed-concentration condition respectively:

$$g_3(\xi,\tau,z)=\frac{F(\xi)}{p}\left\{\frac{2}{\sqrt{4\pi D_z\tau}}\exp\left[-\frac{(z-w\tau)^2}{4D_z\tau}\right]-\frac{w}{2D_z}\exp\left(\frac{wz}{D_z}\right)\operatorname{erfc}\left(\frac{z+w\tau}{\sqrt{4D_z\tau}}\right)\right\} \tag{7}$$

$$g_3(\xi,\tau;z)=c_0(\xi)\frac{z}{\sqrt{4\pi D_z\tau^3}}\exp\left[-\frac{(z-w\tau)^2}{4D_z\tau}\right] \tag{7 bis}$$

where:

w is the vertical component of the pore water velocity (m s^{-1});
$D_z=\alpha_z u$ is the dispersion coefficient in the z-direction (m^2 s^{-1});
z is the depth of the sampling point below the watertable, positive downward;
p is the effective porosity of the aquifer;

F is the tritium flux density per unit area of the watertable (Bq m^{-2} s^{-1}); and
c_0 is the concentration of tritium at the watertable.

The main approximation in the analytical expression above resides in the assumption that the field of water velocity is uniform in a vast domain around the sampling point. In a real situation, this is not exactly true, but the approximation is not totally unrealistic since, in a large domain of the aquifer, *u* and *w* vary only moderately with *x* and *z*.

(E20) The height of the watertable above the aquifer bottom, *h*, and the horizontal and vertical pore water velocity, *u* and *w* respectively, are given from the water balance of the unconfined aquifer by:

$$h = \left[h_0^2 + \frac{V}{K}(L^2 - x^2) \right]^{1/2}$$

$$u = \frac{V}{p}\frac{x}{h}$$

$$w = \frac{pu^2}{K}\left(1 - \frac{z}{h}\right) \qquad (8)$$

where:

h_0 is the height of the watertable at the receiving stream (m);
p is the effective porosity of the aquifer;
x is the horizontal distance of the flow divide to the sampling point oriented positive in the direction of groundwater flow (m);
K is the permeability of the aquifer (m s^{-1});
L is the distance from the flow divide to the receiving stream (m); and
V is the Darcy vertical recharge rate (m s^{-1}).

The velocities u and w decrease with *x* and *z*, but only at a moderate rate in the central part of the aquifer where the flow is nearly horizontal. In this central domain, *u* and *w* can be considered, in a first approximation, as nearly constant and equal to the values estimated from (8) at the distance *x* of the sampling point and level $z = 0$ of the watertable.

(E21) Other analytical models have been tentatively applied by two of the participants: (i) the 1-D vertical transient diffusive-convective Bear's formula (1) given above; (ii) the 2-D Gaussian formula which is classically used for predicting atmospheric dispersion under steady state conditions.

E4. RESULTS AND DISCUSSION

(E22) Nine participants undertook the calculations related to the aquatic pathway as a result of infiltration through the overlying unsaturated soil layer on the basis of Scenario 1.4. These results are presented below. The transport processes and the general modelling approaches have been described in Section E3.1 and E3.2. A brief comparison of modelling approaches can be found in Table E1. Detailed descriptions of individual models are given in Annex I–B.

(E23) Figures E1 and E2 show the vertical profile of HTO concentration in groundwater 1 km downstream from the source, with the boundary condition of a prescribed constant flux at the watertable, for low and high dispersivity respectively:

— In the case of a low vertical dispersivity of 0.05 m (Figure E1), the concentration of tritium just within the entrance of the aquifer at z = 0, is not very different from the concentration of tritium in the entering vertical stream. All the curves obtained lie close together within a factor of two, and show concentrations decreasing by a factor of one thousand at a depth of about 40 m below the watertable, which indicates a low vertical mixing rate. Three of these curves are based on very elaborate numerical models and four of them are based on relatively simple analytical models that have been adapted to the conditions of the scenario (cf. Table E1).

— In the case of a high vertical dispersivity of 0.5 m (Figure E2), there is a significant decrease of concentration at the passage of the watertable, owing to the predominance of dispersion over convection. As in the previous case, the curves lie close together and give similar values within a factor of two, but show a reduction in concentration of only ten at the bottom of the aquifer. This indicates a very high vertical mixing rate, as could be expected from the high vertical dispersivity that was assumed in the calculation.

(E24) Figures E3 and E4 refer to the vertical profiles of HTO concentration in groundwaters, with the boundary condition of a prescribed constant concentration at the watertable, for respectively the same low and high dispersivity as considered above. With this new boundary condition, the concentration is strictly the same on each side of the watertable at z = 0, for any value of the vertical dispersivity:

— In the case of low dispersivity (Figure E3), five curves lie close together. An isolated curve diverges appreciably from the others, by showing a much reduced vertical mixing. No explanation can be found for the divergence between this curve and the others. The five grouped curves are very similar to those previously obtained for low dispersivity for the case of a prescribed-flux condition.

— In the case of high dispersivity (Figure E4), there are also five curves that lie close together and, as above, two curves that differ appreciably from the others due to some error that has not been identified until now. The five consistent curves are quite different from those obtained for the case of high dispersivity with a prescribed-flux condition. This dissimilarity is explained in the next paragraph.

(E25) In the calculations above, two ways of defining the watertable boundary condition have been addressed, which leads to very dissimilar results in the case of high dispersivity. The main difficulty then consists in choosing, among the two different boundary conditions, the one that is the most suitable to describe adequately a real situation. This problem was formerly considered by Kreft and Zuber (1978). These authors studied the physical meaning of the dispersion equation and its solutions for different boundary conditions. They have shown that the different boundary conditions correspond to different ways of measuring the solute concentration. The prescribed-flux condition corresponds to a measure of the solute in the resident fluid at a given fixed point, while the prescribed concentration condition corresponds to a measure of the solute in the fluid passing through a given cross section. If one wishes to estimate the concentration of tritium in the resident fluid of the aquifer, which is the quantity one tries to measure in the field, it is more appropriate to use the prescribed flux boundary condition rather than the prescribed concentration boundary condition.

(E26) It appears from the results that the shape of the vertical profiles of tritium concentration in the aquifer is very sensitive to the value of the vertical dispersivity. For the high dispersivity values used herein, appreciable amounts of tritium invade the aquifer down to its bottom. In contrast, for the low dispersivity values, the vertical mixing of tritium appears to be very limited, even after a few decades of atmospheric releases, which leads to a stratification of most of the tritium in the upper part of the aquifer. In a real situation, the vertical mixing of tritium in an aquifer will depend greatly on the dispersive properties of the aquifer. In a critical review of data on field-scale dispersion in aquifers, Gelhar et al. (1992) insist on the fact that very low vertical dispersivities have been observed at many sites, and that the high values sometimes advanced should be considered with caution.

E5. CONCLUSIONS

(E27) This model-model intercomparison research exercise concerning HTO infiltration to groundwaters, has shown that the results were dependent on the choice of the boundary condition at the watertable, and of the dispersivity of the medium. It was agreed that it was appropriate to choose a prescribed flux boundary condition, rather than a prescribed concentration boundary condition. It was shown that the results were very sensitive to the dispersivity parameter, and that the value of this parameter must be selected very carefully from the data available in the literature. In the simple yet realistic conditions of the scenario, it was verified that many numerical or analytical models arrived at similar results. But this did not mean that both approaches could be used equivalently in any situation, since it was evident that certain heterogeneities encountered in real situations could only be treated by numerical simulation. The experience gained in the model-model intercomparison showed that the correct use of numerical models for this specific problem was rather sensitive, and full attention had to be paid to the time and space discretisation used in the model.

TABLE E1. COMPARISON OF MODELLING APPROACHES USED IN THE MODEL-MODEL INTERCOMPARISON EXERCISE BASED ON SCENARIO 1.4 (GROUNDWATER TRANSPORT)

Institution (Modeller)	Steady Water Flow in Unconfined Aquifer determined from:	HTO Transport in Aquifer determined from:
ANDRA (C. Meurville)	MODFLOW code (USGS) 3D finite-difference Preconditioned conjugate gradient method	MT3D code (SSP&A). 3D explicit finite-difference.
BEAK (D. Lush)	*Not considered*	IMPACT code: 1D vertical transport equation solved by an explicit finite difference technique. Constant concentration at watertable.
Consultant (Y. Belot)	Analytical approximations of the horizontal and vertical velocities (flow conservation)	2D analytical solution of the transient transport equation, obtained by integration of impulse responses.
CEA (G. Guinois)	METIS code (Ecole des Mines) 3D finite-element module	METIS code. Transient transport finite-element module.
FZK (W. Raskob)	Analytical approximation of the horizontal velocity Vertical velocity assumed negligible	2D Gaussian solution of the steady state transport equation.
NIPNE (D. Galeriu)	Analytical approximations of the horizontal and vertical velocities (flow conservation)	Analytical solution.
STUDSVIK (O. Edlund)	Analytical approximations of the horizontal and vertical velocities (flow conservation)	2D analytical solution of the transient transport equation, obtained by integration of impulse responses.
VNIIEF (A. Golubev))	Analytical solution of the hydraulic equation	Transport equation solved by a finite-difference method.
ZSR (M. Täschner)	Analytical approximation of the horizontal velocity Vertical velocity equal to infiltration velocity	1D analytical solution of the transient transport equation.

REFERENCES TO PART E

[1] BEAR, J., Dynamics of Fluids in Porous Media, Elsevier, New York (1972).

[2] GELHAR, L.W., WELTY, C., REHFELDT, K.R., A critical review of data on field-scale dispersion in aquifers, Water Resour. Res. **28** (1992) 1955–1974.

[3] KREFT, A., ZUBER, A., On the physical meaning of the dispersion equation and its solutions for different initial and boundary conditions, Chem. Engng. Sci. **33** (1978) 1471–1480.

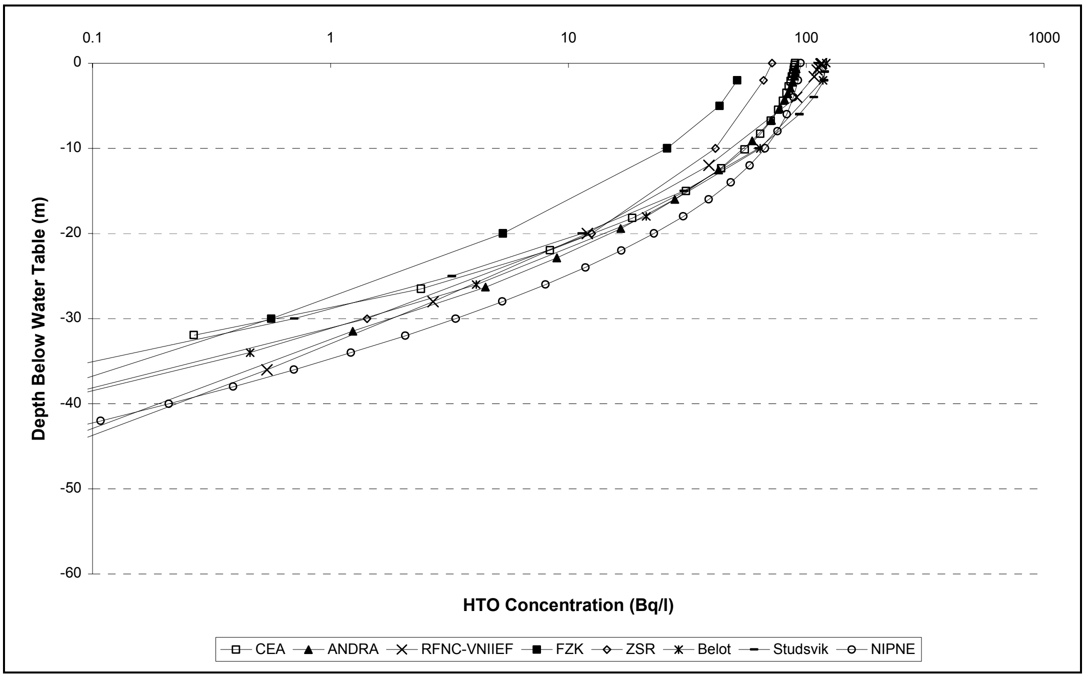

FIG. E1. Vertical profile of HTO concentration in an aquifier 1km from the HTO source and at 20 years after steady state has been achieved at the water table; low dispersivity, prescribed-flux boundary condition.

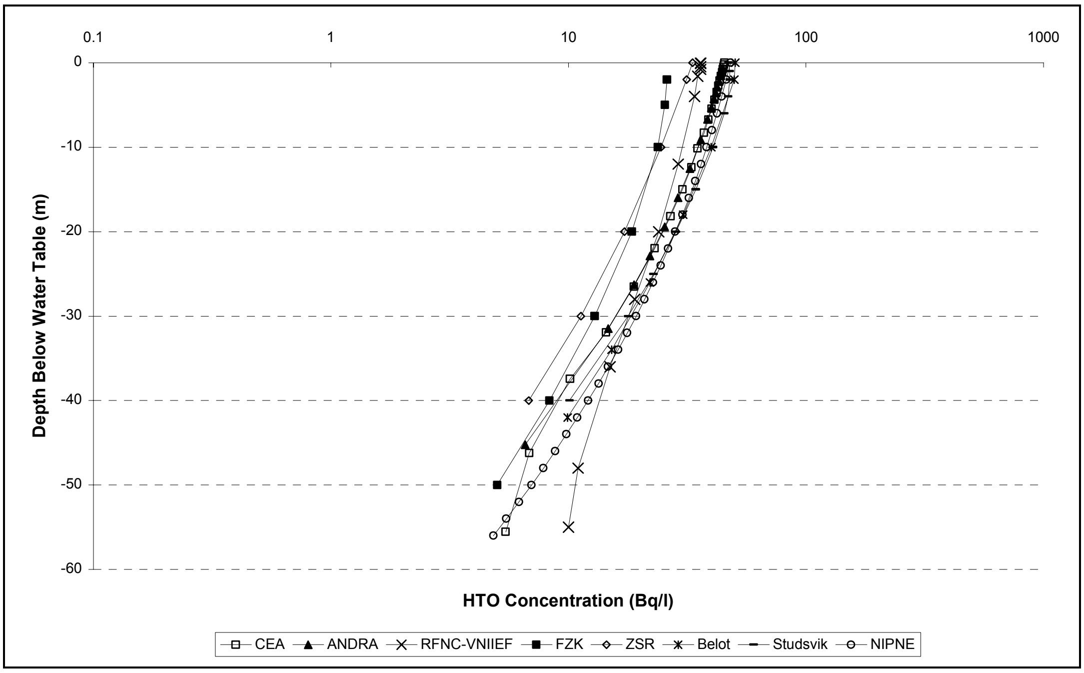

FIG. E2. Vertical profile of HTO concentration in an aquifier 1km from the HTO source and at 20 years after steady state has been achieved at the water table; high dispersivity, prescribed-flux boundary condition.

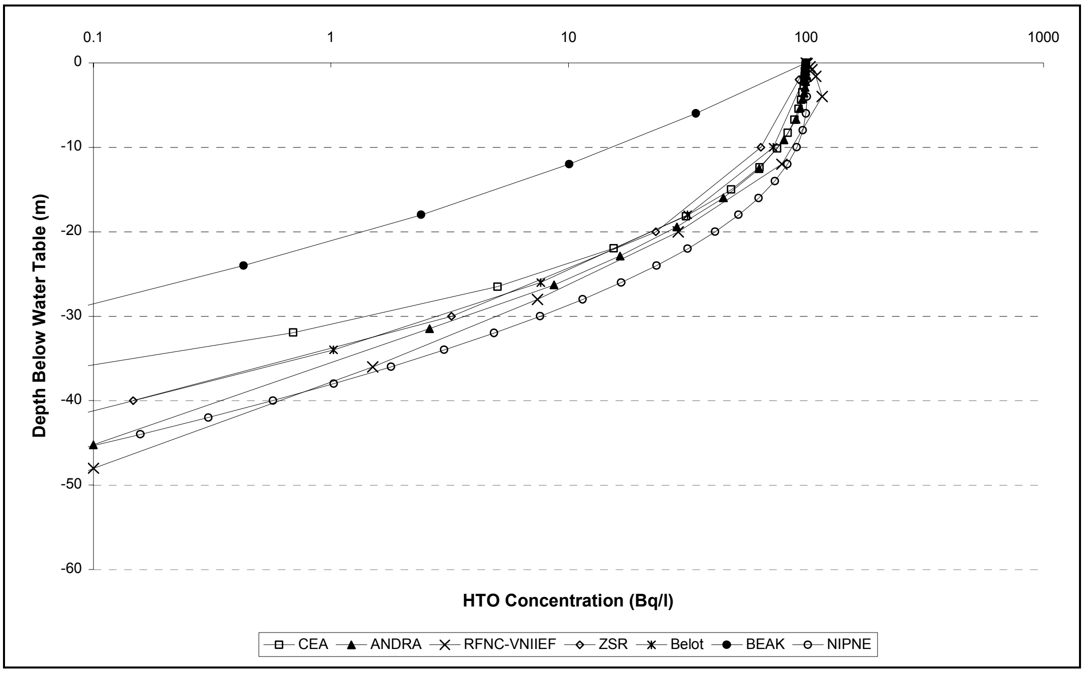

FIG. E3. Vertical profile of HTO concentration in an aquifer 1km from the HTO source and at 20 years after steady state has been achieved at the water table; low dispersivity, prescribed-concentration boundary condition.

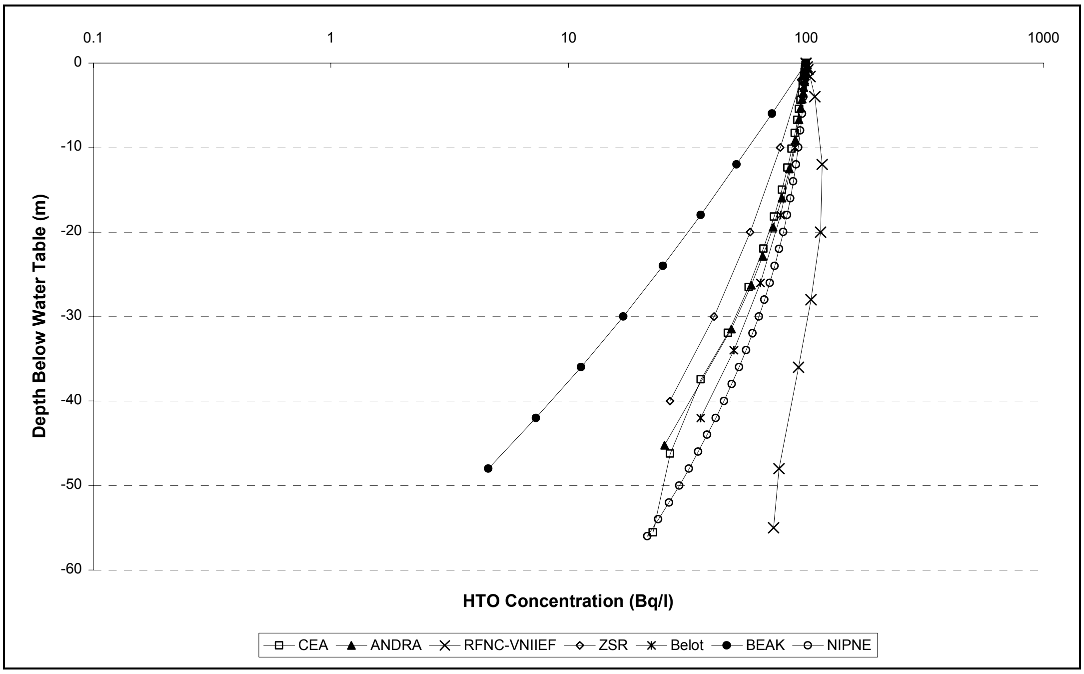

FIG. E4. Vertical profile of HTO concentration in an aquifer 1km from the HTO source and at 20 years after steady state has been achieved at the water table; high dispersivity, prescribed-concentration boundary condition.

PART F

MODELLING THE ENVIRONMENTAL TRANSPORT OF TRITIUM IN THE VICINITY OF PERMANENT ATMOSPHERIC SOURCES:

Model-model intercomparison exercise on predicting the rise of tritium from contaminated groundwaters

F1. BACKGROUND AND OBJECTIVES

(F1) Precipitation that infiltrates a contaminated soil or buried waste can leach tritium as well as other compounds that could be present. The leachate can move downward into the water table and cause groundwater contamination, sometimes over a large area. Even when the source of tritium has been eliminated, it may take many years for natural processes to remove tritium from the contaminated aquifer. During this phase, the tritium-labelled groundwaters may be a source of contamination for the uncontaminated unsaturated soil layer situated above and for the vegetation rooted in that soil. The problem is then to predict the biosphere contamination that may result from groundwater contamination, given the depth of the contaminated groundwaters and the properties of the soil above.

(F2) This problem is not specific for tritium, but concerns any solute, radioactive or not, that might be dissolved in groundwaters and that might be transported up to the roots of the vegetation above, with potential detrimental effects to the vegetation itself or to those that consume the vegetation. A similar problem was considered earlier in lysimeter experiments carried out at Imperial College (University of London, UK). These experiments studied the movement of various radionuclides from a contaminated shallow aquifer to soil and crops using lysimeters. The modelling of moisture and radionuclide movement in the upper unsaturated soil was carried out in parallel to the experimental work. The data from the experiments served as a benchmark test of models in the framework of the second phase of the international Biosphere Model Validation Study (BIOMOVS II) programme (BIOMOVS II, 1996; Butler et al, 1999).

(F3) In the research programme mentioned above, the movement of tritium was not one of the radionuclides considered. The modelling of tritium transport is dissimilar to that of other radionuclides, since tritium can partly volatilise to the air present in soil and can evaporate to the atmosphere through the soil, or through plant leaf surfaces following uptake from contaminated soil water. Tritium is also mobile in soil since it does not interact appreciably with the dry soil material. This means that tritium can move up and down through the soil column according to the soil moisture status and other related factors. The present work specifically addresses the modelling of tritium transport between groundwaters and the atmosphere through unsaturated soil and vegetation. The main objective of the BIOMASS exercise was to help modellers to develop modelling tools that could be adapted to the problem of tritiated water movement in unsaturated soils and that could provide an assessment of the consequences of the presence of tritium in groundwaters. To achieve this main objective, the second of the set of scenarios developed by the BIOMASS Tritium Working Group (TWG) was specifically designed to test and intercompare different deterministic models developed to address this particular issue. Since no experimental data were available for testing models, a model-model intercomparison exercise was developed early in the TWG work programme.

(F4) A draft of the model test scenario, called Scenario 2, was first outlined and presented for consideration in IAEA (1996). At the first TWG meeting held in Cadarache from 22–24 April 1997 it was decided to focus attention on modelling the processes by which tritium could be transferred from contaminated groundwaters to the biosphere through the overlying unsaturated zone of soil. A first version of the scenario description was provided for discussion at the TWG 1997 autumn meeting, and subsequently distributed to participants in amended versions following discussions at the 1998 and 1999 TWG meetings. Preliminary modelling results were discussed at the spring 1998 meeting and revised results were presented and analysed at the autumn 1998 and the two 1999 meetings following each revision of the scenario description. Final results were discussed at the 2000 spring meeting and these are the results presented here.

F2. SCENARIO DESCRIPTION

F2.1. EVOLUTION OF THE SCENARIO

(F5) Scenario 2 in its final form is given in detail in Annex II–F. Schematically, the scenario considers a contaminated perched aquifer, which is limited by a water table that does not appreciably fluctuate during the course of a year (see Figure II–F.1 in Annex II–F). The aquifer is assumed to be covered by a 1m-thick layer of uniform well-characterised soil. The tritium concentration in the aquifer is assumed to be constant throughout the period of study. The horizontal movement of tritium is not considered, because the horizontal extent of the contaminated area is assumed to be large compared to the vertical extent of the unsaturated soil layer. Participants undertaking scenario calculations were provided with soil data, hourly meteorological data and hourly evaporation data for soils both with and without vegetation. From this information they were asked to predict the vertical profile of tritium concentration in soil water, and the flux of tritium to the atmosphere as a function of time over a period of at least one year, both for bare and vegetated soils. The modellers were asked to start from the assumption that the column of soil does not contain any tritium at the beginning of the simulation exercise.

(F6) In the initial version of the scenario the hourly evaporation data were not provided and modellers had to determine such information from the hourly weather data. However, the calculated evaporation rates were different from one model to another and this prevented any further examination and intercomparison of the performance of the tritium transport models. So, it was decided to omit the evaporation calculations and concentrate instead on the transport phase itself. Consequently, in the final version of the scenario, all the modellers were invited to use the same pre-calculated values of evaporation and transpiration rates, and to focus their attention on the transport processes. They were asked to first test the relative importance of diffusion, dispersion and convection processes (Scenario 2.4), and secondly to give results for tritium transport in the same soil which is either bare or vegetated (Scenario 2.5).

(F7) The main simplifying assumption concerns the water table, which is considered to remain at a stable level during the course of a year. It is appreciated that this may be quite different from reality in those cases where the water level changes appreciably as a function of the seasonal water supply. At this stage in the development of transport models for aquatic sources of tritium, the simplification was imposed due to the difficulty of model intercomparisons that would have arisen if a more complex situation had to be modelled. It was considered that it would be more beneficial to start with simple models that could then be used as a basis for the development of more complex ones in the future.

F2.2. SOIL DATA

(F8) **Hydraulic functions:** The most important hydraulic functions for moisture movement in the unsaturated zone are the relationships between water content (θ), pressure head in the soil (h), and hydraulic conductivity (K). The relationship $\theta(h)$ varies widely between different soils. So does the companion relationship K(h). These relationships are strongly non-linear.

During the last fifty years many methods were developed to determine these relationships in situ and from soil samples in the laboratory. The expressions of θ(h) and K(h) that are given in the scenario description have been taken from van Genuchten (1980). In these expressions, there are four fitting parameters that vary according to the type of soil considered, and that can be derived from a data assembly and analysis review by Schaap and Leij (1998). Average values of the parameters are given in this review for twelve different types of soil. These values result from the analysis of extensive experimental data. The particular parameter values that are imposed in the scenario description correspond to sandy loam type soil composed of 70% sand, 20% silt and 10% clay.

(F9) **Dispersivity:** The dispersion is characterised by the coefficient $D = D_m + \alpha v$, where D_m is the molecular diffusion coefficient, α is the dispersivity, and v the absolute value of the pore water velocity. The first term represents the effect of molecular diffusion and the second term accounts for mechanical dispersion. The dispersivity coefficient increases with the degree of irregularities of the flow patterns, and has been shown by theory to increase when the water saturation of the porous medium decreases. Most of the very few experimental values of dispersivity that have been determined until now for unsaturated soils are in the range 0.01–0.10 m (Forrer et al, 1999). Unfortunately, the volume of experimental measurements available is quite inadequate to examine the influence of the factors that may affect the dispersivity of unsaturated soils. In Scenario 2, the dispersivity of the soil in the vadose zone is assumed to be on average equal to 0.05 m.

F2.3. EVAPORATION AND TRANSPIRATION DATA

(F10) The evaporation and transpiration data used in Scenario 2 were derived by one of the participants (W. Raskob, FZK) from a reference set of hourly meteorological data. These reference data, including wind speed, precipitation, air temperature, air humidity, air stability and net radiation, cover a period of one year, and are representative of the region around Karlsruhe in Germany.

(F11) Hourly evaporation and transpiration rates were estimated by Raskob using a numerical model that simulates the movement of water together with the evaporation or transpiration in a soil profile. This numerical model is a part of the program UFOTRI (Raskob, 1993). It considers a 1 m layer subdivided into 10 sub-layers and an additional layer of 1 cm on the top. Evapotranspiration is determined using the Penman-Monteith equation (Monteith, 1981) that introduces the concept of surface resistance. In the case of a bare soil, the surface resistance is an additional resistance of the soil surface, which is in series with aerodynamic and boundary layer resistances and reduces evaporation below potential rates. In the case of a vegetated soil, the surface resistance is the resistance of the canopy to the transpirational water flux. The model was tested against measurements performed in the framework of the Weiherbach experiment (Kolle and Fiedler, 1992; Plate, 1994). Good agreement was achieved without tuning any of the parameters. The model was also applied with great success to predict evaporation from a lysimeter in the BIOMOVS II exercise cited in Section F1 above (BIOMOVS II, 1996).

(F12) The participants were thus provided not only with a set of meteorological hourly data, including precipitation rates, but also with a set of hourly evaporation and/or transpiration rates for a bare soil or a vegetated soil. The balance of the evaporation (or evapotranspiration) and precipitation rates is very different whether the soil is bare or vegetated. The monthly balance of precipitation and evaporation for a bare soil, from January to December, shows a net downward flux of water (positive values) for each month of the year as follows:

36.8 : 55.6 : 57.7 : 7.7 : 7.5 : 79.3 : 3.1 : 52.9 : 4.3 : 50.8 : 11.1 : 55.6 mm.

(F13) The monthly balance of precipitation and evapotranspiration over a year for a soil covered with wheat shows a net upward flux (negative values) for the months of April, May, June, July and September as follows:

38.1 : 56.5 : 54.7 : -17.7 : -62.5 : -7.1 : -87.9 : 23.6 : -12.8 : 44.6 : 9.3 : 55.1 mm.

F3. GENERIC NUMERICAL APPROACH

(F14) There are multiple processes implied in the coupled transport of moisture and tritiated water in an unsaturated soil layer. The tritiated water can be considered to be a solute in the soil liquid phase. It is thus subject to the processes of miscible displacement that play a primary role in the distribution of solutes within a soil profile. These processes, including convection, dispersion and molecular diffusion, although having been recognised for at least one century, have only been studied intensively in the last decades in conjunction with enhanced interest in water quality.

(F15) The numerical models used by the ANDRA, CEA and JAERI participants in the present intercomparison exercise differ from each other by their degree of complexity (see Annex I–B). The most comprehensive and versatile models can take into account every process that may influence the tritium movement. Such models solve a set of coupled transport equations for fluid velocities, capillary pressure, temperature, and concentration of tritium in the liquid and vapour phases of the unsaturated soil. These equations may be solved in their two or three dimensional, transient or steady state form.

(F16) The simpler models (used by Belot, FZK, SES, ZSR) are based on a series of simplifying assumptions. For example: the transport is considered to be one dimensional; the soil column is presumed to be composed of an homogeneous isothermal porous material; and the transport of tritium in the vapour phase is assumed to be only due to the diffusive process. Many of these models are based on the following set of two coupled governing equations that describe respectively the moisture flow and the tritium transport:

$$\frac{\partial h}{\partial t} = \frac{1}{Q(h)}\frac{\partial}{\partial z}\left[K(h)\left(\frac{\partial h}{\partial z} - 1\right)\right] + \frac{\omega(z)}{Q(h)} \tag{1}$$

$$\frac{\partial(\theta C)}{\partial t} = \frac{\partial}{\partial z}\left[D(h)\frac{\partial C}{\partial z}\right] - \frac{\partial(qC)}{\partial z} + \sigma(z) \tag{2}$$

the two equations being linked by:

$$q(h) = -K(h)\left(\frac{\partial h}{\partial z} - 1\right) \tag{2bis}$$

(F17) The first equation is the classical Richard’s equation for moisture flow in the soil, where:

h is the capillary pressure head, negative in the unsaturated zone, expressed as a unique function of the volumetric water content θ;

z is the depth from surface oriented positively downward;

$K(h)$ is the unsaturated water conductivity;

$Q(h)$ is the specific water capacity defined as $Q(h) = d\theta / dh$; and

$\omega(z)$ is a local source or sink term respectively positive or negative for inflow or outflow.

(F18) The second equation of the system is the classical convection-diffusion equation that expresses tritium transport in porous media. In this equation, $C(z)$ is the activity concentration of tritium in soil water, $D(h)$ is the apparent dispersion coefficient of tritiated water through a horizontal section of the soil column and $\sigma(z)$ is a local source or sink term respectively positive or negative for any appearance or disappearance of the species under consideration. The first term on the right hand side describes the longitudinal dispersion of tritiated water through molecular diffusion and convective dispersion; the second term, proportional to the convective flux in the liquid phase $q(h)$, accounts for convection of tritiated water through the soil column; and the third term represents the local appearance or disappearance of tritium.

(F19) Eq.(2) is coupled with Eq.(1) through the convective flux $q(h)$ that can be estimated by Eq.(2bis). The water conductivity K and the volumetric water content θ that appear respectively in the two equations are functions of pressure head h through strongly non-linear relations discussed above in the section concerning soil data. For moisture flow, the upper boundary condition depends on the balance of infiltration and evaporation, and the lower condition by setting the pressure head equal to zero in a supplementary layer at the bottom of the soil column for instance. For tritium transport, the upper condition is written in terms of transpirational flux and/or tritiated water exchange at the soil top layer(s). The lower condition is expressed by assuming a constant concentration in the (supplementary) bottom layer.

(F20) The moisture-flow equation is generally solved using the pressure head as a dependent variable as shown above instead of the volumetric water content which is more rarely used. The moisture-flow and tritium-transport equations are respectively solved for pressure head and tritium concentration using the same time steps and grid layout. The linkage between the two equations is performed at each step by calculating the convective water fluxes and estimating the volumetric water content. Numerically, the partial derivative equations are solved in tandem using a finite-difference or a finite-element method. Full descriptions of the models used by the different participants in the present exercise are given in Annex I–B. A brief summary of the models (including method of solution and the discretisation scheme used) is shown in Table F1.

F4. TENTATIVE ANALYTICAL APPROACH

(F21) Part of the modelling exercise was to examine if an analytical model could be used to estimate, at least approximately, the rise of tritium from contaminated groundwaters up to the soil surface. A strong incentive for this approach was that an analytical solution, even if restrictive regarding the conditions of application, would be of interest for a rapid estimation of tritium dispersion and would not suffer from some of the errors that may be associated with numerical solutions.

(F22) An analytical solution of tritium transport through a soil column can only be obtained when the transport equation is linear with constant coefficients over space and time. In a very strict sense, this would require the soil column to maintain constant uniform properties from top to bottom over the whole duration of the time interval considered. In the current problem, this condition is not fulfilled, but the space varying and time-fluctuating coefficients can nevertheless be approximated by their averages calculated over a certain interval of space and time. With this approximation, the transport of tritium can be described by a simple transport equation with constant coefficients (3), and the associated Dirichlet boundary condition (3bis):

$$\frac{\partial C}{\partial t} = D\frac{\partial^2 C}{\partial x^2} - v\frac{\partial C}{\partial x} - \lambda C \tag{3}$$

$$C_{x=0} = C_0 \tag{3bis}$$

where:

C	is the concentration of tritium in liquid phase;
t	is the time;
x	is the distance from the boundary;
D	is the dispersion coefficient; and
v	is the pore water velocity and λ is the radioactive decay constant.

For a semi-infinite medium with origin at the boundary, the transient solution of the system (3) and (3bis) can be taken from Bear (1972), or, if it is considered that the radioactive decay can be neglected, from the simpler formula of Lapidus and Admunson (1952):

$$\frac{C(x,t)}{C_0} = \frac{1}{2}erfc\left(\frac{x-vt}{\sqrt{4Dt}}\right) + \frac{1}{2}\exp\left(\frac{vx}{D}\right)erfc\left(\frac{x+vt}{\sqrt{4Dt}}\right) \tag{4}$$

where the distance x and the pore water velocity can be changed to x = 1-z and v = -w , in which z is the depth above ground level taken positive downwards, and w is the pore water velocity also taken to be positive when oriented downwards.

(F23) The main problem is to evaluate the average value of the pore water velocity, w_m, and the average value of the dispersion coefficient, D_m, for the period of interest. The average velocity w_m is proportional to the infiltration flux, which is generally positive but may be negative when capillary rise dominates. The average dispersion coefficient D_m, mostly related to mechanical dispersion, is proportional to the water flux regardless of its direction. Taeschner (ZSR) (this work), as described in his soil model (Annex II–B), assumes that the water flux so defined, although actually varying through the soil column, can be approximated for the entire soil column by the mean value of precipitation and infiltration fluxes (absolute values).

F5. INFLUENCE OF ELEMENTAL PROCESSES ON TRITIUM TRANSPORT

(F24) The results to be intercompared are presented and discussed in Section F6 below. They were obtained by taking into account all three main processes that contribute to the transport of tritium in the soil, namely convection, molecular diffusion and mechanical dispersion. One important first task initially assigned to the modellers was to assess the relative importance of the three different transport processes. The participants in the exercise were asked to calculate the profiles of tritium concentration at a given date, when taking into account all three processes together or only selected ones, switching off the others (see Scenario 2.4 description in Annex II–F). This exercise was limited to the case of a bare soil, the specific configuration of soil and watertable given in the scenario description and the set of evaporation data provided to the modellers.

(F25) The results demonstrating the influence of the different processes are illustrated in Figure F1 which gives the tritium profiles calculated for the end of July for a bare soil. The profiles obtained when assuming only convection and molecular diffusion processes are operating differ considerably from those obtained when assuming mechanical dispersion also operates. The concentration at a 10 cm-depth is at least six orders of magnitude lower in the first case than in the second one. This indicates that the mechanical dispersion due to the irregularities of the flow pattern must be considered, at least for the conditions of the proposed scenario.

TABLE F1. COMPARISON OF MODELS USED FOR SCENARIO 2

Institution (Modeller)	Modelling Approach for Transient Moisture Flow and Tritium Transport
ANDRA (C. Meurville)	Approach: 3-D finite-volume code (PORFLOW developed by ACRI). *Solution Method*: Preconditioned conjugate gradient for pressure; Alternate Direction Implicit method (ADI) for transport *Discretisation*: Vertical 1-D grid: 196 layers 0.005 m, 2 boundary layers 0.0025 m. Time increment: modified by user to ensure stability (360 s for Scenario 2.4 and 36 s for Scenario 2.5)
Consultant (Y. Belot)	*Approach*: 1-D finite-difference code (TRIMOVE developed by Y. Belot). *Solution Method*: Implicit method for moisture flow and tritium transport Discretisation: vertical 1-D grid: 101 layers 0.01 m. Time increment to ensure stability (30 s)
CEA (G. Guinois)	*Approach*: 2-D finite-volume code (METIS developed by Ecole des Mines). *Solution method*: Conjugate gradient method Discretisation: 100 layers of 0.01 m. Time increment automatically calculated
FZK (W. Raskob)	*Approach*: 1-D compartment model (developed by W. Raskob) *Solution method*: Explicit method for moisture flow and tritium transport Discretisation: 10 layers of 0.1 m and 1 surface layer of 0.01 m. Time increment 360 s
JAERI (H. Yamazawa)	*Approach*: 1-D finite-difference code with tritium routines (SOLVEG developed by H. Yamazawa) *Solution method*: semi-implicit for dispersion; explicit for transport (low numerical dispersion scheme) Discretisation: 200 layers of 0.005 m. Time increment: 2 s
NIPNE (D. Galeriu)	*Approach*: 1-D finite-difference code *Solution method*: Implicit method. Discretisation: 40 layers of 0.025 m. Time increment 3.6 s to 324 s
STUDSVIK (O. Edlund)	*Approach*: 1-D finite-difference code *Solution method*: Implicit method for moisture flow and tritium transport *Discretisation*: vertical 1-D grid: 101 layers of 0.01 m. Time increment to ensure stability (30 s)
VNIIEF (A. Golubev)	*Approach*: 1-D finite-difference code (developed by S. Mavrin) *Solution method*: implicit method *Discretisation*: 50 layers of 0.02 m. Automatic time increment 1 s to 86 s
ZSR (M. Täschner)	*Approach*: Analytical solution of the mass transport equation for an homogeneous semi-infinite medium with prescribed concentration at the boundary (Bear 1972). *Solution method*: The pore water velocity is proportional to the infiltration flux. The dispersion coefficient is proportional to the mean value of precipitation and infiltration fluxes.

(F26) These very preliminary calculation tests can only be considered to be indicative. They were not sufficient to study the interdependency of the different elemental processes that operate within the soil, and the contribution of each of them to the movement of tritium and its evaporation at soil surface. This was studied more deeply by one of the TWG participants (Yamazawa, 2000). In this parallel work, H. Yamazawa (JAERI) carried out simulations in which the different factors contributing to tritium movement were varied in order to get an insight into their respective influence. It appears that the balance of precipitation over evaporation is the most important factor in the movement of tritiated water from a sub-surface source. Tritium has a tendency to move downward when the balance is positive and upward when the balance is negative. But in the case of the downward movement some tritium lags behind, while in the case of upward movement some tritium is transported faster. This behaviour is the result of mechanical dispersivity, which plays an important role in determining the distribution of tritium concentration through the soil profile. Molecular diffusion is generally negligible in comparison to mechanical dispersion.

F6. RESULTS AND DISCUSSION

(F27) The results that are considered in the present analysis are those which were released at the beginning of year 2000. They correspond to calculations for the final version of the scenario (Scenario 2.5) as given in Annex II–F and to the transpiration/evaporation data supplied with the scenario description. The results that were previously obtained are not presented here, for two main reasons: (i) the scenario has been partially revised to facilitate intercomparison of model results (see Section F2); and (ii) a few participants have detected deficiencies or errors in their model calculations, and have made subsequent corrections. Nine modellers, whose name and affiliation are given in Table F1, participated in the inter-comparison exercise.

F6.1. PROFILES OF SOIL WATER CONTENT

(F28) The majority of participants obtained the profiles of water content by numerical solution of the classical Richard's equation, using the capillary water head h, or the water content θ as a variable. Most modellers used small depth increments (0.005 m to 0.01 m), while only two of the participants have used large increments (0.1 m) (see Table F1). The time increment, chosen to ensure stability of calculation, varied from a few seconds to several hours depending on the selected depth increment. As requested in the scenario, the vertical profiles of volumetric water content (v/v) have been derived from the average values obtained over 10 cm intervals at specified depths below the soil surface and at fixed dates and time (28 February and 28 July at 12:00 h). The results shown in Figures F2 to F5 correspond respectively to the February profile for a bare soil, the February profile for a vegetated soil, the July profile for a bare soil and the July profile for a vegetated soil. The profiles are shown with linear co-ordinates.

(F29) The water content increases quasi linearly from the top layer (0–10 cm) to the bottom layer (90–100 cm). In February, the water content varies on average between 0.25 and 0.37 from top to bottom. In July, it varies also from 0.23 to 0.37 for a bare soil, but from 0.07 to 0.37 for a vegetated soil. In the latter case the deficit in the near-surface soil water content is caused by the strong evapotranspiration that occurs at this time of the year. The average value in the bottom layer approaches the value of water content at saturation. If the results of the different models are compared, it can be seen that the majority of the different profiles in each set of curves lie generally very close together. At a given depth below ground level, the difference between the extreme results is less than 10% of the average value, except for two out of the nine participants whose results lie in certain cases outside of this interval. The slope of the profile with linear co-ordinates, although increasing only extremely slightly from top to bottom, is varying very gradually in most of the cases. The slightly lower slope in the surface layers is a result of evapotranspiration.

F6.2. PROFILES OF TRITIUM CONCENTRATION

(F30) The profiles of tritium concentration in soil water were determined from the numerical solution of the dispersion-convection equation using the dispersivity given in the scenario description and the pore water velocity obtained from the solution of the Richard's equation. Both equations, generally coupled, were operated with the same time and depth increments. Results of tritium concentrations were requested for the same segments of the soil column and the same dates/time as the water contents. The results are given in Figures F6 to F9 for February and a bare soil, February and a vegetated soil, July and a bare soil, July and a vegetated soil, respectively. The results are shown with semi–logarithmic co-ordinates, with concentrations on the logarithmic scale.

(F31) The tritium concentrations increase in a nearly exponential mode from the top to bottom layer with a slight curvature in the upper layers which is imputable to tritium loss from plants and the soil surface. In February, the concentrations increase from about 2.10^{-5} to 5.10^{+3} Bq/L, in the case of bare or still scarcely vegetated soil. In contrast, in July there is a variation of about 5.10^{-1} to 5.10^{+3} Bq/L for the bare soil, compared to a variation of 5.10^{+2} to 9.10^{+3} for the fully vegetated soil. This shows the importance of root uptake in determining tritium rise from a shallow water table. The factors involved in tritium rise could be further explored by varying the water table depth and the nature of the unsaturated soil above, but this was outside the objective of the present work. The results obtained here show that the various concentration profiles, although being similar, are not as closely grouped as they are for water content. If the curves are generally well grouped in deep layers where the concentrations differ generally only by a factor 2 or 3, they are not so well grouped in the upper 20 cm layer, particularly in the case of a vegetated soil during the Summer period. This is probably due to a difference in the modelling of the water and tritium balance in the upper layers where evapotranspiration occurs. It is recommended that this aspect should be further examined.

(F32) One of the participants (Täschner, ZSR) used the analytical solution of the transport equation for a semi-infinite medium, assuming constant coefficients. The profiles obtained are not very different from those obtained from numerical models. But, these profiles strongly rely on the method employed to determine the average of the dispersion coefficient over the whole extent of the soil column. It is not certain that the method that is used here for shallow groundwaters would be applicable to deep groundwaters. Some work remains to be done to delineate the conditions of application of the analytical model.

F6.3. FLUXES OF TRITIUM FROM SOIL TO THE ATMOSPHERE

(F33) The flux of tritium from a bare soil to the atmosphere is usually determined by an exchange between the topsoil layer and the atmosphere just above. The flux from a vegetated soil originates from both soil and vegetation. During both Spring and Summer months, the flux from vegetation dominates; it was calculated by the participants simply as the weighted product of the transpiration rate and the tritium concentration in the different layers of the root zone.

(F34) The monthly densities of tritium flux from soil/plant to the atmosphere, expressed in Bq m^{-2} per month, are shown in Figures F10 and F11 for bare and vegetated soil respectively, assuming a constant aquifer concentration of 10^{4} Bq L^{-1}. The flux is maximal in July and August. If the soil is bare, it varies between 2.10^{+1} to 4.10^{+2} Bq m^{-2} per month, with the exception of the results of one participant that lie mainly outside this range. If the soil is vegetated, the flux was calculated to vary between 9.10^{+4} and $1.8.10^{+5}$ Bq m^{-2} per month, except by two out of nine participants. The enhancement of tritium flux caused by vegetation is related to an enhancement of water and tritium rise from the water table, during the months of April to September when there is a strong excess of evapotranspiration over precipitation. All modellers ignored the diffusive contribution to fluxes from the soil surface because this was considered to be very small in comparison with other exchanges.

F7. CONCLUSIONS

F7.1. NUMERICAL ASPECTS

(F35) As the divergence of results is greater for tritium transport than for moisture flow, the following discussion is focused on the reasons that may induce differences in the estimation of tritium movement. These reasons are mainly related to numerical aspects of the transport models being used.

(F36) The scenario required modellers to simulate the upward transport of tritium from a contaminated aquifer into an initially uncontaminated overlying soil column. During the first months of tritium transport, the gradient of tritium concentration in the bottom layers of the soil column is very steep. It appears that, at least at the beginning of the simulation, the spatial resolution must be very fine to describe accurately the diffusion front and to obtain results that should be acceptable. This was demonstrated by one of the participants (Yamazawa, JAERI, personal communication) who simulated the transport of tritium by diffusion into a soil column of uniform water content. By comparing numerical and analytical results he showed that the numerical solution is correct for a depth increment of 0.005m (200 layers), but becomes more and more erroneous as the depth increment increases. This shows that, at least in the present scenario, a numerical model with a depth increment of 0.1m for instance (10 layers) leads to erroneous results in the very first months of the simulation. Nevertheless, such a coarse resolution can be used for later simulation periods, because the relative error becomes smaller and smaller as the transport of tritium in the soil column progresses.

(F37) The error associated with the dispersion term is explained as follows. If Δz is the depth increment and C the tritium concentration in soil water, the dispersion term can be approximated by:

$$F = \frac{D}{\Delta z^2}\left[C(z+\Delta z) - 2C(z) + C(z-\Delta z)\right] \tag{5}$$

(F38) By using Taylor's expansion series, this expression yields:

$$F = D\frac{\partial^2 C}{\partial z^2} + D\frac{\Delta z^2}{6}\frac{\partial^4 C}{\partial z^4} + \varepsilon^4 \tag{6}$$

(F39) The first term on the right hand side corresponds exactly to the dispersion term itself and the rest to the numerical error that rapidly increases with the increment depth. This error does not depend on the time increment or whether the resolution scheme is implicit or explicit. This error can be reduced only by improving the spatial resolution, which means taking smaller depth increments.

(F40) The numerical error associated with the convection term does not occur if one uses a centered difference approximation of $?C / ?z$, since this approximation cancels the second-order error. It occurs only if one uses a forward (or backward) difference approximation, but in the latter case the numerical error can be canceled by a correction procedure.

F7.2. PROBLEMS RELATED TO THE MODELLING APPROACH

(F41) It was observed that the tritium concentration results obtained from different models, even if similar for deep layers, are rather different for the upper layers, particularly when strong evapotranspiration occurs. This is probably due to the fact that some models preserve mass and activity balances better than others. Care should be taken that the transport equation for the root zone is applicable to a substance that evaporates to the atmosphere. The models that have been designed for non-volatile substances are only transposable to volatile substances with some modifications. This needs further study.

(F42) The scenario exercise also raised the question of the advantages of numerical versus analytical models. It has been explained that the use of analytical models is based on the rather bold assumption that the pore water velocity and the dispersion coefficient can be averaged over space and time. While this appears to be feasible for determining the transport of tritium from shallow groundwaters, it is not certain that this approach would also be feasible in the case of groundwaters situated at greater depths, or in the case of soils with a much lower permeability. Anyway, due to the complexity of the processes and the heterogeneity of the transmitting medium, the analytical approach cannot serve as a reference approach to modelling at this stage.

F7.3. CONCLUSIONS OF THE INTERCOMPARISON EXERCISE

(F43) Most importantly, this exercise has helped modellers to develop modelling tools that could be applied to the problem of tritiated water movement in unsaturated soils and especially that would allow the assessment of the consequences of tritium rise from shallow contaminated groundwaters. For this specific application, some participants adapted flexible models of a commercial type, which are designed to solve a wide range of environmental problems, including flow, heat and mass transport in geologic media. Other participants developed their own codes based on process models and numerical techniques published by others. All of them were helped in this adaptation or new development by this modelling intercomparison exercise, the technical discussions and exchanges of ideas within the BIOMASS Tritium Working Group.

(F44) The application of different models to the problem proposed in Scenario 2, lead to results that were relatively close together, and that were in many cases grouped within a factor of about two. This rather good agreement was obtained by imposing on the modellers the use of the same soil characteristics and evaporation data, and by giving them the occasion to discuss the models to arrive at an acceptable convergence of methods and results. There would have been a wider spread in results in an assessment exercise where the model users would have selected or determined their own soil properties and evaporation data. Some important issues were highlighted. Firstly the necessity of using very small depth and time increments in numerical models. Secondly the need for a close examination of the moisture flow and tritium transport in the plant root zone and at the soil surface where evapotranspiration takes place. The use of the proposed analytical model, although interesting, was felt to be questionable, due to its oversimplification and the question of its applicability to the transport of tritium from deep groundwaters.

(F45) All the modellers agreed and/or showed that the balance of precipitation and evaporation, and the mechanical dispersion process, were the key factors in the transport of tritium in the unsaturated soil layer situated above a shallow watertable. The ensemble of results showed that tritium rise, although being rather moderate, was significant, for the conditions of the scenario and particularly in the case of a vegetated soil. In the latter case, the deficit of water, due to an excess of evapotranspiration over precipitation, induces a replenishment of the upper soil water through the capillary rise process and a simultaneous upward movement of tritium. It is considered that this process can only be significant when the watertable is very close to the soil surface. The results obtained for the conditions of Scenario 2 would have been certainly quite different, if the depth of the watertable and/or the permeability of the soil had been different. However, the main interest was to develop and compare models that would be able to predict the magnitude of the tritium rise as a function of the watertable depth, the weather statistics and the soil properties and this was accomplished.

REFERENCES TO PART F

[1] BEAR, J., Dynamics of Fluids in Porous Media, Elsevier, New York (1972).

[2] BIOMOVS II, Model validation studies of water flow and radionuclide transport in vegetated soils using lysimeter data, BIOMOVS II Technical Report No. 15, Published on behalf of the BIOMOVS II Steering Committee by SSI, Stockholm (1996).

[3] BUTLER, A.P., CHEN, J., AGUERO, A., EDLUND, O., ELERT, M., KIRCHNER, G., RASKOB, W., SHEPPARD, M., Performance assessment studies of models for water flow and radionuclide transport in vegetated soils using lysimeter data, Journal of Environmental Radioactivity **42** (1999) 271–288.

[4] FORRER, I., KASTEEL, R., FLURY, M., FLÜHLER, H., Longitudinal and lateral dispersion in an unsaturated field soil, Water Resour. Res. **35** (1999) 3049–3060.

[5] KOLLE, O., FIEDLER, F., Messung und numerische Simulation der Energie- und Feuchtebilanz der Bodenoberfläche, In: Schlußbericht zur 1, Phase des Weiherbachprojekt, Hrsg.: E.J. Plate, Mitteilungen des Instituts für Hydrologie und Wasserwirtschaft, Nr. 41, Universität Karlsruh (1992) 131–156.

[6] LAPIDUS, L., AMUNDSON, N.R., Mathematics of adsorption in beds, VI, The effects of longitudinal diffusion in ion exchange and chromatographic columns, Journal of Physical Chemistry **56** (1952) 984–988.

[7] MONTEITH, J.L., Evaporation and surface temperature, Q. J. R. Meteorol. Soc. **107** (1981) 1–27.

[8] PLATE, ERICH, J., Weiherbachprojekt: Zwischenbericht 1994, Institut für Hydrologie und Wasserwirtschaft (IHW), Universität Karlsruhe (1994).

[9] RASKOB, W., Description of the new version 4.0 of the tritium model UFOTRI including user guide, Report KfK 5194 (1993).

[10] SCHAAP, M.G., LEIJ, F.J., Database related accuracy and uncertainty of pedotransfer functions, Soil Science **163** (10) (1998) 765–779.

[11] VAN GENUCHTEN, M.TH., A closed form equation for predicting the hydraulic conductivity of unsaturated soils, Soil Sci. Soc. Am. J. **44** (1980) 892–898.

[12] YAMAZAWA, H., Numerical study on soil-atmosphere tritiated water transfer, Proceedings of the International Workshop of the Environmental Behaviour of Tritium, Kumatori, Japan, May 8–9 (2000).

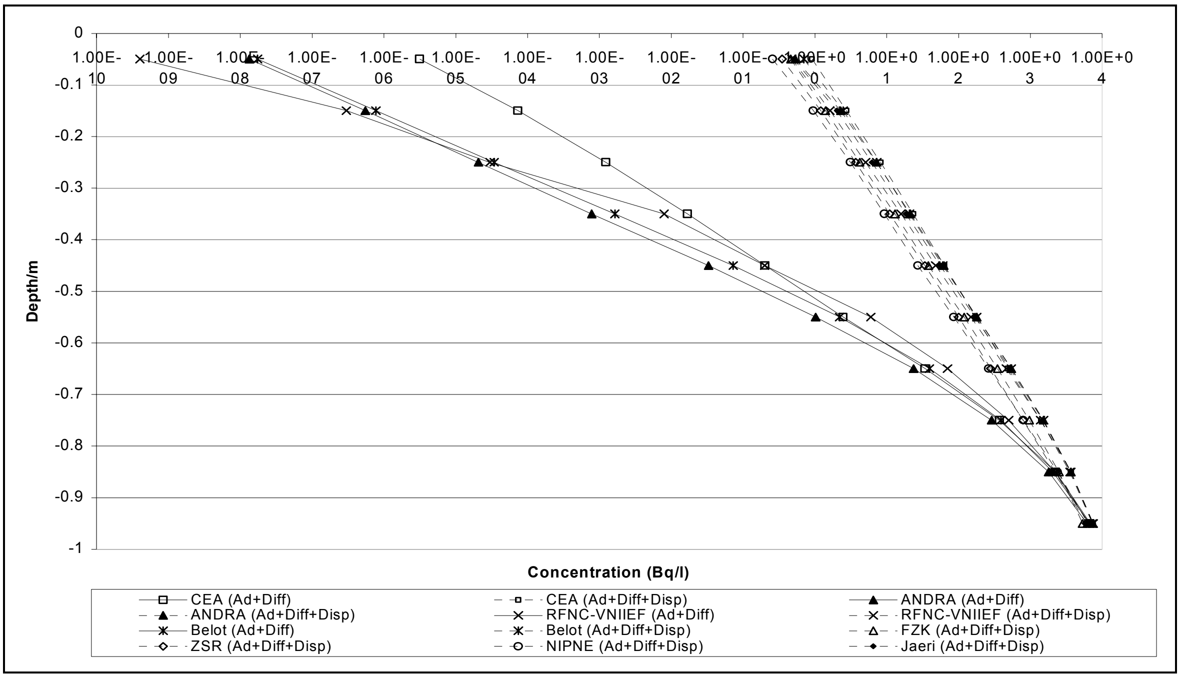

FIG. F1. July HTO profile – Bare soil with and without dispersion.

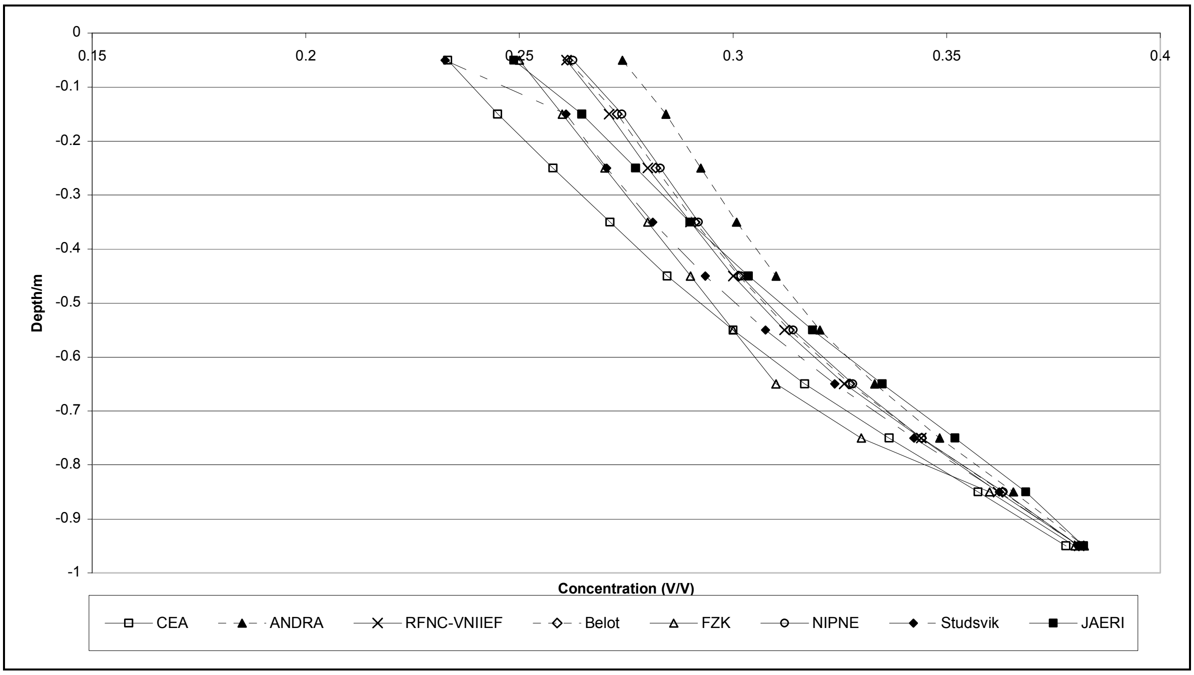

FIG. F2. February H_2O profile – Bare soil.

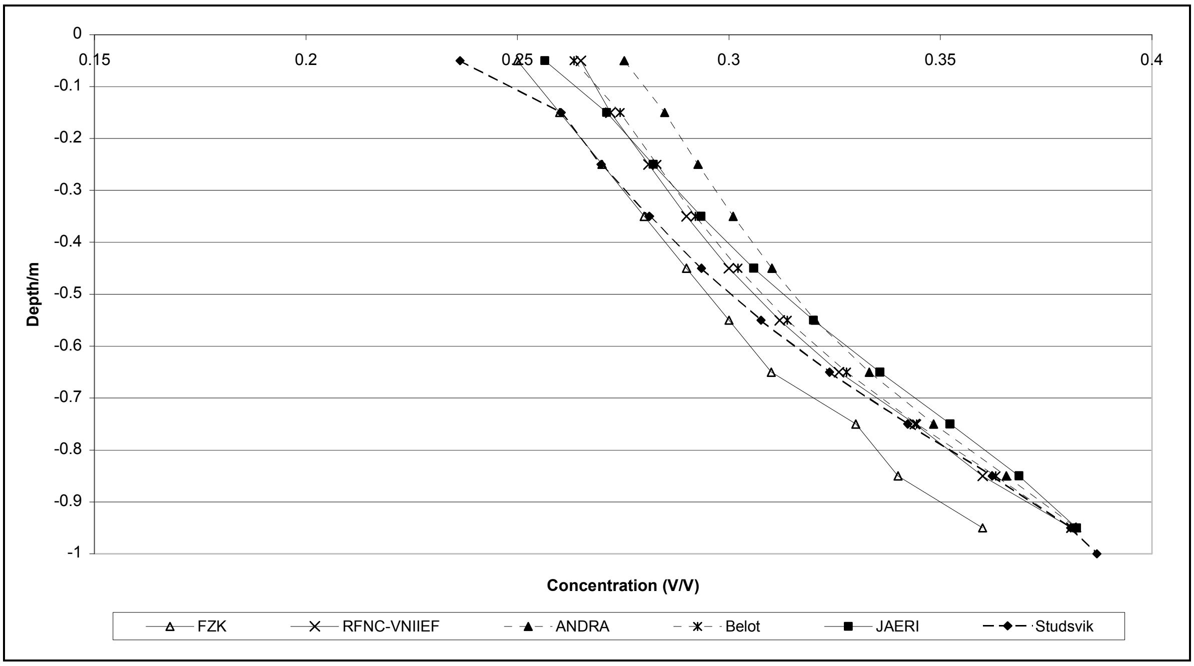

FIG. F3. February H_2O profile – Vegetated soil

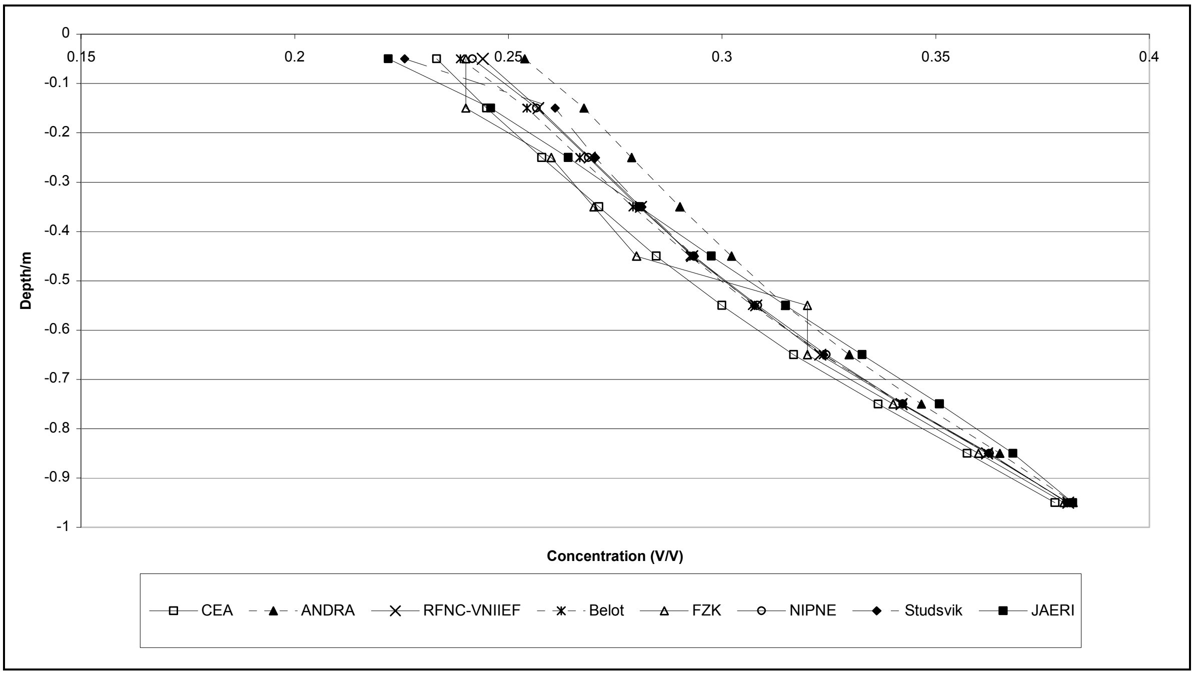

FIG. F4. July H_2O profile – Bare soil.

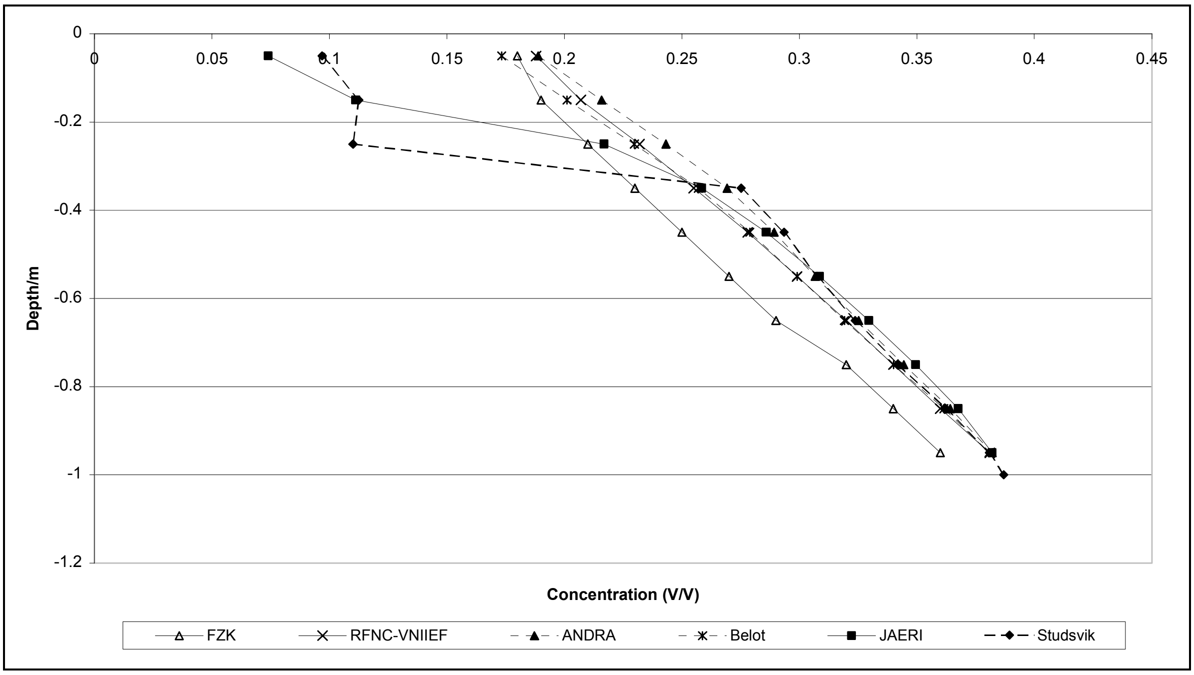

FIG. F5. July H_2O profile – Vegetated soil.

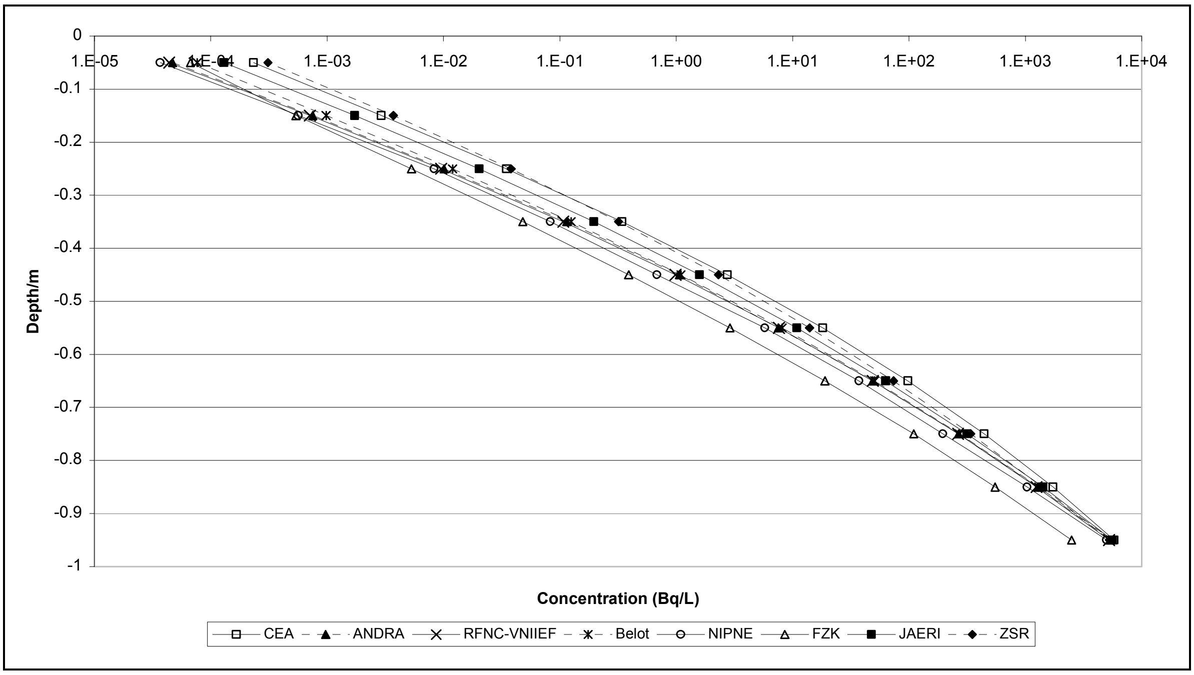

FIG. F6. February HTO profile – Bare soil.

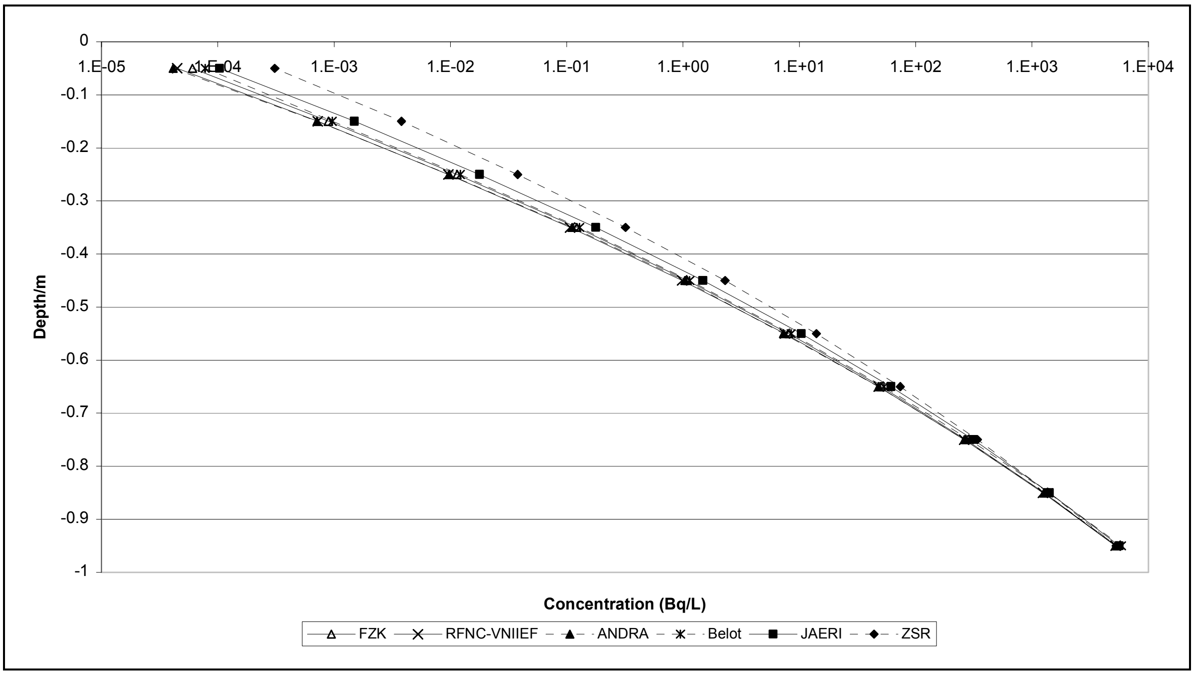

FIG. F7. February HTO profile – Vegetated soil.

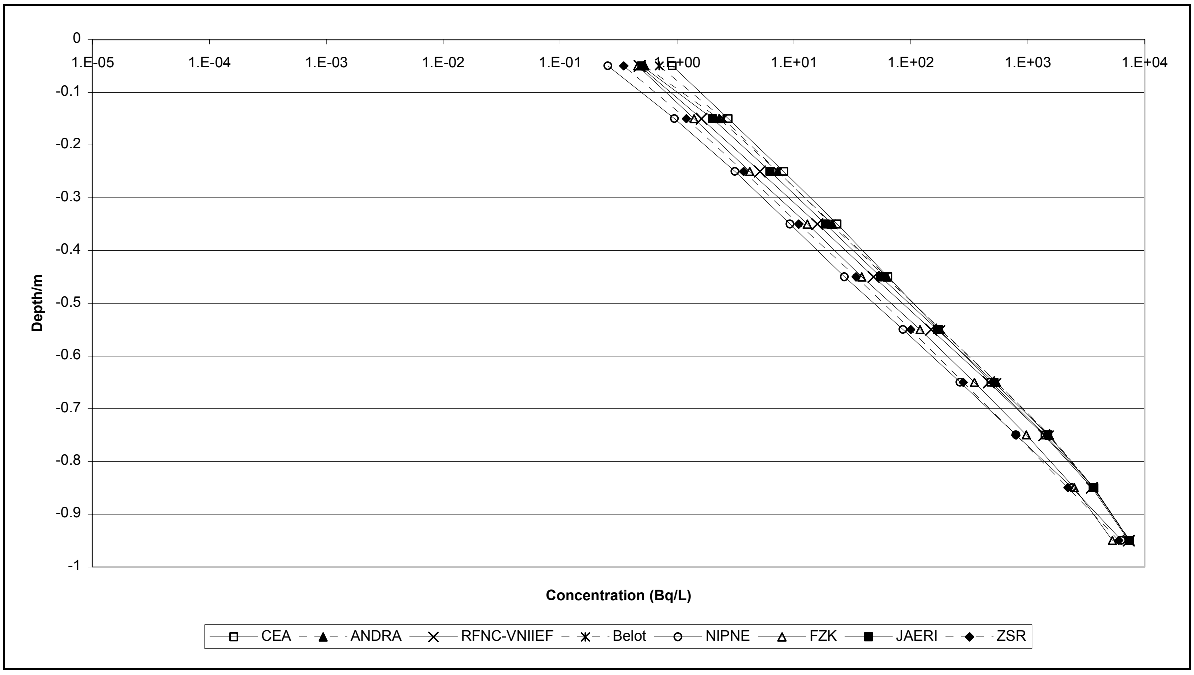

FIG. F8. July HTO profile – Bare soil.

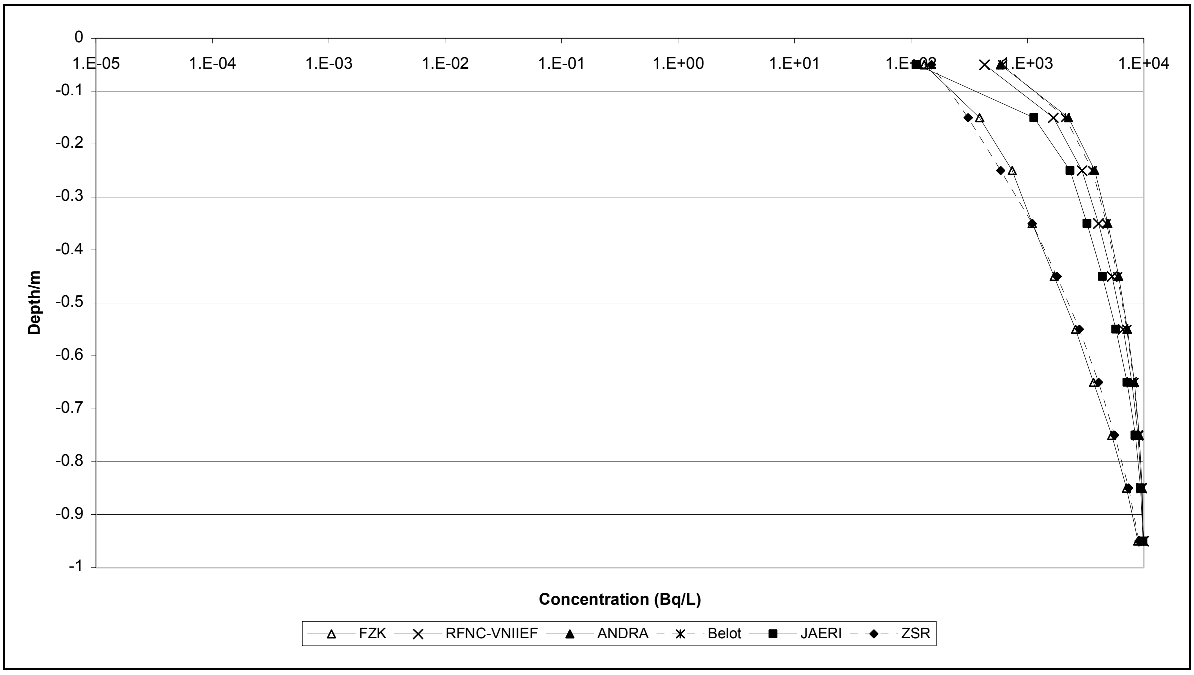

FIG. F9. July HTO profile – Vegetated soil.

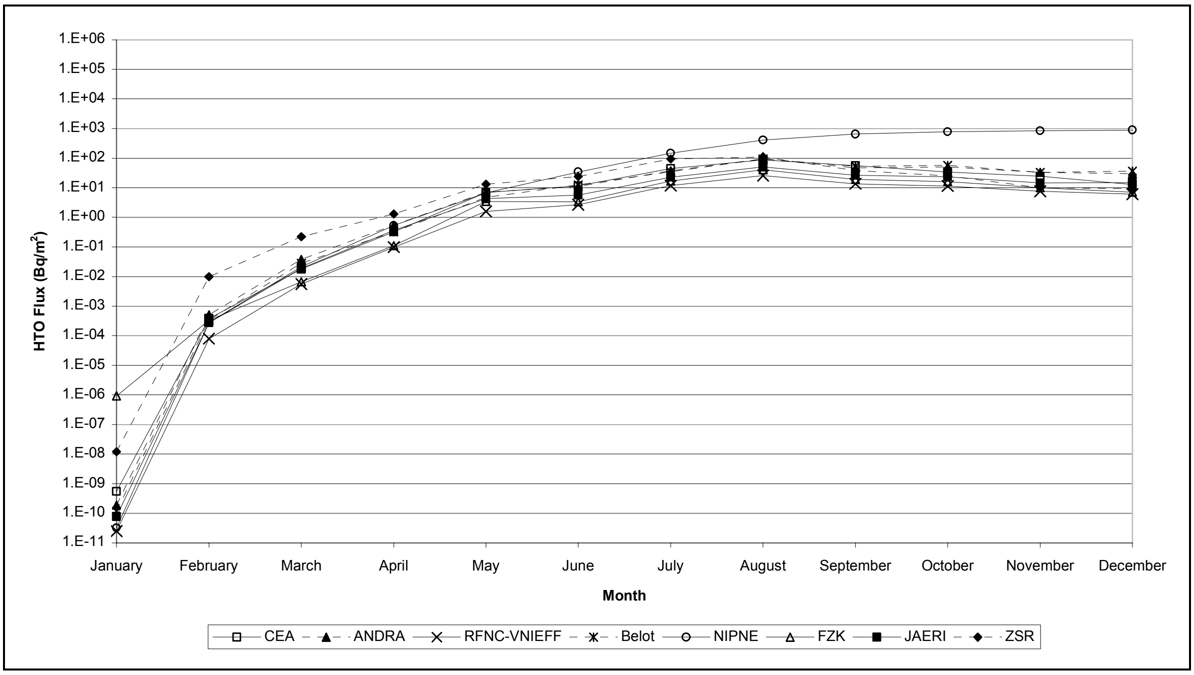

FIG. F10. HTO fluxes – Bare soil.

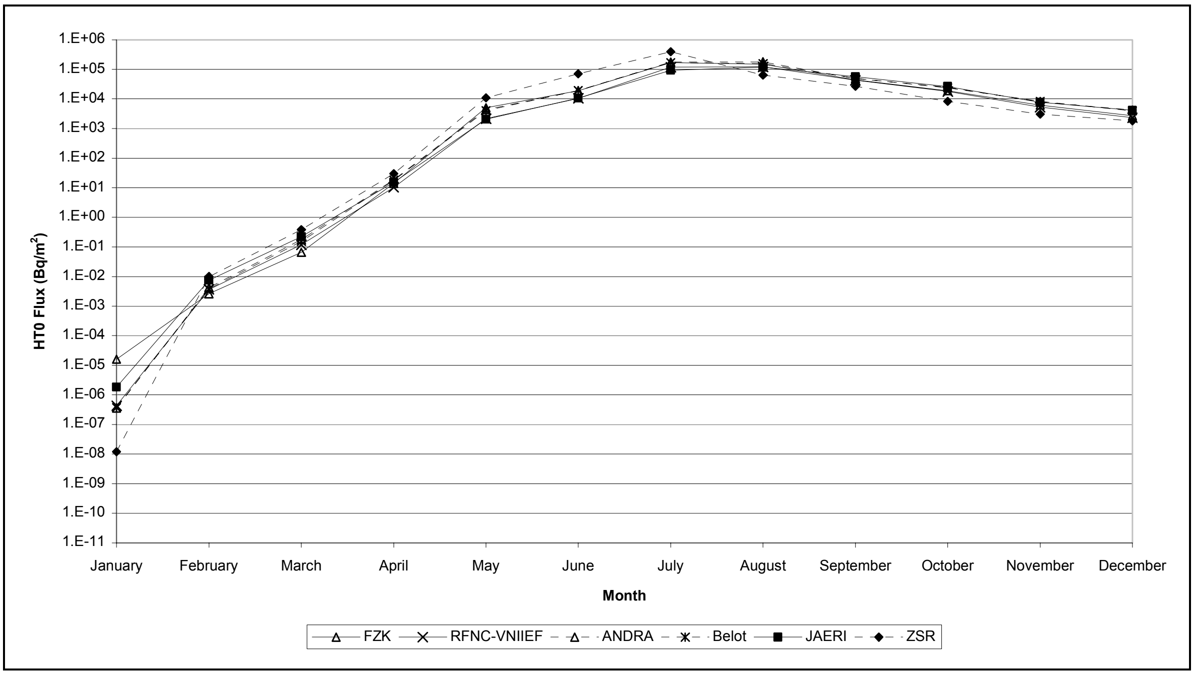

FIG. F11. HTO fluxes – Vegetated soil.

PART G

MODELLING THE ENVIRONMENTAL TRANSPORT OF TRITIUM IN THE VICINITY OF PERMANENT ATMOSPHERIC SOURCES:

Field data for wet and dry deposition of tritium

G1. INTRODUCTION

(G1) During its work on the environmental effects of tritium releases, the BIOMASS Theme 3 Tritium Working Group (TWG) identified a need for new models to asses the impact of long term continuous releases. Scenario 1 was designed to study chronic atmospheric releases of tritium. In modelling the buildup of tritium in soil water, it became evident that insufficient data are available to help decide the relative importance of the wet and the dry deposition processes and whether both processes should be included in the assessment models. To answer this question, specially designed experiments are required because normal monitoring does not provide air, rain and soil samples at the same location.

(G2) In the case of an HTO release, it was assumed by several participants that the concentration of tritium in soil water is mainly attributable to wet deposition. The argument is drawn from experiments and modelling, since it appears that, in the case of short term releases, a major part of the dry-deposited HTO is rapidly re-emitted to the atmosphere and does not remain appreciably in the soil. Therefore, researchers from CEA/DAM/DASE, France in collaboration with German colleagues from the ZSR institute of the University of Hannover decided to undertake an experimental program to investigate the consequences of wet and dry deposition processes following chronic releases of tritium to the atmosphere.

G2. EXPERIMENTAL PROGRAM

(G3) In March 1998, monitoring equipment was set up to gather data on soil, air and rain concentrations in sectors around an emission point which receive either mainly dry or mainly wet deposition. The sampling program ceased in December 1999 after collection of data for 20 months.

(G4) Data on HTO concentrations were derived from the following samples:

- Air moisture (sampled continuously and averaged monthly).
- Rain samples (one composite sample per month).
- Soil moisture (one core at the end of the air and rain sampling interval).

(G5) The soil cores were taken down to a depth of 20 cm and then divided into 4 layers each of 5 cm thickness which were analysed separately.

(G6) It must be noted that soil samples were taken on specific dates, but data on tritium concentrations in air moisture and in rain were obtained from monthly averaged samples.

G2.1. SELECTION OF SAMPLING SITES

(G7) Three monitoring stations were set up at selected points around a stack emitting tritium (more than 90% in the form of HTO) at a site near Paris, France that fulfilled the requirements of parallel sampling of the environmental water compartments of atmosphere, precipitation and soil. The height of the stack is 40 m. The terrain is flat (see Figures G1 and G2). The co-ordinates of the three sampling points (SP) are given below:

— East SP is positioned at 70° from North at a distance of 300 m from the stack (i.e., the plume is present at this site during times when the wind blows from Southwest, the direction of the maximum of the joint frequency of wind and rain);

— West SP is positioned at 255° from North at a distance of 460 m from the stack (i.e., the plume is present at this site during times with north-easterly winds, which are mostly dry); and

— South SP is positioned at 140° from North at a distance of 365 m from the stack.

(G8) After analysing the distribution of wind directions and of the joint frequency of wind and rain, the data from the South SP were considered to be of no help for the task of this report, because it appeared that neither wet nor dry deposition dominated overall during the sampling period. Therefore data from the South SP are not discussed further.

G2.2. COLLECTION OF SAMPLES

(G9) Samples of air humidity, rainwater and soil were collected at the monitoring stations described above. The term 'station' designates a 2 m × 2 m location, established and equipped for taking samples of different types at almost exactly the same place in order to obtain a parallel historical series of data over a long period of time. At the centre of the sampling station is a peg that supports two cylindrical housings, as shown on the two accompanying photographs (Figures G1 and G2). The first housing, closed at the top contains a passive sampler for air humidity collection. The second housing, opened at the top contains a precipitation collector. The base of both housings is pierced with annular holes to allow air to enter, or water to exit.

(G10) Monthly samples of air humidity were collected at a height of 1.5 m, using passive samplers very similar to those that were developed and completely validated by Otlet et al (1992). Each of these samplers is made of a 1000 ml plastic bottle containing 200g of pre-dried silica gel and connected to the atmosphere through a simple tube, 73 mm long and 22 mm wide, covered with 100 mesh stainless steel gauze. The diffusion rate of humidity through the tube is controlled only by its physical parameters. The susceptibility of the sampling rate to air draughts is almost cancelled by the fine mesh gauze that covers the upper end of the tube, and by the housing that isolates the sampler from rainfall. The collection quantity of air humidity is between 1g and 5g of water for an exposure time of about 4 weeks, which was sufficient, in the present case, for liquid scintillation counter measurements. To calculate the HTO concentration of the air humidity, it is necessary to correct the measured HTO concentrations of the silica gel water sample due to dilution by exchangeable water; this was found by experimentation to be approximately 4% w/w of the silica gel. The relative uncertainty of the HTO concentrations of single air samples was evaluated and found to lie in the range of 30% to 50%. The uncertainty of the air samples is dominated by the uncertainty of the correction factor for dilution.

(G11) Monthly samples of rainwater were collected in 500 ml glass bottles using simple plastic funnels of 6 cm diameter to avoid overflow of water in the event of heavy precipitation. To each precipitation collector, 100 ml of cyclohexane was added to prevent exchange between the collected water and atmospheric vapour. There was no satisfactory technique for protecting snow, but fortunately the frequency of snowfall was very low for the particular sampling programme reported here. The absolute uncertainty of HTO concentrations in rain was evaluated and found never to exceed 5 Bq/l plus 0.1 times the measured concentration.

(G12) At the end of each month, soil samples were collected within the station at a distance close to the base of the peg that supports the samplers described above. Because of the particular structure of the sampled soil it was rather difficult to collect the samples by using a hand–driven auger tool and so a different technique was used. It consisted of clearing vegetation in a 20 cm × 20 cm area and removing the soil material in successive layers of 5 cm thickness down to a 20 cm depth using a small scraper-like tool. The sub-samples were put in bottles with large openings and covered with cyclohexane to avoid any exchange with ambient atmosphere.

G2.3. SAMPLE TREATMENT AND ANALYSIS

(G13) Water was first extracted from the silica gel and soil samples. This was achieved by the technique of azeotropic distillation, using cyclohexane as a solvent. The sample was introduced into the distillation flask of a Dean-Starck apparatus. An appropriate amount of cyclohexane was added into the flask so that the sample remained covered throughout the entire distillation process. Water and cyclohexane form an azeotropic mixture and distil together, at a temperature of 69.8°C, into a receiving funnel where cyclohexane separates from water and floats on the top. The distillation process was complete within 3 to 4 hours. The water that was extracted from the silica gel or soil material was analysed for tritium by liquid scintillation counting. The rainwater samples were measured directly without any pre-treatment. The uncertainty for single measurements was evaluated and found to be below 20% at HTO concentrations above 100 Bq/l. At lower concentrations, the uncertainty was higher but the absolute uncertainty never exceeded 3 Bq/l plus 0.2 times the measured concentration.

(G14) The formulae for calculating the uncertainties of the air, rain and soil samples given above were used for all the following uncertainty estimations.

G2.4. METEOROLOGICAL INFORMATION

(G15) In parallel to the rain, air and soil samples, meteorological data were collected continuously at a frequency of one record per 10 min. The following information was provided by the owner of the tritium handling facility:

- wind direction, wind speed, temperature and air humidity at different heights and
- rainfall rate.

(G16) The overall sampling interval of this study was 632 days. It covered 20 months; the average duration of each sampling interval was 31.6 days (minimum 23 days, maximum 42 days).

(G17) Each sampling point was assumed to lie at the centre of a 20° sector in order to decide whether the plume was present over the samples at a given time. Thus, if the wind direction was between 240° and 260° a contamination event was counted for the East SP; the direction was 65° to 85° for the West SP. The wind rose and the distribution of the joint frequency of wind and rain are shown in Figure G3; an overview of the meteorological data is given in Table G1.

(G18) Figure G3 shows that the East SP is near to the sector of the main wind direction. Therefore the East SP is affected by dry contamination events 2.6 times more often than the West SP. The frequency of events with contaminated rain is even higher: the East SP is affected by wet contamination events 4 times more often than the West SP. For this reason it was hoped that these two sampling points could help to answer the question of the relative importance of the wet and the dry deposition process.

TABLE G1. OVERVIEW OF METEOROLOGICAL DATA FOR THE SAMPLING INTERVAL FROM 18 MARCH 1998 TO 10 DECEMBER 1999 FOR EAST AND WEST SAMPLING POINTS (SP)

Overall number of counted 10-min. events	91008	
Number of events with precipitation	2883	
Precipitation	1072 mm	
Average duration of sampling intervals	31.6 days	
Overall sampling interval in days	632 days	
Number of days with precipitation events	309 days	
Events with wind at	**East SP**	**West SP**
Number of contamination events	9594	3635
Fraction of all events	10.5%	4.0%
Number of days with contamination events	427	222
East to West ratio of numbers of all wet and dry contamination events: 2.6		
Events with rain and wind at	**East SP**	**West SP**
Number of wet contamination events	301	74
Fraction of all events	0.33%	0.08%
Fraction of all wet events	10.4%	2.6%
Number of days with wet contamination events	114	22
East to West ratio of numbers of wet contamination events: 4.1		

(G19) More detailed meteorological information is shown in Figures G4 and G5. The counted 10-minute contamination events are compressed to daily frequencies and are plotted against time together with the precipitation rate and the soil sampling dates, which also mark the beginning and end of the respective sampling intervals for air humidity and rain water.

G3. RESULTS

(G20) The collated meteorological data presented in Figures G4 and G5 show that the East SP is affected by dry and wet contamination events during all monthly sampling intervals. The West SP is affected much more sparsely, in particular there are several months without any wet contamination event at the West SP. This makes the interesting difference for the task of this report, namely that the West SP is apparently less affected by wet deposition than is the East SP. Nevertheless, even at the West SP there is wet deposition of atmospheric HTO during all the sampling intervals, although concentrations in rain are likely to be very low because the primary plume is not present.

(G21) The data on HTO concentrations in the three different water compartments (air, rain and soil) are shown in Figures G6 to G9. The data are plotted on logarithmic scales in order to emphasise equally the scatter of data at higher and lower values. Overall data are presented in Table G2. The HTO data for soil are compressed to the averages of the four analysed layers (0 to 20 cm, see Figure G8), but the topsoil layer values are shown separately (Figure G9). The spread of data exceeds one order of magnitude for the 20 month sampling interval. The data on HTO concentrations are very scattered from one month to the next. At the East SP, the average HTO concentrations are similar in the soil and rain compartments (with an average of about 300 Bq/l), but the concentrations in the air compared to soil and rain are higher by a factor of five. At the West SP the average concentrations in soil are twice the concentrations in rain, and, the concentrations in the air are higher by a factor of twelve compared to those in soil.

TABLE G2. OVERVIEW OF HTO CONCENTRATIONS IN AIR, RAIN AND SOIL WATER FOR THE SAMPLING INTERVAL FROM 18 MARCH 1998 TO 10 DECEMBER 1999 FOR EAST AND WEST SAMPLING POINTS (SP)

Averages and spread of HTO concentration data at East SP

HTO concentration in	Air humidity (Bq/l)	Rain water (Bq/l)	Moisture of topsoil layer (Bq/l)	Average of all soil layers (Bq/l)
Arithmetic mean	1647	310	387	322
Relative standard deviation	71%	95%	101%	61%
Maximum	4431	938	1490	753
Minimum	173	21	29	58

Averages and spread of HTO concentration data at West SP

HTO concentration in	Air humidity (Bq/l)	Rain water (Bq/l)	Moisture of topsoil layer (Bq/l)	Average of all soil layers (Bq/l)
Arithmetic mean	1227	50	96	99
Relative standard deviation	94%	99%	93%	62%
Maximum	5056	178	377	273
Minimum	327	4	15	26

(G22) The time-courses of the HTO concentrations of the different water compartments do not show a pronounced seasonal trend (Figures G6 to G9). The soil moisture contents were measured and varied between 3% v/v (late summer) and 25% v/v (autumn). Also, there was no correlation between the HTO concentrations of the different water compartments and dry or wet frequency of contamination events.

(G23) The overall averages of the HTO concentrations of the different compartments are indicated in Figures G6 to G9 by straight lines and, on the right-hand axis, the values of the geometric means are given for each sampling point. Note that in figures with logarithmic scales the indicated averages are geometrical, but the tables contain arithmetic averages. The geometric mean represents the median value (which is appropriate to logarithmic plots), whereas the arithmetic average represents the expectation value of the respective data.

G4. DISCUSSION

(G24) As a first step to answer the question of the relative importance of wet and dry deposition, ratios of the measured concentrations of the different compartments have been calculated and are shown in Table G3. The most pronounced difference between the two sampling points appears to be the ratio of HTO concentration in air humidity to that in rainwater – at the West SP this ratio is about 5 times higher than that at the East SP.

(G25) These data give the first indication of the pronounced importance of the dry deposition process at the West SP. But simply comparing arithmetic averages of data that spread over more than one order of magnitude might be misleading, because it stresses the importance of high values. Also there is the question as to whether monthly averages of air and rain actually reflect the conditions of the soil at the particular sampling time.

TABLE G3. RATIOS OF AVERAGES OF HTO CONCENTRATIONS IN WATER OF DIFFERENT COMPARTMENTS FOR THE SAMPLING INTERVAL FROM 18 MARCH 1998 TO 10 DECEMBER 1999 FOR EAST AND WEST SAMPLING POINTS (SP)

Compartment A	Compartment B	Ratio A to B at East SP	Ratio A to B at West SP
Top Soil	Rain	1.2	1.9
Top Soil	Air	0.24	0.08
Soil (0–20 cm)	Rain	1.0	2.0
Soil (0–20 cm)	Air	0.20	0.08
Air	Rain	5	24

(G26) A different approach is to look for correlation of HTO concentrations in different environmental media compartments. Figure G10 shows some evidence of a correlation of HTO in rain to HTO in air at the East SP, but there is hardly any correlation at the West SP. Although the correlation is not strong, there is a trend that HTO concentrations are high in rain when they are high in air, which is surely not surprising for locations where rain occurs frequently, because the source for HTO in rain is also atmospheric. For sites where the joint frequency of rain and plume presence is low, the rain may fall at times when the air concentration is far from its average value and no correlation can be expected between rain and air concentrations on a monthly basis.

(G27) Single correlation of HTO concentrations in soil to rain and air are shown in Table G4 and Figures G11 to G14. At the East SP, HTO in soil moisture is found to be highly correlated with HTO in rainwater (Figures G11 and G13); but at the West SP the compartment that is correlated to soil water concentration is air humidity (Figures G12 and G14). This stresses the importance of the wet deposition process at the East SP and of the dry deposition process at the West SP.

(G28) Overall at West SP, higher regression coefficients are obtained for the averaged soil values than for the topsoil values. This is the effect of more rapid and dynamic exchange of HTO from the upper soil layer to the atmosphere than from deeper soil layers. It also indicates that the average HTO concentration of the whole soil column is more related to the conditions of the previous month than it is with the topsoil layer.

TABLE G4: REGRESSION COEFFICIENTS (R^2) OF THE CORRELATION OF HTO CONCENTRATIONS IN THE COMPARTMENTS OF SOIL, AIR AND RAIN WATER

Compartment 1	Compartment 2	East SP	West SP	Comment
Top Soil	Rain	0.73	0.02	see Figure G11
Top Soil	Air	0.29	0.42	see Figure G12
Soil (0–20 cm)	Rain	0.66	0.13	see Figure G13
Soil (0–20 cm)	Air	0.24	0.60	see Figure G14

Therefore, the averaged soil values are used for further evaluations of the relative importance of the wet and dry pathways of HTO to the soil. Firstly, the ratios of HTO in soil to that in rain or in air are examined to see if there is a relationship between that ratio and the HTO concentration in the third compartment. Secondly, the data were examined to see if there is a relationship between the HTO ratios of soil to rain or air and the amount of uncontaminated rain that fell after the last wet contamination event. It would be expected that less contaminated rain would reduce the HTO concentration of the soil. Thirdly, analyses were performed to see if it is possible to reduce the scatter of data if the age of wet or dry contamination events is taken into account, and if there is a seasonal trend. If the release rate was constant over time, contamination events at the beginning of a sampling period should be of minor importance compared with later events.

(G29) The respective ratios of HTO in soil and rain or air are presented in Figures G15 to G19. The ratios of the most correlated compartments are well within an order of magnitude: the geometric mean of HTO ratios for soil to rain is about 1.4 at the East SP and about 2.5 at the West SP (Figures G15 to G17). The geometric mean of HTO ratios for soil to air is about 0.1 at the West SP and about 0.2 at the East SP (Figures G18 and G19). The uncertainties for the means of the ratios are between a factor of 2 and 2.5. The ratios for the non-correlated, or less correlated, compartments are scattered over more than an order of magnitude (soil to rain at West SP and Soil to air at East SP). The investigated relationships do not show any clear trend with the third compartment (Figures G15 and G17), or the age of wet contamination events (Figure G17), or the age of dry contamination events (Figure G19). The numbers on the dots of Figures G17 and G19 indicate the month of the year, but again there is no seasonal trend. It must be assumed that fluctuations of the release rate are large enough to cover all trends that could be expected for the ratios. There is no method to reduce the scatter of data.

G5. CONCLUSIONS

(G30) During work on Scenario 1 (see Part A), the question arose as to the importance of including dry deposition in a model. An experimental program was initiated in France to collate data on the effects of wet and dry deposition on tritium concentrations in rain, air and soil. The experimental work and sample analysis were supervised by G Guinois (CEA, France), and M Täschner (ZSR, Germany) performed the analysis of the results from the sampling programme.

(G31) The overall conclusion is that both wet and dry deposition must be considered when evaluating tritium concentrations in soil moisture from the activity concentrations of HTO in air humidity and in rain water. Two sampling points were investigated with different contributions of HTO in the environmental compartments of rain and air to soil water concentrations. One important finding is that the HTO concentration in air is very much higher than the HTO concentrations in soil moisture and in rain. This does not prove the importance of the dry deposition process by itself, and, in fact, at one sampling point the HTO concentration in soil moisture is correlated to that in rain. But at the other sampling point, the HTO concentration in soil moisture is twice the concentration in rain, and the analyses show a significant correlation between HTO concentrations in soil and those in air. That sampling point is located in a sector where the joint frequency of wind and rain is low. In this case, the effective pathway for HTO to soil is via dry deposition.

(G32) The task of this experimental program was not to answer the question of whether the current models are able to predict correctly HTO concentrations in soil via dry and wet deposition from release and meteorological data, i.e., within acceptable limits of uncertainty. Further work is required to clarify the relative importance of the washout process of HTO compared to dry deposition, as this has not yet been fully validated for sites other than the ones investigated here. Once suitable data sets are available, the models then need to be tested for their ability to predict the appropriate environmental concentrations following the wet and dry deposition processes. Until then, this report shows that if HTO concentration in rain is taken as a basis for evaluating HTO in soil, and if wet deposition is considered solely as a pathway of HTO to soil, then the models are certain to underestimate soil, and consequently plant, concentrations.

(G33) The ratios of HTO in soil moisture to HTO in air humidity reported here of between 0.08 and 0.2 on average reflect the specific conditions of the sites investigated. For dose assessment calculations it is strongly recommended that the dry deposition process of HTO to the soil compartment is included. Given the uncertainty for these ratios of 2 for monthly samples over a 20-month period, the data for both sampling sites can be summarised by the statement that soil activity can be estimated by taking a value of 0.2 times the HTO concentration of the air humidity.

(G34) Further experimental work should include higher sampling frequencies, in order to obtain a better correlation between variations in tritium concentrations and the frequently sampled meteorological conditions in order to understand more fully the various tritium transport processes involved in deposition to the soil.

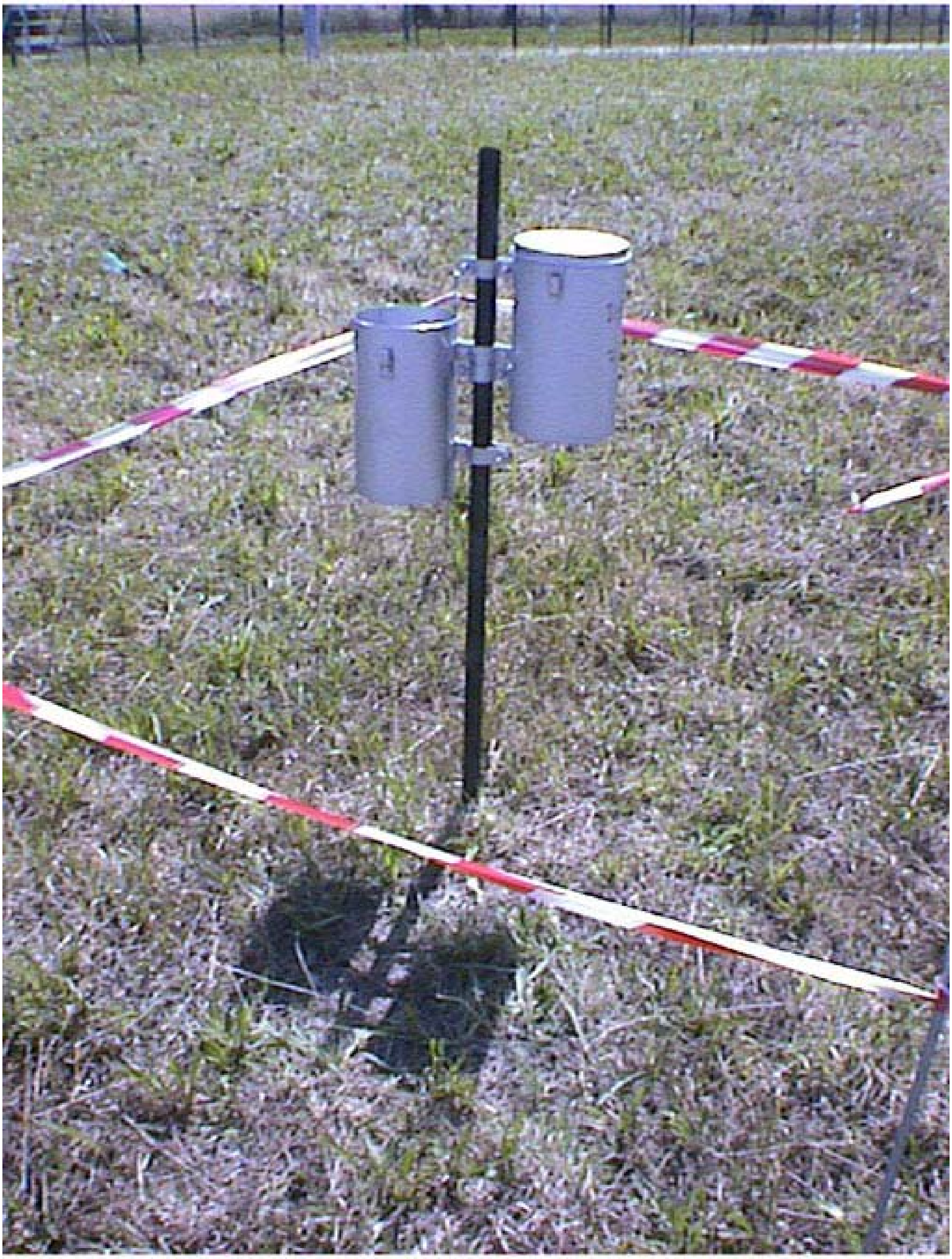

FIG. G1. Photograph of the sample collection equipment in normal operation. The housing closed at the top contains a passive sampler for air humidity collection (on the right). The second housing, opened at the top contains a precipitation collector (on the left).

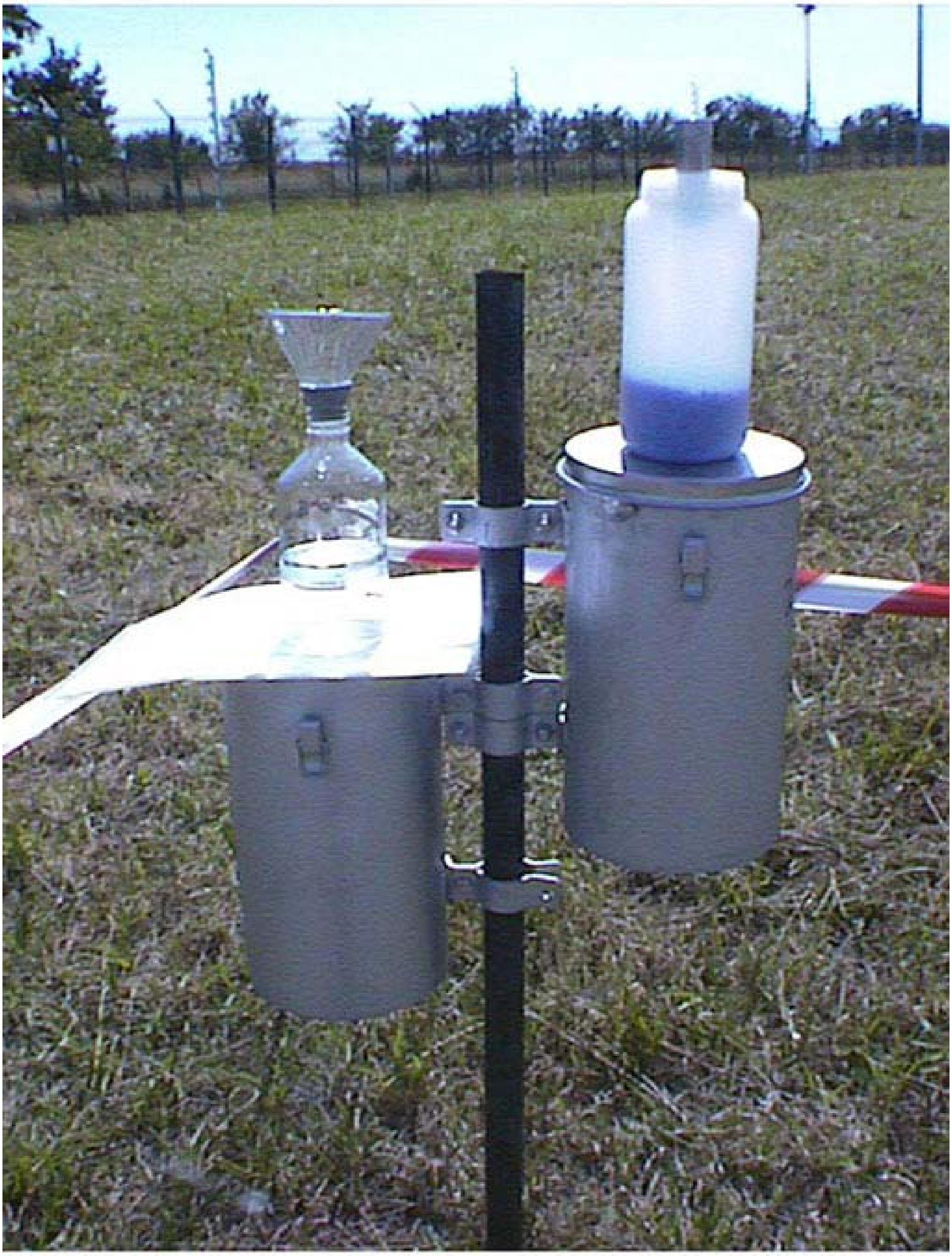

FIG. G2. Photograph of collectors placed on top of their housings for the purposes of the photograph (on the right: passive sampler for air humidity collection; on the left: precipitation collector). In normal operation, the collectors are contained within the housings.

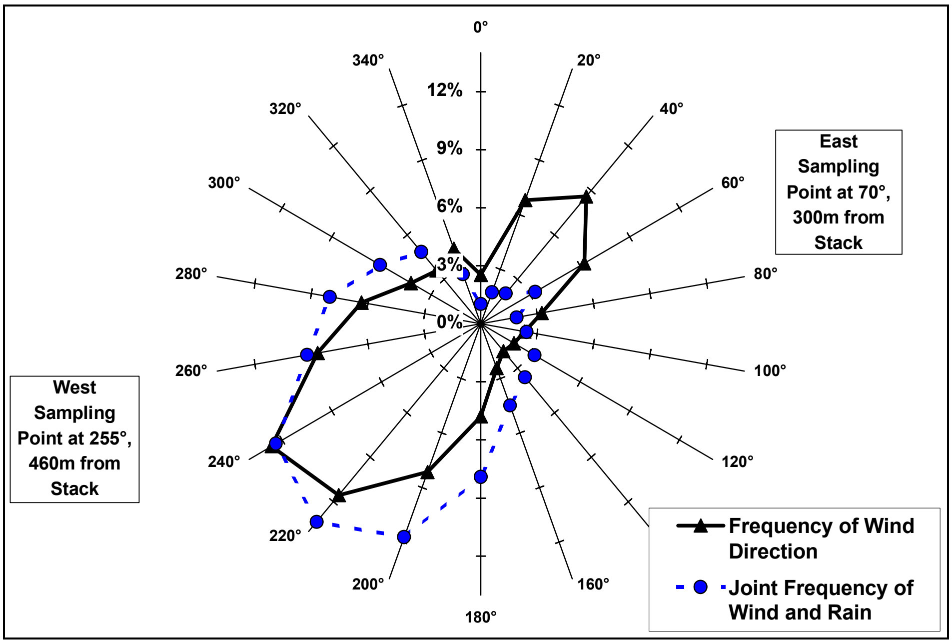

FIG. G3. Distribution of the wind directions (triangles), i.e. the frequencies of wind blowing from the direction within of each of the respective 20°-sectors. The main wind direction is Southwest to Northeast. Distribution of the joint frequency of wind and rain (circles). Sampling period is from 18 March 1998 to 10 December 1999. The joint frequency is given in relative units (the frequency values sum up to 100% which represents the number of 10-minute events with precipitation which actually is a fraction of 3.4% of all recorded 10-minute events). It has a maximum at Southwest, i.e., when precipitation occurs the wind blows predominantly from Southwest. Also indicated are positions of the Sampling Points East and West.

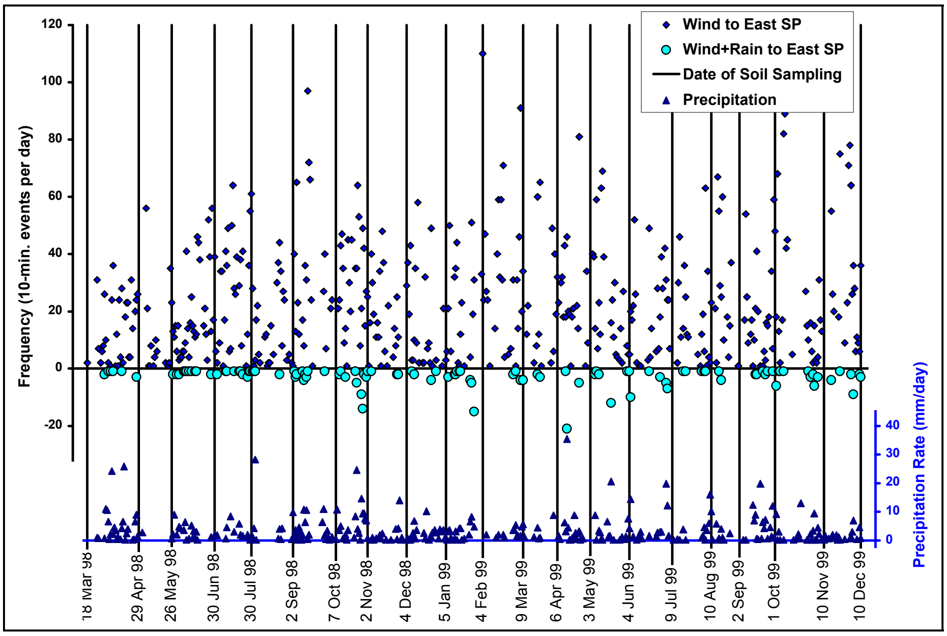

FIG. G4. Time-course of frequency of all wet and dry contamination events (i.e. the daily number of 10-minute meteorological records with wind blowing from the stack) (diamonds) and wet contamination events (joint frequency of rain and wind from the stack, plotted on the negative axis) (circles) at East Sampling Point (East SP). Precipitation rate is shown on a separated y-axis (triangles).

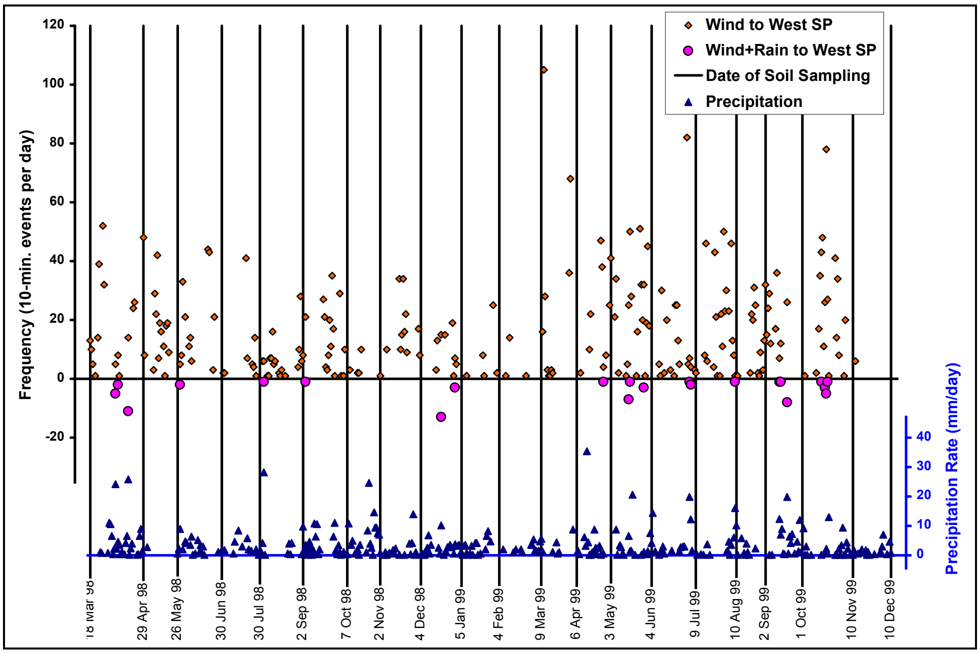

FIG. G5. Time-course of frequency of all wet and dry contamination events (i.e. the daily number of 10-minute meteorological records with wind blowing from the stack) (diamonds) and wet contamination events (joint frequency of rain and wind from the stack, plotted on the negative axis) (circles) at West Sampling Point (West SP). Precipitation rate is shown on a separated y-axis (triangles).

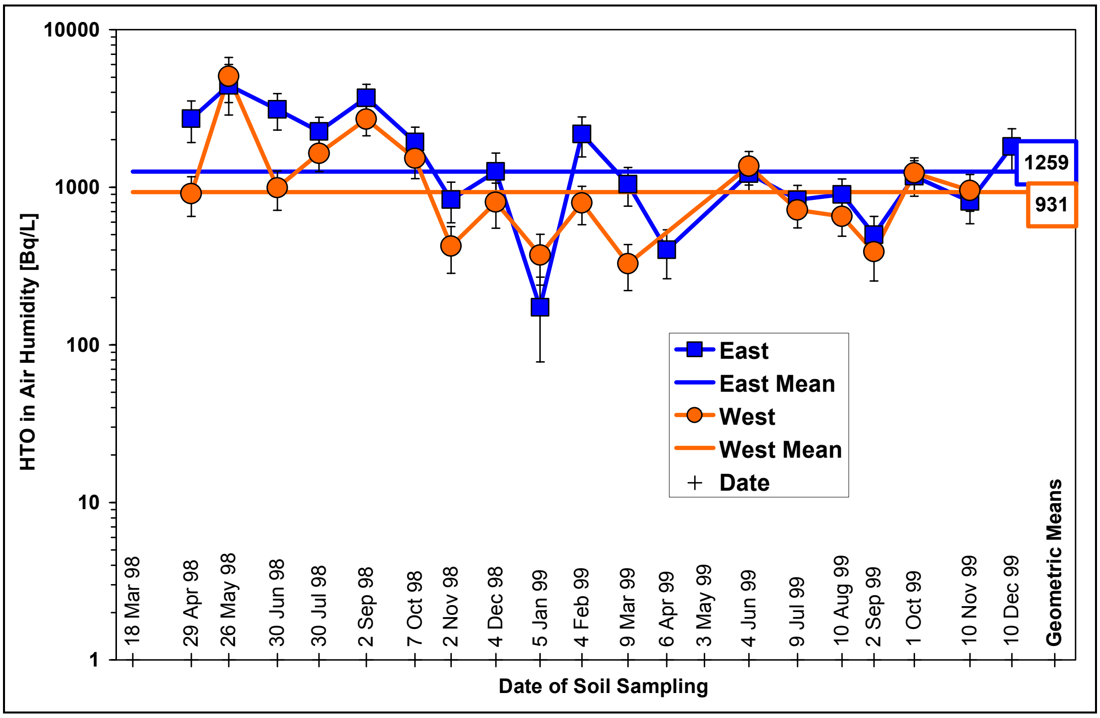

FIG. G6. HTO concentration in air humidity at East SP and at West SP. The horizontal lines indicate the geometric means of all samples during the sampling period at the respective SP. Symbol bars indicate the uncertainty of the HTO determination.

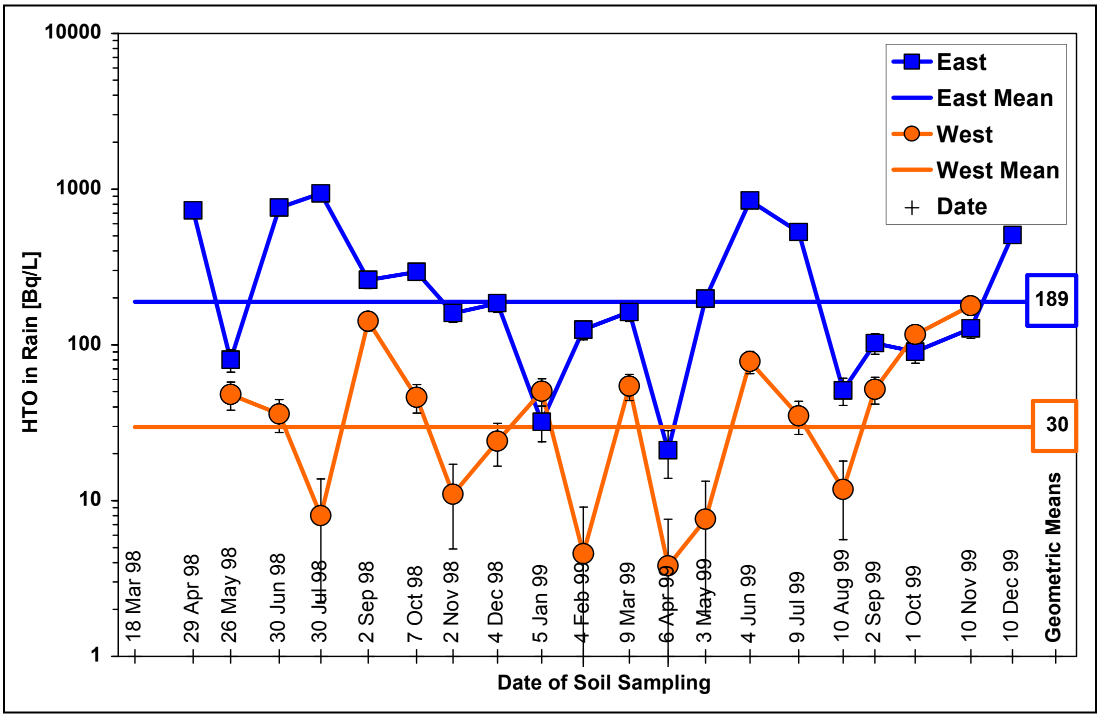

FIG. G7. HTO concentration in rainwater at East SP and at West SP. The horizontal lines indicate the geometric means of all samples during the sampling period at the respective SP. Symbol bars indicate the uncertainty of the HTO determination.

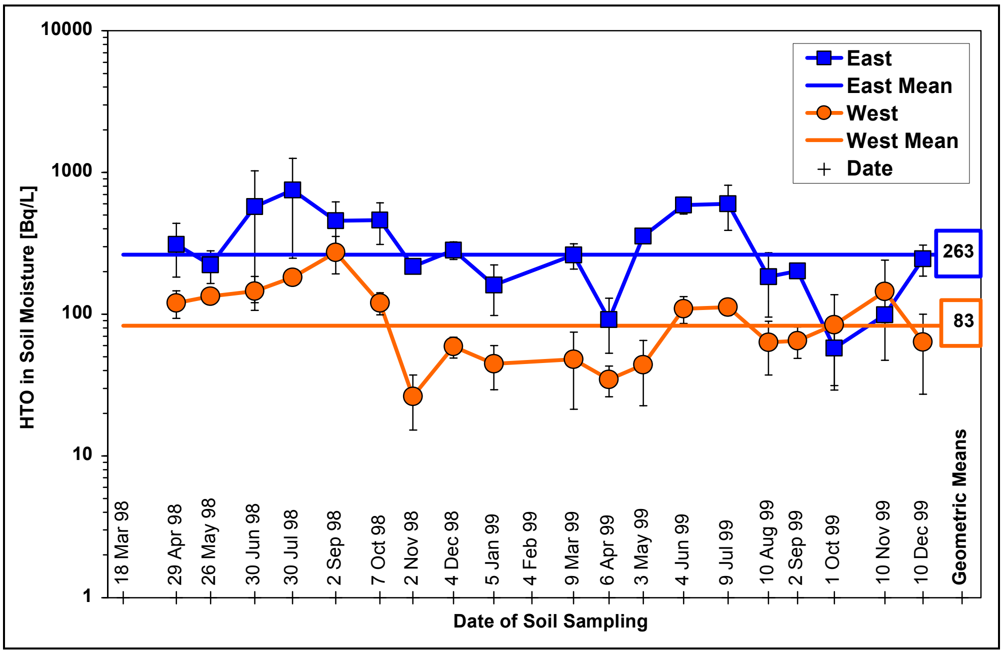

FIG. G8. HTO concentration in soil moisture (average of all four 5-cm layers, total depth is 20cm) at East SP and at West SP. The horizontal lines indicate the geometric means of all samples during the sampling period at the respective SP. The symbol bars indicate the variation within the four layers contributing to the average. The uncertainty of the HTO determination is indicated in Figure G9.

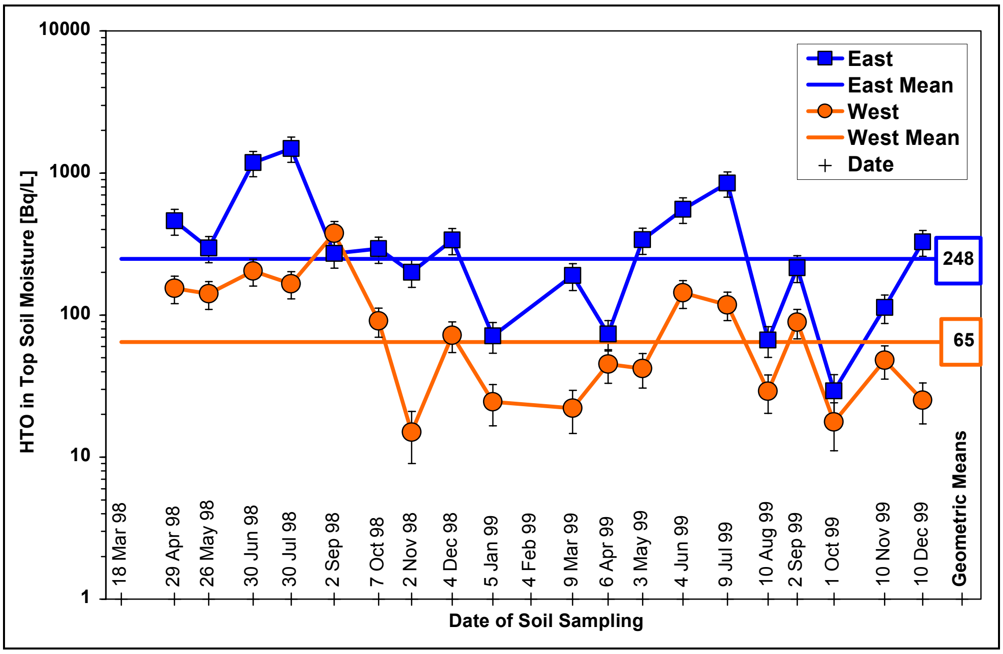

FIG. G9. HTO concentration in soil moisture of the top 5-cm soil layer. The horizontal lines indicate the geometric means of all samples during the sampling period at the respective SP. Symbol bas indicate the uncertainty of the HTO determination.

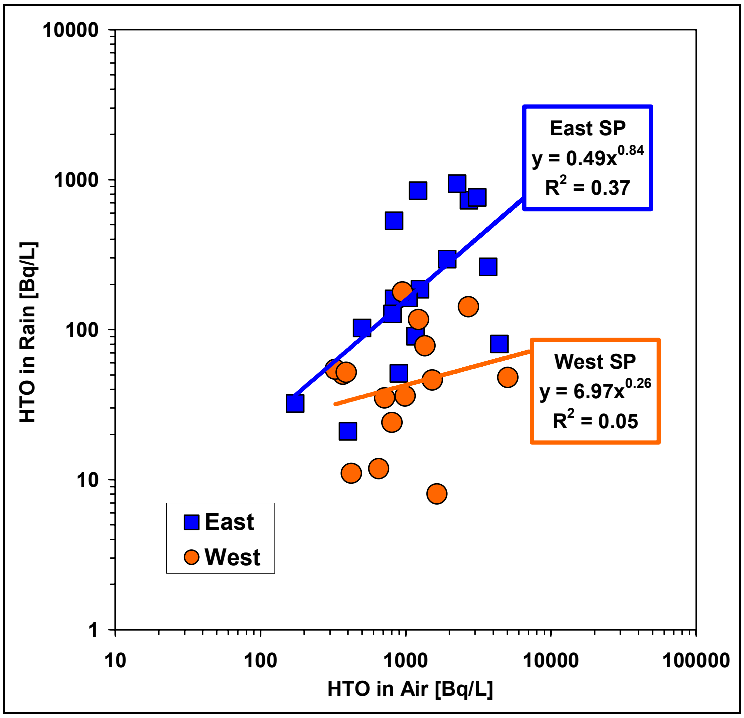

FIG. G10. Correlation of HTO concentrations in rainwater and in air humidity at East and West SP.

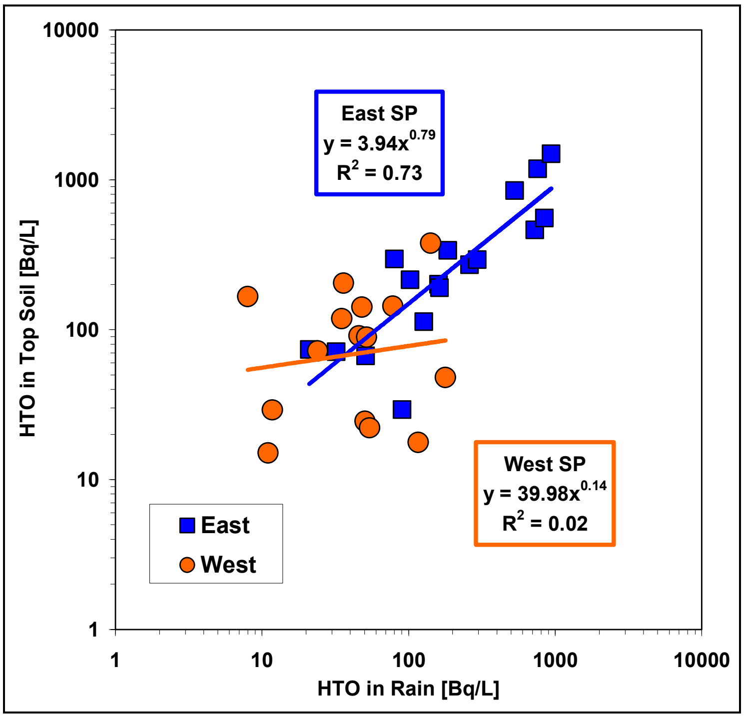

FIG. G11. Correlation of HTO concentrations in moisture of topsoil layer and in rain at East SP. There is no significant correlation at West SP.

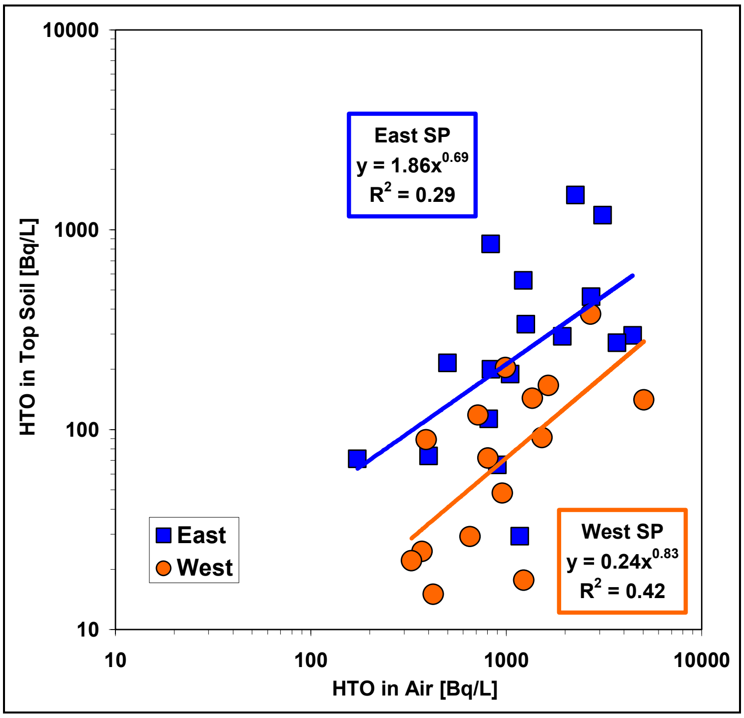

FIG. G12. Correlation of HTO concentrations in moisture of topsoil layer and in air humidity at West SP. There is less significant correlation at East SP.

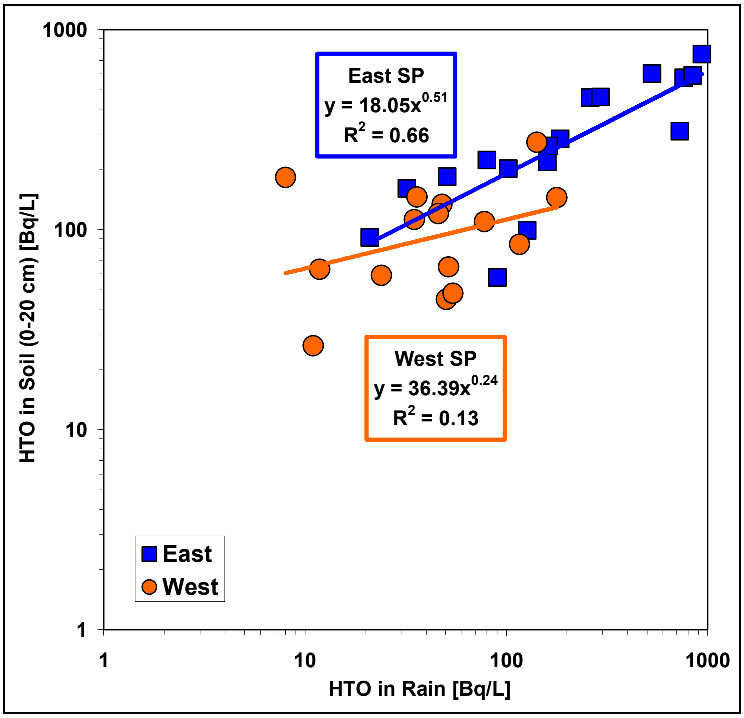

FIG. G13. Correlation of HTO concentrations in soil (0 to 20cm layer) and in rainwater at East SP. There is no significant correlation at West SP.

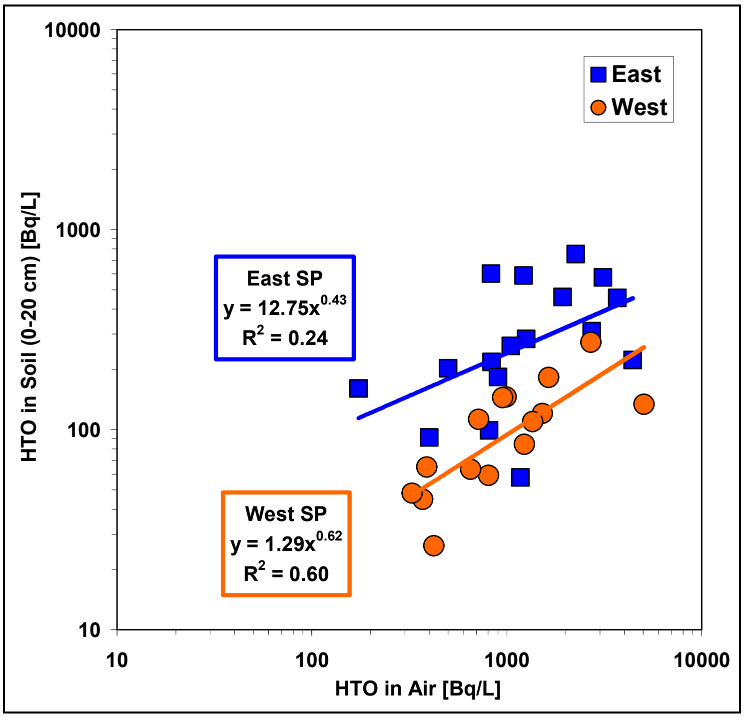

FIG. G14. Correlation of HTO concentrations in soil (0 to 20cm layer) and in air at West SP. There is less significant correlation at East SP.

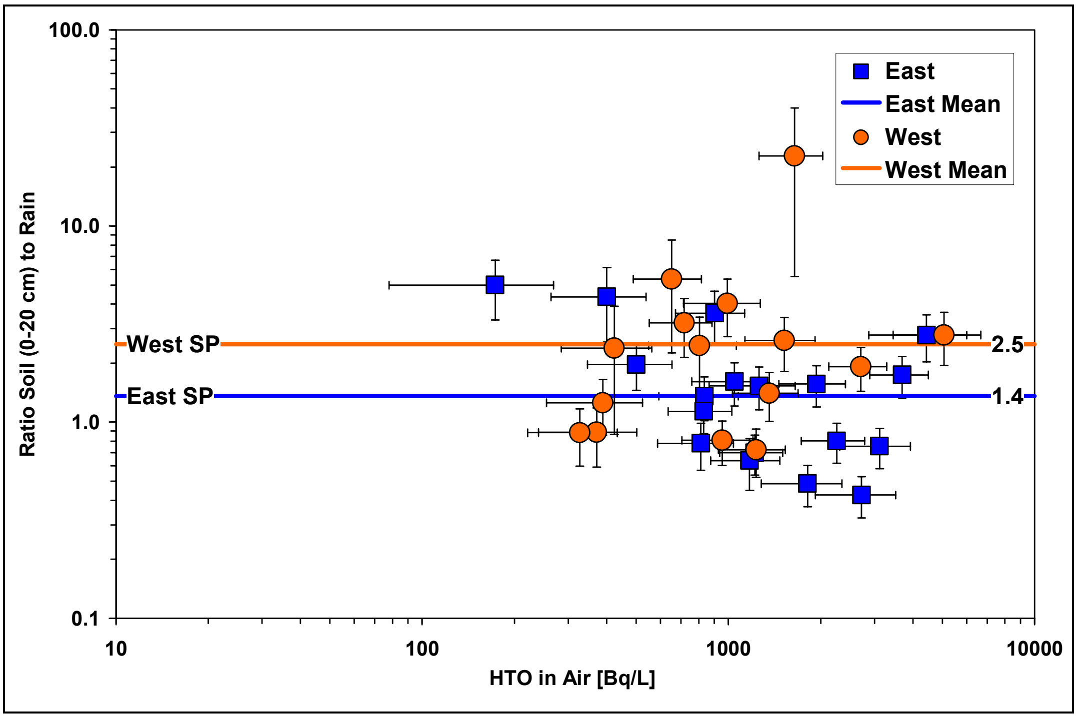

FIG. G15. Relationship between the ratios of HTO concentrations in soil and in rain and the HTO concentrations in air humidity. The symbol bars indicate the uncertainty of the determination of the ratios and of the HTO concentrations.

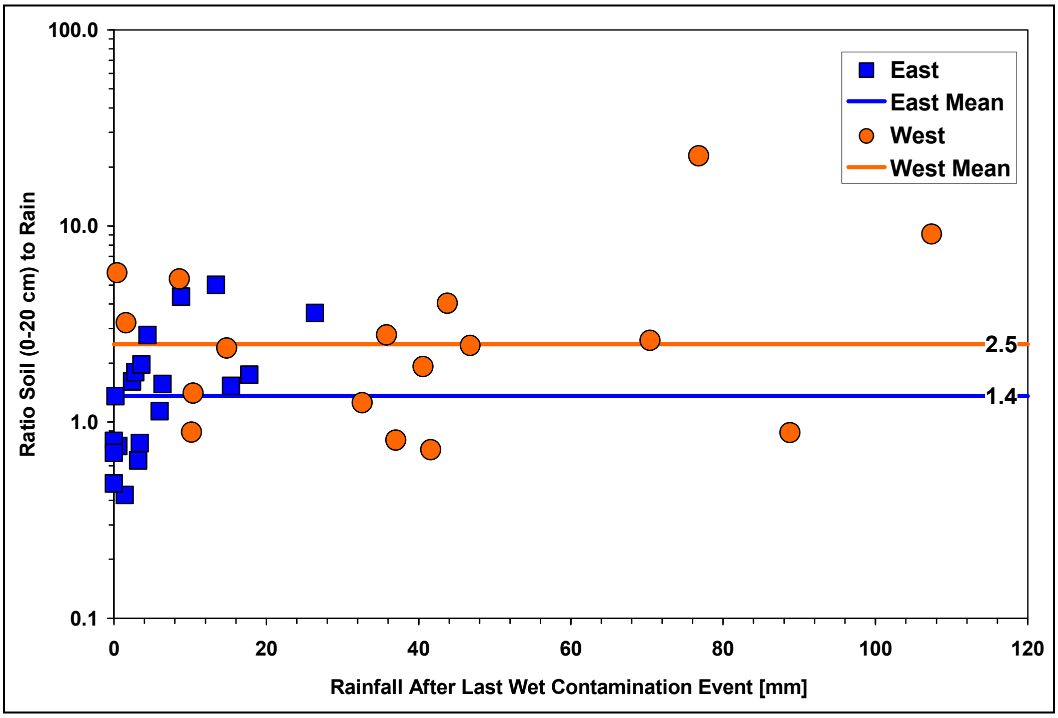

FIG. G16. Relationship between the ratios of HTO concentrations in soil and in rain and the rainfall after the last wet contamination event before sampling.

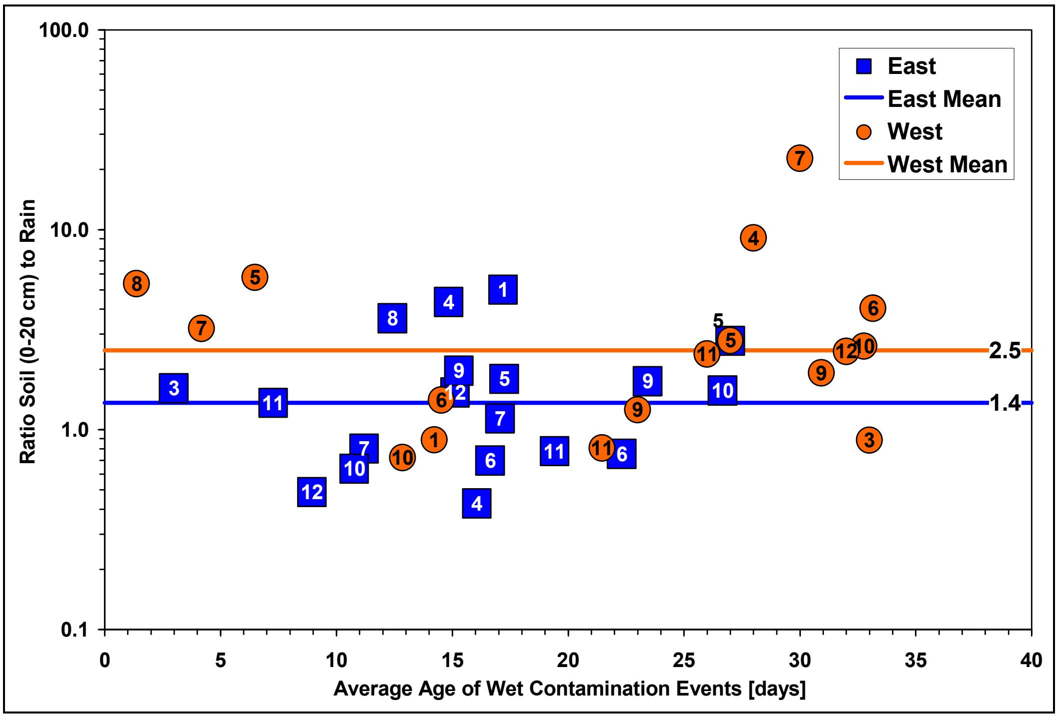

FIG. G17. Relationship between the ratios of HTO concentrations in soil and in rain and the average ages of the wet contamination events of the sampling period (the numbers on the symbols for East and West SP indicate the month of sampling).

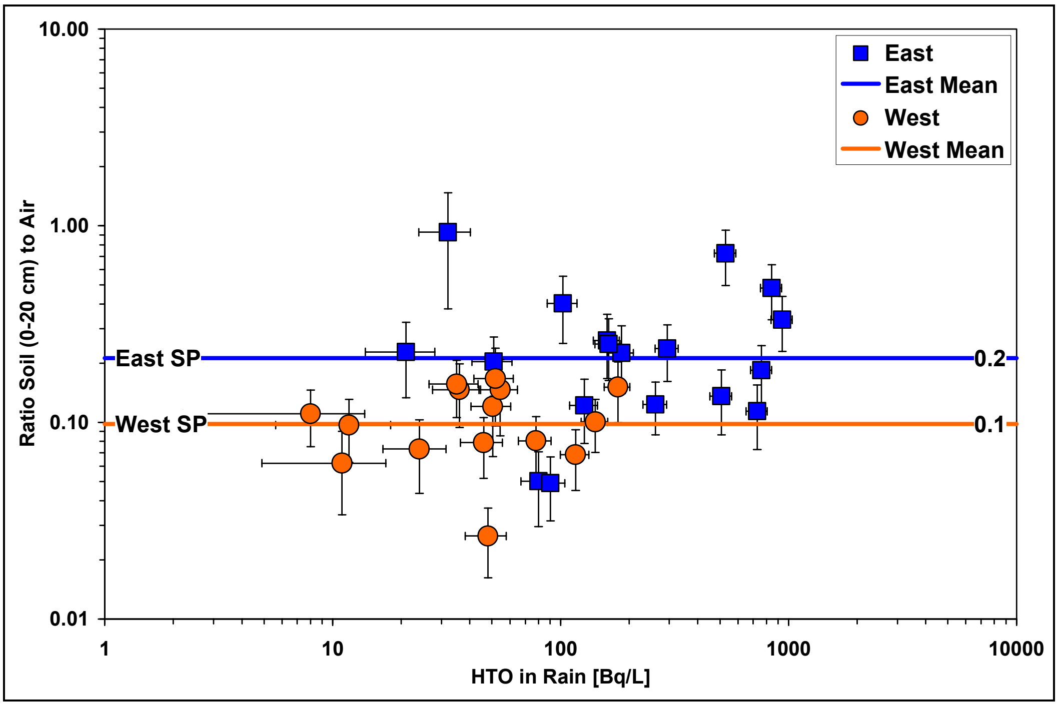

FIG. G18. Relationship between the ratios of HTO concentrations in soil and in air to the HTO concentrations in rain. The symbol bars indicate the uncertainty of the determination of the ratios and of the HTO concentrations.

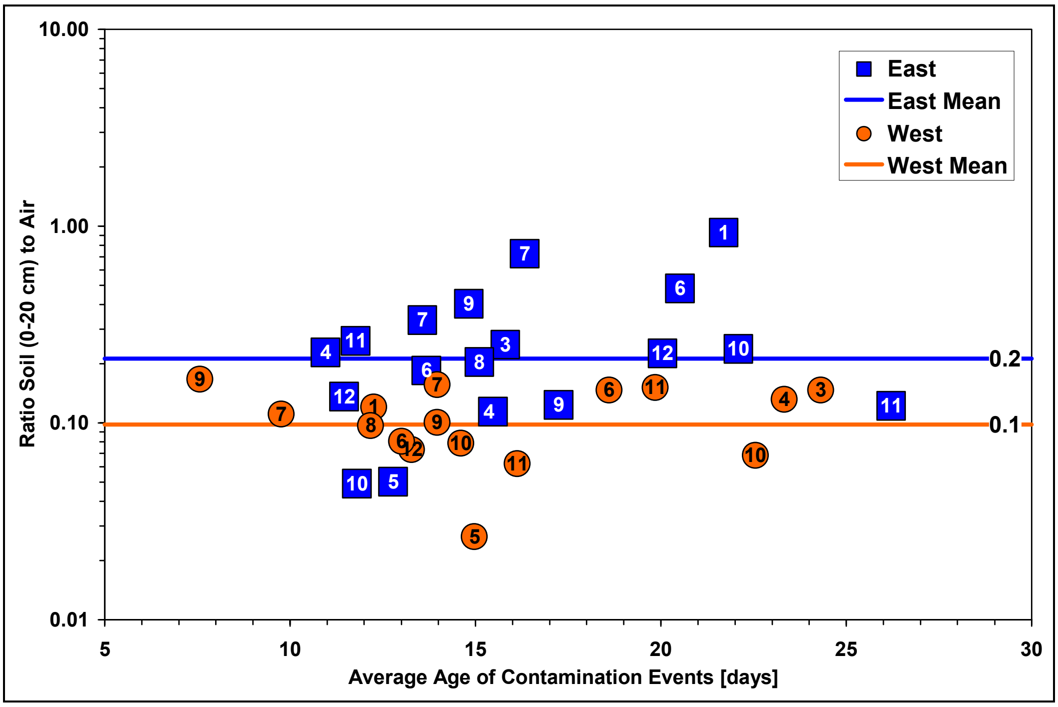

FIG. G19. Relationship between the ratios of HTO concentrations in soil and in air and the average ages of the contamination events of the actual sampling period (the numbers on the symbols for East and West SP indicate the month of sampling).

GENERAL CONCLUSIONS

(1) The global level of tritium is currently much lower than during the period of nuclear testing and concentrations have now fallen to near natural background levels. Nevertheless, some areas in the vicinity of chronic atmospheric or sub-surface sources of tritium still show elevated concentrations. Modelling the environmental transport of tritium from chronic sources, and the subsequent concentrations in different environmental media, cannot be carried out by direct application of multi-purpose generic assessment models, which are not suitable due to the unique properties and behaviour of tritium compounds in the environment. Whilst specific models for short term or accidental releases of tritium have previously been developed and tested in various international fora (e.g. see BIOMOVS II, 1996 a, b; Barry et al, 1999), this has not been the case for models for chronic releases. When the TWG was inaugurated within the IAEA BIOMASS programme in December 1996, the participating modellers and experimentalists agreed that their activities should concentrate in four main areas related to chronic sources of tritium.

(i) Testing whether the existing models for calculating long term air concentrations are suitable for assessing concentrations of HTO and HT in air following chronic atmospheric releases.

(ii) Testing and modifying appropriate models for calculating HTO concentrations in near-surface soil moisture and plants following chronic atmospheric releases.

(iii) Modifying or developing models for processes involved in tritium transport down through deeper soil layers to groundwater and up through unsaturated media to the soil surface as a result of long term atmospheric or sub-surface sources respectively.

(iv) Identifying a key modelling problem for which observational data were lacking so that experimentalists and modellers could collaborate in the development of a suitable sampling programme to provide the required data.

(2) Six different model test scenarios (four concerned with atmospheric pathways and two with sub-surface pathways) and a 20-month environmental sampling programme were undertaken to address these four main areas of interest. Conclusions arising from these activities are provided below together with recommendations for model improvements, data acquisition methods and future studies.

ATMOSPHERIC PATHWAYS

(3) Four different model test scenarios were developed for chronic atmospheric releases of tritium either as HTO or HT. The first scenario was a relatively simple model-model test exercise that was undertaken whilst sets of relevant observational data from sites in Canada, Russia and France were collated to provide the basis for three model-data exercises. In each case, modellers were asked to calculate concentrations of HTO in air moisture, soil moisture and plant tissue free water (TFW) and concentrations of organically bound tritium (OBT) in dry plant matter. Each of these exercises presented the modellers with specific challenges. For example, the scenario based on Canadian data required the modellers to consider multiple emission sources and to explain temporal and spatial variability in the observations. The scenario based on Russian data was concerned with a non-continuous, but chronic, source where emissions decreased significantly over the twenty years of observations. The scenario based on French data required consideration of multiple sources and the effects of rolling terrain on air concentrations. A comparison of the four sets of results enabled a number of conclusions to be drawn concerning modelling HTO concentrations in each environmental

medium. Most participants used models based on simple equilibrium concepts but some employed time-dependent codes that simulated the transport processes in detail.

HTO releases: Air moisture concentrations

(4) All the participating models were based on the traditional Gaussian dispersion formulae. The first scenario (a model-model inter-comparison exercise) considered a single stack that continuously emits a constant concentration of HTO under well-defined average weather conditions. The weather statistics were provided in the scenario description and all the modellers used a sector-averaged approach to the dispersion calculations. Predicted concentrations of HTO in air moisture were all within a factor of two, except in the immediate vicinity of the stack where the concentrations are very low if re-emission from the contaminated soil was neglected and much higher if the re-emission was taken into account. The divergence in the results that were obtained at more than a few hundred metres from the source was considered to be acceptable. However, the question remained as to how the models would perform in 'real' assessment type situations where modellers must interpret data and adapt their model to reflect conditions at the site of interest.

(5) The three subsequent scenarios were blind test exercises in which predictions from the different models were compared with observations. In most cases predictions agreed with the observed air concentrations within a factor of three for the Canadian and French sites, and within a factor of five for the Russian site. The results are considered acceptable for the scenarios based on Canadian and French data. It is interesting to note that in the case of the French site with rolling terrain, some participants actually obtained better results when ignoring topography than those modellers who included it. On the basis of these results, it appears that topographic effects need not be taken into account, at least for sites of moderate relief and for receptors up to a few kilometres from the source(s). The more divergent results for the Russian site were attributable to two main causes. The first was a problem with the meteorological data which were not supplied in the normal format used in the models. As a consequence the modellers interpreted the data differently and used different techniques to obtain suitable meteorological statistics as input for their models. Secondly, results for air moisture concentrations were most divergent for just one of the sampling locations (Sampling Point 4). In fact, calculations for this sampling point actually helped to demonstrate that there was a problem with the observational data. Upon further investigation it was found that there was a second source of emission near Sampling Point 4 that was not known to the scenario developer until the last phase of the scenario test exercise. So, although the additional emission was much weaker than the main source it nevertheless affected the air concentrations. The modelling results would have been closer to observations had modellers been able to take the second source into account. Overall, it appears that the existing models are satisfactory for predicting HTO concentrations in air moisture.

(6) In theory, the models should account for the contribution of re-emitted tritium to the air concentration. In fact, the calculation of secondary air concentrations is not a simple matter. Summing the contribution from all ground level sources is really the only way to estimate contributions from this process. Although the dispersion part of such calculations is relatively straightforward there are a number of uncertainties involved, the most notable of which is the height at which to measure wind speed. It is also a non-trivial matter to estimate re-emission fluxes. But secondary re-emission to air from soil probably contributes less than 10% to the air moisture concentrations of HTO under most circumstances. So, it was considered that re-emission could be ignored *unless* calculations are required for areas very close (within 500 m) to an elevated point source or when the source is below ground.

HTO releases: Soil moisture concentrations

(7) In contrast to results for air concentrations, predictions for HTO concentrations in soil water were more divergent. For the first scenario, results varied by more than a factor of seven. For the scenario based on Canadian data, the predicted soil water concentrations differed from the observations by a factor of less than ten, although this was reduced when soil concentrations were normalised to air concentrations in order to eliminate the influence of different modelling approaches on atmospheric dispersion. In the scenario based on Russian data, snow lying on the soil surface for any length of time was shown to prevent the ingress of HTO into the soil until snow melt occured in spring. Snowmelt also appeared to cause some retention of tritium in the soil but more information is required before firm conclusions can be made on this.

(8) The differences in predicted soil concentrations were due to differences in calculated air concentrations (see above) combined with differences in modelling approach. Some modellers used an activity balance approach in their calculations. This generally gives soil/air ratios close to unity, a result much higher than most observations. It appears that a steady state assumption is unrealistic, and/or that the method for formulating the balance of activity in soil is oversimplified. Some modellers ignored the contribution of dry deposition to soil concentrations. Others included semi-empirical representations of both wet and dry deposition processes. The predictions underestimated the observed soil/air ratios if only wet deposition was included in the models, and overestimated the ratios when both dry and wet deposition were included. It appears that dry deposition must be considered in calculating long term average soil concentrations but it is not yet clear how to quantify it properly.

(9) It was decided to commission a field survey with the specific objective of collecting data on the relative contributions of wet and dry deposition of HTO to soil water concentrations (see Objective 4 above). The work was undertaken collaboratively by CEA/DAM/DASE, France and ZSR of the University of Hannover, Germany and carried out at a site near Bruyeres-le-Chatel, France. Concentrations of HTO were measured monthly in air moisture, rain and soil moisture at two stations that received either mainly dry or mainly wet deposition. The results of the 20-month sampling programme showed that dry deposition does contribute to soil moisture concentrations. The experimental work also showed that a better estimate of soil moisture concentrations is obtained if they are related to HTO concentrations in air averaged over the period of study rather than to average concentrations in rainwater as often previously assumed. Moreover, the ratio of soil/air concentrations showed a spatial variability that depended on the joint frequency of precipitation occurrence and wind direction. These data will provide the first step toward the development of better models for predicting soil concentrations. Until then, from the ensemble of data obtained from the Bruyeres-le-Chatel field experiment (Part G) and the Chalk-River field survey (Part B), the following recommendation can be made. The concentration of tritium in soil moisture (Bq l^{-1}) can be assumed to be 0.3 times the concentration of tritium in atmospheric moisture (Bq l^{-1}); a higher ratio of 0.5 possibly could be used for conservative assessments. It is recommended that further work is undertaken on the activity balance and semi-empirical modelling approaches in the hope of finding a more general, theoretically-based model that can account for variations among sites. Although uncertainties in calculations of soil moisture concentrations are larger than uncertainties in predictions for other environmental compartments, HTO concentrations in soil do not contribute much to dose estimates and so a moderate level of uncertainty in modelling soil concentrations can be tolerated.

(10) It is often assumed that, where field observations and model predictions disagree, it is the predictions that are at fault. However, this is not always the case since field data are always subject to errors. This is examined further in the discussion below on how to improve field survey data.

HTO releases: Plant aqueous and organic phase concentrations

(11) The spread of results for predictions of plant tissue free water tritium (TFWT) and organically bound tritium (OBT) for all the atmospheric pathway scenarios was smaller than the divergence of results for soil moisture concentrations. Predictions and observations were generally in agreement within a factor of two to three for the model-model inter-comparison and the Canadian and French scenarios, and less than a factor of five for the Russian scenario. This is not surprising as model calculations depend primarily on air, not soil, concentrations. All the participating models for plant leaf uptake are similar. Overall, the models over-estimated the proportion of HTO taken up from the atmosphere probably because they are based on the assumption that all the water in plant leaves is accessible for exchange with water in the atmosphere and this is not true for all plants. Generally, the TFWT and OBT over-estimates were relatively small because plant water concentrations are forced by specific activity concepts to be lower than concentrations in air humidity. The relatively small errors are probably acceptable if assessments require conservative estimates of doses to humans from consumption of foodstuffs. However, care needs to be taken that summing of conservative estimates over all the environmental compartments does not result in unrealistic predictions. The observational data for OBT concentrations in tree leaves and tree rings (in the French scenario) emphasised that information is lacking on the behaviour of OBT in plants and trees.

(12) Overall, it is considered that models for plant leaf uptake of HTO into TFW are acceptable. However, transport of TFWT to other plant parts such as to tubers, root vegetables, shrub and tree fruits, and particularly development of models for OBT in plants (and animals) used for food by humans all require further study.

HT releases: Air moisture concentrations

(13) HT releases were only considered in the first, model-model intercomparison, scenario. Concentrations of HTO in air moisture following an HT release are entirely controlled by oxidation of HT at the soil surface and subsequent re-emission of HTO to the atmosphere. Model predictions were spread over a factor of ten. This is not surprising given the difficulty of simulating the oxidation and re-emission processes. This is one area where more information and data are required. Until this is forthcoming, it is suggested that the empirical ratios derived from the 1994 HT chronic release experiment conducted at Chalk River Laboratories (CRL), Canada are used, namely that HTO in air (Bq m^{-3}) due to an HT release is 0.04 times the predicted HT concentration in air (Bq m^{-3}). Uncertainties that would arise by using this ratio are likely to be lower than those that would occur in trying to model deposition and retention in soil, re-emission and dispersion in the atmosphere. However, it should also be recognised that there are uncertainties associated with the data obtained from the experiment and that the ratios may not be appropriate for sites where the climate, plants or soil differ markedly from those at CRL.

HT releases: Soil moisture concentrations

(14) As for air moisture concentrations, it is suggested that empirical ratios derived from the 1994 HT chronic release experiment at CRL provide the best way to calculate soil moisture concentrations. The recommended tritium concentration in soil moisture (Bq l^{-1}) is 6 times the concentration of HT in air (Bq m^{-3}). Once the HTO concentrations in air and soil are known, the rest of the model for HT releases is identical to the model for HTO releases.

SUB-SURFACE PATHWAYS

(15) An effort was made to model the transport of tritiated water both down to, and up from aquifers in the vicinity of tritium facilities. There was no ambition to be totally comprehensive in the processes to be studied as this was neither a hydrological nor a soil study. The aim was to improve models for tritium assessment purposes. The first problem given to modellers involved tritium transport down through the soil and the consequent contamination of a previously uncontaminated shallow aquifer. The second problem involved a sub-surface source of tritium that had resulted in the contamination of an aquifer and the resulting upward movement of tritium through a previously uncontaminated soil. These are issues that must be considered either for the protection of groundwaters or for the isolation of buried wastes from the overlying soil medium.

(16) Although detailed soil and hydrological models are generally available, there has been no previous attempt to couple these with the specific problem of modelling tritium transport in unsaturated media. At the start of the TWG four-year programme, it was hoped that at least one data set would become available for testing the models. Despite a concerted effort to obtain such data from various sources this goal was not realised. Consequently, two model-model inter-comparison exercises were developed so that modellers could develop or adapt appropriate models and discuss the modelling problems that arose. Most importantly, these two exercises helped modellers to develop modelling tools that can now be applied to the problem of tritiated water movement in saturated and unsaturated media.

(17) Different models were applied to the two problems posed in the scenarios. Some modellers adapted flexible models of a commercial type that are normally used to solve a wide range of environmental problems, including flow, heat and mass transport in geological media. Other participants developed their own codes based on process models and numerical techniques formerly developed by others. A few modellers attempted to elaborate analytical models. The application of the different models to the two problems led to results that were relatively close together, and in many cases were grouped within a factor of two. Nevertheless, some important issues were highlighted during the study. The numerical models were found to be more flexible than the analytical models and could be more readily adapted to the complex processes involved in tritium transport. But, great care is required with temporal and spatial discretisation. Use of small time steps and a large number of thin soil layers appeared to be most suitable for the problems in hand. However, one modeller was able to 'tune' certain parameters and transfer coefficients in order to retain a model with a small number of thick soil layers that gave comparable results to the more complex models. Regardless of the number of layers used, how to treat the variability within the layers still needs to be addressed. The two modelling exercises were approached in a research context and the question remains as to whether complex models would perform adequately in an assessment situation where all the relevant data required for their operation might not be available. Certainly in the two inter-comparison scenarios the simple models also appeared to perform well. Indeed, the steep

tritium concentration gradients imposed in the second sub-surface scenario were rather artificial. It may be that with the shallower gradients seen in nature, models with a small number of thick layers would perform adequately. So, without actual observational data it is not possible to unequivocally recommend the highly sophisticated models.

(18) A number of other conclusions were drawn during the work on the two scenarios. First, there is a need to examine closely if the models conserve the activity balance during the evolution of the systems involved in either downward or upward transport of tritium. Secondly, it was evident that water infiltrating down through the soil, or water being drawn up and evaporating from the soil surface, together with mechanical dispersion are the key factors in the transport of tritium in saturated or unsaturated media. Thirdly, the transport of tritium is very sensitive not only to water flow, but also to the value assigned to the dispersivity parameter that expresses the degree of irregularity of the flow pattern and which increases when local velocities vary strongly along the flow path. Experiments using tracers are required in order to have more information and data on dispersivity. Fourthly, from the second of the sub-surface scenarios, it was shown that a vegetated soil increases the upward movement, and the consequent flux of tritium from the soil surface, by more than three orders of magnitude compared to a bare soil. This is a function of the transpiration processes at work when plants are present. It was shown that a soil cover of one metre depth above a contaminated aquifer would only be sufficient to act as a protecting barrier to tritium fluxes from the soil surface if the soil is not vegetated. For containment purposes a greater soil depth should be used if plants are to be established in the overlying soil medium.

GENERAL RECOMMENDATIONS

(19) As a result of the six model test exercises and the field sampling programme undertaken by the TWG during the four-year international collaborative programme, a number of recommendations that derive from the conclusions above can be made concerning: a) modelling tritium behaviour due to chronic atmospheric and sub-surface sources; b) field sampling and data acquisition methods; and c) future studies.

MODELLING

(i) Dry deposition is an important process that contributes to long term average soil moisture concentrations of HTO and should be included in models.

(ii) Secondary sources of HTO due to re-emission from soil can be ignored for ground level atmospheric sources and at distances >500 m from elevated sources but must be considered if the source is sub-surface.

(iii) To calculate near-surface soil moisture concentrations due to an atmospheric source, a more accurate estimate is made if soil moisture concentrations are related to air rather than rain concentrations.

(iv) In the absence of a suitable model, the assumption that the soil moisture concentration (Bq l^{-1}) is 0.3 times the air concentration (Bq l^{-1}) can be used. In screening assessments, a conservative value of 0.5 can be adopted.

(v) For HT releases, air and near-surface soil concentrations of HTO can be obtained from empirical data obtained in the CRL chronic HT release experiment.

(vi) For tritium transport down through deeper soil layers, and up from contaminated aquifers, the division of the model soil compartment into a large number of thin layers is likely to give more accurate results than if a small number of thick layers is used.

DATA ACQUISITION METHODS

(i) It is essential to have good source data and accurate measurements for model inputs (e.g. well-defined meteorological data statistics, soil properties) in order to achieve good assessment predictions and for developing, testing and applying models.

(ii) One of the reasons for the differences between predictions and observations in the atmospheric scenarios may lie in a mismatch between the assumptions of the models and the realities of the data. Most of the models assume equilibrium conditions when in fact the air concentrations over a given sampling site fluctuate continually in response to changing atmospheric conditions. Moreover, the observed soil and grass concentrations are normally determined from samples taken irregularly throughout the growing season. Averages of these samples may not reflect true mean values, which are what the models are designed to predict. Sampling programmes should be planned to yield mean concentrations, which are the quantities of primary interest in dose assessments.

(iii) Models can be used to highlight problems with observational data and it should not be automatically assumed that model predictions are inaccurate if they do not agree with the observations.

FUTURE STUDIES

(i) We have adequate models for assessing air moisture, soil moisture and plant TFWT concentrations of HTO resulting from both short term and chronic releases of HTO. Work is now required to develop and test models for OBT formation and translocation in food crops, animals and aquatic systems. More work is also needed to understand and model tritium deposition to snow and the fate of the tritium when the snowpack melts.

(ii) Further experimental work is needed to confirm the concentration ratios determined in the CRL HT chronic release study and to extend the ratios obtained to sites with climate, soil and plant properties different from those at CRL.

(iii) Data sets are required to test models for sub-surface processes and pathways involved in tritium transport in saturated and unsaturated media following chronic atmospheric or sub-surface sources of tritium.

(iv) Data are required to improve modelling of wet and dry deposition to soil.

(v) Further work is needed to determine if tritium can be retained in the environment to a significant extent if a previously constant source of tritium is reduced or cut off.

(vi) Tracer experiments are required to provide information on tritium dispersivity in the saturated and unsaturated zones.

REFERENCES

[1] BARRY, P.J., WATKINS, B.M., BELOT, Y., DAVIS, P.A., EDLUND, O., GALERIU, D., RASKOB, W., RUSSELL, S., TOGAWA, O., Intercomparison of model predictions of tritium concentrations in soil and foods following acute airborne HTO exposure, Journal of Environmental Radioactivity **42** (1999) 191–207.

[2] BIOMOVS II, Tritium in the Food Chain: Intercomparison of model predictions of contamination in soil, crops, milk and beef, after a short exposure to tritiated water vapour in air, Published on behalf of the BIOMOVS II Steering Committee by the Swedish Radiation Protection Institute, Sweden, ISBN 91-972134-7-0 (1996a).

[3] BIOMOVS II, Tritium in the Food Chain: Comparison of Predicted and Observed Behaviour, A: Re-emission from soil and vegetation, B: Formation of organically bound tritium in grain of Spring Wheat, Published on behalf of the BIOMOVS II Steering Committee by the Swedish Radiation Protection Institute, Sweden ISBN 91-972958-2-5 (1996b).

ANNEX I

MODEL DESCRIPTIONS

I–A. MODELS FOR ATMOSPHERIC RELEASES

I–A.1. Model used by JAERI, Japan

H. Amano, M. Andoh, T. Takahashi

ETDOSE (Environmental Tritium model for DOSE estimation), was developed by M.A. Andoh, T. Takahashi and H. Amano for dose assessment of tritium emissions in the surface environment. ETDOSE calculates tritium concentrations in air; soil, plant free water and OBT, and estimates dose impact by inhalation of air and ingestion of food for an acute and a chronic release of HT and HTO [1].

I–A.1.1. Structure of the model

ETDOSE includes two systems that user can choose for calculation of atmospheric distribution patterns of tritium. One is "rectangular grid system". This system is based on TRIMOD, which was developed by Dr. Belot [2]. In this system, the downwind area from the release point to the sampling point is divided into rectangular elements. Tritium dispersed into a given sector deposits on each rectangular element and re-emits to the atmosphere soon from the area source.

Another is "numerical integral system". In this system, not only the downwind area to the sampling point, but also the upwind area and the downwind area from the sampling point are included for calculations of secondary tritium dispersion. In a circle area, with the center of the source point and the radius of twice the length of the distance from the source to the sampling point, tritium is dispersed under given condition of the wind direction. Tritium re-emitted from the deposition point is dispersed to the sampling point according to the wind direction.

We calculated scenario 1 (atmospheric transport) by using "rectangular grid system" for HTO release and "numerical integral system" for HT release.

I–A.1.2. Primary dispersion

The basic equation is the sector averaged Gaussian equation. Deposited concentration of tritium is postulated to be equal in the same downwind distance in the given sector. It needs the frequency of wind blows into the chosen direction, wind speed at effective height of release and stability as input data. The tritium concentration is calculated by superimposing of all results for each weather stability class multiplied by that frequency.

I–A.1.3. Secondary dispersion

Re-emission from soil surface is considered to occur one time. Flux of re-emission is assumed to be equal to flux of deposition that given in scenario 1; 3.0E-4m/s for HT release and 3.0E-3 for HTO release. In both HT and HTO release, the chemical form of re-emission is HTO. User can give wind velocity for re-emission plume as input data, and in the calculation of scenario 1, we used wind velocity at 60m height.

I–A.1.4. Wet deposition

Wet deposition is assumed to occur only for HTO (for primary release of HTO and re-emission) and affect the soil HTO concentration and the re-emission rate. The wet deposition rate is calculated by using the washout coefficient. The tritium concentration in rainwater is obtained by dividing the wet deposition rate by the average precipitation rate.

I–A.1.5. Buildup in soil and vegetation

Soil: The tritium concentration in soil water is assumed to be equilibrium with that in the air moisture on the soil surface. The tritium concentration in soil water is obtained by multiplying the tritium concentration in the air moisture by the isotopic ratio HTO/H_2O in liquid and vapor (=1.1), and adding the tritium concentration of rainwater.

Plant HTO: A plant takes water from both the soil and the atmosphere. The relative humidity coordinates which amount of tritium comes from atmosphere or from the soil. The concentration in plant free water (C_{pw}) is calculated by the next equation,

$$C_{pw} = aEC_{aw}^{p} + (1-E)C_{SW}$$

where a is the isotopic ratios HTO/H_2O in liquid and vapor (=1.1), C_{aw}^{p} is the concentration of HTO in air humidity at the plant leaf surface, C_{sw} is the concentration in soil surface water, E is the relative humidity. In the calculation for scenario 1, HTO concentration in air humidity at the plant leaf surface was same value as the specific activity in soil surface air because the plant was assumed to be short grass.

Plant OBT: The tritium concentration in plant organic matter (OBT) is calculated by multiplying the HTO concentration in the plant free water by the ratio of OBT/HTO in an equilibrium state. The ratio of OBT/HTO was determined as 0.8 for calculation of Scenario 1.

References

[1] ANDOH, M., TAKAHASHI, T., AMANO, H., Development of an environmental tritium model; ETDOSE, Proceedings of the Cross-Over Symposium "New Approach for Studies on Environmental Radioactivity ", JAERI-Conf 99-001, 161–169 (1999) (in Japanese).

[2] BELOT, Y., CAMUS, H., A code to predict the atmospheric concentration of HTO following an accidental release of HT, in Tritium in the Environment and Work Place, Final report on Fusion Safety and Environment for the period 1989–1991, Institut de Protection et de Sureté Nucléaire, France (1991).

I–A.2. MODEL USED BY COMMISSARIAT À L'ÉNERGIE ATOMIQUE, FRANCE

Y. Belot

TRIMASS1, is a code written in Fortran 77, that was developed at CEA by Y. Belot and G. Guinois for assessment of tritium atmospheric dispersion during routine operations. This is a multi-source, sector–averaged model, that requires the user to define as input data the source(s), and terrain characteristics and the weather annual-averaged conditions. The model is applicable to flat terrains and to a certain extent to rolling terrains showing small elevational differences.

I–A.2.1. Structure of the model

The average concentrations of tritium in air humidity, rain water, soil moisture, plant water and plant organics are obtained from the code, as output data, at given points, and/or at the points of an uniform user–specified rectangular grid. The resulting data matrix can be optionally visualised as contour plots.

The calculation grid is defined by contiguous rectangular terrain elements of given size and number in two rectangular directions. The size and the number of the terrain elements can be chosen, but an increase in the number of elements is at the expense of an increase in the calculation time (about half-an-hour for 201 × 201 terrain elements).

The main primary source is placed at the centre of the grid. The position of each of the other primary sources, and also of all receptors, is defined with respect to the main primary source, taking the Ox axis from West to East direction, and the Oy axis from South to North direction.

I–A.2.2. Primary dispersion

The basic equation is the sector-averaged Gaussian equation for a 'continuously' emitting point-source. This equation is based on the assumption that that all wind directions within a given sector occur with equal probability. It uses the probability distributions of wind direction, wind speed and stability given as input to the model. No provision is made for plume broadening at the source nor for plume depletion.

The vertical dispersion parameter is expressed as a function of both distance and mesoscale roughness length by using the Hosker's formulae (1974) derived from Smith's results (1972), and assuming that the airflow displacement height is negligible in the sampling zones of interest. As an alternative, the user can choose the Brigg's results (Briggs 1973) which have been collated for unspecified small roughness lengths (between 0.03 and 0.3 m).

The wind speed is extrapolated to the height of each source by using the vertical profiles proposed by van Ulden and Holtslag (1985). In case of several sources, the contribution of each source is calculated in the same manner with only changes in the relative coordinates of each new source and receptor(s). The total primary concentration is determined by superimposing the contributions of all sources.

I–A.2.3. Secondary dispersion

The secondary concentration of tritium as HTO, due to reemission of tritium deposited on the soil surface, is determined by estimating as indicated below, in the section on soil and re-emission, the upward flux of tritium at each terrain element (or grid node), and summing up over space the contributions of each of the terrain elements to the secondary concentration at each point of the grid.

It is assumed that the secondary and primary dispersion proceed under identical weather conditions, except for the wind speed which is assumed to be substantially reduced close to the ground where the re-emitted tritium comes from. As suggested by Smith and Singer (1966), the wind speed is extrapolated to the height 0.6 σ, where σ is the vertical dispersion parameter. This extrapolation is made by using the vertical profiles of wind speed referenced in the section above.

I–A.2.4. Wet deposition

The wet deposition of HTO is determined from a formula based on the use of an apparent washout coefficient. The long-term time averaged wet deposition flux at the receptor is estimated by the sector-averaged formula:

$$F_w = Q\Lambda\Phi/(u\rho\theta)$$

where Q is the average emission rate; Λ is the washout rate of tritiated water for the average precipitation rate during the period of interest; Φ is the joint frequency of rain and wind into the sector containing the receptor j; u is the average wind speed; ρ the distance between source and receptor and θ the angle of the wind direction sector.

The washout rate of tritiated water depends on source height, distance from the source and rain intensity. In the case of elevated sources, the washout rate coefficient is nearly constant over a wide area (Belot 1998). The average concentration of tritium in rainwater is simply obtained by dividing the wet deposition flux so obtained by the corresponding average precipitation rate.

I–A.2.5. Buildup in soil and vegetation

The estimation of the soil water concentration is obtained by writing the balance of tritium average inputs and outputs to and from the root layer. The inputs are attributable to dry and wet deposition, the outputs to infiltration, plant uptake and re-emission from soil surface, the losses due to radioactive decay being negligible. The steady-state concentration of tritium in the soil water so obtained is independent of the thickness of the root layer and depends only on the relative magnitude of inputs and outputs. This yields the following formula:

$$C_s = (v_t\chi + F_w)/(v_e\rho_s + I_r)$$

where C_s is the concentration of tritium in soil water; v_t is the transfer velocity of HT or HTO from atmosphere to soil; χ is the average concentration of tritium in the atmosphere; F_w is the average flux density of tritium wet deposition; v_e is the exchange velocity of HTO between soil and the atmosphere; ρ_s is the water concentration in air saturated at soil surface temperature; I_r is the infiltration rate of water through the root layer. The density of the re-emission flux is assumed to be equal to $v_e\rho_sC_s$, that is to be proportional to the concentration of tritium in soil water.

The main difficulty resides in the estimation of the transfer / exchange velocities. If we consider only HTO, the transfer velocity v_t is assumed to be equal to the exchange velocity ve, and is set equal to a value comprised between 0.001 and 0.003 m s-1 depending of average soil moisture and mean wind speed close to ground level. For HT, the transfer velocity is assumed to be ten times lower than the exchange velocity.

The concentrations in plant water are predicted using the equation of Raney and Vaadia (1965) that relates the concentration plant water to the concentrations in air humidity and soil moisture. The concentrations of non-exchangeable tritium in the combustion water of organic matter in leaves is predicted by multiplying the concentrations in leaf water by an isotopic discrimination factor taken to be 0.6 (Kim and Baümgartner, 1994).

I–A.2.6. Application of the model to BIOMASS scenarios

Scenario 1: The concentrations in air are determined from both primary and secondary dispersion for the weather conditions given in the scenario. The vertical dispersion parameters are taken from Briggs. The average exchange velocity at soil surface is 0.003 m s^{-1} and the washout coefficient is 6×10^{-4} s^{-1} for a precipitation intensity of 1 mm hr^{-1}.

Scenario 3: The concentrations in air are determined from the primary dispersion only, using the weather conditions given in the scenario. The vertical dispersion parameters are taken from Briggs. The average exchange velocity at soil surface is 0.003 m s^{-1} and the washout coefficient is 6×10^{-5} s^{-1} for a precipitation intensity of 1 mm hr^{-1}.

Scenario 5: The model, theoretically devoted to nearly flat terrains, is nevertheless applied to the Valduc terrain, in spite of the fact that the terrain shows elevational differences of about 100 m over several km in certain directions. This is supported by the observation made elsewhere that elevational differences in excess of 50 m over several km do not show significant topographical effects (Hinds 1970). The concentrations in air are determined by summing the contributions of primary and secondary dispersion. The vertical dispersion parameters are taken from Hosker (1974), and correspond to a mesoscale roughness length of 1m, which is assumed to be representative of the patchy forested area that surrounds the Valdux center. The average exchange velocity at soil surface is 0.002 m s^{-1} and the washout coefficient is 6×10^{-5} s^{-1} for a precipitation intensity of 1 mm hr^{-1}.

References

[1] BELOT, Y., Predicting the washout of tritiated water from atmospheric plumes, presented at the workshop of the IEA Task group on tritium Safety and Environmental Effects, held at AECL, Chalk River, Canada, on May 11–12 (1998).

[2] BRIGGS, G.A., Diffusion estimation for small emissions (draft), ATDL contribution file No. 79, Atmospheric Turbulence and Diffusion Laboratory, Oak Ridge, Tennessee (1973).

[3] HINDS, W.T., Diffusion over coastal mountains of Southern California, Atmospheric Environment **4** (1970) 107–124.

[4] HOSKER, R.P., in Proc. Symp. on Physical Behaviour of Radioactive Contaminants in the Atmosphere, November 1973, Vienna IAEA, p 291 (1974).

[5] KIM, M.A., BAUMGÄRTNER, F., Equilibrium and non-equilibrium partition of tritium between organics and tissue water of different biological systems, Appl. Radiat. Isot. **45** (1994) 353–360.

[6] RANEY, R., VAADIA, Y., Movement and distribution of THO in tissue water and vapor transpired by shoots of Helianthus and Nicotiana, Plant Physiology **40** (1965) 383–388.

[7] SMITH, F.B., A scheme for estimating the vertical dispersion of a plume from a source near ground level, In Proc. Third Mtng of the Expert Panel on Air Pollution Modeling, Paris, France, NATO-CCHS report 14, Brussels (1972).

[8] SMITH, M.E., SINGER, I.A., An improved method of estimating concentrations and related phenomena from a point source emission, J. Appl. Meteor. **5**, (1966) 631–639.

[9] VAN ULDEN, A.P., HOLSTLAG, A.M., Estimation of atmospheric boundary layer parameters for diffusion applications, J. Climate Appl. Meteor. **24** (1985) 1196–1207.

I–A.3. MODEL USED BY AECL, CANADA

P. Davis

I–A.3.1. Introduction

The AECL model was developed by P.A. Davis of Chalk River Laboratories, Canada, in 1997. It is a simple analytical model implemented in FORTRAN 77. It is meant to calculate realistic concentrations of tritium in air, rain, soil and plants due to chronic releases of tritiated hydrogen (HT) and tritiated water vapour (HTO) to the atmosphere. The model was developed specifically for use in BIOMASS as an aid in evaluating and revising the Canadian derived release limit model for tritium. The model is described by Davis (1998) but the code is not available to the public.

I–A.3.2. Modelling approach

Structure of the model: Average tritium concentrations in air moisture, rainwater, soil moisture, plant water and plant organic material are calculated by the code from input information consisting of source strength, meteorological data, plant properties and various transfer parameters. Concentrations are calculated at an arbitrary number of downwind distances in a given wind direction sector. The model can handle only one source at a time.

Primary dispersion: Air concentrations of HT and HTO in the primary plume are calculated using a standard sector-averaged Gaussian plume model (CSA 1987). This model adopts a laterally uniform concentration across each sector under the assumption that all wind directions within the sector occur with equal probability. Input to the dispersion model includes emission rate, effective height of release, downwind distance, the frequency with which the wind blows into the sector of interest, the frequency of occurrence of stability classes and the average wind speed for each stability class. No provision is made for plume broadening at the source, and plume depletion due to deposition is not considered. The model calculates the vertical dispersion parameter, σ_z, according to Briggs' (1973) scheme, as required by Scenario 1. The wind speed is extrapolated to the height of the source by using the vertical profiles provided in Scenario 1. The model does not account for complex topography in any way but is believed to provide reliable results for rolling terrain.

Secondary dispersion: The contribution to air concentrations of HTO re-emitted to the atmosphere from soil and plants following deposition from the primary plume is not explicitly considered for an HTO release. However, re-emission of dry-deposited HTO is implicitly accounted for since the plume is not depleted by deposition in the first place. Air concentrations for the HTO release therefore reflect the primary plume plus secondary re-emission for downwind distances beyond the point where the plume reaches the ground. Closer to the stack, deposition occurs through precipitation scavenging. Re-emission of this material is not considered, with the result that air concentrations in this region may be underestimated.

Air concentrations of HTO resulting from a continuous release of HT are estimated from empirical relationships observed during the 1994 chronic HT release experiment at Chalk River Laboratories (Davis et al. 1995). The ratio of the HTO concentration in air to the HT concentration in air is assumed to be 0.022 at a downwind distance of 100 m, increasing to 0.04 at 10 km. Subsequent re-analysis of the Chalk River data following completion of the

BIOMASS calculations (Davis and Bickel 2000) suggests that this ratio is constant with downwind distance, with a value of 0.032 for the absolute humidity assumed in Scenario 1.

Deposition: For an HTO release, only tritium that is deposited with precipitation is assumed to contribute to the permanent HTO inventory in soil (Raskob 1994). The wet deposition flux is calculated using a washout coefficient (Engelmann 1 968), which is set to a fixed value representative of the average rainfall rate during the period of interest. The calculation takes into account the joint frequency of occurrence of rain and plume presence at the site in question. It uses the wind speed for neutral conditions since in Scenario 1 rain is assumed to fall only when the atmosphere is neutral. The average concentration of tritium in rainwater is obtained by dividing the wet deposition flux by the average precipitation rate.

Deposition of HT is not considered explicitly. Rather HT concentrations in soil are calculated using empirical data as described in the following section.

Concentrations in soil and vegetation: For an HTO release, the HTO concentration in soil is assumed equal to the HTO concentration in rainwater. For an HT release, the HTO concentration in soil is calculated using empirical data observed during the CRL chronic HT release experiment (Davis et al. 1995). The ratio of the HTO concentration in soil water to the HT concentration in air is assumed to be 6 Bq $L^{-1}/(Bq\ m^{-3})$ at a downwind distance of 100 m, increasing to 10.6 Bq $L^{-1}/(Bq\ m^{-3})$ at 10 km. Subsequent re-analysis of the Chalk River data following completion of the BIOMASS calculations (Davis and Bickel 2000) suggests that this ratio has a fixed value of 6 Bq $L^{-1}/(Bq\ m^{-3})$ for all downwind distances.

For both HT and HTO releases, HTO concentrations in plant water are calculated from the predicted HTO concentrations in air moisture and soil water, weighted by the atmospheric relative humidity (Raney and Vaadia 1965, Murphy 1984). The concentration of non-exchangeable OBT in the combustion water of plant organic material is assumed to be the same as the HTO concentration in plant water apart from an isotopic discrimination factor.

I–A.3.3. Application of the model to BIOMASS scenarios

Scenario 1: The AECL model was applied only to Scenario 1, for which most of the input parameters were defined. The washout coefficient Λ was set equal to $5.5 \times 10^{-5}\ s^{-1}$, corresponding to a mean rainfall intensity I of 0.86 mm h^{-1} (750 mm a^{-1} occurring 10% of the time) and an assumed variation of Λ with I given by $\Lambda = 6 \times 10^{-5}\ I^{0.6}$. The isotopic discrimination factor used in the calculation of OBT concentrations was set equal to 0.8. The empirical ratios used to estimate the HTO concentrations in air and soil for an HT release are documented above.

References

[1] BRIGGS, G.A., Diffusion estimation for small emissions, ATDL Contribution No. 79, Atmospheric Turbulence and Diffusion Laboratory, Oak Ridge, Tennessee (1973).

[2] CANADIAN STANDARDS ASSOCIATION, Guidelines for calculating derived release limits for radioactive material in airborne and liquid effluents for normal operation of nuclear facilities, Standard CAN/CSA-N288.1-M87, CSA, Rexdale, Ontario (1987).

[3] DAVIS, P.A., Evaluation of the Canadian DRL model for tritium through the BIOMASS program, COG Report COG-98-233-I, Document Centre, AECL, Chalk River (1998).

[4] DAVIS, P.A., BICKEL, G.A., Environmental HTO/HT ratios arising from a chronic atmospheric HT release, Presented at the KURRI International Workshop on the Environmental Behaviour and Biological Effects of Tritium, 8–9 May 2000, KURRI, Kumatori, Osaka, Japan (2000).

[5] DAVIS, P.A., GALERIU, D.C., SPENCER, F.S., AMIRO, B.D., Evolution of HTO concentrations in soil, vegetation and air during an experimental chronic HT release, Fusion Technology **28** (1995) 833–839.

[6] ENGELMANN, R.J., The calculation of precipitation scavenging, In: Meteorology and Atomic Energy, D.H. Slade, D.H., (Ed) USAEC TID-24190 (1968).

[7] MURPHY, C.E. Jr., The relationship between tritiated water activities in air, vegetation and soil under steady-state conditions, Health Physics **47** (1984) 635–639.

[8] RANEY, R., VAADIA, Y., Movement and distribution of THO in tissue water and vapor transpired by shoots of Helianthus and Nicotiana, Plant Physiology **40** (1965) 383–388.

[9] RASKOB, W., Description of NORMTRI: a computer program for assessing the off-site consequences from airborne releases of tritium during normal operation of nuclear facilities, KfK 5364, Forschungszentrum Karlsruhe (1994).

I–A.4. MODEL USED BY STUDSVIK ECO & SAFETY AB, SWEDEN

O. Edlund

USTEVA is a code, written in Fortran 77, that has been developed by O. Edlund for assessment of atmospheric dispersion attributed to both accidental and routine releases of tritium as well as tritium transport in soil water. In the following section the atmospheric model is described.

The code can be applied for multisources and uses as input, besides special parameter values even hourly meteorological data records. The environment around a source of release is divided in sectors of arbitrary sizes concerning angles.

I–A.4.1. Structure of the model

The concentrations of tritium in air humidity, rain water, soil moisture, plant water and plant organics are calculated for each hour, and in the case of routine releases average values over a given time period can be estimated. The main primary source is placed at the centre of the grid. The position of each of the other primary sources, and also of all receptors, is defined with respect to the main primary source, taking the x-axis from west to east direction, and the y-axis from south to north direction.

I–A.4.2. Primary dispersion

The dispersion for each hour is calculated using the basic Gaussian equation using Briggs' dispersion parameter set (Briggs, 1973). Plume broadening can be included if necessary (Rasmussen, 1975). Plume depletion is neglected. The wind speed is extrapolated to the height of each source by using a vertical logarithmic wind-speed profile. Plume rise is estimated by using the methods described in DOE/TIC-27601.

I–A.4.3. Secondary dispersion

The dispersion from secondary (re-emitted) plume is not considered.

I–A.4.4. Wet deposition

The wet deposition of HTO is determined for each hour using a washout coefficient combined with the rain intensity and assuming integration of tritium adsorbed on the raindrops passing through the plume (Karlberg, 1971).

I–A.4.5. Buildup in soil and vegetation

The concentration of tritium in the soil and vegetation is calculated using an iterative air-soil-plant micrometeorological resistance model, schematically shown in Figure I–A.4.1. In this model the Monin-Obuchov's length (L), friction velocity (u_*), the resistances (R) and the potential evaporation rate (E) are the key parameters, which have to be calculated (Golder, 1972, Businger et al, 1971, Venkatram, 1980 and Monteith, 1965).

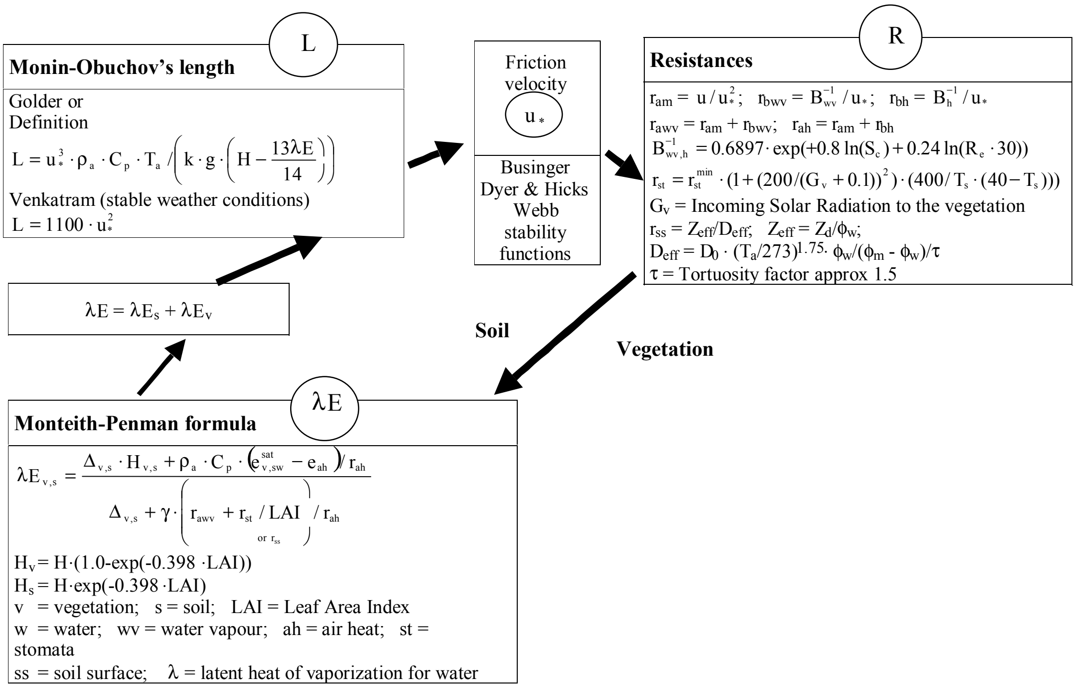

FIG. I–A.4.1. Flowscheme of the resistance model.

When the values for these parameters are estimated, the true evaporation and transpiration have to be calculated and depend on the amount of available water in the soil. For that purpose a special model has been developed and described below.

I–A.4.6. Transpiration of water through the vegetation

The amount of transpired water through the vegetation depends on how much water, which is available in the soil. If the soil water content is lower than the so-called wilting point, (see Figure I–A.4.2 below) no water can be transpired. At present it is assumed in the model that the water content in the vegetation is constant even if there normally is some variation, ~± 30 % in Scenario 3, for example. The distribution of the root system can be given as input in the model, which means how much the root system is shared between the given soil layers. The evaporation from the vegetation is compensated for through the transpiration from the soil.

One soil layer containing roots is now considered:

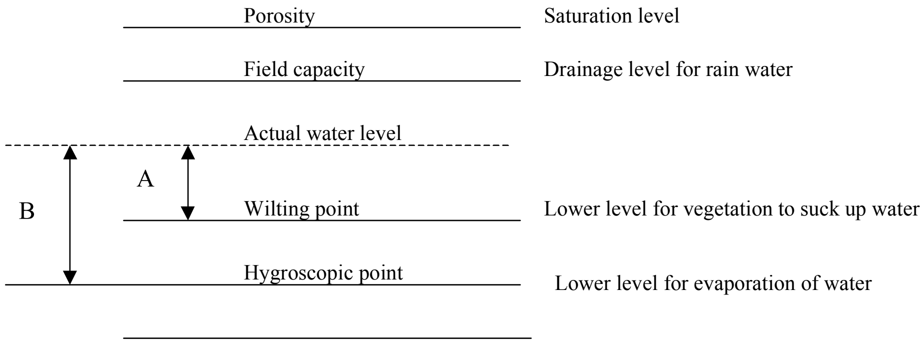

A Available part of the soil water for transpiration.
B Available part of the soil water for evaporation from the soil surface.

FIG. I–A.4.2. Definitions of characteristic soil parameters concerning soil water content.

If the actual water level is higher than the wilting point there is a "competition" between how much water that is evaporated from the soil surface and transpired through the vegetation, depending on the relative estimated values of the potential evaporation from the soil and vegetation, respectively.

If the estimated potential evaporation from the soil and transpiration through the vegetation is designated E_S and E_V, it is assumed in the model that $\left[\frac{E_s}{E_s+E_v}\cdot A\right]$ is evaporated from the soil surface and $\left[\frac{E_v}{E_s+E_v}\cdot A\right]$ is transpired through the vegetation.

This partition has influence on how much tritium contained in the soil water that follows the water to the leaves of the vegetation. If the total potential evapotranspiration is estimated to be more than A, see Figure I–A.4.2, the rest is evaporated from the soil surface and taken from the part between the wilting point and the hygroscopic point. If there is no water available in a special soil layer, the next layer is considered and so on.

I–A.4.7. Interception of rain by the vegetation

Some of the rain is intercepted on the vegetation, here grass. It is assumed that rain within an intensity of 1-3 mm, either accumulated during several hours or precipitated during one hour, is intercepted by the grass and later on evaporated. Further rain, more than 1-3 mm, is falling down to the ground. Of this at most 3 mm is drained down into the soil, while for the rest >3 mm, if the rain intensity $\geq$(4-6) mm, is considered as runoff.

I–A.4.8. Transfer of tritium between the soil, vegetation and the atmosphere

The transfer of tritium between the atmosphere and the soil as well as the vegetation is simulated applying the exchange velocity method. The direction of the transfer depends on the direction of the tritium concentration gradient between the atmosphere and the soil and vegetation, respectively.

I–A.4.9. Estimation of Organic Bound Tritium (OBT) in the vegetation

The calculation of the OBT concentration in the vegetation is carried out in a very simple way by multiplying the TFWT-concentration by a factor varying between 0.6 and 1.0, taken from the literature.

I–A.4.10. Application of the model to BIOMASS scenarios

Scenario 3: The tritium concentration in the rainwater, soil water, tissuefree water in grass and OBT in grass were estimated. The exchange velocity method was applied. The washout coefficient is $6 \cdot 10^{-5}$ s^{-1} for a precipitation intensity of 1 mm/h.

Scenario 4: Besides the atmospheric dispersion, also the plume rise for each hour was estimated according to Randerson (1984). The tritium concentration was calculated in all points given in the scenario description.

References

[1] Atmospheric Science and Power Production, DOE/TIC-27601. Darryl Randerson, Editor. U.S. Department of Commerce, National Technical Information Service, Springfield, VA. 22161 (1984).

[2] BRIGGS, G.A., Diffusion Estimation for Small Emissions (draft), ATDL contribution file No. 79, Atmospheric Turbulence and Diffusion Laboratory, Oak Ridge, Tennessee (1973).

[3] BUSINGER, J.A., et al., Flux-Profile Relationships in the Atmospheric Surface Layer, Journal of the Atmospheric Sciences **28** (1971) 181.

[4] GOLDER, D., Relations Among Stability Parameters in the Surface Layer, Boundary Layer Meteorology **3** (1972) 47–58.

[5] KARLBERG, O., UNIDOSE – A Computer Program for the Calculation of Individual and Collective Doses from Airborne Radioactive Pollutants, Studsvik Energiteknik AB, Sweden (STUDSVIK-79/1) (1971).

[6] MONTEITH, J.L., Evaporation and Environment, The State and Movement of Water in Living Organisms, Symposium of the Society for Experimental Biology **19**, 205–224, Cambridge University Press (1965).

[7] RANDERSON, D., (Ed.), Atmospheric Science and Power Production, Technical Information Center, Office of Scientific and Technical Information, United States Department of Energy, (DOE/TEC-27601, Chapter 8) (1984).

[8] RASMUSSEN, Calculations of Reactor Accident Consequences, WASH-1400 (NUREG 75/014) Appendix VI to Reactor Safety Study, US Nuclear Regulatory Commission (1975).

[9] VENKATRAM, A., Estimating the Monin-Obukov Length in the Stable Boundary Layer for Dispersion Calculations, Boundary-Layer Meteorology **19** (1980) 481–485.

I–A.5. MODEL USED BY NIPNE, ROMANIA

D. Galeriu

DISPT was developed for assessment of tritium atmospheric releases during routine operations. It treats dispersion with the statistical (sector–averaged) Gaussian model or with the straight-line Gaussian using a series of hourly meteorological data with defined wind directions. The model can address up to 3 sources and is applicable to flat terrain and, to a certain extent, rolling terrain.

I–A.5.1. Structure of the model

DISPT is a simple code written in MS Fortran. The model first calculates the air concentration and wet deposition of tritium and next the tritium concentrations in soil, plant water and organic plant parts. The calculations are done in turn for each receptor of interest. Re-emission of HTO from soil and plant to air following an HTO release is not treated. The air HTO concentration after an HT release is computed using experimental data.

I–A.5.2. Primary dispersion

The basic equation is the sector-averaged Gaussian equation for a "continuously" emitting point-source or the straight-line Gaussian equation for a plume emitted for one hour (Hanna 1982). For the sector-averaged case, input to the model is the triple joint frequency distribution of wind direction, wind speed and stability class. For a series of short-term releases, hourly values of wind direction and wind speed are required, as well as an indication of atmospheric stability. If measurements of lateral and vertical wind direction fluctuations and vertical temperature gradient are available, similarity theory is used to define the dispersion parameters. In the absence of direction fluctuations and temperature gradients, the dispersion parameters are determined from the stability class using one of a number of sigma schemes supported by the model. The scheme selected is the one that best matches the height of release and roughness length of the area of interest. By default, the averaging time is assumed to be 1 hour and the lateral dispersion parameter is corrected if obtained at shorter averaging times (Hanna 1982). Also, if the roughness length of the actual site differs from that in the sigma scheme used, a correction is done for the vertical dispersion parameter (Hanna 1982). If necessary, the dispersion parameters are increased to account for initial plume broadening due to building wake effects using standard procedures (Hanna 1982, IAEA 1986).

Wind speeds are extrapolated from measurement height (z_{ref}) to the height of each source (h) using the vertical profiles proposed by van Ulden and Holtslag (1985):

$$U(h) = U_{ref}\,(h/z_{ref})^{p}\ .$$

The exponents p were set by considering the recommendations of Panitz (1989), Simmonds (1995) and Irwin (1979) and are listed in Table I–A5.1.

TABLE I–A.5.1. POWER LAW EXPONENT FOR THE VERTICAL WIND SPEED PROFILES

Roughness Length (m)	Stablity Class A	B	C	D	E	F
0.1	0.07	0.1	0.12	0.18	0.40	0.47
0.5	0.12	0.16	0.19	0.25	0.49	0.57
1.0	0.15	0.20	0.23	0.30	0.54	0.64

DISPT also considers plume rise due to excess momentum or bouyancy in the stack gases using the Briggs' formalism (Simmonds 1995, Hanna 1982). For the present calculations, only the final rise is considered, as all receptors in the BIOMASS scenarios are far from the source. In stable situations, iteration is needed to compute plume rise and the effective release height, which are functions of wind speed.

Complex terrain is treated in a simplified manner (Witek 1985) by adapting the effective release height h_{eff} to reflect the height difference Dz between the receptor and the base of the stack. Complex terrain effects are ignored under stable conditions if the slope of the land in the surrounding area is less than 0.01, and under neutral or unstable conditons if the slope is less than 0.1. Otherwise, the effective release height is calculated according to the following algorithm:

Dz > 0 (receptor higher than base of stack):

$$h_{eff} = H + Dz\ (f_t - 1.)$$

where:

$$f_t = 1. - 0.2\ (\text{istab} - 1).$$

istab is the numerical value of stability class (A=1, B=2 and so on) and H is the effective release height in the absence of topography.

Dz < 0 (receptor lower than base of stack):

$h_{eff} = H$ for unstable and neutral conditions

$h_{eff} = H + |Dz|$ for stable conditons

In the case of several sources, the contribution of each source at each receptor is calculated independently using the above methods. The total primary air concentration is determined by summing the contributions from all sources.

I–A.5.3. Secondary dispersion

For an HTO release, the secondary concentration of HTO in air due to reemission of tritium deposited on the soil surface is not determined in DISPT. The secondary plume is partly accounted for by ignoring plume depletion, although close to elevated sources neglect of reemission results in an underestimate of air concentrations. For an HT release, the HTO in air and in soil water is computed using empirical factors determined in the chronic HT release experiment in 1994 in Canada (Davis et al. 1995). The ratio of HTO in air (Bq m^{-3}) to HT in air (Bq m^{-3}) is:

$$Ra = 0.022 + 0.018\ (x - 0.1),$$

and the ratio of HTO in soil water (Bq L^{-1}) to HT in air (Bq m^{-3}) is:

$$Rs = 6 + 4.6\ (x - 0.1)\ ,$$

where x is the downwind distance in km.

I–A.5.4. Wet deposition

The wet deposition of HTO is determined from a formula based on the use of an apparent washout coefficient. The long-term time-averaged wet deposition flux (F_w, Bq m^{-2} s^{-1}) at the receptor is estimated by the sector-averaged formula:

$$F_w = Q\ \Lambda\ \Phi\ /(u\ x\ \Delta\theta)$$

where Q (Bq s^{-1}) is the average emission rate; Λ (s^{-1}) is the washout coefficient of tritiated water for the average precipitation rate during the period of interest; Φ is the joint frequency of rain and wind in the sector containing the receptor; u (m s^{-1}) is the average wind speed; x (m) is the distance between source and receptor; and Δθ is the angular width of the wind direction sector.

The value of Λ for tritiated water depends on source height, distance from the source and rain intensity. In the case of elevated sources, Λ is nearly constant over a wide range of conditions (Belot 1998). For all BIOMASS calculations, Λ was assumed to vary linearly with precipitation intensity but to be independent of release height. The average concentration of tritium in rainwater was obtained by dividing the wet deposition flux by the corresponding average precipitation rate.

I–A.5.5. Buildup in soil and vegetation

The estimation of soil water concentration is obtained by summing the contributions of wet deposition, conversion of HT to HTO and dry deposition of HTO. The first two of these processes have been discussed above. The contribution of HTO dry deposition is acounted for in a simplified manner by assuming that the soil concentration is a fraction of the HTO concentration in air moisture. This fraction was taken to be 0.15, which was determined using experimental values of reemision rates and a simple model that predicted soil concentrations resulting from a sequence of 1-hour deposition periods followed by 11-hour reemission phases, repeated until soil concentrations came into equilibrium.

Concentrations in plant water (C_{pw}) are predicted using the equation of Raney and Vaadia (1965) that relates C_{pw} to the concentrations in air humidity and soil moisture. The concentrations of non-exchangeable tritium in the combustion water of organic matter in leaves is predicted by mutiplying the concentrations in leaf water by an isotopic discrimination factor taken to be 0.6 (Kim and Baumgartner, 1994) and adjusted to 0.7 for conservatism.

I–A.5.6. Application of the model to BIOMASS scenarios

Scenario 1: As requested, Briggs' dispersion parameters were used and the washout coefficient was taken as 6×10^{-4} s^{-1} for a precipitation intensity of 1 mm h^{-1}.

Scenario 3: The concentrations in air were determined from primary dispersion only, using the weather conditions given in the scenario. The straight-line Gaussian model was used with hourly data and the KFK 50-m dispersion parameters (Panitz 1989). These parameters were obtained at Julich and Karlsruhe for 1-hour averaging times, a release height of 50 m and a roughness length of 1.2 m. These conditions correspond closely to those at the CRL site, which is highly forested with small hills. In practice, the roughness length used in the calculations was chosen to be 1 m. Two sources (the reactor exhaust stack and the reactor building) were considered. The effective plume height was established at 45 m for the stack and 15 m for NRU. The initial dispersion parameters were set to $\sigma_z = \sigma_y = 3$ m for the stack and to $\sigma_z = \sigma_y = 10$ m for the reactor building.

For the assessment of wet deposition, the washout coefficient was assumed to vary linearly with rain intensity, with $\Lambda = 7\ 10^{-5}\ s^{-1}$ for an intensity of 1 mm h^{-1}. The wet flux was computed hourly for each source and summed to give the total for the study period.

In addition to the model described above, an alternative way to compute HTO concentrations in soil was used in this scenario. The second model was time-dependent and assumed constant moisture content and uniform tritium concentration in the soil column, piston-flow of (tritiated) rainwater and a simplified treatment of the dry deposition/reemision process based on an exchange velocity of 0.002 m s^{-1} in an active upper layer of 0.5 cm. This model gave higher soil concentrations than the one described above and was not better with respect to the data.

The uncertainties in air concentration are estimated to be a factor 3 (20-30 % from wind speed, 100 % from wind direction, 100 % from stability classification and 100% from the sigma scheme used). The same uncertainty is expected in the wet flux.

Scenario 4: The Mol dispersion parameters (obtained for 1-h releases at a height of 69 m over a surface of roughness 0.3 m) were used. Other sigma schemes were tried but only Briggs' scheme, uncorrected for averaging time and roughness, resulted in (slightly) better predictions. Plume rise was accounted for but was important only for station 1. Air concentrations were calculated using meteorological data for the summer period only, for winter and for all year. The variability was found to be less than a factor 2 but the meteorological data are uncertain. There are many clusters in the wind velocity distribution, there is no information on the roughness length at the meteorological station and it is not clear how stability class was determined.

The dry deposition velocity to snow was set to $1.6\ 10^{-3}$ m s^{-1} and a fraction 0.7 of the amount deposited was assumed to be retained in the snowpack until melt. The washout coefficient for snow was set to $1.46\ 10^{-5} * 0.6$ (where 0.6 cm h^{-1} is the snow intensity). The washout coefficient for rain was asssumed to depend nonlinearly on rain intensity and was set to $\Lambda = 6.5\ 10^{-5}\ (1.3)^{0.7}\ s^{-1}$, where 1.3 mm h^{-1} was the average rainfall rate.

Scenario 5: For the Valduc site, the model was applied with the simple complex terrain algorithm described above. This model was initially developed for receptors at greater elevations than the source. However, at Valduc we have the opposite situation in which the receptors are mostly lower than the sources and the model systematically mispredicted. The rest of the model was as in Scenario 4. A tentative model to account for wind direction shear was attempted but without clear improvement in the predictions.

References

[1] BELOT, Y., Predicting the washout of tritiated water from atmospheric plumes, Presented at the Worshop of the IEA Task Group on Tritium Safety and Environmental Effects, AECL, Chalk River, Canada, May 11–12 (1998).

[2] DAVIS, P.A., GALERIU, D.C., SPENCER, F.S., AMIRO, B.D., Evolution of HTO concentrations in soil, vegetation and air during an experimental chronic HT release, Fusion Technology **28** (1995) 833–839.

[3] HANNA, S.R., Review of atmospheric diffusion models for regulatory applications, World Meteorological Organization Tech. Note **177** (1982).

[4] INTERNATIONAL ATOMIC ENERGY AGENCY, Atmospheric dispersion models for application in relation to radionuclide releases, IAEA-TECDOC-379, Vienna (1986).

[5] IRWIN, J.S., A theortical variation of the wind profile power-law exponent as a function of surface roughness and stability, Atmos. Envir. **13** (1979) 191.

[6] KIM, M.A., BAUMGÄRTNER, F., Equilibrium and non-equilibrium partition of tritium between organics and tissue water of different biological systems, Appl. Radiat. Isot. **45** (1994) 353–360.

[7] PANITZ H.J., et al. UFOMOD atmospheric dispersion and deposition, KFK-4332, Karlsruhe, Germany (1989).

[8] RANEY, R., VAADIA, Y., Movement and distribution of THO in tissue water and vapor transpired by shoots of *Helianthus* and *Nicotiana*, Plant Physiology **40** (1965) 383–388.

[9] SIMMONDS, J.R., et al., Methodology for assessing the radiological consequences of routine releases of radonuclides to the environment, European Commission, Radiation Protection, EUR 15760 (1995).

[10] VAN ULDEN, A.P., HOLSTLAG, A.M., Estimation of atmospheric boundary layer parameters for diffusion applications, J. Climate Appl. Meteor. **24** (1985) 1196–1207.

[11] WITTEK, P., A survey of atmospheric dispersion models applicable to risk studies for nuclear facilities in complex terrain, KfK-3870, Karlsruhe, Germany (1985).

I–A.6. MODEL USED BY VNIIEF, RUSSIAN FEDERATION

A. Golubev, et al.

I–A.6.1. Provisional observations

The concentration of tritium oxide was assumed to be in equilibrium in all compartments. The HTO concentrations in all environmental compartments are determined by using the equation of material balance [1]. For the case of the pronounced period with the snow cover, the vegetation period and the period with the snow cover are examined separately. The HT emission and HTO emission are considered separately or HTO+ HT. For the HT emission, there were assumed no dry deposition onto the snow blanket and no wet deposition.

I–A.6.2. Atmospheric dispersion, primary source

The average concentrations of impurities in the air, resulted from the emission from the primary source, are calculated using the Gauss model for the long-term point source [2] depending on the distance from the source and on the averaged weather conditions. To calculate dispersion parameters of impurities, the Briggs method was used [3]. The frequency of the atmosphere stability category, the oblongness function of the wind rose, the average speed of wind at the altitude of the source calculated for each stability class are used as input parameters. The depletion of the emission plume due to dry and wet deposition is not taken into account. The wind speed at the height of the source is calculated with the assumption of the parabolic profile of the wind speed. For the case of a number of sources, the superposition of concentrations induced by all sources is taken. The height variation between the source base and the calculation point of the ground-surface concentration can be taken into account.

I–A.6.3. Secondary dispersion

In case of only HT emission from the primary source, the HTO atmospheric concentration due to the re-emission from the soil is calculated. The precipitation and evaporation from the soil surface are assumed to be uniform throughout the entire region. The complete *HT* oxidation takes place in the surface layer of the soil. The *HT* conversion to *HTO* is assumed to occur instantaneously. It is valid for the calculation of average annual concentrations. The total *HTO* generated during the year is diluted in X *mm* precipitations fallen out during the same period. The *HTO* concentration in the soil moisture is equal to:

$$C^{HTO} = \frac{V_d \cdot C^{HT}}{X} \tag{1}$$

where V_d – is the speed of *HT* precipitation on to the ground (*m·s-1*).

The HTO is re-emitted due to water evaporation from the surface. (*X–I*) *mm* precipitations is evaporated during the year. Consequently, the flow of evaporated *HTO* in the atmosphere is:

$$J_{\uparrow}^{HTO} = (X - I) \cdot C^{HTO} \tag{2}$$

where *I* – is the soil infiltration during a year (*mm*).

The secondary source is split into a variety of elementary sources each of which is assumed to be approximately a point one. The annually averaged *HTO* concentration in the atmospheric moisture for the given stability class is determined by the superposition of concentrations induced by all elementary surface sources [4]:

$$C^{HTO} = \sum_{i} \left(J_{\uparrow\ i}^{HTO} \cdot \Delta_i \right) \cdot G(r_i), \tag{3}$$

where:

$J_{\uparrow}^{HTO} \cdot \Delta_i$ is the intensity of the elementary source (*Bq/s),*

$G(r_i)$ is the Gauss formula.

We obtain the annually averaged HTO concentration by averaging it over categories of atmosphere stability.

I–A.6.4. HTO concentration in soil moisture

The HTO concentration in the soil moisture is determined by the combination of dry and wet deposition fluxes. At that, with the dry deposition, the equilibrium HTO content is assumed to be achieved within the depth of 0.2 meters and the HTO content in the rainwater is assumed not to exceed 0.4 of the equilibrium HTO concentration in the air [5]. The ratio of moisture volumes in the soil as the result of condensation and of precipitations is 0.2:0.8, respectively [6].

While calculating the HTO concentration in case of HT emission, the HT conversion to HTO in the soil is assumed to occur instantaneously.

I–A.6.5. HTO concentration in free moisture of plants

The content in the soil moisture is generated due to rain precipitations, to condensation of atmospheric moisture by spring melting snow. The HTO content in free moisture of plants was estimated in accordance with [5] as the combination of HTO content in soil moisture and in atmospheric moisture with the relative contribution of 0.25 $\tilde{N}_{soil}$+0.75 $\tilde{N}_{air,}$ respectively. The concentration in free moisture of plants is assumed to be determined only by the HTO concentration in atmosphere. With the emission of only HT, the HTO concentration in soil moisture is determined using (1).

I–A.6.6. The HTO concentration in the organic matter of plants

The tritium content in the organic matter of plants (OBT) is determined as $\tilde{N}_{obt}/\tilde{N}_{tfwt}$=0.03 [7].

The stationary HTO concentration in water equivalent of organically bound tritium corresponds to the stationary HTO concentration in free moisture of plants.

I–A.6.7. The HTO concentration in rain moisture

The calculations are based on the equality of HTO fluxes due to rain moisture and due to HTO wash-out from the atmosphere. The ultimate formula is:

$$C_{rain} = \frac{\Lambda \cdot Q}{2\pi \cdot r \cdot U \cdot I} \tag{4}$$

where Q – is the intensity of emission, r is the distance from the source, U is the speed of the wind, Λ is the coefficient of wash-out, I is the rain intensity.

I–A.6.8. HTO concentration in melt water

In case of two calculated periods, the HTO content in moisture produced by melt snow is calculated. The concentration in melt water is generated due to HTO wash-out from atmosphere by snow and due to isotopic exchange between the atmospheric moisture and the snow cover calculated using Henry constant [5]. With the emission of only HÒ, with the assumption of absence of dry and wet HT deposition on the surface of snow cover, there is no HTO in melt water.

I–A.6.9. Application of the model to BIOMASS scenarios

Scenario 1: In case of HTO emission, the concentration in atmospheric moisture is determined by the primary source. With the emission of HT, the concentration in atmosphere is determined by the re-emission from the soil. The HTO concentrations in soil moisture, in free moisture of plants, the concentrations of organically bound tritium and HTO in water equivalent of organically bound tritium were determined. The deposition velocity on to the soil is 3E-3 m/s for HTO and is 3E-4 m/s for HT. The wash-out coefficient for the rain with the intensity of 1mm/hour is 6E-5 s-1. The average meteodata, the dispersion parameters are described in scenario.

Scenario 4: Two periods were examined, namely, the vegetation one (from May till September) and the period with snow cover (from December till March). The snow precipitations were assumed to take place during the period with snow cover. Using the meteorological data, the wind rose and the average absolute humidity, the frequency of stability category were calculated for each period. The entire 20-year period of emissions was split into 4 intervals. The averaged emission intensity was taken for each interval. The emissions in previous time intervals were assumed not to affect the following ones. The deposition velocity on to the soil is 1.7E-3 m/s for HTO and is 3E-4 m/s for HT. The wash-out coefficient for the rain with the intensity of 1mm/hour is 6E-5 s-1. The HTO concentrations in atmospheric and soil moisture, in free moisture of plants, in melt water were calculated.

Scenario 5: A number of point sources were specified. The height variation between source bases and sampling points was taken into account. For the specified points, the annually averaged tritium concentration in the air, the ÍÒÎ concentration in free moisture of plants, in organically bound moisture, in rain moisture were calculated. The deposition velocity on to the soil is 1.7E-3 m/s for HTO and is 3E-4 m/s for HT The wash-out coefficient for the rain with the intensity of 1mm/hour is 6E-5 s-1.

References

[1] BELOVODSKY, L.F., VERESHCHAGA, A.N., GOLUBEV, A.V., MAVRIN, S.V., STEN'GACH, A.V.. "Scenario 1. Calculation results", RFNC-VNIIEF report on the IAEA "BIOMASS" program, Tritium Working Group Meeting, April 22–24 1997, Cadarache, France (1997).

[2] GUSSEV, N.G., Radioactive emissions in the atmosphere, M.: Energoatom (1991).

[3] The atmospheric turbulence and simulation of impurities propagation, Edited by F.T.M. Newstadt and H. Van Dop, L., Gidrometeoizdat (1985).

[4] BELOT, Y., WATKINS, B., Modelling of tritium behaviour in the environment of permanent sources, BIOMASS Theme 3 Tritium Working Group Scenario 1 (1998).

[5] MURPHY, C.E., Jr., "Tritium transport and cycling in the environment", Health Physics **65** 6 (1993) 683–697.

[6] BUNNENBERG, C., TASCHNER, M., Discussions during Cadarache Tritium Working Group Meeting, April 22–24 (1997).

[7] DIABATE, S., STRACK, S., "Organically bound tritium", Health Physics **65** 6 (1993) 698–712.

I–A.7. MODEL USED BY CEA, FRANCE

G. Guinois

TRIMASS1: is a code written in Fortran 77, that was developed at CEA by Y. Belot and G. Guinois for assessment of tritium atmospheric dispersion during routine operations. This is a multi-source, sector–averaged model that requires the user to define as input data the source(s), and terrain characteristics and the annual-averaged weather conditions. P. Armand (CEA) has now made this model applicable to multi-sources, rolling terrain and plume rise due to gas ejection (TRIMASS2).

I–A.7.1. Structure of the model

The average concentrations of tritium in air humidity, rain water, soil moisture, plant water and plant organic material are obtained from the code, as output data, at given points, and/or at the points of a uniform user–specified rectangular grid. The resulting data matrix can be optionally visualised as contour plots.

The calculation grid is defined by contiguous rectangular terrain elements of given size and number in two rectangular directions. The size and the number of the terrain elements can be chosen, but an increase in the number of elements is at the expense of an increase in the calculation time (about half-an-hour for 201 × 201 terrain elements).

The main primary source is placed at the centre of the grid. The position of each of the other primary sources, and also of all receptors, is defined with respect to the main primary source, taking the Ox axis from West to East direction, and the Oy axis from South to North direction.

I–A.7.2. Primary dispersion

The basic equation is the sector-averaged Gaussian equation for a 'continuously' emitting point-source. This equation is based on the assumption that all wind directions within a given sector occur with equal probability. It uses the probability distributions of wind direction, wind speed and stability given as input to the model. No provision is made for plume broadening at the source nor for plume depletion.

The wind speed is extrapolated to the height of each source by using the vertical profiles with an exponential function. In the case of several sources, the contribution of each source is calculated in the same manner with only changes in the relative coordinates of each new source and receptor(s). The total primary concentration is determined by superimposing the contributions of all sources.

I–A.7.3. Secondary dispersion

The secondary concentration of tritium as HTO, due to reemission of tritium deposited on the soil surface, is determined by estimating as indicated below, in the section on soil and re-emission, the upward flux of tritium at each terrain element (or grid node), and summing up over space the contributions of each of the terrain elements to the secondary concentration at each point of the grid.

It is assumed that the secondary and primary dispersion proceed under identical weather conditions, except for the wind speed which is assumed to be substantially reduced close to the ground where the re-emitted tritium arises. As suggested by Smith and Singer (1966), the wind speed is extrapolated to the height 0.6 σ, where σ is the vertical dispersion parameter. This extrapolation is obtained using the vertical profiles of wind speed proposed by Van Ulden and Holstag (1985).

I–A.7.4. Topographic effect

The topographic effect is very simple as the recommendation from Briggs (1975), Egan (1975) and Egan,d'Errico and Vaudo (1975) is used.

Trimass uses a file that contains the height of every point of the grid. For each point, the height of the source is modified as follows:

- If DZ (difference between z altitude of the source and z altitude of the station) is lower than H (height of the stack) and if we have unstable and neutral classes then we have H = H+ DZ/2.
- If DZ is lower than H and if we have stable classes then we have H= H.
- If DZ is higher than H and if we have unstable and neutral classes then we have H= H+DZ/2.
- If it is lower than H and if we have unstable and neutral classes then we have H = H + 10.

I–A.7.5. Wet deposition

The wet deposition of HTO is determined from a formula based on the use of an apparent washout coefficient. The long-term time averaged wet deposition flux at the receptor is estimated by the sector-averaged formula:

$$F_w = Q\Lambda\Phi/(u\rho\theta)$$

where Q is the average emission rate; Λ is the washout rate of tritiated water for the average precipitation rate during the period of interest; Φ is the joint frequency of rain and wind into the sector containing the receptor; u is the average wind speed; ρ the distance between source and receptor and θ the angle of the wind direction sector.

The washout rate of tritiated water depends on source height, distance from the source and rain intensity. In the case of elevated sources, the washout rate coefficient is nearly constant over a wide area (Belot 1998). The average concentration of tritium in rainwater is simply obtained by dividing the wet deposition flux so obtained by the corresponding average precipitation rate.

I–A.7.6. Buildup in soil and vegetation

The estimation of the soil water concentration is obtained by writing the balance of tritium average inputs and outputs to and from the root layer. The inputs are attributable to dry and wet deposition, the outputs to infiltration, plant uptake and re-emission from soil surface, the losses due to radioactive decay being negligible. The steady-state concentration of tritium in the soil water so obtained is independent of the thickness of the root layer and depends only on the relative magnitude of inputs and outputs. This yields the following formula:

$$C_s = (v_t\chi + F_w)/(v_e\rho_s + I_r)$$

where Cs is the concentration of tritium in soil water; v_t is the transfer velocity of HT or HTO from atmosphere to soil; χ is the average concentration of tritium in the atmosphere; F_w is the average flux density of tritium wet deposition; v_e is the exchange velocity of HTO between soil and the atmosphere; ρs is the water concentration in air saturated at soil surface temperature; I_r is the infiltration rate of water through the root layer. The density of the re-emission flux is assumed to be equal to $v_e\rho_s C_s$, that is to be proportional to the concentration of tritium in soil water.

The main difficulty resides is the estim vt is assumed to be equal to the exchange velocity v_e, and is set equal 0.003 m s^{-1}. For HT, the transfer velocity is assumed to be ten times lower than the exchange velocity.

The concentrations in plant water are predicted using the equation of Raney and Vaadia (1965) that relates the concentration in plant water to the concentrations in air humidity and soil moisture. The concentrations of non-exchangeable tritium in the combustion water of organic matter in leaves is predicted by multiplying the concentrations in leaf water by an isotopic discrimination factor taken to be 0.6 (Kim and Baümgartner, 1994).

I–A.7.7. Application of the model to BIOMASS scenarios

Scenario 1: The concentrations in air are determined from both primary and secondary dispersion for the weather conditions given in the scenario. The vertical dispersion parameters are taken from Briggs. The average exchange velocity at the soil surface is 0.003 m s^{-1} and the washout coefficient is 6 × 10-5 s^{-1} for a precipitation intensity of 1 mm hr^{-1}.

Scenario 3: The concentrations in air are determined from the primary dispersion only, using the weather conditions given in the scenario. The vertical dispersion parameters are taken from Briggs. The average exchange velocity at soil surface is 0.003 m s^{-1} and the washout coefficient is 6 × 10-5 s^{-1} for a precipitation intensity of 1 mm hr^{-1}.

Scenario 4: The concentrations in air are determined from both primary and secondary dispersion for the weather condition calculated from the meteorological data that have been given. The vertical dispersion are taken from Briggs. The average exchange velocity at the soil surface is 3.10-3 m/s for rain and 1.6 10-3 m/s for snow and the washout coefficient is 6.10-5 s^{-1} for rain and 1.46 10-5 s^{-1} for snow.

Scenario 5: The concentrations in air are determined by summing the contributions of primary and secondary dispersion. The vertical dispersion parameters are taken from Briggs. The average exchange velocity at soil surface is 0.003 m s^{-1} and the washout coefficient is 6 × 10^{-5} s^{-1} for a precipitation intensity of 1 mm hr^{-1}.

References

[1] BELOT, Y., Predicting the washout of tritiated water from atmospheric plumes, Presented at the workshop of the IEA Task group on Tritium Safety and Environmental Effects, held at AECL, Chalk River, Canada, on May 11–12 (1998).

[2] BRIGGS, G.A., Diffusion estimation for small emissions (draft), ATDL contribution file No 79, Atmospheric Turbulence and Diffusion Laboratory, Oak Ridge, Tennessee (1973).

[3] HINDS, W.T., Diffusion over coastal mountains of Southern California, Atmospheric Environment **4** (1970) 107–124.

[4] HOSKER, R.P., in Proc. Symp. on Physical Behaviour of Radioactive Contaminants in the Atmosphere, Nov. 1973, IAEA, Vienna (1974) 291.

[5] KIM, M.A., BAUMGÄRTNER, F., Equilibrium and non-equilibrium partition of tritium between organic and tissue water of different biological systems, Appl. Radiat. Isot. **45** (1994) 353–360.

[6] RANEY, R., VAADIA, Y., Movement and distribution of THO in tissue water and vapour transpired by shoots of Helianthus and Nicotiana, Plant Physiology **40** (1965) 383–388.

[7] SMITH, F.B., A scheme for estimating the vertical dispersion of a plume from a source near ground level, In Proc. Third Meeting of the Expert Panel on Air Pollution Modeling, Paris, France, NATO-CCHS report 14, Brussels (1972).

[8] SMITH, M.E., SINGER, I.A., An improved method of estimating concentrations and related phenomena from a point source emission, J. Appl. Meteor. **5** (1966) 631–639.

[9] VAN ULDEN, A.P., HOLSTLAG A.M., Estimation of atmospheric boundary layer parameters for diffusion applications, J. Climate Appl. Meteor. **24** (1985) 1196–1207.

[10] BRIGGS, G.A., Plume rise predictions, In: Lecture on air pollution and environmental impact analyses, Workshop Proceedings of the Atm. Meteorol. Soc., Boston (Massachussets) USA (1975).

[11] EGAN, B.A., D'ERRICO, R., VAUDO, C., Estimating air quality levels in region of high terrain under stable atmospheric conditions, In: Lecture on air pollution and environmental impact analyses, Workshop Proceedings of the atm. Meteorol. Soc., Boston (Massachussets) USA (1975).

[12] EGAN, B.A., Turbulent diffusion in complex terrain, In: Lecture on air pollution and environmental impact analyses, Workshop Proceedings of the atm. Meteorol. Soc., Boston (Massachussets) USA (1975).

I–A.8. MODEL USED BY BEAK, CANADA

D. Lush

IMPACT (*I*ntegrated *M*odel for the *P*robabilistic *A*ssessment of *C*ontaminant *T*ransport) is a product from BEAK Consultants. The model has been programmed with an icon-based user interface using C++. Some adaptation was to be made to treat the special case of HTO or HT releases that were considered in the BIOMASS exercises.

I–A.8.1. Structure of the model

During a simulation, contaminants are tracked over time as they are released from sources and move from one block to another by a variety of processes. *Blocks* represent compartments of specified environmental media where contaminants can move or accumulate. This definition is quite broad, and encompasses a range of compartments such as Plume, Soil, Groundwater, Water Column, Sediment. Each block resides within an owning *polygon*, that is a 2-D area with similar characteristics, giving the block a spatial reference.

The processes are modelled mathematically using equations that incorporate the attributes of the polygons and blocks that are involved. *Reactions* represent any process that causes the consumption of a parent contaminant, and the production of a daughter contaminant. The reactions can be described by first-order kinetics or as a simple ratio between the parent and daughter contaminant concentration. 'First-order reactions' are for instance used to simulate precipitation, volatilisation, oxidation etc.. 'Ratio reactions' are useful as a way of representing processes that establish equilibrium quickly in living organisms.

I–A.8.2. Atmospheric dispersion

The basic equation is the traditional sector-averaged Gaussian equation for a 'continuously' emitting point-source as described in CSA, 1987. This equation is based on the assumption that that all wind directions within a given sector occur with equal probability. It uses the probability distributions of wind direction, wind speed and stability given as input to the model. It calculates the long-term average concentrations of contaminants in air (here tritium) at distances within a radius of approximately 20 km from the point of release.

The plume model uses the concept of a single virtual point-source, with a setback factor calculated as a function of the spatial separation of each sub-source. Plume depletion as resuspension from soil can be considered. The area covered by a plume block is subdivided into 16 compass sectors centred at the location of the virtual source. For the purposes of calculating dispersion, the distance which contaminants travel is calculated as the radius from the virtual source to the centre of each polygon, giving each polygon a unique dispersion value. Every polygon in a scenario can potentially receive input from each atmospheric source, unless the wind frequency in that sector (for all stability and velocity classes) is zero. Each sector covers an angle of 22.5°, with the first sector centred about 0° North (bearing -11.25° to +11.25°).

The vertical dispersion parameter is expressed as a function of both distance and mesoscale roughness length by using Hosker's formulae (1974) derived from Smith's results (1972). The mesoscale roughness length can be changed according to the surface type and land use, ranging from 0.01 m for lawn grass and bodies of water, 0.4 m for rural areas, 1 m for forested areas to 4 m for cities with tall buildings. The wind speed used in the basic formula is the mean wind speed for each stability class at a standard height of 10 m above ground level. The meteorological data required is triple-joint frequency data for each sector/stability class/ velocity class combination. A default dataset can be used which assumes uniform frequencies in all directions, but has variable stability classes and velocity classes typical of average Canadian climatic conditions.

The plume model sums the discharges from all linked plume sources and calculates the total loading rate to the plume. Concentrations of airborne contaminants are then calculated for each polygon based on the polygon's relative position (angle and distance) to the Plume block and the distance from the virtual point source to the centre of the polygon. The concentrations of contaminants in the air at each location of interest are then used to calculate the concentration in soil and plants.

I–A.8.3. Buildup of tritium in soil and vegetation

IMPACT does not model evapotranspiration from the soil. In addition, the mass-balance equation for the soil does not include the mass losses due to volatilisation. This approximation is overly conservative for HTO. Therefore, a *net* rate of HTO deposition to soil must be used in the model calculations. The net deposition rate (from wet and dry deposition) is determined such that the specific activity of HTO in soil water equals 1.1 times the specific activity of HTO in air humidity. The factor 1.1 accounts for the fact that HTO has a lower vapour pressure than HHO. The relation is then:

$$C_{sw} = 1.1C_{aw}$$

where C_{sw} is the specific activity of near-surface soil water, and C_{aw} the specific activity of air humidity. It should be noted that this estimate corresponds to the true conservative value of the average soil water concentration, given the process of HTO exchange between soil water and atmospheric humidity.

The concentrations in plant water are predicted using the equation of Raney and Vaadia (1965) that relates the concentration in plant water to the concentrations in air humidity and soil moisture:

$$C_{pw} = 1.1\left[C_{aw} \cdot H_r + C_{sw}(1 - H_r)\right]$$

where H_r is the average relative humidity of the atmosphere.

Concentrations of non-exchangeable tritium in the combustion water of organic matter in leaves is predicted by mutiplying the concentrations in leaf water by an isotopic discrimination factor taken to be 0.6 (Kim and Baümgartner, 1994; Galeriu, 1994).

I–A.8.4. Application of the model to BIOMASS scenarios

Scenario 1: The air concentrations were calculated by using standard deviations from Hosker's formulae and not by the recommended Brigg's formulae. The meteorological dataset used in the calculation was the default dataset implemented in the model. The wind velocities used in the dispersion formula were those given in the meteorological data set for the standard 10 m height above ground level, without any further correction for effective source height. It was assumed that the 'net deposition rate' of tritium to the soil surface was $5.22\text{x}10^{-4}$ and $5.22\text{x}10^{-5}$

m/s for HTO and HT respectively. These values were based on the rationale that is presented above in the Section on Buildup of Tritium in Soil. The OBT/HTO specific activity ratio was taken equal to 0.6.

Scenario 5: As the windrose data for Valduc consider 18 compass sectors covering 20° each, a conversion of the data was undertaken using a weighted conversion process. The Valduc data, relevant to a height of 150 m, were also converted to the velocities at 10 m using the power-law equation. A surface roughness length of 0.4 m was used as representative of the entire area in question. The 'net deposition rates' used in the Scenario 5 calculations were those already used in Scenario 1 calculations. The analysis of historical occurrences for 1983 to 1988 was completed using a single plume with characteristics based on average characteristics of the three distinct sources examined in detail. For the calculation of OBT concentrations in Bq per kg of equivalent water, the ratio OBT / HTO ratio was taken equal to 0.6.

References

[1] CANADIAN STANDARDS ASSOCIATION, Guidelines for Calculating Derived Release Limits for Radioactive Material in Airborne and Liquid Effluents for Normal Operation of Nuclear Facilities, CAN/CSA-N288.1-M87 (1987).

[2] GALERIU, D., Transfer parameters for routine release of HTO – Consideration of OBT, Atomic Energy of Canada Limited Report AECL-11052 (1994).

[3] HOSKER, R.P., in Proc. Symp. on Physical Behaviour of Radioactive Contaminants in the Atmosphere, Nov 1973, IAEA, Vienna (1974) 291.

[4] KIM, M.A., BAUMGÄRTNER, F., Equilibrium and non-equilibrium partition of tritium between organics and tissue water of different biological systems, Appl. Radiat. Isot. **45** (1994) 353–360.

[5] RANEY, R., VAADIA, Y., Movement and distribution of THO in tissue water and vapor transpired by shoots of *Helianthus* and *Nicotiana*, Plant Physiology **40** (1965) 383–388.

[6] SMITH, F.B., A scheme for estimating the vertical dispersion of a plume from a sourcenear ground level, In Proc. Third Meeting of the Expert Panel on Air Pollution Modeling, Paris, France, NATO-CCHS report 14, Brussels (1972).

I–A.9. MODEL USED BY ANDRA, FRANCE

C. Meurville

The ANDRA model has been especially developed to reach the aquifer source term for Scenario 1, even though ANDRA is not specialised in “ atmospheric dispersion ” modelling.

After the isolation of the groundwater modelling in the scenario, ANDRA still provided its results to the working group as a way to allow the identification of the main processes for tritium atmospheric dispersion.

I–A.9.1. Structure of the model

This code is a one-source analytical sector averaged model. It was developed with Excel spreadsheets after a bibliographic review (references given below). For each wind direction sector, the model calculates the average concentrations of tritium in air humidity, rain water, soil moisture, plant water and plant tissues at given distances from the source.

The model takes into account the following processes:

- Air concentration is obtained with a yearly sector averaged analytical Gaussian atmospheric dispersion model, considering one source with a constant flux. Time dependant sources or secondary sources (reemission from soil) are not considered.
- Soil concentration is obtained by the computation of the balance of input and output flux. Input flux is based on wet and dry deposition from the primary plume. Output flux from soil include: infiltration in deeper layers of soil (by water advection), plant root uptake. Outputs by reemission or surface run off are not included in the model.
- Plant concentration: concentration in free water is derived from air and soil water concentrations by a classical formula. OBT concentration is derived from concentration in free water using an isotopic discrimination factor of 0.8.

I–A.9.2. Application of the model to BIOMASS scenarios

Scenario 1: Calculation are performed for HTO release only (because reemission, which is not considered in the model, is an important phenomena for HT release).

Scenario 3, 4 and 5: As this model does not take into account more than one source, time dependant sources and reemission, calculation have not been performed.

References

[1] Air pollution meteorology, Encyclopedia of environmental Science and Engineering, Third edition revised and updated, **1** A-I (1992) 56–66, Gordon and Breach Science Publishers.

[2] HANN, S.R., BRIGGS, G.A., HOSKER, R.P. JR., Handbook on atmospheric diffusion, (DOE/TIC-11223 - DE82002045) (1982).

[3] Guide de l’évaluation de l’impact de rejets radioactifs atmosphériques, EDF (1989).

I–A.10. MODEL USED BY LLNL, USA

S-R. Peterson

DCART: (Doses from Continuous Atmospheric Releases of Tritium) was developed by S. Ring Peterson of Lawrence Livermore National Laboratory, USA and P.A. Davis of Chalk River Laboratories, Canada in 1998. DCART is a simple analytical model implemented on a spreadsheet. The purpose of the model is to calculate doses (inhalation/skin absorption and ingestion) to adult, child (age 10) and infant (age 1) from chronic releases of tritium gas (HT or T_2) and tritiated water (HTO) to the atmosphere. Doses should not be underestimated. DCART can be used for regulatory purposes. DCART is not available to the public and has not been published.

I–A.10.1. Structure of the model

The average concentrations in air moisture, rainwater, soil moisture, plant water and plant organics, all in units of Bq L^{-1}, are obtained from the code as output for each set of input data. The dispersion code is separate from the environmental transport code and is used to calculate concentrations in air (Bq m^{-3}) based on emission rate (Bq s^{-1}), effective height of release, and distance from source (m) for each location of interest. Input for the environmental transport code includes air concentration (Bq m^{-3}), fraction HTO in air after an HT release, parameter values for dry and wet deposition calculations, relative humidity, absolute humidity, the fraction of HTO retained by the soil, and the isotopic discrimination factor for OBT. Output can only be calculated for one location at a time, so all input has to be location-specific.

I–A.10.2. Primary dispersion

Air concentrations of HT and HTO in the primary plume are calculated using one of two standard sector-averaged Gaussian plume models, the Canadian Standard N288.1 (CSA, 1987) and CAP88-PC (Parks, 1992). Both models are based on the assumption that all wind directions within a given sector occur with equal probability. Probability distributions of wind direction, wind speed and stability class are given as input. No provision is made for plume broadening at the source, and plume depletion is not considered.

Default values for the plume dispersion parameter, σ_z, in CSA-N288.1 are those of Hosker (1974). In CAP88-PC, plume dispersion is modeled with Pasquill's sigma scheme (1961) as modified by Gifford (1976).

The wind speed is extrapolated to the height of each source by using the vertical profiles provided in Scenario 1. When there are several sources, a separate wind speed is calculated for each source. Concentrations due to emissions from each source are added together at a given location to get the total air concentration due to primary dispersion.

I–A.10.3. Secondary dispersion

Secondary concentration of HTO, due to re-emission of deposited HTO, is not considered. However, air concentrations of HTO after a release of HT were estimated based on empirical relationships observed at the 1994 chronic HT release experiment at Chalk River Laboratories (Davis et al., 1995). The fraction of HTO in air relative to the air HT concentration due to resuspension following an HT release was assumed to be 0.04 (HTO in air to HT in air, both in Bq m^{-3}). Since completion of the BIOMASS scenarios, based on re-analysis of the Chalk

River data (Davis and Bickel 2000), this fraction is now calibrated so that the ratio of HTO in air moisture to HT in air is conservatively set to 8 Bq L^{-1} / (1 Bq m^{-3} HT) (the best estimate is now believed to be 4 Bq L^{-1}/(Bq m^{-3} HT). The fraction or percentage thus depends on the absolute humidity. For an absolute humidity of 0.08, the fraction would be 0.064.

I–A.10.4. Deposition

Wet deposition of HTO is calculated using the equation of Engelmann (1968). The average concentration of tritium in rainwater is simply obtained by dividing the obtained wet deposition flux (Bq m^{-2}) by the corresponding average precipitation rate.

Dry deposition (Bq m^{-2}) is obtained by multiplying air concentrations of HT or HTO (Bq m^{-3}) by a deposition velocity (m s^{-1}).

I–A.10.5. Buildup in soil and vegetation

The total concentration of HTO in soil water (Bq L^{-1}) is achieved by dividing dry deposition (Bq m^{-2}) by the corresponding average precipitation rate (m), adding the contribution from wet deposition (Bq m^{-3}), converting from m^3 to litres, and multiplying by the fraction retained in the soil water. For HTO, this fraction is calibrated so that the ratio of HTO in soil water (Bq L^{-1}) to HTO in air moisture (Bq L^{-1}) is 0.25, the average fraction observed for chronic releases at Chalk River Laboratories.

The amount of HTO converted from HT retained in soil moisture was obtained by calibrating the ratio of HTO in soil (Bq L^{-1}) to HT in air (Bq m^{-3}) to 6.0, the ratio observed over natural soil during the Chalk River experimental HT release of 1994 (Davis et al. 1995, Davis and Bickel 2000).

Concentrations in plant water are calculated with the classical formula of Raney and Vaadia, (1965). The concentrations of non-exchangeable tritium in the combustion water of plant organic matter are predicted by multiplying the concentrations in plant water by an isotopic discrimination factor of 0.8.

I–A.10.6. Application of the model to BIOMASS scenarios

Comparative values for unvarying parameters are as follows:

	Scenario 3	Scenario 4	Scenario 5
Dry deposition velocity, HT (m s^{-1})		$2.68\ 10^{-4}$ $2.0\ 10^{-6}$ (snow)	$2.53\ 10^{-4}$
Dry deposition velocity, HT0 (m s^{-1})	$4.08\ 10^{-3}$	$4.44\ 10^{-3}$ $2.3\ 10^{-3}$ (snow)	$3.92\ 10^{-3}$
Washout coefficient (s^{-1})	$1.56\ 10^{-4}$	$8.51\ 10^{-5}$ $2.41\ 10^{-5}$ (snow)	$1.3\ 10^{-4}$
Fraction HTO retained by soil, HT release		0.75 0.9 (snow)	0.81
Fraction HTO retained by soil, HTO release	0.08	0.20 0.5 (snow)	0.15

Scenario 3: The dispersion model of CSA-N288.2 was used assuming a roughness length of 0.4 m. The model, “HOTSPOT” (Homan 1994), was used to estimate plant water and soil moisture concentrations at the specific times requested in the scenario description. HOTSPOT is a model to evaluate accidental releases involving radioactive materials. It uses Briggs methodology (1975) to determine $?_y$ and $?_z$. Uncertainty was estimated to be the spread between the results resulting from running DCART using the highest and lowest estimated parameter values.

Scenario 4: The dispersion model of CSA-N288.1 was used assuming a roughness length of 0.4 m. CSA-N288.1 was modified to handle 10 rather than 16 sectors.

Scenario 5: CAP88-PC was the model used for dispersion, in spite of its being a model for flat terrain. The roughness length is 0.1 m by default in CAP88-PC. CAP88-PC was modified to handle 18 rather than 16 sectors. For OBT in tree rings, a discrimination factor of 0.4 was assumed, rather than the 0.8 assumed for leaves.

References

[1] BRIGGS, G.A., Plume rise predictions, In: Lectures on Air pollution and Environmental Impact Analyses, Workshop Proceedings, American Meteorology Society, Boston, MA 58–111 (1975).

[2] DAVIS, P.A., BICKEL, G.A., Environmental HTO/HT ratios arising from a chronic atmospheric HT release, Presented at the International Workshop on the Environmental Effects of Tritium, 8–9 May 2000, KURRI, Kumatori, Osaka, Japan (2000).

[3] DAVIS, P.A., GALERIU, D.C., SPENCER, F.S., AMIRO, B.D., Evolution of HTO concentrations in soil, vegetation and air during an experimental chronic HT release, Fusion Technology **28** (1995) 833–839l.

[4] ENGELMANN, R.J., The calculation of precipitation scavenging, In: Meteorology and Atomic Energy, Slade D.H. (Ed), USAEC TID-24190 (1968).

[5] GIFFORD, F.A., Jr., Turbulent diffusion type schemes: A review, Nuclear Safety **17** 1 (1976) 68–86.

[6] HOMAN, S.G., HOTSPOT: Health Physics Codes for the PC, Lawrence Livermore National Laboratory.,UCRL-MA-106315 (1994).

[7] HOSKER, R.P. Jr., Estimates of dry deposition and plume depletion over forests and grassland, Proceedings of IAEA Symposium, Physical Behaviours of Radioactive Contaminants in the Atmosphere, Vienna, November 1973, IAEA, Vienna (1974).

[8] PASQUILL, F., The estimation of the dispersion of windborne material, Meteorology Magazine **90** 33 (1961).

[9] RANEY, R., VAADIA, Y., Movement and distribution of THO in tissue water and vapor transpired by shoots of Helianthus and Nicotiana, Plant Physiology **40** (1965) 383–388.

I–A.11. MODEL USED BY FZK, GERMANY

W. Raskob

NORMTRI was developed by W Raskob as a model for dose assessments of tritium emissions during normal operations, which can cope with releases of tritium as a gas (HT) as well as with releases of tritiated water (HTO) (Raskob, 1994). It has been applied in the Frame of the SEAFP (Safety and Environmental Aspects of Fusion Power) and ITER (International Thermonuclear Experimental Reactor) studies and was defined as standard model for assessing the off site consequences from tritium releases under normal operation conditions. NORMTRI is written in FORTAN 77 and can be obtained on request.

I–A.11.1. Atmospheric dispersion calculations

I–A.11.1.1. Primary plume

The computer code ISOLA V (Hübschmann, and Raskob, 1990) has been applied for the calculation of the atmospheric dispersion of tritium (HT and/or HTO) around nuclear installations for long term quasi stationary release situations. ISOLA V is a so-called 'statistical Gaussian dispersion model'. This means, for all different dispersion situations during the considered time period, a double Gaussian distribution of the released radionuclides is assumed throughout the plume. ISOLA V uses hourly meteorological data of a station near the source. Therefrom a four-parameter statistics will be prepared. It includes meteorological parameters such as wind speed, wind direction, stability classes and rain intensities. A frequency distribution will be calculated for each of the different dispersion conditions which have been identified occurring during the investigation period. Thereafter, for all the sampled dispersion conditions, the activity concentrations of the air near the ground and the ground contamination will be calculated. The activity concentrations calculated for these dispersion situations around the nuclear installation will be summarised, where their frequency of occurrence is taken into account. This leads to a mean load during the considered time period. The area under consideration is treated as a polar co-ordinate system with an angular resolution of 5 degrees (72 sectors) and a maximum number of 20 radii.

I–A.11.1.2. Area source module

The statistical dispersion model ISOLA has been also used for calculating the transport and dispersion from the area sources. Every area source (12 per distance band times up to 20 distances) will release their tritium content with the identical weather conditions of the primary dispersion process. Thus the program ISOLA will be applied up to 240 times (with the different locations of the area sources) during one weather period. Here it should be mentioned, that one year, which is the standard application period, will be subdivided into two winter weather sequences (from January 1. to March 31. and from October 16. to December 31.) and one vegetation period (from April 1. to October 15.). To save computing time the newly deposited tritium will not be considered for a second reemission step, which may slightly underestimate the influence of the re-emitted HTO.

A simplified assumption has been used which replaces the area source by a single source point in the centre of the area, with a given initial widening of the plume. This method presents the least difficulties in programming combined with an acceptable accuracy.

I–A.11.2. Foodchain module

I–A.11.2.1. Plants

It is assumed that the specific tritium content (HTO) in vegetation water is influenced by tritium in soil and atmosphere. The relative humidity coordinates which amount of tritium comes from atmosphere or from the soil. Additionally a discrimination factor which results from differences in molar weights of water vapour and HTO of about 1.1 has to be taken into account if equilibrium between air and plant water is assumed. Thus the basic equation describing the HTO content in plant water is:

$$C_{pw,HTO} = 1.1\ \rho\ C_{air,HTO} + (1 - \rho) * C_{soil,HTO}$$

where:

$C_{pw,HTO}$ is the specific HTO concentration in plant water;
$C_{air,HTO}$ is the specific HTO concentration in air humidity;
$C_{soil,HTO}$ is the specific HTO concentration in soil water; and
ρ is the relative air humidity (ranging from 0. to 1.).

The relative humidity in Europe and most non-arid regions range from 70% to 80% during the year; the first value more applicable for summer, the latter one for winter conditions. The tritium concentration in the organic material (OBT) is assumed to be in equilibrium with the tritium in the plant water. Another point which often may be ignored in case of tritium modelling for normal operation conditions is that one has to cope with concentrations, resulting from the past. This means especially for tritium that the equilibrium conditions has not to be reached but is already existing.

Differing from the other nutriment plants it is assumed for potatoes and root vegetables that the specific concentration in the edible parts (e.g. tubers) is dominated by the tritium in soil water. But for the OBT concentration in e.g. tubers, the air concentration is the source.

I–A.11.2.2. Soil

The HTO concentration in soil is calculated separately for an HT and HTO release. In case of an HTO-release, only the wet deposited tritium - resulting from the primary or from the reemission process - is used for the calculations of tritium in plants. The dry deposited tritium is assumed to evaporate totally back into the atmosphere. In case of an HT-release the dry deposited HT - wet deposition is negligibly small - is converted into HTO, which is reemitted again into the atmosphere. The reemitted HTO is then the source for the tritium in plants and livestock. The converted and reemitted HTO is treated as if it was primarily an HTO release. However, the dry deposition process from HT is different from that of HTO. Here the conversion of HT into HTO due to microbiological activities is the dominating factor for determining the dry deposition rate. From experimental results it is known that the HT-gas penetrates deeper into the soil than HTO. It is converted into HTO and the remaining HT is directly evaporated back into the atmosphere, as it is not bound to the soil or the water in soil. Due to these processes, which are different from those found for HTO, it is assumed in NORMTRI, that not all the converted HTO evaporates back into the atmosphere. It is assumed that 20% of the primarily deposited HT, which is converted into HTO, remains in the soil and contributes to the specific tritium content in soil water together with the wet deposited HTO from the area sources.

I–A.11.2.3. Application of the model to BIOMASS scenarios

Scenario 1: NORMTRI has been applied with the parameters defined in the scenario descriptions including the reemission part.

Scenario 3: The sigma parameter set of MOL was used, as this seemed to fit best with the properties of the site. Calculations are only provided for B600 and ARS, as these two sites are mostly influenced by the two single sources stack and NRU. Reemission from these 2 sources was considered. The third source, the area source was not considered in the calculations. Apart from the standard approach in NORMTRI, the nighttime TWT concentrations in grass at ARS and B600 were corrected by a factor of 0.38 and 0.34 respectively. The daytime TWT concentrations were corrected by a factor of 0.9. The 24 hour averages were calculated without any correction factor.

Scenario 4: The standard version of NORMTRI with the sigma parameter set of MOL was applied. Problems were encountered when evaluating the meteorological file, in particular the rain intensities and the stability classes caused problems. Uncertainty in the results due to these problems might be considerably high.

References

[1] HÜBSCHMANN, W., RASKOB, W., ISOLA IV – A FORTRAN 77-Code for Calculation of the Long-Term Concentration Distribution in the Environment of Nuclear Installations, Report KfK-4604, Kernforschungszentrum Karlsruhe (1990).

[2] RASKOB, W., Description of the Tritium Model NORMTRI for Releases under Normal Operation Conditions, Report KfK-5364, Kernforschungszentrum Karlsruhe (1994).

I–A.12. MODEL USED BY ZSR, UNIVERSITY OF HANNOVER, GERMANY

M. Täschner

The ZSR model was developed for scientific purposes by M. Täschner and C. Bunnenberg on the basis of the German regulation guide AVV (Gumprecht et al 1992). According to that guide the behaviour of tritium in the environment after continuous releases of tritium is modelled with a specific activity approach. T he ZSR model generally uses annual averages of the meteorological data, but it is made more dynamic (with up to hourly steps) for some scenarios. The model is applicable to flat terrains according to the applicability of the used dispersion parameters.

I–A.12.1. Structure of the model

The model predictions are calculated on spreadsheets. It is based on a sector–averaged one-dimensional Gaussian plume model for a single elevated source, that requires as input data the source strength and the weather conditions (e.g. annual or hourly averages, see Application of the model). The average concentrations of tritium in air humidity, rainwater, soil moisture and plant water are calculated at given points.

I–A.12.2. Primary dispersion

The basic equation is the sector-averaged Gaussian equation for a continuously emitting point-source. This equation is based on the assumption that all wind directions within a given sector occur with equal probability. It uses the probability distributions of wind direction, wind speed and stability given as input to the model. Building wake effects are considered only with Scenario 3. Plume depletion is neglected.

The vertical dispersion parameter is expressed as a function of both distance and stability class using the Briggs' results (Briggs 1973), which have been collated for unspecified small roughness lengths (between 0.03 and 0.3 m). The wind speed is extrapolated to the height of the source by using the vertical profiles proposed by Briggs.

In the case of several sources (e.g., Scenario 3), the contribution of each source is calculated in the same manner with changes in the relative co-ordinates of each source. The total primary concentration is determined by superimposing the contributions of all sources.

I–A.12.3. Secondary dispersion

The secondary concentration of tritium after primary HTO releases, due to re-emission of tritium deposited on the soil surface, is not considered directly. But neglecting plume depletion is assumed to compensate for the secondary pathway of tritium to the atmosphere in the long term.

If the source emits HT primarily, empirical constants for long-term ratios of HTO concentrations at different levels above the soil can be derived from the 1987 Canadian field experiments. The HTO concentration at 1.5 m above ground is assumed to be a quarter of the HTO concentration at the soil surface (this ratio was found to be the four-day average).

I–A.12.4. Wet deposition

The wet deposition of HTO is determined from a formula based on the use of an apparent washout coefficient, which is described in more detail by Belot (1998). The washout rate of tritiated water depends on source height, distance from the source and rain intensity. In case of elevated sources, the washout rate coefficient is nearly constant over a wide area (Belot 1998). The average concentration of tritium in rainwater is simply obtained by dividing the wet deposition flux so obtained by the corresponding average precipitation rate.

I–A.12.5. Buildup in soil and vegetation

According to the specific activity approach the HTO concentrations in soil and plant water are attributable to the HTO concentrations of the air humidity and of the rainwater.

Dry HTO transfer from air to soil is coupled to the condensation pathway of air humidity. The activity concentration in the condensate is set to that in the air humidity of the primary plume. The rate of 150 mm a^{-1} is an estimate for the annual average condensation rate for Germany and is considered a typical rate for temperate climates. The HTO concentration in air humidity is calculated by dividing the HTO concentration in air by the mean air humidity of the respective time interval.

It is possible to calculate an effective HTO deposition velocity that can be compared with the value of $3{\cdot}10^{-3}$ m s^{-1} given in Scenario 1. Given the condensation rate of 150 mm a^{-1}, an average air humidity of 10 cm^3 m^{-3} and an infiltration rate of 150 mm a^{-1}, which is a fraction of 1/6 of the annual total water deposit of 900 mm to the soil, the resulting effective HTO deposition velocity is about $8{\cdot}10^{-5}$ m s^{-1}. This is less than 3% of the HTO deposition velocity of this scenario and indicates that more than 97% of tritium that would be deposited with $3{\cdot}10^{-3}$ m s^{-1} would not penetrate into deeper soil layers but would re-enter the atmosphere.

The HTO concentrations in soil water are weighted averages of the specific activities of the air humidity (17%) and of the rainwater (83%). The fraction of 17% of air humidity results from a condensation rate of 150 mm a^{-1} and the fraction of 83% of rain water results from a precipitation rate of 750 mm a^{-1}, summing up to 900 mm a^{-1} of water uptake per year.

Similarly, plant water is assumed to be a mixture of air humidity by a fraction of h, and of soil water, by a fraction of $1-h$; h is the average relative humidity. This composition of the plant water is related to the aerial part of plants and would be different for tubers, for example.

Non-exchangeable tritium in the combustion water of organic matter in leaves (OBT) is not treated in this model and the reported OBT results are copies of the HTO concentrations in the plant water.

I–A.12.6. Application of the model to BIOMASS scenarios

Scenario 1: The HTO concentrations in air are determined from primary dispersion for the weather conditions given in the scenario. In the case of an HT release HTO is released to the atmosphere by a secondary process but the dispersion is related to the primary plume of HT. The vertical dispersion parameters are taken from Briggs. The HTO concentration in rainwater is calculated with a constant washout factor ($6{\cdot}10^{-5}$ s^{-1} per 1 mm h^{-1}) and is inversely proportional to the wind speed and to the distance from the source. Therefore, the HTO concentrations in rain, plant and soil water are highest near the source. The radioecological situation in the immediate vicinity of the stack (distance < 200 m) is not considered further. The average relative humidity is set to $h = 0.7$.

Scenario 3: For this scenario the HTO exchange between air and soil is made dynamic with hourly recalculations of HTO concentrations in air humidity, soil moisture and plant water.

HTO is moved via advection with the water (rain, condensation and evaporation) and via diffusive exchange between the atmosphere and the upper soil layer. For plant water the specific activity approach is extended from annual averages to hourly changes of the HTO concentrations of the water of air and soil.

I–A.12.6.1. Primary dispersion (Scenario 3)

The concentrations in air are determined from primary dispersion, using the weather conditions (hourly averages) given in the scenario. The vertical dispersion parameters are taken from Briggs. The washout coefficient is $6{\cdot}10^{-5}$ s^{-1} per 1 mm h^{-1}. In a second run of the model, atmospheric HTO concentrations are taken from observations.

The vertical dispersion of the primary plume is calculated with Briggs parameters. The wind speed measured at 61 m is limited to 1 m s^{-1} at the minimum. According to Briggs' power law the wind speed is further reduced to the effective release height of the source: i.e. 46 m for releases from the stack and, in case of ARS, 30 m for the NRU source. Building wake effects are neglected by ZSR predicting HTO concentrations at ARS.

The HTO concentration in rainwater is calculated commonly with a constant washout factor ($6{\cdot}10^{-5}$ s^{-1} per 1 mm h^{-1}).

In a second edition of calculations, ZSR also predicted HTO concentrations at the B600 site. Compared with measurements, it became evident that the effective release height of the NRU source has to be reduced in order to meet measured air concentrations. Therefore, the ZSR predictions for B600, submitted after the release of the observations, were calculated with an effective release height of 15 m and included wake effects of the NRU building, which was the main contributor of HTO to the B600 site. All other modelling approaches were the same as with ARS.

I–A.12.6.2. Soil compartment (Scenario 3)

The soil is divided into 10-cm layers. Soil moisture is set to 5 % v/v at minimum and 40 % v/v at maximum. Water exchange between deeper layers is not considered unless overflow of the first layer happens. HTO exchange between deeper layers via diffusion is considered.

Water exchanges via condensation and evaporation (Monteith/Penman) between upper soil layer and atmosphere. The water content of plants is invariable. Precipitation is introduced to the upper soil layer. Heavy rain contributes also to the moisture of deeper layers.

HTO is moved via advection with the water (rain, condensation and evaporation) and via diffusive exchange between the atmosphere and the upper soil layer. The initial deposition rate for HTO to uncontaminated soil is set to 3.0 E-3 m s^{-1} for a soil moisture of 10.3% v/v. The initial HTO content of soil water is set to 94 Bq L^{-1} (ARS) or 230 Bq L^{-1} (B600).

I–A.12.6.3. Plant compartment (Scenario 3)

The water content of the plants is kept constant. The initial HTO concentration of the plant water is set to 94 Bq L^{-1} (ARS) or 230 Bq L^{-1} (B600). The specific activity ($C_{pw,new}$, Bq L^{-1}) of the new plant water that enters the plant during the actual time step is calculated according to the following equation:

$$C_{\mathrm{pw,new}} = h\, C_{\mathrm{am}} + (1 - h)\, C_{\mathrm{s}} ,$$

where h is the relative humidity, C_{am} (Bq L^{-1}), is the HTO concentration in air moisture and C_{s} (Bq L^{-1}) is the HTO concentration in soil water. The actual HTO concentration of the plant water (C_{pw}, Bq L^{-1}) is calculated from the new plant water concentration ($C_{\mathrm{pw,new}}$, Bq L^{-1}) at a given hour and the old plant water concentration for the previous hour ($C_{\mathrm{pw,old}}$, Bq L^{-1}):

$$C_{\mathrm{pw}} = \alpha\, C_{\mathrm{pw,old}} + (1 - \alpha)\, C_{\mathrm{pw,new}} .$$

The weighting factor α is introduced to reflect the rate at which the plant concentration comes into equilibrium with the current air and soil concentrations. For daytime conditions (net radiation $R_{\mathrm{N}} > 0$), when exchange between the plant and its surroundings is rapid, α is chosen to be 0.5 (half life: one hour). For $R_{\mathrm{N}} < 0$, α is set to 0.94, implying much slower exchange (half life: 12 hours).

I–A.12.6.4. OBT compartment (Scenario 3)

The organic compartment is treated dynamically with OBT decaying slowly with a 100-hour half-life and newly-formed OBT that has the same concentration as plant water. The initial OBT concentration is set to 94 Bq L^{-1} (ARS) or 230 Bq L^{-1} (B600). The OBT concentration is calculated hourly from

$$C_{\mathrm{OBT}} = \beta\, C_{\mathrm{OBT,old}} + (1 - \beta)\, \mathrm{C}_{\mathrm{pw}} ,$$

where $\beta = 0.993$. Isotopic discrimination in OBT formation is not accounted for.

I–A.12.6.5. Soil and plant HTO concentrations at specific times (Scenario 3)

It was found that the above atmospheric modelling was not able to reproduce observed (CRL) air concentrations that were included within the scenario. Therefore, the model was run a second time, using air HTO concentrations for each hour derived from CRL measurements. Missing data were replaced by the average of 3.5 Bq m^{-3}. The results for plant water differed very much for the two runs. The endpoint results for selected times for plant water are given as averages of the two runs.

References

[1] BELOT, Y., Predicting the washout of tritiated water from atmospheric plumes, presented at the Workshop of the IEA Task Group on Tritium Safety and Environmental Effects, held at AECL, Chalk River, Canada, May 11-12 (1998).

[2] BRIGGS, G.A., Diffusion estimation for small emissions (draft), ATDL contribution file No 79, Atmospheric Turbulence and Diffusion Laboratory, Oak Ridge, Tennessee (1973).

[3] GUMPRECHT, D., MÜLLER-NEUMANN, M., Modelle, Annahmen und Daten mit Erläuterungen zur Berechnung der Strahlenexposition bei der Ableitung radioaktiver Stoffe mit Luft oder Wasser zum Nachweis der Einhaltung der Dosisgrenzwerte nach § 45 StrlSchV. Veröffentlichungen der Strahlenschutzkommission. Bd. 17, G. Fischer, Stuttgart, Jena, New York (1992).

I–B. SOIL AND GROUNDWATER MODELS

I–B.1. MODELS USED BY COMMISSARIAT À L'ÉNERGIE ATOMIQUE, FRANCE

Y. Belot

I–B.1.1. Soil model

TRIMOVE is a numerical model for simulating both soil moisture flow and tritium transport through a column of unsaturated soil. The model, written by Y. Belot, is intended to describe the one–dimensional vertical movement of tritium in the soil-atmosphere continuum. Implied in the choice of the simulation method is the prospect of potential uses ranging from management to research. The main purpose is to study the effects of boundary and initial conditions, soil characteristics, and weather inputs on the vertical movement of water and tritium within and from a soil column, including the exchange of tritium between the soil surface and the atmosphere.

The model deals with bare or vegetated soils considered as isothermal and homogeneous over the whole extent of the soil column. The model describes the transient transport of both ordinary water and tritiated water by means of two sub-models working in parallel at space and time scales that can be changed according to the problem and / or the process to be treated. Most of the model has taken advantage of process models developed by others.

I–B.1.1.1. Structure of the model

The core of the model is a system of coupled partial derivative equations that represent the transient processes of moisture flow and tritium transport through the 1-D unsaturated zone of interest. To solve the problem, the soil column is subdivided into a series of regular layers, which correspond to a fixed space increment ?z=D /N, where D is the total column depth and N the number of soil layers. The system of the two equations is solved by a finite-difference method.

Boundary and initial conditions, soil characteristics and weather data are given as inputs to the model. The weather data are provided as a set of hourly values of wind speed, precipitation, air temperature, air humidity, atmospheric stability and net radiation. Optionally, hourly evaporation and transpirational rates can also be provided, which eliminates the need to estimate these rates by the model.

The results of the model calculations are the profiles of water content and tritium concentration, and the fluxes of tritium from soil to the atmosphere, these profiles and fluxes being given at a fixed date or as monthly averages.

I–B.1.1.2. Moisture flow

The soil moisture flow through the unsaturated zone is described by the Richard's equation with a sink / source term. The equation is written with the pressure head h taken as dependent variable, the time t and the depth z below ground level as independent variables.

The most important hydraulic functions that intervene in the equation are the relationships between water content (θ), pressure head in the soil (h), and hydraulic conductivity (K). The relationship θ(h) is strongly non-linear and varies widely between different soils. So does the companion relationship K(h). The expressions of θ(h) and K(h) are taken from van Genuchten (1980), using fitting parameters collated by Schaap and Leij (1998). If the actual hourly evaporation and transpiration rates at the upper boundary are not provided as input data, the potential values of these parameters are determined by using the Penman-Monteith relation (Monteith 1981).

The Richard's equation is replaced by a system of N algebraic equation which is obtained by using a fully implicit discretisation scheme. In these algebraic equations, the interlayer conductivity is approximated by the geometrical mean of the adjacent central conductivities as recommended by Haverkamp and Vauclin (1979). The top and bottom boundary conditions are embedded in the first and last equation of the system. The system is solved numerically at each time step using the classical tridiagonal algorithm which appears to be very efficient (Remson et al. 1971).

The self-limiting process of water evaporation at soil surface is simulated by suppressing numerically the evaporation when the pressure head of the top layer falls under a certain limiting value, and giving to the evaporation rate its potential rate when the pressure head exceeds this value. A limiting value of -100m, established by test calculations, is convenient to simulate and estimate appropriately the actual evaporation rate.

I–B.1.1.3. Tritium transport

The classical mass transport equation is solved in parallel with the moisture flow equation. In this equation the change in tritium concentration at a given level is related to a convection term, a dispersion term, and a term for local appearance or disappearance of tritium.

The convection term ensures the linkage between the tritium transport equation and the moisture flow equation, since the convection term is proportional to the convective flux of soil moisture. The dispersion term depends on molecular diffusion, but mostly on mechanical dispersion imputable to irregularities of the flow patterns. The dispersion is characterised by a coefficient $D = D_m + \alpha v$, where D_m is the molecular diffusion coefficient, α is the dispersivity and v is the absolute value of pore water velocity.

At each time step, the mass transport equation is solved in parallel to the moisture flow equation using the same numerical technique. The evaporation of tritiated water at soil surface is expressed by writing that the flux of tritium is proportional to the difference in tritium concentration across the lowest part of the soil-atmosphere boundary layer, that is:

$$J = v_a(\chi - \rho_s C_s)$$

where v_a is the exchange velocity, χ is the concentration of tritium in the air in Bq m^{-3}, ρ_s is the absolute humidity in air at soil temperature in kg m^{-3} and Cs is the concentration of tritium in the water of the top soil layer in Bq kg^{-1}. The exchange velocity is derived from the Chamberlain's formula (Chamberlain 1968), but set equal to zero when the top soil layer is dry in the sense explained above.

I–B.1.1.4. Application of model to BIOMASS scenarios

Scenario 2 considers a 1 m-thick layer of uniform sandy loam soil situated above a water table that does not appreciably fluctuate during the course of a year. The tritium concentration in the aquifer is assumed to be constant throughout the period of study. The soil column is assumed to be devoid of tritium at the beginning of the simulation exercise. The concentration of tritium in air is assumed to be negligible.

The TRIMOVE model is applied for the special initial and boundary conditions of the scenario. As the gradient of tritium concentration is very steep at the beginning of the simulation exercise, a fine spatial resolution is needed to describe accurately the dispersion front and minimise the truncature errors in the numerical approximation of the dispersion term. From test calculations, it appears that the space increment should be = 0.01 m. This requires the division of the unsaturated 1m–layer into 100 sublayers or more. The computational time step should be then sufficiently small to avoid any computation instability that would appear if a sublayer was completely filled up or emptied out in the course of a time step. So, the time step is to be taken the smaller as the depth increment is the smaller. In the present problem, a constant time step equal to 30 s has been chosen for 0.01-m sublayers, and 10 s for 0.005-m sublayers.

References

[1] CHAMBERLAIN, A.C., Transport of gases to and from surfaces with bluff and wave-like roughness elements, Quart. J. Roy. Meteo. Soc. **94** (1968) 318–322.

[2] HAVERCAMP, R., VAUCLIN, M., A note on estimating finite difference interblock hydraulic conductivity values for transient unsaturated flow problems, Water Resour. Res. **15** 1 (1979) 181–187.

[3] MONTEITH, J.L., Evaporation and surface temperature, Q.J.R. Meteor. Soc. **107** (1981) 1–27.

[4] REMSON, I., HORNBERGER, G.M., MOLZ, F.J., Numerical Methods in Subsurface Hydrology, John Wiley, New York (1971).

[5] SCHAAP, M.G., LEIJ, F.J., Database related accuracy and uncertainty of pedotransfer functions, Soil Science **163** 10 (1998) 765–779.

[6] VAN GENUCHTEN, M.Th., A closed form equation for predicting the hydraulic conductivity of unsaturated soils, Soil Sci. Soc. Am. J. **44** (1980) 892–898.

[7] VAUCLIN, M., HAVERKAMP, R., VACHAUD, G., Etude de la résolution numérique de l'infiltration d'eau en milieu non saturé, Final Report, Contract 75-102-01, Grenoble, France (1978).

I–B.1.2. Groundwater model

The transport of tritium in groundwaters is estimated by using an analytical approach instead of the numerical approach usually adopted in treating such a problem. It was felt that an analytical solution, even if restrictive regarding the conditions of application, would possess a greater flexibility and would not suffer from some of the errors that may be associated with numerical solutions. The model, developed by Y. Belot, is partly based on the classical treatment of the water flow in an homogeneous aquifer, and partly based on the use of Green's functions in solving the partial derivative equation that governs the mass transport of tritium in the aquifer.

I–B.1.2.1. Steady flow in an unconfined aquifer

In an unconfined aquifer, the fact that the water table is also the upper boundary of the region of flow complicates flow determinations. An approximate solution can nevertheless be obtained from the water balance of the unconfined aquifer (Polubarinova–Kochina 1962). In the case of an homogeneous unconfined aquifer resting on an horizontal impervious surface, the height, *h,* of the water table above the aquifer bottom can be written:

$$h = \left[h_o^2 + \frac{V}{K}\left(L^2 - x^2\right) \right]^{1/2}$$

where h_o is the height of the watertable at the receiving stream; x is the horizontal distance of the flow divide to the point of interest (oriented positive in the direction of groundwater flow); K is the permeability of the aquifer; L is the distance from the flow divide to the receiving stream; V is the Darcy vertical recharge rate.

The field of the horizontal, *u,* and vertical, *w,* pore water velocities in the aquifer can be estimated from the relations: $u = Vx/(ph)$ and $w = (pu^2/K)(1 - z/h)$, where p is the porosity of the aquifer and z is the depth below water table.

I–B.1.2.2. Transport of tritium in the aquifer

The method used to derive an analytical expression of the transient transport of tritium in the steady flow of the aquifer is based on solving the advective-dispersive partial differential equation by the use of Green's functions, otherwise called 'impulse responses in the terminology of signal theory. A Green's function is simply the concentration as a function of time and space arising from an unit instantaneous source.

The current problem can be reduced to the estimation of the tritium transport in a vertical 2D-plane. The concentration of tritium at horizontal distance x from the flow divide, and at depth z below the watertable at time t after beginning of release, is:

$$c(x,z,t) = \int_0^t \int_{l_1}^{l_2} g_1(\xi,\tau;x) g_3(\xi,\tau;z) \exp(-\lambda\tau) d\xi d\tau$$

where g_1 refers to the transport of tritium in the horizontal x-direction and g_3 to the transport of tritium in the vertical z-direction; λ_1 and λ_2 are empirical limits of integration along the x–axis.

The function g_1 refers to the transport of tritium in the horizontal x-direction which can be considered as unbounded. This function is known to be Gaussian with a shift to describe the main water flow in the x-direction:

$$g_1(\xi,\tau;x) = \frac{1}{\sqrt{4\pi D_x \tau}} \exp\left[-\frac{(x - \xi - u\tau)^2}{4D_x\tau} \right]$$

where u is the average horizontal component of the pore water velocity and $D_x = \alpha_x u$ is the dispersion coefficient in the x-direction.

The function g_3 which refers to the transport of tritium in the vertical z-direction is more complicated because of the water table boundary condition. Function g_3 is the solution obtained for the instantaneous injection of a tracer at the boundary of a semi-infinite bed. The following solutions are those reported by Kreft and Zuber (1978) for a prescribed-flux condition or a prescribed-concentration condition respectively:

$$g_3(\xi,\tau,z) = \frac{F(\xi)}{p}\left\{\frac{2}{\sqrt{4\pi D_z\tau}}\exp\left[-\frac{(z-w\tau)^2}{4D_z\tau}\right] - \frac{w}{2D_z}\exp\left(\frac{wz}{D_z}\right)\operatorname{erfc}\left(\frac{z+w\tau}{\sqrt{4D_z\tau}}\right)\right\}$$

$$g_3(\xi,\tau;z) = c_0(\xi)\frac{z}{\sqrt{4\pi D_z\tau^3}}\exp\left[-\frac{(z-w\tau)^2}{4D_z\tau}\right]$$

where co is the concentration of tritium at the water table; w is the average vertical component of the pore water in the zone considered in the aquifer; z is the depth below water table; F is the tritium flux density per unit area of water table and Dz = ?zu is the dispersion coefficient in the z–direction. The average values of these parameters in the case of an unconfined aquifer is drawn from a water-balance of the aquifer, as shown in the section just above.

I–B.1.2.3. Application of model to BIOMASS scenarios

In the conditions of Scenario 1, at 6000 m downstream from the flow divide, the average values of pore water velocities which are taken in the above formulae are u=54.3 m a-1 and w=0.28 m a-1. These approximations are not too unrealistic, since in the domain considered, u and w vary only moderately with x and z.

References

[1] POLUBARINOVA-KOCHINA, P.Y., Theory of groundwater movement, trans. R.J.M. DeWiest, Princeton, N.J. Princeton University Press (1962).

[2] KREFT, A., ZUBER, A., On the physical meaning of the dispersion equation and its solution for different initial and boundary conditions, Chem. Engng. Sci. **33** (1978) 1471–1480.

I–B.2. MODELS USED BY STUDSVIK ECO & SAFETY AB, SWEDEN

O. Edlund

I–B.2.1. Soil model

USTEVA is a code, written in Fortran 77, and developed by O. Edlund for assessment of atmospheric dispersion attributed to both accidental and routine releases of tritium as well as tritium transport in soil water. In the following section the water transport part in the soil model is described. The tritium transport model does not work adequately at present and is therefore not included in the description.

I–B.2.1.1. Structure of the model

The movement of water in an unsaturated soil column is solved numerically with Richard's equation used as the basic equation. The column is divided in regular layers, which correspond to a fixed space increment $\Delta Z = D/N$, where D is the total column depth and N the number of soil layers. All necessary parameters characterising several soils are introduced in the code.

I–B.2.1.2. Moisture flow

For a special soil the relationships between water content (θ), pressure head in the soil (h) and hydraulic conductivity (K) are given.

The relationship $\theta(h)$ is strongly non-linear and varies widely between different soils. So does the companion relationship K(h). The expressions of $\theta(h)$ and K(h) are taken from van Genuchten (1980), using fitting parameters collated by Schaap and Leij (1998). If the actual hourly evaporation and transpiration rates at the upper boundary are not provided as input data, the potential values of these parameters are determined according to the resistance model described in the atmospheric model. The code can handle the situation even if the hourly evaporation and transpiration rates are given as input. During the calculation of the transport of water from one layer to another the water content is checked relative the hygroscopic point and the field capacity in each layer. The water balance at the top layers of the soil is checked when rain, evaporation and transpiration through vegetation are considered.

I–B.2.1.3. Application of the model to BIOMASS scenarios

Scenario 2 considers a 1-m thick layer of uniform sandy loam soil situated above a water table that does not appreciably fluctuate during the course of a year.

The water content in the unsaturated zone is assumed to correspond to the field capacity in each layer and is calculated according to a given formula. The soil layer is divided in 100 1-cm layers and the water profile is estimated at the time points given in the scenario.

References

[1] SCHAAP, M.G., LEIJ, F.J., Database related accuracy and uncertainty of pedotransfer functions, Soil Science **163** 10 (1998) 765–799.

[2] VAN GENUCHTEN, M.Th., A closed form equation for predicting the hydraulic conductivity of unsaturated soils, Soil Sci. Soc. Am. J. **44** (1980) 892–898.

I–B.2.2. Groundwater model

The transport of tritium in the ground water is estimated using the model developed by Y. Belot. In the simulations the MATHCAD-code system has been used. A complete explanation of the model can be found in the model description written by Yves Belot.

I–B.3. MODEL USED BY NIPNE, ROMANIA

D. Galeriu

I–B.3.1. Groundwater model

I–B.3.1.1. Steady flow in an unconfined aquifer

As a first approach, an approximate velocity field is assessed:

$$V_x = Vi*x/H$$

$$V_z = Vi*(1-z/H)$$

as a simple solution of flow conservation for isotropic hydraulic tensor with Vi the pore water velocity from infiltration (inf_rate/porozity m/y) H the depth of aquifer and x,z coordinates.

The dispersion coefficients are also increasing with x and decreasing with z (but Dxx is constant with z).

After the first interaction with the group members, I used an approximation obtained from the water balance of the unconfined aquifer (Polubarinova–Kochina 1962). In the case of an homogeneous unconfined aquifer resting on an horizontal impervious surface, the height, *h,* of the water table above the aquifer bottom can be written:

$$h = \left[h_0^2 + \frac{V}{K}\left(L^2 - x^2\right) \right]^{1/2}$$

where ho is the height of the watertable at the receiving stream; x is the horizontal distance of the flow divide to the point of interest (oriented positive in the direction of groundwater flow); K is the permeability of the aquifer; L is the distance from the flow divide to the receiving stream; V is the Darcy vertical recharge rate.

The field of the horizontal, u, and vertical, w, pore water velocities in the aquifer can be estimated from the relations: $u = Vx/(ph)$ and $w = (pu^2/K)(1 - z/h)$, where p is the porosity of the aquifer and z is the depth below water table.

I–B.3.1.2. Transport of tritium in the aquifer

As explained in the introduction, I take the analytical solution from a unique event, convolute and add radioactive decay. I checked that we can ignore the y dimension and finally, the approximate formulae are similar to those deduced by the TWG leader. After correcting a mistake in the fluid velocity, the results are also numerically similar.

The concentration of tritium at horizontal distance x from the flow divide, and at depth z below the watertable at time t after beginning of release, is:

$$c(x,z,t) = \int_0^t \int_{l_1}^{l_2} g_1(\xi, \tau; x)\, g_3(\xi, \tau; z)\, \exp(-\lambda\tau)\, d\xi\, d\tau$$

where g_1 refers to the transport of tritium in the horizontal x-direction and g_3 to the transport of tritium in the vertical z-direction ; l_1 and l_2 are empirical limits of integration along the x–axis.

The function g_1 refers to the transport of tritium in the horizontal x-direction that can be considered as unbounded. This function is known to be Gaussian with a shift to describe the main water flow in the x-direction:

$$g_1(\xi,\tau;x)=\frac{1}{\sqrt{4\pi D_x\tau}}\exp\left[-\frac{(x-\xi-u\tau)^2}{4D_x\tau}\right]$$

where u is the average horizontal component of the pore water velocity and $D_x = \alpha_x u$ is the dispersion coefficient in the x-direction. For solving in the x direction, the infinite media is adopted and the limit of the integral l_1,l_2 are infinite.

As explained for the function g_3 which refers to the transport of tritium in the vertical z-direction we take initially the expressions for infinite and later for semi-infinite media (Moltyaner) and finally our formulae are similar to those used by Y Belot (TWG Leader) and taken from Kreft and Zuber (1978) for a prescribed-flux condition or a prescribed-concentration condition respectively:

$$g_3(\xi,\tau,z)=\frac{F(\xi)}{p}\left\{\frac{2}{\sqrt{4\pi D_z\tau}}\exp\left[-\frac{(z-w\tau)^2}{4D_z\tau}\right]-\frac{w}{2D_z}\exp\left(\frac{wz}{D_z}\right)\operatorname{erfc}\left(\frac{z+w\tau}{\sqrt{4D_z\tau}}\right)\right\}$$

$$g_3(\xi,\tau;z)=c_0(\xi)\frac{z}{\sqrt{4\pi D_z\tau^3}}\exp\left[-\frac{(z-w\tau)^2}{4D_z\tau}\right]$$

We add the solution for infinite media prescribed concentration:

$$g_3=c_o(\xi)\exp(-\frac{(z-w\tau)^2}{4D_z\tau})\frac{1}{\sqrt{4D\tau}}$$

where c_o is the concentration of tritium at the water table; w is the average vertical component of the pore water in the zone considered in the aquifer; z is the depth below water table; F is the tritium flux density per unit area of water table and $D_z = \alpha_z u$ is the dispersion coefficient in the z–direction. The average values of these parameters in the case of an unconfined aquifer is drawn from a water-balance of the aquifer, as shown in the section just above.

I–B.3.1.3. Application of model to BIOMASS scenarios

Scenario 1: at 6000 m downstream from the flow divide, the average values of pore water velocities which are taken in the above formulae are *u*=54.3 m a-1 and w=0.28 m a-1. These approximations are not too unrealistic, since in the domain considered, u and w vary only moderately with x and z. When applying our first approximation, u is lower at 42 m/s (constant h = H).

The integrals have a singularity at t=0, and must be treated carefully. We used a partition of time interval and two routines from the professional version of IMSL, under Microsoft

Developer Studio: QDAGP for t=0.000001 to 0.01 and QDAG after. The routine QDAGP uses a globally adaptive scheme in order to reduce the absolute error. It initially subdivides the interval [A, B] into NPTS + 1 user-supplied sub-intervals and uses a 21-point Gauss-Kronrod rule to estimate the integral over each sub-interval. The error for each sub-interval is estimated by comparison with the 10-point Gauss quadrature rule. This routine is designed to handle endpoint as well as interior singularities. The routine QDAG is a general-purpose integrator that uses a globally adaptive scheme in order to reduce the absolute error. It subdivides the interval [A, B] and uses a (2k + 1)-point Gauss-Kronrod rule to estimate the integral over each sub-interval. The error for each sub-interval is estimated by comparison with the k-point Gauss quadrature rule. The sub-interval with the largest estimated error is then bisected and the same procedure is applied to both halves. The bisection process is continued until either the error criterion is satisfied, roundoff error is detected, the sub-intervals become too small, or the maximum number of sub-intervals allowed is reached.

The different approaches (infinite media, concentration boundary condition (ic), semi-infinite-concentration (sic) or semi-infinite flux (sif)) for a case with low dispersivity are shown below for the depth profile. We see that at the water table there are differences in concentrations but the shape is similar. Note also that the infinite approach is between the two semi-infinite ones. Generally speaking, the boundary condition at the water table is far from easy to understand, due to physical simplification of the aquifer.

References

[1] POLUBARINOVA-KOCHINA, P.Y., Theory of groundwater movement, trans. R.J.M. DeWiest, Princeton, N.J. Princeton University Press (1962).

[2] KREFT, A., ZUBER, A., On the physical meaning of the dispersion equation and its solution for different initial and boundary conditions, Chem. Engng. Sci. **33** (1978) 1471–1480.

[3] MOLTYANER, G. M., Migration of radionuclides in porous media AECL-8254 1984, Dispersion of contaminants in saturated porous media AECl-9520 (1987).

[4] ENGESGAARD, P., JENSEN, K.H., Large scale dispersion in a sandy aquifer, Simulation of subsurface transport of environmental tritium, Water Resources Researches **32** (1996) 3253.

I–B.4. MODELS USED BY VNIIEF, RUSSIAN FEDERATION

A. Golubev, L. Belovodsky, S. Mavrin, et al.

I–B.4.1. Soil model

SM_Moist is the numerical 1-D model intended to study the processes of water and tritium transport in the area of soil aeration. The model allows the investigation of the effect of initial conditions, soil properties, meteorological conditions and vegetation on the process of tritium transport both from the soil to the atmosphere and from the atmosphere to the soil. The model takes into account the following physical processes: the water motion in the soil, tritium transport in the liquid phase and tritium transport in the gaseous phase. For the specified time points, the said model allows the calculation of:

- water profiles;
- tritium profiles in the liquid phase;
- tritium profiles in the gaseous phase;
- tritium profiles in the soil as the total in liquid and in gaseous phases;
- the total amount of water in the soil;
- the total amount of water entered the soil with precipitations;
- the total amount of water escaping the soil due to evaporation;
- the total amount of water escaping the soil due to transpiration;
- the total water run off over the surface;
- the total amount of water entered the aquifer;
- the total amount of tritium in the liquid phase;
- the total amount of tritium in the gaseous phase;
- the total amount of water tritium, escaping the soil due to evaporation;
- the total amount of water tritium, escaping the soil due to transpiration;
- balance on water;
- balance on tritium.

Upon completion of calculations, the model yields the following monthly averaged values:

- the amount of water entering the soil/escaping the soil, precipitation's, evaporation, transpiration, water run off over the surface and the amount of water, entering the aquifer/escaping the aquifer,
- the amount of tritium entering the soil/escaping the soil,
- the amount of tritium escaping the soil due to evaporation and transpiration.

I–B.4.1.1. Structure of the model

The model is represented by the system involving 3 differential equations in partial derivatives and one algebraic equation:

- the Richardson equation, modeling the motion of water,
- the equation of convective diffusion modeling the tritium transport in the liquid phase,
- the diffusion equation modeling the tritium transport in the gaseous phase,
- the equation of equilibrium between liquid and gaseous phases.

This system is solved numerically using the method of splitting over physical processes with the employment of the method of finite differences. All the equations are solved on a single spatial and time grid.

The set of equations being solved is non-linear (all coefficients in the equations depend on the soil moisture). Therefore, the coefficient iterations are employed to solve it (Samarsky, 1989).

I–B.4.1.2. The motion of water

The motion of water is described by the Richardson equation with run-offs, which models transpiration. The equation is solved in the h-form. The dependencies of humidity derivative on the potential (dθ/dh) and of the coefficient of hydraulic conductivity on the humidity Ê (θ) are the coefficients in this equation. Over the range of humidity variation from θmin to θmax, these coefficients change by several orders of magnitude leading to the essential non-linearity of the equation being solved. If one cannot attain the desirable accuracy of solution by using the coefficients iteration, the automatic reduction of time step takes place. The reduced time step is used only to solve the Richardson equation. The diffusion equations possess insignificant non-linearity, therefore they are solved with constant time step, which is specified at the beginning of calculations.

The h(θ) and Ê(θ) dependencies can be specified in any analytical form. The evaporation and the transpiration can be specified both using the external file and can be calculated using models (Poluektov et al, 1996, Gussev and Nanosova, 1998).

I–B.4.1.3. Tritium transport in the liquid phase

To describe the tritium transport in the liquid phase, the equation of convective diffusion is used. The soil moisture and the speed of water motion are taken from the solution of the Richardson equation. The diffusion coefficient is written as follows:

$$D=D_m+\alpha V,$$

where D_m is the coefficient of molecular diffusion, α is the dispersion coefficient, V is the speed of water motion. While calculating Scenario 2.5, the boundary condition on the upper boundary was specified in the following way:

$$J_{HTO}=J_{evap}C_s,$$

where J_{HTO} is the tritium flux into the atmosphere, J_{evap} is the evaporation, C_s is the tritium concentration in the 5-sm-thick surface layer. The employment of the average value in the thin surface layer rather than the concentration in the upper computational cell as C_s allows the size of the computational cell to be independent with the essential variation of HTO concentration in the vicinity of the surface.

I–B.4.1.4. Tritium transport in the gaseous phase

Since isothermal conditions are specified in Scenario 2.5, it is quite permissible to use the diffusion equation without sources and convection. The boundary condition on the surface is $C_{HTO}=0$. The said condition ensures the maximal flow in the gas phase.

I–B.4.1.5. The balance between liquid and gaseous phases

The process of achieving balance between the liquid and the gaseous phases occurs much faster then the transport processes in the said phases. Proceeding from the above-said, the employment of the Henry law is quite acceptable.

I–B.4.1.6. Application of the model to BIOMASS scenarios

For the calculations under *Scenario 2.5*, the uniform spatial grid with the spacing of $\Delta Z=0.02$ m was used. The employment of a finer grid and of the non-uniform one, whose spacing was reduced in the vicinity of boundaries did not lead to essential variation of results. The time step in calculations was $\Delta\tau=10^{-3}$ days and nights (it could self-reduce with the solution of the Richardson equation).

For the calculations under Scenario 2.5, evaporation, precipitation and transpiration were specified as boundary conditions and were taken from files provided by W. Raskob.

The accounting of diffusion in the gaseous phase led to the variation of results by several percent.

It follows from the modeling that the key mechanism for tritium propagation in the soil is the hydromechanical dispersion. This means that while resolving practical problems, one should measure hydrophysical properties of soils very accurately and, using them, calculate the speed of water motion with high degree of accuracy.

References

[1] SAMARSKY, A.A., The theory of difference schemes, M.: Nauka (1989).
[2] POLUEKTOV, R.A., KUZNETSOV, M.YA., VASSILENKO, G.V., Water exchanges modeling in agroecosystems, Saint Petersburg (1996).
[3] GUSSEV, E.M., NANOSOVA ,O.N., Parametrization of heat and moisture exchange on the land surface with the conjugated hydrologic and climatic models, Vodnie resursi, **25** 4 (1998) 421–431.

I–B.4.2. Groundwater model

The calculation problem of tritium concentration in the ground water over the period of 20 years involves two sub-problems. The first sub-problem is the calculation of flow in the non-head aquifer. While solving this problem, one can neglect the change of the velocity of the flow vertically, since the height of the aquifer is much less than its length. Proceeding from that, it is quite permissible to use 1-D model (Mironenko and Ruminin, 1998). The second sub-problem is the tritium transport in the said aquifer. The 3-D model should be used for this sub-problem for two reasons. First, for the period of 20 years, the contamination does not reach the base of the aquifer in the watershed area (Golubev et al., 2000). Second, the initial contamination is distributed in the X-Y plane, according to the radial law (Scenario 1.4).

I–B.4.2.1. Steady flow in an unconfined aquifer

The speed of filtration and the height of an aquifer are determined from the analytical solution of the 1-D equation of mass balance. These solutions have the following form:

$$h(x)=\left(-\frac{\varepsilon x^{2}}{K}+h_{2}^{2}+\frac{\varepsilon L^{2}}{K}\right)^{1/2}$$

$$V(x)=\frac{1}{2}[h(x)]^{-1/2}[-\varepsilon x]$$

where h(x) is the height of the aquifer at the point with the x coordinate, ε - is the infiltration entering the aquifer, h_2=1m, L=10000 m, Ê is the filtration coefficient of the aquifer, V(x) is the speed of filtration at the point with the x-coordinate.

The vertical speed is assumed to be zero, since accounting for it essentially does not lead to the change of results.

I–B.4.2.2. Transport of tritium in the aquifer

The method of finite differences is used to solve the 3-D equation of convective diffusion. To eliminate the numerical dispersion, the computation of convective transport is performed using the method of particles in cell (PIC) (Golubev et al., 2000). As is well known, to reduce the computation errors to minimum, it is expedient to use the rectangular grid in the method of finite differences. In the problem under consideration, the height of the aquifer varies more than by a factor of ten (on the left boundary its height is 69 m, on the right side it is 1 m). To use the rectangular grid in the computations, the transformation of coordinates is performed in the model, which converts the physical non-rectangular X-Z region to the computational rectangular one (Golubev et al., 2000). The coefficients of hydromechanical dispersion are written down as follows:

$$D_x=D_m+V(x)\ \delta_x;\ D_y=D_m+V(x)\ \delta_y;\ D_z=D_m+V(x)\ \delta_z$$

Here, Dm is the coefficient of molecular diffusion, $\delta_x, \delta_y, \delta_z$ are the coefficients of mechanical dispersion, namely, the longitudinal, transverse and vertical ones, respectively.

V(x) is the filtration speed at the point with the x coordinate.

I–B.4.2.3. Application to BIOMASS scenarios

In the conditions of *Scenario 1*, at 6000 m downstream from the flow divide, the average values of pore water velocities which are taken in the above formulae are V=60.2 m a^{-1}.

References

[1] MIRONENKO, V.A., RUMININ, V.G., The problems of hydroecology, **1** M.: Publishing House of Moscow State University of Mines (1998).
[2] GOLUBEV, A.V., MAVRIN, S.V., STENGACH, A.V., The model of tritium dispersion by the ground water, Journal of Engineering Physics and Thermophysics, **73** 4 (2000).
[3] BIOMASS Theme 3, Tritium Working Group, Scenario1.4, Description (1998).

I–B.5. MODELS USED BY CEA, FRANCE

G. Guinois

I–B.5.1. Soil model

The code **METIS** (Modelisation des Ecoulements et des Transferts avec Interaction en milieu Saturé) has been written by P. Goblet from the Paris school of Mines. The code is a finite element model which solves 2D problems in unsaturated media. It was developed in 1996 for the unsaturated part of the model to calculate the impact of radio-elements. METIS is applied to practical problems in hydrological, geological, and nuclear applications.

I–B.5.1.1. Moisture flow

METIS solves the Richard's equation with a conjugate gradient method. METIS can calculate permanent and transient state. The time step is automatically deduced from the space discretisation and the water flux. We can give a time step maximum. The boundary conditions are given as a flux which is positive if the water goes out of the system and negative if it moves in.

I–B.5.1.2. Tritium transport

METIS resolves the convection, dispersion and molecular diffusion equations. METIS models fractured media as a double media with matrices which can retain a pollutant. METIS can transport other radionuclides even with a decay and it takes into account the progeny of a radionuclide.

I–B.5.1.3. Application of model to BIOMASS scenarios

Scenario 2 considers a 1 m-thick layer of uniform sandy loam soil situated above a water table that does not appreciably fluctuate during the course of a year. The tritium concentration in the aquifer is assumed to be constant throughout the period of study. The soil column is assumed to be devoid of tritium at the beginning of the simulation exercise. The concentration of tritium in air is assumed to be negligible.

The METIS model is applied for the special initial and boundary conditions of the scenario. The soil layer is divided in 100 sub-layers. The time step is automatically calculated by the code, a maximum time step of one hour has been imposed. A concentration of 107 Bq/m^3 is imposed at the bottom of the model. The flux on the surface, which is the difference between the evaporation rate and the amount of rain, is imposed. For the transpiration of the plant a flux is imposed on the node concerned.

References

[1] Programme METIS- Simulation d'écoulement et de transport miscible an milieu poreux et fracturé – Notice de conception – P. Goblet – Ecole des Mines de Paris – centre d'informatique géologique de Fontainebleau - LHM/RD/89/23 (1989).

[2] Programme METIS- Simulation d'écoulement et de transport miscible an milieu poreux et fracturé – Notice d'emploi – P. Goblet – Ecole des Mines de Paris – centre d'informatique géologique de Fontainebleau - LHM/RD/99/18 (1999).

[3] Programme METIS- Simulation d'écoulement et de transport miscible an milieu poreux et fracturé en milieu insaturé – à paraître– P. Goblet – Ecole des Mines de Paris – centre d'informatique géologique de Fontainebleau (to be published).

I–B.5.2. Groundwater model

The code METIS (Modelisation des Ecoulements et des Transferts avec Interaction en milieu Saturé) has been written by P. Goblet from the Paris school of Mine. The code is a finite element model which solve 2D and 3D problem in saturated media. It has been developed in 1989 to modelise the impact of storage of radio-elements. METIS is applied to practical problem in hydrological, geological, and nuclear applications.

I–B.5.2.1. Moisture flow

METIS solves the Darcy equation with a conjugate gradient method. METIS can calculate permanent and transient state. The time step is automatically deduced from the space discretisation and the water flux.

I–B.5.2.2. Tritium transport

METIS resolved the convection, dispersion and molecular diffusion equations. It allowed the modelling of fractured media as a double media with matrices which can retain a pollutant. METIS can transport other radio-elements even with a decay and it can take into account transport of chain of radio-elements.

METIS is able to couple thermal flow and transfer (thermo – convection).

I–B.5.2.3. Application of model to BIOMASS scenarios

Scenario 1 is modelled in 3 D dimension. A condition of imposed potential is used to simulate the river. We introduce a uniform permeability of 10^{-4} m/s in the model and we give a flux rate for the rain all over the model. The flux of tritium is imposed on upper nodes, porosity and dispersivity have the values given in the scenario. The discretisation of the model is 25m in the Oy axis, 12.5m in Ox axis and progressive from 0.2m to 8m in the Oz axis at 1 km from the source.

References

[1] Programme METIS- Simulation d'écoulement et de transport miscible an milieu poreux et fracturé – Notice de conception – P. Goblet – Ecole des Mines de Paris – centre d'informatique géologique de Fontainebleau - LHM/RD/89/23 (1989).

[2] Programme METIS- Simulation d'écoulement et de transport miscible an milieu poreux et fracturé – Notice d'emploi – P. Goblet – Ecole des Mines de Paris – centre d'informatique géologique de Fontainebleau - LHM/RD/99/18 (1999).

[3] Programme METIS- Simulation d'écoulement et de transport miscible an milieu poreux et fracturé en milieu insaturé – à paraître– P. Goblet – Ecole des Mines de Paris – centre d'informatique géologique de Fontainebleau (to be published).

I–B.6. MODELS USED BY ANDRA, FRANCE

C. Meurville

I–B.6.1. Soil model

I–B.6.1.1. Introduction

PORFLOW is a code developed by ACRi (Analytic & Computational Research, Inc.). It is a numerical 3D model for the simulation of transient or steady state multiphase fluid flow, heat transfer and mass transport in variably saturated porous (or fractured) media.

PORFLOW is a highly modular program which has been applied to a wide range of practical problems in petrochemical, hydrological, geological, nuclear and chemical industry applications.

It provides a unified theoretical treatment of concepts relevant to fluid flow and transport with various levels of dynamic interaction and coupling between different components of the flow system. Some of the physical processes incorporated in the software, useful for the modelling of tritium transport in a soil layer, are:

- for fluid flow: multiphase flow, hydraulic conduction, fluid sources and sinks,
- for mass transport: convection, diffusion, dispersion, mass sources or sinks, decay.

Detailed descriptions can be obtained with Internet:

- Presentation: http://www.acri.fr/English/Products/PORFLOW/porflow.html
  http://www.acri-us.com/software/porflow/por.htm
- Code manual: http://www.acri.fr/English/manual.html

I–B.6.1.2. Structure of the model

PORFLOW solves a set of coupled transport equations for fluid velocities, pressure and concentration of chemical species in multiphase variably saturated porous media flow. The governing equations are based on the conservation principles of fluid mechanics, except that the Darcy's equations are used in place of the Navier-Stokes equations. Auxiliary equations are used for characteristic saturation relations and hydraulic conductivity (Van Genuchten). These equations are solved in their three dimensional transient state form, with a finite-volumes approach (Nodal Point Integration).

Input data to be given to the model must include:

- space discretisation;
- soil characteristics;
- boundary conditions (fixed or time-dependant with corresponding history);
- initial conditions;
- duration of the simulation and time steps.

Moisture flow:

Variables used: Pressure, Saturation

Spatial discretisation scheme: central difference scheme with first order approximation.

Inter-element conductivity calculated with harmonic mean.

Spatial temporal scheme: semi-implicit (only saturation is considered explicitly) with first order approximation.

Solving method used: conjugate gradient method including:
- preconditioning by incomplete Cholesky factorisation
- conjugate gradient accelerator.

Input data: imposed pressure, imposed flux (derived from ETR calculation), initial pressure profile.

Tritium transport:

Variable used: Concentration in water

Spatial discretisation schem: hybrid scheme

If Peclet number < 2: central difference scheme (with second order profile)

If Peclet number > 2: upwind scheme (first order profile).

Spatial temporal scheme: semi-implicit with second order

Solving method used: ADI algorithm (alternating direction implicit method)

Advection and diffusion terms are treated in a unified manner

Source terms treated individually

Input data: imposed concentrations, initial concentration profile.

Application:

The soil, supposed unsaturated, is modelled as an homogeneous column (1 square meter surface and 1 m thick) with an imposed recharge (or evaporation) flux at the top (and in the root zone) and an aquifer at the bottom.

Space discretisation:

Regarding the location of the sink and sources (the aquifer at the bottom, the root zone and the atmosphere at the top), it appeared necessary to extend the refinement the grid near at the boundaries to the rest of the grid.

The grid, automatically generated by the code, is made of 198 meshes (200 nodes):
- the boundary elements (2) are 0.025 m thick,
- the other elements (196) are 0.05 m thick.

Boundary conditions

The net water flux (recharge >0 or evaporation <0) is imposed at the upper limit of the top element. The transport boundary condition is a constant null concentration (assuming a diffusive outflux only).

Plant uptake is a flux applied homogeneously to each layer of the root zone (0-10cm, 10-20cm, 20-30cm).

The vertical boundaries are supposed to be no flow limits.

At the lower boundary, the aquifer is represented by a constant head and a constant concentration.

Time discretisation:

The time steps are adapted to ensure the calculation stability: pressure and solute transport are solved simultaneously with the same time steps.

For monthly averaged data, the time step used is the one given per default by the code:

- first time step: 3.16E+4 s (total duration / 1000) ~ 1/3 day
- geometric ratio multiplier: 1.01

For hourly data, the time step is maintained constant: 360 s ~ 6 minutes.

For hourly data and plant transpiration, the time step is maintained constant: 36 s ~ 0.5 minutes.

I–B.6.2. Groundwater model

I–B.6.2.1. Introduction

MODFLOW and **MT3D** have been used for the modelling of tritium transport in groundwater. These two codes are commonly used in hydrogeology and contaminant transport modelling.

MODFLOW is developed by the US Geological Survey, and MT3D is developed by SSP&A. These codes are numerical 3D models for the simulation of transient or steady state water flow and dissolved mass transfer in saturated porous media.

MODFLOW includes a various set of packages to handle all kind of natural boundary conditions such as wells, flow from rivers, flow into drains. A specific package is needed to produce a file dedicated to the use of MT3D.

MT3D can take into account various processes such as advection, dispersion, diffusion, sorption, decay, chemical reactions. It is also adapted to the different kind of hydrogeological boundary conditions considered in MODFLOW.

References are given below and detailed descriptions can be obtained with internet:

http://water.usgs.gov/nrp/gwsoftware/modflow.html

http://hydro.geo.ua.edu/mt3d/mt3dhome.htm

I–B.6.2.2. Structure of the model

Groundwater flow

MODFLOW solves the classical equation describing the movement of groundwater of constant density through a porous material. This equation is solved in its three dimensional transient state form, with a finite-differences approach.

Variable used: Water head

Spatial discretisation scheme: central difference scheme with first order approximation.

Effective hydraulic conductivity calculated with harmonic mean.

Spatial temporal scheme: backward differences (implicit with first order approximation).

Solving method used: The most commonly algorithm used is preconditioned conjugate gardients method (PCG2). Strongly implicit procedure (SIP) or slice-successive overrelaxation method can also be used.

Input data to be given to the model must include:
- space discretisation,
- aquifer characteristics,
- boundary conditions (fixed or time-dependant with corresponding history),
- initial conditions,
- duration of the simulation and time steps.

Groundwater contaminant transport

MT3D solves the classical equation describing the fate of transport of species in a transient groundwater flow system. This equation is solved in its three dimensional transient state form, with one of the three major class of transport solutions techniques available in MT3D – standard finite-difference method:
- particle-tracking based Eulerian-Lagrangian methods,
- finite-volume third order total-variation-diminishing (TVD) method.

The characteristics of the standard finite-difference method are given below.

Variable used: Concentration in water

Spatial discretisation scheme: two schemes are available

Central difference scheme (with second order profile)

Upwind scheme (first order profile).

Spatial temporal scheme: implicit or explicit according to the solving method used.

Solving method used:

Explicit method (without iterative solver),

Iterative solver: Conjugate gradient solver with preconditioning option (Jacobi, symmetric successive over relaxation or modified incomplete Cholesky).

Input data: imposed concentrations or flux, initial concentrations.

I–B.6.2.3. Application

Space discretisation

As the aquifer thickness decreases from more than 60 m to 1 m, the horizontal stepsize is adapted to obtain a stable piezometric profile, especially near the boundary condition.

Regarding the source location (at the surface of the aquifer) and the calculation endpoints (vertical profiles), the vertical geometry of the grid to the head profile is adapted in order to have the same number of meshes on each vertical profile.

The horizontal stepsize is:

- varying from 500 m at 5 km upstream the stack to 200 m at 4 km upstream the stack,
- constant (100 m) from 4 km upstream to 4.5 km downstream the stack,
- varying from 50 m at 4.5 km downstream the stack to 1 m at 5 km downstream the stack.

The vertical stepsize is increased with depth, and decreased with the thickness of the aquifer.

The final grid has 18 layers of 100 meshes per layer.

Layer	5 km upstream	Under the stack	1 km downstream	3 km downstream
1	0.3 m	0.3 m	0.3 m	0.2 m
5	0.9 m	0.7 m	0.7 m	0.5 m
10	1.7 m	1.5 m	1.4 m	1.0 m
15	4.3 m	3.7 m	3.5 m	2.6 m
18	25.8 m	22.4 m	20.7 m	15.6 m

Time discretisation

The hydraulic solution is to be obtained with a steady-state simulation.

The transport calculation was made with the explicit finite difference method. This method is subject to various stability constraints on the size (length) of the (constant) transport time step which are listed below for the different transport components:

- Advection: $\Delta t \leq \dfrac{1}{\dfrac{v_x}{\Delta x}+\dfrac{v_y}{\Delta y}+\dfrac{v_z}{\Delta z}}$
- Dispersion: $\Delta t \leq \dfrac{0.5}{\dfrac{D_{xx}}{\Delta x^2}+\dfrac{D_{yy}}{\Delta y^2}+\dfrac{D_{zz}}{\Delta z^2}}$
- Sink/source: $\Delta t \leq \dfrac{\theta}{|q_s|}$
- Chemical reaction: $\Delta t \leq \dfrac{\lambda}{2}$

The transport stepsize estimated by the code are about:

- 170 s with the high dispersivity case
- 1700 s with the low dispersivity case.

Note: The dispersivity applied to small meshes leads to very small time steps (less than 1 second). The dispersivity has been reduced in the downstream part of the model (> 4.5 km downstream) to obtain the stepsize given above.

References

[1] McDONALD, M.G., HARBAUGH, A.W., A modular three-dimensional ground-water flow model, U.S. Geological Survey Techniques of Water Resources Investigations, Book 6, Chapter A1, 586 p. (1988).

[2] HILL, M.C., Preconditioned conjugate-gradient 2 (PGC2), a computer program for solving ground-water flow equations: U.S. Geological Survey Water-Resources Investigations, Report 90-4048, 43 p. (1990).

[3] ZHENG, C., WANG, P.P., MT3DMS: A modular three-dimensional multispecies model for simulation of advection, dispersion and chemical reactions of contaminants in groundwater systems, Documentation and User's Guide. Contract Report SERDP-99-1, U.S. Army Engineer Research and Development Center, Vicksburg, MS (1999).

I–B.7. MODELS USED BY FZK, GERMANY

W. Raskob

I–B.7.1. Soil infiltration model

I–B.7.1.1. Introduction

The program used for the calculation of the water and tritium flux in soil following a contamination of groundwater is a standalone version of individual modules that are part of the program UFOTRI /RAS90/ and /RAS93/ for assessing the consequences of accidental tritium releases. This program is not operational but serves as a tool to gain a better insight in the processes involved in the transfer of tritium and water in the infiltration zone. Results might be incorporated into any further versions of UFOTRI.

I–B.7.1.2. Soil/atmosphere exchange processes

The exchange soil/atmosphere and thus the evaporation of water is modelled according to the resistance approaches. These transfer resistances (aerodynamic r_{av} , boundary layer r_{bv} and soil r_{soil} resistance) determine the uptake of tritium and water by the soil as well as their loss

The aerodynamic resistance r_{av} characterises the transfer from the free atmosphere to the surroundings of the leaf, whereas the boundary layer resistance r_{bv} describes the mass transfer through the quasi laminar air layer directly connected to the surface (see /TOM69/ and /BRU82/ Since r_{av} and r_{bv} depend on the atmospheric stability and the surface properties, the commonly used Dyer-Businger equations are used in calculating the friction velocity /BRU82/.

The evaporation of water vapour from soil is calculated by applying Monteith's equations usually used for canopies only. However replacing the canopy resistance by the soil resistance, this equation can be used for the soil too /RIE72/:

$$\lambda E_a = \frac{\delta R_a + \varsigma c_p (e_s - e_a) / r_{av}}{\delta + \gamma (1 + r_{soil} / r_{AV})}$$

where λ is the latent heat of evaporation in J kg^{-1}, c_p is the specific heat of air at constant pressure in J kg^{-1} K^{-1}, E_a is the actual evapotranspiration, R_a is the incoming solar radiation in W m^{-2}, e_s is the actual saturation vapour pressure of air in N m^{-2}, e_a is the actual vapour pressure of air in N m^{-2}, δ is the gradient of the vapour pressure curve at ambient temperature in J m^{-3} K^{-1}, γ is the psychrometer constant in J m^{-3} K^{-1}, r_{AV}: is the sum of the atmospheric and the boundary resistance. The surface resistance r_{soil} is described in terms of path length and diffusivity. The diffusion coefficient itself depends on the temperature and on the water content in soil.

Theoretical considerations and some practical analysis /SFS82/ show that for calculating the soil resistance, the water content in a soil layer of 0.5 to 1 cm depth is decisive. However, the water module considers only a first soil layer of 10 cm depth. Therefore a so-called 'help layer' with the depth of 1 cm is introduced into the code for calculating the soil resistance only. The water content of this upper layer is calculated in a simple manner; it increases in case of rainfall and decreases by evaporation. Water transport due to matrix forces is neglected in this help layer. The varying depth of the 'dry' soil layer z is considered. In addition, a minimum resistance: r_{sm} is introduced because a zero resistance seems to be unreasonable, also if the soil is saturated with water. This drying layer determines the difference between the ‘potential’ and the so called ‘actual’ evaporation.

The soil is subdivided into 11 layers, 10 for the more or less unsaturated soil with a depth of 10 cm and one for the aquifer. The water transport in soil between each layer due to matrix forces is considered. The pressure head Ψ, the degree of saturation S, and the conductivity K are key parameters. The water movement $V_{1,2}$ from layer 1 to layer 2 is calculated by using a simplified version of Darcy’s law /WAL82/:

$$V_{1,2} = K_{1,2} \cdot \frac{\Psi_1 - \Psi_2}{(\Delta z_1 + \Delta z_2)/2} - 1$$

where Δz_1 and Δz_2 are the thickness of layer one and two, respectively, Ψ_1 and Ψ_2 are the pressure head of layer one and layer two, respectively and $K_{1,2}$ is the mean conductivity of the two layers. This equation is solved in an explicit numerical scheme.

I–B.7.1.3. Tritium transport

Tritium movement, as described earlier, is simply coupled to the movement of water. An explicit scheme is used to estimated water and thus the tritium transport for one time step. As described earlier the soil is subdivided into 11 layers (10 with 10 cm thickness and the ground water layer) and a time step of 6 minutes was applied for this realisation. Upper boundary is the flux to the atmosphere calculated by Monteith's equations whereas the lower boundary is defined by a constant concentration of tritium in the aquifer. For scenario 2.1 to 2.3, the diffusion of tritium was not considered explicitly. In later scenarios a transfer parameter for tritium representing the flux from one layer to another was introduced.

I–B.7.1.4. Application of model to BIOMASS scenarios

In *Scenario 2.1 and 2.2* a different parameter set for calculating the suction tension and conductivity was used /CLA78/. From *Scenario 2.3* onward, the water movement is calculated according to the approach proposed by Van Genuchten and documented in the scenario description. The water movement itself was still calculated with the approach explained above, however the suction tension and conductivity is defined in the new manor as done by Van Genuchten. In addition, a dispersion parameter for tritium was introduced and set to a value of 0.07 %/h for the revised *Scenario 2.4 and Scenario 2.5*. In scenario 2.5 not only evaporation from bare soil was applied but also the transpiration from vegetation. To this purpose, the wheat module from UFOTRI was extracted and coupled to the infiltration module. Transpiration of water and flux of tritium to the atmosphere is modelled in a similar manor as for soil. However the soil resistance is exchanged by the canopy resistance. In addition, water and tritium is extracted by the root system from a depth up to 30 cm. More details of the vegetation submodule are described in /RAS93/.

References

[1] BRUTSAERT, W.H., Evaporation into the Atmosphere, D. Reidel Publishing Company, Dordrecht, Holland (1982). /BRU82/

[2] CLAPP, R.B., HORNBERGER, G.M., Empirical equations for some soil hydraulic properties, Water Resources Research **14** (1978) 601–604. /CLA78/

[3] RASKOB, W., UFOTRI: Program for Assessing the Off-Site Consequences from Accidental Tritium Releases, Report KfK-4605, Kernforschungszentrum Karlsruhe, June (1990). /RAS90/

[4] RASKOB, W., Description of the New Version 4.0 of the Tritium Model UFOTRI Including User Guide, Report KfK-5194, Kernforschungszentrum Karlsruhe, August (1993). /RAS93/

[5] RITCHIE, J.T., Model for Predicting Evaporation from a Row Crop with Incomplete Cover, Water Resources Research **8** 5 (1972) 1204–1213. /RIE72/

[6] SHU FEN SUN, Moisture and Heat Transport in a Soil Layer Forced by Atmospheric Conditions, M.Sc. thesis University of Connecticut (1982). /SFS82/

[7] MCINTOSH, D.H., THOM, A.S., Essentials of Meteorology, Wykeham Science Series 3, London (1969). /THO69/

[8] WALLEY, W.J., HUSSEIN, D.E.D.A., Development and Testing of a General Purpose Soil-Moisture-Plant Model, Hydrological Sciences Journal **27** 1 (1982) 1–17. /WAL82/

I–B.7.2. Groundwater model

I–B.7.2.1. Introduction

For calculating the transport and dispersion of HTO in groundwater, the area source module of NORMTRI /RAS94/ was applied. The standard area source module of NORMTRI was extracted from the computer code and coded as a stand-alone version. This realisation is not operational and will be not part of any further code system for ground water transport. The main aim was to test if simple Gaussian type approaches can describe simple geometrical cases for ground water dispersion.

Only the selected dispersion and transport parameters differ from an application in the atmosphere. No time dependency can be calculated. Steady state conditions are assumed. Source term for the area source module is the estimated flux to the ground water table (in Bq/year).

I–B.7.2.2. Area source module

The area under consideration is treated as a polar coordinate system with an angular resolution of 5 degrees (72 sectors) and a maximum number of 20 radii. Every area source (12 per distance band times up to 20 distances) is located at the top of the aquifer and the source strength is defined by the flux to the ground water. Steady state conditions are assumed. However, radioactive decay is considered as the transport velocity is rather low in the aquifer.

A simplified assumption has been used which replaces the area source by a single source point in the centre of the area, with a given initial widening of the plume. This method presents the least difficulties in programming combined with an acceptable accuracy.

The sigma parameterisation was adapted to the aquatic conditions and the following equations were used for defining the dispersion parameters:

$$\sigma_z = \sqrt{2D_z x}$$

$$\sigma_y = \sqrt{2D_y x}$$

where:

σ is the sigma in y and z direction;
D is the diffusivity in y and z direction; and
x is the distance from the source point.

The transport velocity was set to a constant value all over the aquifer.

I–B.7.2.3. Application of the model to BIOMASS scenarios

Scenario 1: As the present model originates from atmospheric applications, parameters have been adapted for the use of such Gaussian type models in the aquatic media. This adaptation contains mainly the parameters diffusivity and transport velocity. The diffusivity D in horizontal direction was set to 5 and 0.5 for the high and low diffusivity case, respectively. The values for the vertical diffusivity were estimated to 0.5 and 0.05 for the two cases. The average transport velocity was set to 42 m a^{-1}.

The Gaussian transport equations were solved for various depth in the aquifer. Steady state conditions were assumed.

References

[1] RASKOB, W., Description of the Tritium Model NORMTRI for Releases under Normal Operation Conditions, Report KfK-5364, Kernforschungszentrum Karlsruhe, (1994). /RAS94/

I–B.8. MODELS USED BY ZSR, UNIVERSITY OF HANNOVER, GERMANY

M. Täschner

I–B.8.1. Soil model

The ZSR model is an analytical approach to simulate the one–dimensional vertical transport of tritium through a column of unsaturated soil. It was developed by M. Täschner and C. Bunnenberg for scientific purpose to study the effects of different boundary conditions (e.g. location of the tritium source) and of changes in soil parameter values (e.g. porosity, moisture content, hydrodynamic dispersivity, pore water velocity) on the exchange of tritium between the soil surface and the atmosphere. The model deals with bare or vegetated soils considered as isothermal and homogeneous over the whole extent of the soil column.

I–B.8.1.1. Structure of the model

The model is an application of Bear's formula (Bear 1972), with a modified hydrodynamic dispersion parameter D to apply for the variety of pore water velocities within the soil column. Bear's formula is a time-dependent analytical solution of the one-dimensional convective-dispersive system that represents the movement of tritium in an unsaturated soil layer. To use the formula the following parameters have to be defined: pore water velocity (amount and direction), hydrodynamic dispersivity (fixed at 0.05 m for Scenario 2) and the source of tritium (strength and location).

At the ground water table the advective transport of tritium from the groundwater to the unsaturated soil is governed by the infiltration flux and is taken to determine the pore water velocity to drive Bear's solution. But as it applies to a semi-infinite homogeneous soil column and to a constant water flux through the whole column, that solution cannot treat correctly the limited soil column with different conditions at the top and the bottom. The water flux at the soil surface is rather vivid due to precipitation and evapo-transpiration compared to the slow water flux at the groundwater table. To represent the conditions of the whole soil column, the hydrodynamic dispersion parameter is assumed to be governed by the average of the precipitation and the infiltration flux rather than by the infiltration flux itself (as it is with Bear's formula).

The results of the application of the modified Bear's formula are the profiles of tritium concentration in the soil. These profiles are given at fixed dates (e.g. at the end of months) and are used to calculate the fluxes of tritium from the soil to the atmosphere (e.g. as monthly averages).

I–B.8.1.2. Moisture flow

The soil moisture flow through the unsaturated zone is not treated in this model. Data on the movement of soil water (precipitation, evaporation and transpiration in case of vegetated soil), which have to be supplied from elsewhere, are used to calculate the pore water velocities as ratios of the flux of soil water and the average moisture content. The soil moisture of the soil column is calculated at steady state (i.e. no loss or gain of soil water at soil surface or at ground water table) with help of the Van Genuchten expression (Van Genuchten, 1980) and is averaged for ZSR modelling between groundwater table and soil surface.

The hourly data provided for precipitation, evaporation and transpiration are compressed into (e.g. monthly) averaged fluxes The infiltration flux is considered to be the difference of the precipitation and the combined evapo-transpiration flux, i.e. there is no surface run-off.

I–B.8.1.3. Tritium transport in soil

According to Scenario 2 tritium penetration into the soil water starts with the contact to contaminated ground water by the beginning of the year of simulation. The HTO profiles at the end of each month are calculated with averaged water fluxes determined cumulatively by summing the infiltration or precipitation amount from the beginning of the year when the contamination started to the end of the respective month and dividing by the time interval from the start of the contamination.

The profiles are calculated with Bear's formula, in which the dispersion term depends on molecular diffusion, but mostly on mechanical dispersion imputable to irregularities of the flow patterns. The dispersion is characterized by the coefficient $D = D_{\text{mol}} + \alpha v$, where D_{mol} is the molecular diffusion coefficient, α is the dispersivity and v is the absolute value of pore water velocity. According to ZSR modelling the effective pore water velocity, which represents the whole column with respect to hydrodynamic dispersion during the time of contamination, is calculated as the ratio of the averaged soil water flux (i.e. the average of the cumulative precipitation and the infiltration fluxes) and the average moisture content.

The advective transport of tritium at the ground water table into the unsaturated soil column is assumed to be governed by the infiltration flux. Note, that the infiltration flux may be negative, when capillary rise of ground water occurs. In times of ground water recharge the infiltration flux is positive and tritium from the ground water can enter the soil column only by dispersion.

I–B.8.1.4. Tritium transport from soil to atmosphere

To determine the monthly fluxes of tritium from the soil to the atmosphere, the HTO profiles are calculated at the end of each month of the year of simulation. The HTO concentration of the released soil water by evaporation and transpiration is estimated according to these profiles. It is assumed to have the same concentration as the soil water at an appropriate depth. This depth is determined by the thickness of a soil layer containing an equal amount of water that is lost to the atmosphere during the month.

I–B.8.2. Groundwater model

The transport of tritium in groundwaters is modelled at ZSR by M. Täschner and C. Bunnenberg by using an time-dependent analytical approach. The vertical transport is described according to a solution of Bear (Bear 1972) of the one-dimensional convective-dispersive system. The lateral dispersion is neglected, but the longitudinal transport is considered. The ZSR model was developed for scientific purpose, to provide a different method apart from numerical models to study the effect of different boundary conditions (e.g. constant concentration or constant flux at the groundwater table) and changes in aquifer parameter values (e.g. porosity, hydrodynamic dispersivity, pore water velocity).

Scenario 1 assumes uncontaminated soil and groundwater initially and uptake of tritium from the atmosphere. Therefore, the concentration gradient in the soil water is highest downwards and Bear's formula is used to calculate the vertical profiles at points of interest at different times. His formula applies to constant concentration conditions at the groundwater table and the result is the function $C(x,z,t)$, the HTO concentration of the groundwater at the distance x form the stack, at the depth z below the groundwater table, at time t after the arrival of the tritium front at the groundwater table. The following parameters have to be defined: the vertical pore water velocity, v_z = 0.5 m a^{-1}, (derived from infiltration rate and porosity), hydrodynamic dispersivity, A_z = 0.5 m (or A_z = 0.05 m, in case of low dispersivity), and the effective dispersion coefficient for the vertical transport in the aquifer, $D = D_{\mathrm{mol}} + A_z\, v_x$, where D_{mol} is the molecular diffusion coefficient of HTO in soil (about 0.04 m^{-2} a^{-1}), and v_x = 42 m a^{-1} is the quasi-horizontal longitudinal pore water velocity. The value of D is about 21 m^2 a^{-1} (or 2.1 m^2 a^{-1} with low dispersivity).

During the dispersive movement of tritium into deeper layers of the aquifer there is an increasing effect of the longitudinal flow within the aquifer. In order to estimate the effect of the longitudinal transport, an appropriate point of infiltration in the upstream direction is determined that is related to the depth of the respective layer of the aquifer. For that purpose a theoretical concentration profile $C_t(z,t)$ is calculated according to:

$$C_{\mathrm{t}}(z,t) = \frac{1}{2}\ \mathrm{erfc}\left[\frac{(z - v_z\, t)}{\sqrt{4 D t}}\right] + \frac{1}{2}\ \exp\left[\frac{v_z\, z}{D}\right] \mathrm{erfc}\left[\frac{(z + v_z\, t)}{\sqrt{4 D t}}\right]$$

which is the concentration profile of a non-decaying substance that is dispersed within the aquifer in the same way as tritium. The difference of the $C_t(z,t)$ profile to the $C(x,z,t)$ profile is attributed to the decay of tritium (with λ = 0.056 a^{-1}, the decay constant) and is used to define an effective travel time $t_{\mathrm{eff}}(z,t)$:

$$t_{\mathrm{eff}}(z,t) = -\ln\left[\frac{C(x,z,t)}{C_0(x) \cdot C_{\mathrm{t}}(z,t)}\right] \cdot \frac{1}{\lambda}$$

where $C_0(x)$ is the tritium concentration of the infiltrating soil water given in the scenario description. The related point of infiltration to the depth z is located at a distance of $v_x \cdot t_{\mathrm{eff}}(z,t)$ in the upstream direction. Finally, the corrected vertical profile of tritium in the aquifer at the distance x from the stack, $C_{\mathrm{corr}}(x,z,t)$, is given by:

$$C_{\mathrm{corr}}(x,z,t) = \frac{C(x,z,t)}{C_0(x)}\, C_0(x - v_x\, t_{\mathrm{eff}})$$

and is reported as result of the ZSR model.

A different boundary condition can be considered: constant tritium flux at the groundwater table. The profiles are calculated according to an analytical solution taken from Parlange and Starr (1978) (reported in: van Genuchten, 1980) and are corrected for the longitudinal transport in the same way as described above.

References

[1] BEAR, J., Dynamics of Fluids in Porous Media. Elsevier, New York (1972).

[2] VAN GENUCHTEN, M.Th., A closed form equation for predicting the hydraulic conductivity of saturated soils, J. Soil Sci. Soc. Am. **44** (1980) 892–898.

I–B.9. SOIL MODEL USED BY JAERI, JAPAN

H. Yamazawa

SOLVEG, developed by H. Yamazawa and H. Nagai, is originally a ground surface model for simulating surface-atmosphere exchange of physical quantities of meteorological interest such as momentum, heat, water vapour and solar radiation and atmospheric radiation. It has a soil part, a vegetation part and an atmospheric part, each being connected with others rather loosely. The atmospheric part is linked with a separate atmospheric model PHYSIC. In the application to Scenario 2, only the soil part is used. The soil part calculates movement of liquid water, water vapour and heat, and output vertical profile of volumetric water content, specific humidity of soil air and temperature. This model was extended to include tritiated water transfer in unsaturated surface soil layer. Transfer in both gas and liquid phases are considered.

I–B.9.1.1. Structure of model

The model is a one-dimensional multi-layer model with prognostic equations. This version of model has five one-dimensional prognostic equations for liquid water, water vapor in soil pore, temperature, and HTO concentrations in liquid and gas phases. These equations are numerically solved with a finite difference scheme. This scheme is semi-implicit in time for diffusion terms. The advection term in the conservation equation for liquid HTO is solved with a low-numerical-diffusion scheme.

Initial conditions and boundary conditions are externally given as input data. The ground surface boundary condition of the soil model is a time series of wind, temperature, humidity, solar radiation, atmospheric radiation and precipitation. These data are either observed data or predicted values by the atmospheric model. With these input data, the soil model returns various fluxes at the ground surface, which are physically consistent with calculated profiles of physical quantities in soil. An optional function was newly added to the model for the present simulations to enable model executions with inputs of evaporation and transpiration data. With this option, the model calculates sensible heat flux, conductive heat flux (temperature profile in soil), and other quantities so that they altogether keep mass and heat balances at the ground surface. The transfer of HTO is calculated in the similar manner as for liquid water and water vapor. Transport equations for gas HTO and liquid HTO are solved in parallel with other prognostic equations.

I–B.9.1.2. Moisture flow

A one-dimensional Richard's equation is used with volumetric water content η_w in m^3/m^3 as dependent variable and depth z and time t as independent variable. The equation has sink/source terms expressing exchange with water vapor in soil pore (evaporation/condensation) and root-uptake loss due to transpiration, which is always zero in the non-vegetated simulations. A water balance equation specifies the boundary condition at the ground surface. A constant volumetric water content is given at the bottom. The soil moisture characteristic used is of van Genuchten type or Clapp-Hornberger type. The former is used in the present simulations with parameters given in the scenario description.

The model has additional equations for specific humidity of soil air q_s (kg/kg) and soil temperature T_s (K). Both are in the form of one-dimensional diffusion equation. Boundary conditions are specified by continuity of water vapor flux and balance of heat at the ground surface, respectively, together with the meteorological input data. Although this inclusion of temperature effect, in addition to the inclusion of gas phase HTO diffusion, is not strictly along with the scenario's demand, its effect is thought to be small as shown in the results of related simulations, in which gas diffusion was pointed out to be less significant in determining concentration profile and evapo-transpiration of HTO as compared with liquid phase diffusion, dispersion and advection.

I–B.9.1.3. Tritium transport

Transport of HTO is expressed by a combination of a one-dimensional advection-diffusion equation for HTO concentration in liquid phase χw (Bq/m3 water) and a one-dimensional diffusion equation for HTO concentration in gas phase χs (Bq/m3 air). They are linked to each other with a source/sink term expressing evaporation/condensation of HTO. The liquid phase HTO equation contains advection (convection), dispersion and diffusion, while the gas phase HTO equation has gas diffusion only. The advection and the dispersion are solved in parallel with the moisture calculations.

Evaporation of HTO at the ground surface is expressed by a bulk formula:

$$F_\chi = C_\chi u \cdot \left(\chi_{sfc} - \chi_a\right)$$

where χ_{sfc} and χ_a are HTO concentrations at the ground surface and the atmosphere, respectively, Cχ the bulk coefficient of HTO exchange, which is assumed to be identical with that of water vapor and a function of the atmospheric stability and the roughness length scales, and u the wind speed. This equation forms a boundary condition for the gas phase HTO diffusion equation. In the simulation for the vegetated scenario, transpiration rate of HTO is simply assumed to be proportional to the transpiration rate given in the provided data file and to the concentrations of HTO in soil water taken up by vegetation.

I–B.9.1.4. Application of the model to BIOMASS scenarios

The 1 m thick soil layer were evenly divided into 200 layers, each being 5 mm thick. The time increment was 2 seconds, although it might be unnecessarily short when soil is dry. The initial condition and the bottom boundary condition were set as described in the scenario. The values of hydraulic parameters, dispersion coefficient and diffusion coefficient were also taken from the scenario description. It was assumed in the calculation of bulk coefficient of air-surface exchange that the roughness length was 0.23 mm for wind and 0.0115 mm for other passive scalars. The evaporation and transpiration rates provided with the scenario were used to drive the model, by switching off the model's original function of calculating them.

References

[1] KONDO, J., SAIGUSA, N., Modelling the evaporation from bare soil with a formula for vaporization in the soil pores, J. Meteor. Soc. Japan **72** (1994) 413–421.

[2] NAGAI, H., YAMAZAWA, H., Development of one-dimensional atmosphere-soil-vegetation model, JAERI-Data/Code 99-024 (1999) (in Japanese).

[3] YAMAZAWA, H., Development of a Numerical Solution Method for Advection Terms and its Application to the Atmospheric Dynamic Model, PHYSIC, J. Nucl. Sci. Tech., **33** (1996) 69–77.

[4] YAMAZAWA, H., NAGAI, H., Development of one-dimensional bare soil model, JAERI-Data/Code 97-041 (1997) (in Japanese).

[5] YAMAZAWA, H., Numerical Study on Soil-Atmosphere Tritiated Water Transfer, Proceedings of International Workshop on the Environmental Behavior of Tritium, Kumatori, Japan, May 8-9 (2000).

ANNEX II

TRITIUM WORKING GROUP SCENARIO DESCRIPTIONS

ANNEX II–A
SCENARIO 1.3 DESCRIPTION

Modelling of the steady-state behaviour of tritium in the environment when atmospheric releases are assumed to be on average nearly constant and a steady-state equilibrium has been reached

History

Scenario 1.3 drafted by Y. Belot (Working Group Leader, Consultant, France) and B. Watkins TWG (Technical Secretariat, QuantiSci Limited, United Kingdom), June 1998.

Scenario 1.2 drafted by Y. Belot (Working Group Leader, Consultant, France) and B. Watkins TWG (Technical Secretariat, QuantiSci Limited, United Kingdom) to incorporate changes agreed by WG participants at Plenary meeting in Vienna, October 1997.

Scenario 1.1 drafted by Y. Belot (Working Group Leader, Consultant, France) and B. Watkins TWG (Technical Secretariat, QuantiSci Limited, United Kingdom) to incorporate agreed revisions following Cadarache meeting.

Working Group Meeting, Cadarache, France, 22–24 April 1997: Y. Belot (Working Group Leader, Consultant, France). Discussion of scenario description by WG participants. For information on meeting participants, see: IAEA (1997), Notes of BIOMASS Theme 3 Tritium Working Group Meeting, Cadarache, 22–24 April, 1997.

Scenario 1.0 drafted. See IAEA (1996). International Programme on Biosphere Modelling and Assessment Methods (BIOMASS). Theme 3: Biospheric Processes. Tritium Working Group Scope, Objectives and Approaches. 1996-12-20. IAEA, Vienna.

II–A.1. INTRODUCTION

Scenario 1.0 initially provided in IAEA (1996), was first amended to version 1.1 after the 1997 Spring Working Group (WG) meeting, and to version 1.2 after the 1997 Autumn meeting. At the 1998 Spring WG meeting in Deep River (Canada), it was observed that the most sensitive part of the modelling approach was in the evaluation of the accumulation of tritium in the soil. Appreciable differences were obtained in estimates of tritium concentrations in soil water and tritium fluxes at the water table. In consequence, the vertical profiles of tritium concentrations in the aquifer were also different, and the corresponding sub-models could not be easily compared.

It was decided to further revise the scenario description (version 1.3) with the objectives of: (i) continuing to investigate on the best way to model the transport of tritium from a stack to the terrestrial environment; (ii) intercomparing the hydraulic part of the models by starting from a common average source term at the watertable (see Annex II–E).

II–A.2. SCENARIO DESCRIPTION

II–A.2.1. Atmospheric Pathway

A stack of 60 m height emits tritium as tritiated water or tritiated hydrogen, each form at the rate of 1 g tritium per year. The average humidity of atmosphere is assumed to be 0.01 kg m^{-3}. The windrose is uniform in all directions. The frequency of weather categories is shown in Table II–A.1 and is independent of wind direction. The total annual precipitation is 750 mm per year and rain is assumed to occur 10% of the time under stability class D, independently of wind direction. The atmospheric dispersion calculation should be made over a range of 10 km, using 30° wind sectors and dispersion parameters taken from Briggs (see Table II–A.2). The wind speed at source height should be calculated from the wind speed at 10 m given in Table II–A.1 by using the following relationship:

$$u(z) = u_{10}\,(z/10)^n$$

where n equals 0.2, 0.2, 0.2, 0.3, 0.5, 0.7 for the stability categories A, B, C, D, E, F respectively. The roughness length is 0.3 m. The washout coefficient is 6×10^{-5} per second for 1 mm rain per hour. The average dry deposition rate is assumed to be 3×10^{-3} m s^{-1} for HTO and 3×10^{-4} m s^{-1} for HT. It is assumed that soil concentrations in the 360° area of radius 0.5 km around the stack are uniform and the same as those at the 0.5 km point from the stack. The plume depletion due to wet or dry deposition is taken to be negligible at the downwind distances considered.

TABLE II–A.1. METEOROLOGICAL DATA

Pasquill Category	Frequency %	Wind Speed m s^{-1}
A	1	1
B	6	2
C	10	5
D	56	5
E	10	3
F	17	2

TABLE II–A.2. BRIGG'S FORMULAS

Class A	$\sigma_z = 0.20x$
Class B	$\sigma_z = 0.12x$
Class C	$\sigma_z = 0.08x / (1+0.0002x)^{1/2}$
Class D	$\sigma_z = 0.06x/ (1+0.0015x)^{1/2}$
Class E	$\sigma_z = 0.03x / (1+0.0003x)$
Class F	$\sigma_z = 0.016x / (1+0.0003x)$

II–A.2.2. Aquatic Pathway (see also Annex II–E)

The calculation of tritiated water in groundwaters start from an average flux to groundwater surface defined as follows. The flux at the water table should be supposed to be a function of distance x (km) from the stack, everywhere around the stack. The flux F is equal to 2 × 10^4 Bq m^{-2} y^{-1} for $x \leq 0.5$ km, and is inversely proportional to x at larger distances, according to the expression:

$$F(Bq\ m^{-2}\ y^{-1}) = \frac{10^4}{x(km)}$$

The total infiltration rate (or recharge rate) is 150 mm per year. The horizontal extension of the unconfined aquifer is 10 km from the flow divide to the stream. The stack is placed at the midpoint between the divide and the stream (i.e. at 5 km from each) (as shown in Figure II-E.1). The groundwater zone has a permeability of 1 × 10^{-4} m s^{-1}; a porosity of 30%; a longitudinal dispersivity A_x = 50 m; a transverse dispersivity A_y = 5 m; and a vertical dispersivity A_z = 0.5 m.

Calculations can be made by using relatively complex finite element models that simulate the groundwater flow and tritium transport in the aquifer. In this case the data given above are sufficient to perform calculations of the water and tritium transport over the whole extension of the aquifer from the flow divide to the receiving stream.

Calculations can also be made in a more simple way by using analytical models of the Gaussian type. In this case, the water flow in the aquifer has to be approximated by assuming that the flow is nearly uniform within a zone of 3 km radius centred on the stack with a longitudinal pore water velocity of about 42 m y^{-1} and a hydraulic head (aquifer thickness) of 59 m, which have been calculated at the vertical of the stack.

II–A.3. ENDPOINT CALCULATIONS

The requested calculational endpoints are average concentrations of tritium expressed in Bq per litre of real water, or in Bq per litre of equivalent water (combustion water) in the case of plant organic matter. This concerns only tritium in the form of tritiated water (HTO).

For endpoints concerned with tritium concentrations in terrestrial media associated with the atmospheric release (e.g. air humidity, soil water, plant TFWT), calculations should be provided for distances of 0.5 km, 0.6 km, 0.7 km etc. up to 1 km and then every km up to

10 km. The atmospheric water should be given at 1.5 m height; the soil water should be averaged over the top 0.2 m depth.

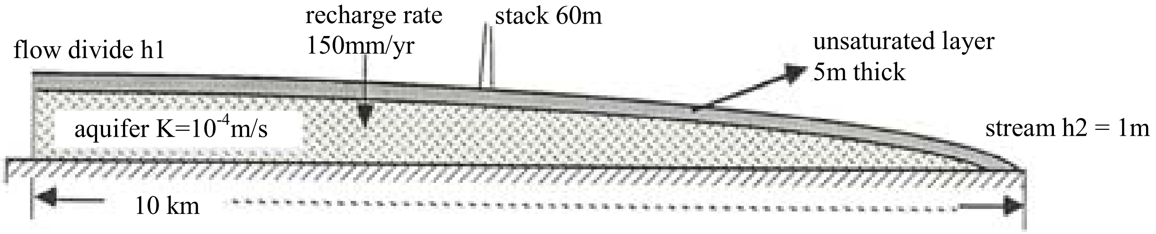

Unconfined aquifer with the bottom resting on a horizontal impervious surface and the top coinciding with the water table

FIG. II–A.1. Diagrammatic representation of Scenario 1.3.

References

[1] GIFFORD, S.A., The turbulent diffusion typing schemes: a review, Nuclear Safety **17** 1 (1976) 68–86.

[2] INTERNATIONAL ATOMIC ENERGY AGENCY, International Programme on Biosphere Modelling and Assessment Methods (BIOMASS), Theme 3: Biospheric Processes, Tritium Working Group Scope, Objectives and Approaches. 1966-12-20 IAEA, Vienna (1996).

[3] INTERNATIONAL ATOMIC ENERGY AGENCY, Notes of BIOMASS Theme 3 Tritium Working Group Meeting, Vienna, 20–24 October 1997, IAEA, Vienna (1997).

[4] INTERNATIONAL ATOMIC ENERGY AGENCY, Notes of BIOMASS Theme 3 Tritium Working Group Meeting, Deep River, Canada, 13–15 May 1998, IAEA, Vienna (1998).

ANNEX II–B
SCENARIO 3.0 (CRL) DESCRIPTION

History

Scenario 3.0 (CRL), Version 1.0. Addendum of additional data and information, issued November 1998.

Scenario 3.0 (CRL), Version 1.0. Issued in June 1998 for discussion at Tritium Working Group Plenary Meeting, October 1998, Incorporates comments on Version 0.1.

Scenario 3.0 (CRL), Version 0.1. Scenario drafted by P.A. Davis (AECL, Canada) and distributed for comment following BIOMASS Theme 3 Tritium Working Group Spring Meeting 1998.

Scenario 3.0 (CRL), Outline scenario proposed by P.A. Davis (AECL) at Tritium Working Group Spring 1998 Meeting.

II–B.1. BACKGROUND

The environment surrounding Chalk River Laboratories (CRL) contains trace amounts of tritium due to routine releases of HTO from reactor facilities and waste management areas. These releases have been going on for many years and concentrations in various parts of the environment are likely to be in equilibrium. Tritium concentrations in air, vegetation and soil were collected twice daily on selected days over a 2-month period in the summer of 1995 at three locations on the CRL site. Hourly measurements of various meteorological parameters were made throughout the period. The data are offered here as a test of models that predict the long-term average tritium concentrations in the environment due to chronic atmospheric releases.

II–B.2. SITE DESCRIPTION

General: CRL is located in the valley of the Ottawa River (Figure II–B.1). The laboratory complex contains about 100 buildings spread over an area of 0.5 km^2 on the southwest bank of the river. Terrain height increases away from the river with low ridges 80 m high running roughly parallel to the shore. Most of the vegetation is mixed forest with tree heights of about 30 m. Soils in the area tend to be sandy with porosities of about 38%.

Tritium Release Points: HTO is released to the atmosphere from three main locations on the CRL site: by direct emission from the NRU reactor building and the 46 m reactor exhaust stack and by evapotranspiration from a lake (Perch Lake) and wetland contaminated by leakage of tritium from a waste management area (Figure II–B.1). Release rates are typically 5×10^{13} Bq a^{-1} from each of the reactor and stack and perhaps 1×10^{13} Bq a^{-1} from the lake and wetland combined.

Environmental Measurement Locations: Tritium concentrations were measured at three locations in the summer of 1995 (Figure II–B.1). The Acid Rain Monitoring Site (ARS) is located 2 km northwest of the reactor stack in a hydro right-of-way about 100 m wide cut through the surrounding forest. Air concentrations at this location are dominated by releases from the stack and, to a lesser extent, from the reactor building. Perch Lake Satellite Station (PL) is located in a meadow about 100 m in diameter on the east shore of Perch Lake. It receives most of its airborne tritium from the lake and wetland. The third sampling site (B600) was located just north of Building 600, a 20 m by 50 m building in the laboratory complex. The terrain is open for the first 150 m from B600 toward NRU but buildings occupy the remaining distance. Air concentrations at B600 are dominated by releases from the reactor building. The local vegetation at ARS and PL is a mixture of natural grasses. At B600, the grass is tended but was left uncut in the sampling area itself. The distances and directions of the sampling sites from the three release points are shown in Table II–B.1.

TABLE II–B.1. DISTANCES AND DIRECTIONS OF THE THREE SAMPLING LOCATIONS FROM THE THREE RELEASE POINTS

	Distance (km) from			Direction from		
	Stack	NRU	Lake	Stack	NRU	Lake
Acid Rain Site	2.2	2.9	3.3	115°	107°	146°
Perch Lake Satellite Station	2.3	2.4	0	348°	011°	316°
Building 600	1.1	0.45	1.7	287°	330°	216°

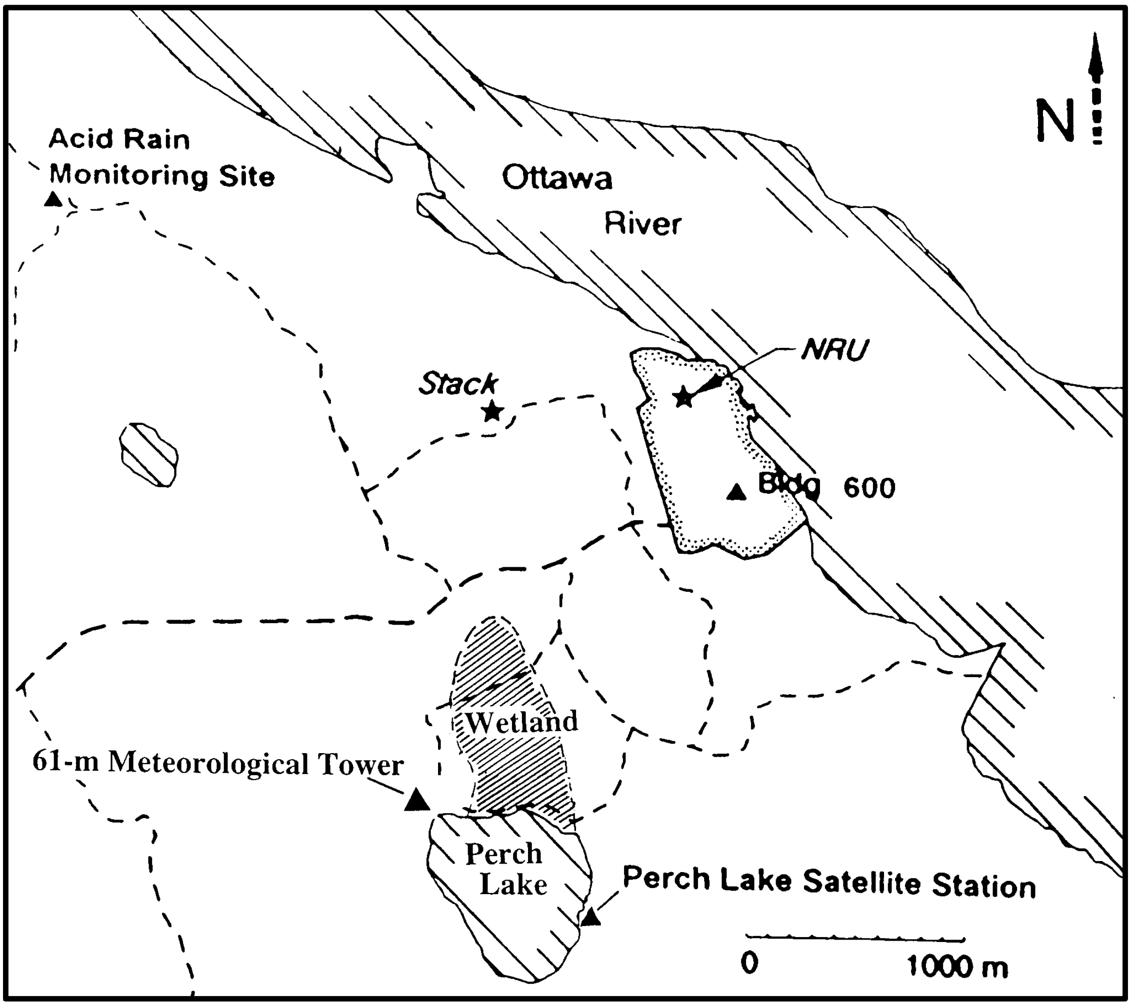

FIG. II–B.1. Location of tritium sources and sampling sites at CRL.

II–B.3. TRITIUM MEASUREMENTS

Air: HTO samples in air were collected 0.5 m above ground at each site with small, portable, active samplers. Air was drawn by a pump through a calibrated flowmeter at a rate of about 90 mL min^{-1} and passed through scintillation vials containing 10 mL of tritium-free water. The tritium concentration in the water was determined by liquid scintillation counting (LSC), taking into account the sampler efficiency and the small amount of water lost from the vial during sampling. Average air concentrations were measured over the time periods 0900–1500 and 1500–0900 each day (Table II–B.2). Daily average concentrations (0900–0900) were determined from these measurements and are included in Table II–B.2. Average concentrations over the entire period of study were 3.54 Bq m^{-3} at ARS, 19.3 Bq m^{-3} at B600 and 8.67 Bq m^{-3} at PL. Uncertainties in the concentrations arise due to counting errors and to uncertainty in determining the volume of air sampled. The total uncertainties in the air concentrations are estimated to be less than 10% in most cases but could reach 20% for some of the lower concentrations.

Vegetation: Approximately 20 g of grass were collected at 0900 and 1500 at each of the three sampling sites. The samples were composites formed by taking subsamples at 3 or 4 random locations within 5 m by 5 m plots. The free water was extracted from the samples by azeotropic distillation with toluene and the tritium concentration determined by LSC. Counting errors for the grass samples were generally less than 5%, although replicate samples would likely have shown larger differences because of natural variability. A few grass samples were oven-dried to remove their free water, washed with dead water to remove exchangeable OBT and then analysed for their fixed OBT concentration using ^{3}He mass spectrometry.

The grass at B600 was identified as upland bent grass (*Agrostis perennans* (Walt.) Tuckerm). This grass was also sampled at PL, along with the rush *Juncus tenuis* Willd. At ARS, the sampled species were witch or couch grass (*Agropyron repens* (L.) Beauv.) and an unidentified grass. Water contents of the samples ranged between 50 and 75% of fresh weight at ARS and B600, and between 60% and 75% at PL.

Soil: Soil cores were taken at 0900 at two of the three sampling sites each day on a rotating basis. Three 10-cm cores were collected within 5 m by 5 m plots and composited. The soil water was extracted from the samples by azeotropic distillation with toluene and the tritium concentrations determined by LSC. Counting errors were generally less than 10% but, as with grass, concentrations in replicate samples would differ by 20% or so because of natural variability. Soil moisture contents in early June were 10.3% of wet weight at ARS, 12.9% at B600 and 21% at PL. The first soil cores taken in the study showed concentrations of 94 Bq/L at ARS, 230 Bq/L at B600 and 139 Bq/L at PL.

Precipitation: Precipitation is collected at ARS but the rain that fell during the study period was not analysed for its tritium content. However, long-term average HTO concentrations in air and precipitation are routinely measured at site MR, which is located 5.8 km and 122^{o} from the stack (6.6 km and 117^{o} from NRU). MR and ARS are thus roughly colinear with the main tritium release points and the ratio R_{PA} of HTO concentration in precipitation to that in air should be approximately equal at the two sites. Precipitation at MR is collected in a bucket under an oil layer and analysed monthly by LSC for its tritium content to an accuracy of about 5%. Air concentrations are 3-month averages obtained using passive diffusion samplers and have an uncertainty of about 30%. The long-term average of R_{PA} at ARS can therefore be deduced to an accuracy of about 30%, but its value over the 2-month study period will contain additional uncertainty because of the different sampling interval used at MR.

TABLE II–B.2. HTO CONCENTRATIONS IN AIR (BQ M^{-3}) AT THE 3 SAMPLING SITES

Daytime (0900–1500)				Night-time (1500–0900)				24-h Average (0900–0900)			
Date	ARS	B 600	PL	Date	ARS	B 600	PL	Date	ARS	B 600	PL
June				June				June			
5	–	34.1	–	5–6	5.8	43.9	–	5–6	–	41.5	–
6	5.5	13.5	–	6–7	3.6	27.0	26.3	6–7	4.1	23.6	–
7	8.4	30.4	–	7–8	1.2	18.9	–	7–8	3.0	21.8	–
8	–	26.3	–	8–9	1.7	15.5	–	8–9	–	18.2	–
9	–	–	–	9–10	–	–	–	9–10	–	–	–
10	–	–	–	10–11	–	–	–	10–11	–	–	–
11	–	–	–	11–12	–	–	–	11–12	–	–	–
12	–	43.4	33.5	12–13	3.3	42.7	13.9	12–13	–	42.9	18.8
13	–	74.2	17.6	13–14	3.2	25.3	13.3	13–14	–	37.5	14.4
14	2.3	30.6	15.0	14–15	1.1	17.0	7.9	14–15	1.4	20.4	9.7
15	1.4	66.3	18.9	15–16	–	–	–	15–16	–	–	–
16	–	–	–	16–17	–	–	–	16–17	–	–	–
17	–	–	–	17–18	–	–	–	17–18	–	–	–
18	–	–	–	18–19	–	–	–	18–19	–	–	–
19	5.8	84.0	43.0	19–20	1.9	34.6	20.9	19–20	2.9	47.0	26.4
20	0.7	11.8	12.9	20–21	1.9	10.7	6.9	20–21	1.6	11.0	8.4
21	4.2	6.9	7.5	21–22	4.0	19.9	8.6	21–22	4.1	16.7	8.3
22	7.5	21.1	13.9	22–23	5.6	16.1	8.8	22–23	6.1	17.4	10.1
23	–	–	–	23–24	–	–	–	23–24	–	–	–
24	–	–	–	24–25	–	–	–	24–25	–	–	–
25	–	–	–	25–26	–	–	–	25–26	–	–	–
26	–	–	–	26–27	9.2	8.1	6.6	26–27	–	–	–
27	4.8	7.0	6.5	27–28	4.2	3.9	2.9	27–28	4.4	4.7	3.8
28	3.6	7.2	5.4	28–29	2.5	3.8	3.4	28–29	2.8	4.7	3.9
29	3.4	7.1	7.1	29–30	6.1	11.2	4.7	29–30	5.4	10.2	5.3
30	–	–	–	30–1	–	–	–	30–1	–	–	–
July				July				July			
1	–	–	–	1–2	–	–	–	1–2	–	–	–
2	–	–	–	2–3	–	–	–	2–3	–	–	–
3	–	–	–	3–4	–	–	–	3–4	–	–	–
4	–	–	–	4–5	–	–	–	4–5	–	–	–
5	7.6	9.9	7.5	5–6	5.8	4.6	2.4	5–6	6.3	5.9	3.7
6	4.3	8.0	2.0	6–7	2.3	12.0	4.5	6–7	2.8	11.0	3.9
7	–	–	–	7–8	–	–	–	7–8	–	–	–
8	–	–	–	8–9	–	–	–	8–9	–	–	–
9	–	–	–	9–10	–	–	–	9–10	–	–	–
10	3.0	6.6	9.6	10–11	8.5	16.2	2.9	10–11	7.1	13.8	4.6
11	–	28.4	19.5	11–12	1.7	21.3	9.6	11–12	–	23.1	12.1
12	1.5	–	8.0	12–13	5.0	15.9	4.4	12–13	4.1	–	5.3
13	8.9	4.1	15.4	13–14	2.1	22.8	15.3	13–14	3.8	18.1	15.3
14	–	–	–	14–15	–	–	–	14–15	–	–	–
15	–	–	–	15–16	–	–	–	15–16	–	–	–
16	–	–	–	16–17	–	–	–	16–17	–	–	–
17	–	–	–	17–18	–	–	–	17–18	–	–	–
18	3.8	26.0	10.3	18–19	1.6	23.5	9.1	18–19	2.2	24.1	9.4
19	1.8	41.4	15.3	19–20	3.0	9.6	6.2	19–20	2.7	17.6	8.5
20	4.4	–	4.3	20–21	2.5	31.5	7.1	20–21	3.0	–	6.4
21	–	–	–	21–22	–	–	–	21–22	–	–	–
22	–	–	–	22–23	–	–	–	22–23	–	–	–
23	–	–	–	23–24	–	–	–	23–24	–	–	–
24	4.4	14.2	10.8	24–25	2.6	21.2	3.1	24–25	3.1	19.5	5.0

TABLE II–B.2. (CONTINUED)

Daytime (0900–1500)				Night-time (1500–0900)				24-h Average (0900–0900)			
Date	ARS	B 600	PL	Date	ARS	B 600	PL	Date	ARS	B 600	PL
July				July				July			
25	5.4	13.1	5.4	25–26	3.6	23.7	4.5	25–26	4.1	21.1	4.7
26	2.4	–	9.2	26–27	1.2	22.7	7.2	26–27	1.5	–	7.7
27	2.5	14.9	10.4	27–28	4.3	13.1	4.5	27–28	3.9	13.6	6.0
28	–	–	–	28–29	–	–	–	28–29	–	–	–
29	–	–	–	29–30	–	–	–	29–30	–	–	–
30	–	–	–	30–31	–	–	–	30–31	–	–	–
31	3.6	12.1	11.9	31–1	1.9	29.4	3.9	31–1	2.3	25.1	5.9
Aug				Aug				Aug			
1	2.1	11.0	6.9	1–2	0.6	10.4	4.3	1–2	1.0	10.6	5.0
2	1.3	3.9	3.3	2–3	2.9	4.7	1.5	2–3	2.5	4.5	1.7
3	1.5	3.1	1.3	3–4	–	–	–	3–4	–	–	–
4	–	–	–	4–5	–	–	–	4–5	–	–	–
5	–	–	–	5–6	–	–	–	5–6	–	–	–
6	–	–	–	6–7	–	–	–	6–7	–	–	–
7	–	–	–	7–8	–	–	–	7–8		–	–
8	–	–	–	8–9	–	–	–	8–9	–	–	–
9	6.8	9.1	6.2	9–10	2.5	7.2	–	9–10	3.6	7.7	–
10	6.0	9.2	–	10–11	–	–	–	10–11	–		–

II–B.4. METEOROLOGICAL MEASUREMENTS

Meteorological data were collected throughout the study at Perch Lake Satellite Station. The measurements made, the instruments used to obtain them, and the measurement heights are summarized in Table II–B.3. Signals from all instruments were sampled at 0.1 Hz and averaged to give hourly means. The data for June 3 are shown in Table II–B.4 and data for the entire study period are contained in file HourMet.xls on diskette. The hourly data were averaged over the air sampling periods (0900–1500 and 1500–0900; Tables II–B.5 and II-B.6; files DayMet.xls and NightMet.xls), over 24-hour periods beginning at 0900 each day (Table II–B.7; file 24HMet.xls) and over the entire duration of the study (Table II–B.8). Note that wind direction and standard deviation in wind direction (σ_θ) have little meaning when averaged over periods longer than a few hours. It is likely that σ_θ was calculated without taking into account the discontinuous change that occurs between 0^o and 360^o, so that values of σ_θ are probably overestimates for wind directions near north.

Absolute humidity was not measured directly but was calculated hourly from the air temperature and relative humidity data measured at 0.5 m height and then averaged over daytime, night-time, 24-hour and full study periods.

Wind speed and direction measurements made at Perch Lake Satellite Station represent conditions close to the ground. Winds aloft (at the height of the reactor stack, for instance) can be quite different, especially at night when the atmosphere tends to become decoupled in the vertical. Accordingly, wind speed and direction measurements made 61 m above ground with Bendix-Friez anemometers on a tower at Perch Lake Main (Figure II–B.1) are also included in the meteorological data sets.

TABLE II–B.3. METEOROLOGICAL MEASUREMENTS AT PERCH LAKE SATELLITE STATION

Variable	Instrument	Measurement Height
Wind speed, wind direction, standard deviation in wind direction	R.M. Young Wind Monitor Model 5305	2.5 m
Air temperature, relative humidity	Vaisala, Model HMD 30YB	0.5 m, 1.5 m
Leaf temperature	Everest Infrared Thermometer Model 112 ALCS	Mounted at 1 m
Soil temperature	Campbell Scientific Thermistors, Model 107B	2 and 7 cm below soil surface
Net radiation	Middleton Net Radiometer Model CN-1	Mounted at 1 m

Rain that fell during the study was collected in a standard precipitation gauge near Building 600 and measured twice per day, at 0800 and 1600. Rainfall intensity was also measured at ARS with a Belfort recording gauge. However, signals from this instrument were output only on chart paper with coarse resolution. Hourly rainfall amounts were deduced by combining the information from these two gauges. The hourly data are likely accurate to no better than a factor of 2, although the uncertainty in the daily totals is only about 20%. Also, the timing of the rainfall events may be off by an hour or two. The rainfall data are included in the meteorological data sets. The joint frequency distribution of rainfall intensity and wind direction (as measured at the 61 m level of the meteorological tower) is shown in Table II-B.9.

All of the meteorological instruments were calibrated before the experiment. Uncertainties in the meteorological data were generally fairly low, on the order of 5-10%.

II–B.5. DATA ON DISKETTE

A diskette is available which contains the meteorological and tritium data specified below on Excel spreadsheets in the following files:

HourMet.xls - hourly meteorological data
DayMet.xls - meteorological data averaged over the period 0900-1500 each day
NightMet.xls - meteorological data averaged over the period 1500-0900 each day
24HMet.xls - meteorological data averaged over the period 0900-0900 each day
Trit.xls - tritium air concentrations at the three sampling sites for the daytime, night-time and 24-h periods.

Missing data are indicated by “M” in each file.

This diskette was distributed to participants at the Spring WG Meeting in Deep River in May 1998. Anyone else requiring a diskette should contact the Technical Secretariat at the address given below.

TABLE II–B.4. HOURLY METEOROLOGICAL DATA

Date	Time Sampling Ended	Wind Speed (m/s)	Wind Direction (true)	Standard Deviation in Wind Direction	1.5-m Relative Humidity (%)	1.5-m Air Temp. (C)	0.5-m Relative Humidity (%)	0.5-m Air Temp. (C)	Leaf Temp. (C)	2-cm Soil Temp. (C)	7-cm Soil Temp. (C)	Net Radiation (W/m2)	Rain (mm)	61-m Wind Speed (m/s)	61-m Wind Direction (true)
	Local Daylight Time														
3-Jun	100	0.03	99.2	28.8	100.1	16.1	100.7	15.8	14.7	15.3	15.1	-7.5	0.0	1.92	339.3
3-Jun	200	0.03	100.3	18.7	100.3	15.8	100.8	15.5	14.3	15.2	14.9	-6.4	0.0	1.25	12.5
3-Jun	300	0.05	87.3	20.4	100.4	15.6	100.9	15.3	14.1	15.0	14.8	-7.3	0.0	2.11	32.7
3-Jun	400	0.07	75.9	68.7	100.4	15.5	100.9	15.2	14.3	14.9	14.7	-7.0	0.0	2.39	30.6
3-Jun	500	0.04	51.7	70.7	100.4	15.5	100.9	15.2	14.6	14.9	14.6	-5.6	0.0	2.31	340.0
3-Jun	600	0.05	94.0	19.1	100.5	15.3	101.0	15.1	14.7	14.8	14.6	-4.5	0.0	1.22	39.5
3-Jun	700	0.03	105.9	78.5	100.5	15.3	101.0	15.1	14.9	14.8	14.5	-1.7	0.0	3.03	31.6
3-Jun	800	0.13	129.7	81.2	100.2	15.6	101.0	15.4	15.8	14.9	14.5	18.8	0.0	4.11	28.2
3-Jun	900	0.27	40.0	78.6	94.5	16.6	95.6	16.5	18.0	15.3	14.6	84.0	0.0	3.22	20.5
3-Jun	1000	0.16	33.4	66.1	90.8	17.5	90.2	17.6	18.7	15.9	14.8	80.4	0.0	1.25	3.7
3-Jun	1100	0.24	27.1	73.4	93.0	17.4	92.5	17.4	18.1	15.9	14.9	60.6	0.0	2.28	348.1
3-Jun	1200	0.32	8.1	81.4	91.1	16.2	91.1	16.2	16.8	15.7	15.0	43.0	0.0	2.64	337.3
3-Jun	1300	0.26	45.4	95.2	90.3	15.9	90.5	15.8	16.7	15.6	14.9	49.7	0.0	3.19	354.8
3-Jun	1400	0.62	324.6	76.6	84.9	17.0	85.4	17.1	18.3	15.9	15.0	106.8	0.0	2.86	318.2
3-Jun	1500	0.64	1.9	90.6	72.0	19.7	71.8	20.1	23.9	17.1	15.2	346.9	0.0	2.17	39.2
3-Jun	1600	0.46	80.1	100.5	68.8	20.9	68.7	21.2	23.2	17.8	15.6	235.6	0.0	0.92	101.2
3-Jun	1700	0.26	121.4	84.4	67.9	21.6	67.7	21.8	22.4	17.9	16.0	175.5	0.0	0.69	101.0
3-Jun	1800	0.07	151.0	69.8	77.2	20.8	76.8	20.9	20.2	17.5	16.1	78.2	0.0	1.61	194.2
3-Jun	1900	0.11	205.5	59.7	78.6	20.7	78.6	20.7	19.4	17.3	16.1	59.4	0.0	1.72	239.4
3-Jun	2000	0.08	195.5	54.8	84.6	19.8	84.8	19.7	17.2	16.9	16.0	12.0	0.0	1.78	259.2
3-Jun	2100	0.34	103.8	9.6	95.1	17.4	94.8	17.1	12.2	16.1	15.8	-26.2	0.0	1.61	280.9
3-Jun	2200	0.30	103.9	14.1	99.0	15.5	99.2	15.1	9.5	15.1	15.5	-15.3	0.0	2.33	309.5
3-Jun	2300	0.30	114.0	30.0	100.0	14.2	100.3	13.8	7.9	14.5	15.1	-15.6	0.0	2.67	326.0
4-Jun	0	0.60	110.4	16.6	100.1	13.2	100.6	12.7	7.3	13.9	14.7	-15.7	0.0	4.47	46.2

TABLE II–B.5. METEOROLOGICAL DATA AVERAGED OVER THE DAYTIME PERIOD (0900–1500)

Date	Wind Speed (m/s)	Wind Direction (true)	Standard Deviation in Wind Direction	1.5-m Relative Humidity (%)	1.5-m Air Temp. (C)	0.5-m Relative Humidity (%)	0.5-m Air Temp. (C)	Leaf Temp. (C)	2-cm Soil Temp. (C)	7-cm Soil Temp. (C)	Net Radiation (W/m2)	Absolute Humidity (g/m3)	Rain (mm)	61-m Wind Speed (m/s)	61-m Wind Direction (true)
3-Jun	0.37	14.1	80.6	87.0	17.3	86.9	17.4	18.7	16.0	15.0	114.6	12.8	0.0	2.40	353.1
4-Jun	0.95	265.7	41.3	44.2	20.6	47.1	21.1	22.4	17.6	14.9	367.4	8.7	0.0	1.53	260.6
5-Jun	2.04	306.5	42.4	46.5	23.6	49.4	24.3	25.4	18.8	15.4	425.6	10.9	0.0	3.70	288.2
6-Jun	0.61	229.8	85.3	56.0	25.8	56.7	26.5	28.3	20.2	16.6	405.4	14.0	0.0	2.14	135.9
7-Jun	0.44	294.5	61.0	71.9	23.7	72.3	24.1	23.7	18.8	16.7	177.5	15.8	1.0	1.26	29.8
8-Jun	1.64	307.6	56.4	46.4	14.5	48.7	15.6	20.7	17.1	14.9	477.9	6.4	0.0	4.12	321.7
9-Jun	0.81	221.1	87.9	36.8	18.4	39.3	19.4	23.2	18.0	15.0	454.9	6.5	0.0	2.22	104.3
10-Jun	0.44	127.4	82.8	46.7	20.4	48.6	21.1	22.3	17.5	14.8	306.5	8.9	0.0	3.18	130.0
11-Jun	0.63	166.1	81.8	82.9	18.7	82.0	19.2	21.1	17.0	15.3	211.8	13.4	1.0	2.58	144.2
12-Jun	3.35	290.8	20.2	42.0	16.9	45.1	18.0	21.3	17.7	15.3	449.8	6.8	0.0	4.84	296.9
13-Jun	1.34	292.4	33.8	54.2	20.4	55.8	21.4	23.5	17.8	14.9	386.3	10.4	0.0	2.69	319.9
14-Jun	1.67	296.5	42.9	41.8	20.3	44.4	21.3	23.8	18.5	15.5	433.8	8.2	0.0	2.67	315.7
15-Jun	1.41	275.9	30.5	38.9	21.4	42.3	22.4	23.7	18.3	15.2	437.2	8.2	0.0	2.54	281.1
16-Jun	0.69	272.8	58.5	42.8	23.9	45.5	24.9	25.4	18.8	15.4	415.8	10.3	0.0	1.70	217.3
17-Jun	1.25	281.5	35.2	51.9	26.6	53.9	27.5	26.9	20.2	16.8	381.5	14.2	0.0	2.72	266.1
18-Jun	1.75	268.7	47.0	54.1	29.1	56.2	29.7	28.8	21.5	18.0	384.5	16.7	0.0	4.38	253.7
19-Jun	2.01	287.2	22.9	63.5	30.9	65.0	31.6	30.7	23.7	20.0	342.2	21.5	0.0	3.46	298.3
20-Jun	0.69	334.4	73.8	53.5	20.4	55.9	21.0	22.0	19.6	18.3	302.1	10.1	0.0	2.66	2.0
21-Jun	0.68	253.9	86.1	40.4	23.6	43.0	24.5	25.8	20.8	17.6	452.8	9.6	0.0	1.27	120.6
22-Jun	0.55	235.7	69.7	46.1	26.0	48.3	26.9	27.2	21.1	17.6	446.1	12.2	0.0	1.68	126.5
23-Jun	0.55	289.2	80.6	53.5	27.7	54.8	28.7	28.5	22.0	18.5	421.4	15.3	0.0	1.16	115.4
24-Jun	0.49	291.5	61.4	60.4	27.6	61.2	28.5	27.9	21.6	18.8	356.2	17.0	0.0	0.69	260.1
25-Jun	0.41	275.2	56.5	61.3	28.5	61.7	29.5	28.5	22.5	19.5	363.3	18.0	0.0	0.58	223.0
26-Jun	0.88	102.1	83.8	39.8	28.5	42.2	29.2	28.2	23.4	20.1	450.9	12.1	0.0	4.65	77.2
27-Jun	0.80	131.6	82.6	49.8	26.1	51.3	27.0	27.3	22.7	19.7	436.8	13.2	0.0	5.77	127.7
28-Jun	0.63	119.9	82.4	58.6	24.9	59.2	25.8	27.0	22.3	19.8	412.6	14.2	0.0	4.48	123.3
29-Jun	0.68	142.7	87.3	65.7	26.6	65.3	27.5	28.9	23.4	20.3	437.3	17.2	0.0	4.69	135.2
30-Jun	0.35	153.8	83.1	80.0	25.1	79.0	25.8	25.6	21.8	20.0	210.4	19.0	6.0	2.74	144.5
3-Jul	0.49	211.1	78.0	58.3	22.0	59.0	23.2	24.0	20.3	17.9	405.3	12.0	0.0	M	M
4-Jul	0.60	113.3	85.1	51.6	24.9	53.2	25.9	26.4	21.3	18.3	451.7	12.8	0.0	M	M
5-Jul	0.54	120.9	79.7	81.5	23.8	80.1	24.6	25.6	20.6	18.7	301.0	18.0	0.0	4.97	132.8
6-Jul	0.63	123.7	83.2	73.4	27.4	73.6	28.0	27.2	22.5	20.3	232.0	20.0	0.8	5.19	179.2
7-Jul	0.55	136.1	82.7	70.5	23.3	72.4	23.6	22.8	21.2	19.9	158.0	15.5	0.0	4.93	206.7
8-Jul	1.84	280.6	22.3	81.9	15.3	82.0	16.0	16.4	18.7	18.2	180.1	11.2	1.6	2.61	283.3
9-Jul	0.59	262.4	65.0	85.6	16.5	85.2	17.2	17.5	17.7	17.0	139.3	12.4	2.0	1.85	218.3
10-Jul	0.59	277.2	59.7	61.1	20.2	62.2	21.4	21.8	19.2	17.4	367.5	11.4	0.0	1.14	227.8

TABLE II–B.5. (CONTINUED)

Date	Wind Speed (m/s)	Wind Direction (true)	Standard Deviation in Wind Direction	1.5-m Relative Humidity (%)	1.5-m Air Temp. (C)	0.5-m Relative Humidity (%)	0.5-m Air Temp. (C)	Leaf Temp. (C)	2-cm Soil Temp. (C)	7-cm Soil Temp. (C)	Net Radiation (W/m2)	Absolute Humidity (g/m3)	Rain (mm)	61-m Wind Speed (m/s)	61-m Wind Direction (true)
11-Jul	0.45	279.5	60.5	68.3	22.8	68.8	23.9	24.2	20.2	17.9	363.3	13.6	0.0	0.97	188.0
12-Jul	0.82	281.0	43.0	62.5	23.9	62.9	25.3	25.9	21.1	18.6	411.7	14.4	0.0	1.59	248.4
13-Jul	0.89	304.3	68.9	62.1	29.3	62.3	30.5	29.6	23.0	19.9	406.9	19.4	0.0	2.39	162.8
14-Jul	1.54	280.7	34.6	61.5	30.1	62.0	31.4	30.9	24.7	21.4	444.0	20.1	0.0	2.63	293.9
15-Jul	2.34	296.4	34.4	72.1	22.9	72.4	23.9	24.3	22.7	21.0	368.2	8.2	0.0	4.29	305.7
16-Jul	0.21	104.3	64.8	77.8	18.8	78.7	19.4	19.0	19.5	19.0	103.8	13.0	10.2	3.66	122.4
17-Jul	0.34	101.4	75.1	97.9	16.5	96.6	16.9	17.7	18.0	17.7	69.7	13.9	1.4	4.03	118.8
18-Jul	0.68	270.2	63.3	91.9	20.1	91.4	20.9	21.6	19.2	18.2	174.6	16.6	12.9	1.89	262.3
19-Jul	1.88	280.0	27.3	72.7	22.3	73.1	23.6	24.7	20.9	18.8	142.6	15.2	0.0	3.15	271.5
20-Jul	0.22	95.9	78.9	96.4	17.6	95.5	18.2	18.8	18.5	18.1	M	14.8	0.4	2.98	112.9
21-Jul	1.79	286.6	23.0	68.7	23.1	69.3	24.4	22.4	21.0	18.7	M	15.2	0.0	3.13	291.5
22-Jul	0.53	129.7	89.3	55.6	26.0	57.9	27.1	M	21.6	18.9	300.5	14.7	0.0	3.75	145.7
23-Jul	0.15	21.2	73.8	93.3	21.7	92.3	22.2	M	19.8	18.9	81.8	18.1	3.6	1.07	335.8
24-Jul	0.47	255.0	76.9	83.3	23.2	81.3	24.4	M	21.3	19.2	288.6	17.0	0.0	2.06	149.2
25-Jul	0.57	118.5	81.4	67.5	26.5	67.6	27.6	M	22.3	19.6	392.7	17.8	0.0	4.00	132.1
26-Jul	0.89	303.9	62.6	77.8	26.3	76.6	27.4	M	22.7	20.5	290.1	20.1	22.0	1.55	358.1
27-Jul	0.61	301.0	82.9	45.9	26.3	50.2	27.3	M	22.1	19.8	437.0	12.7	0.0	1.69	41.1
28-Jul	0.74	123.3	77.0	70.3	26.2	69.8	27.2	M	22.4	20.1	323.9	18.1	0.0	5.75	131.0
29-Jul	2.86	274.1	26.5	56.3	27.2	58.9	28.2	M	23.0	20.8	420.0	15.9	0.0	5.92	262.1
30-Jul	2.22	284.1	23.9	53.9	24.8	56.0	26.2	M	22.5	20.1	430.1	13.7	0.0	3.15	292.8
31-Jul	0.48	245.5	87.8	55.3	29.2	58.5	30.3	M	22.7	20.0	430.0	17.7	0.0	2.69	211.0
1-Aug	0.96	308.4	69.7	76.0	26.5	75.1	27.6	M	22.8	20.8	258.6	20.0	0.6	3.00	345.3
2-Aug	0.61	351.3	86.8	54.8	20.6	55.7	22.0	M	20.7	19.1	374.9	10.7	0.0	1.91	89.7
3-Aug	0.24	105.8	73.4	87.8	20.2	87.2	20.8	M	19.2	18.5	103.2	15.8	0.0	3.09	128.5
4-Aug	1.09	288.6	30.3	87.5	22.9	85.8	23.8	M	20.5	19.3	192.4	18.4	0.4	1.42	313.6
5-Aug	0.36	105.4	86.8	76.5	22.4	76.1	23.2	M	20.5	19.4	187.8	15.8	4.0	2.85	119.8
6-Aug	0.73	46.6	88.3	59.9	23.6	60.9	24.8	M	21.9	19.9	361.7	13.8	0.0	3.85	61.8
7-Aug	0.56	160.0	89.1	62.5	24.6	63.7	25.9	M	21.7	19.2	430.3	15.2	0.0	4.00	140.9
8-Aug	0.54	159.6	87.9	59.6	25.7	60.7	27.0	M	21.7	19.1	426.4	15.3	0.0	3.51	137.4
9-Aug	0.47	142.2	88.9	56.1	25.6	58.1	26.7	M	21.5	18.8	427.7	14.3	0.0	3.68	135.0
10-Aug	0.32	153.8	87.8	60.9	24.4	63.0	25.5	M	20.5	18.2	351.1	14.7	0.0	2.74	138.5
Average	**0.93**	**218.51**	**64.61**	**63.80**	**23.39**	**64.73**	**24.29**	**24.31**	**20.62**	**18.35**	**332.19**	**14.17**	**0.98**	**2.95**	**196.43**

TABLE II–B.6. METEOROLOGICAL DATA AVERAGED OVER THE NIGHTTIME PERIOD (1500–0900)

Date	Wind Speed (m/s)	Wind Direction (true)	Standard Deviation in Wind Direction	1.5-m Relative Humidity (%)	1.5-m Air Temp. (C)	0.5-m Relative Humidity (%)	0.5-m Air Temp. (C)	Leaf Temp. (C)	2-cm Soil Temp. (C)	7-cm Soil Temp. (C)	Net Radiation (W/m2)	Absolute Humidity (g/m3)	Rain (mm)	61-m Wind Speed (m/s)	61-m Wind Direction (true)
02-03 Jun	0.06	102.0	47.7	95.6	16.8	96.1	16.6	16.0	15.7	15.2	15.3	13.5	0.0	1.76	50.6
03-04 Jun	0.43	120.5	42.1	87.4	14.0	89.2	13.7	11.2	14.5	14.6	30.7	10.7	0.0	2.17	308.4
04-05 Jun	0.37	101.6	23.1	80.5	14.7	82.3	14.5	11.4	14.9	14.9	56.0	9.7	0.0	1.92	245.8
05-06 Jun	0.56	82.1	39.1	79.5	19.1	82.0	18.7	15.5	16.3	15.8	57.0	12.6	0.0	2.73	107.0
06-07 Jun	0.18	122.1	40.9	73.0	21.2	76.1	20.9	17.3	17.7	16.9	72.4	12.9	0.0	2.28	183.2
07-08 Jun	0.98	334.9	76.0	84.6	9.1	85.5	8.9	9.5	14.2	15.0	6.6	7.9	4.9	5.46	335.0
08-09 Jun	0.69	87.8	37.5	67.9	11.4	71.1	11.3	9.1	14.2	14.6	63.1	6.7	0.0	2.86	349.6
09-10 Jun	0.11	104.4	35.7	74.3	12.3	76.2	12.2	10.3	14.4	14.7	62.6	7.7	0.0	1.71	115.2
10-11 Jun	0.22	111.0	62.2	75.9	17.0	78.8	17.0	16.4	15.9	15.4	39.7	11.0	4.0	3.20	77.2
11-12 Jun	2.91	291.6	18.7	79.3	14.2	80.3	14.2	13.4	15.0	15.1	18.2	9.9	0.0	4.65	298.7
12-13 Jun	0.84	87.8	20.6	81.1	10.7	83.0	10.6	10.0	14.4	14.8	72.4	6.5	0.0	2.26	270.7
13-14 Jun	0.97	4.8	36.5	65.1	16.8	70.0	16.3	13.1	15.5	15.4	36.1	9.5	0.0	3.26	328.3
14-15 Jun	0.59	87.9	38.0	64.8	13.6	68.3	13.3	9.9	14.6	15.0	51.1	7.3	0.0	3.44	338.4
15-16 Jun	0.38	101.8	24.7	70.8	14.3	73.7	14.2	10.8	14.8	15.0	65.5	8.2	0.0	1.96	290.3
16-17 Jun	0.15	119.5	36.5	73.9	19.6	77.9	19.3	15.8	16.6	16.1	57.8	12.3	0.0	2.55	257.2
17-18 Jun	0.50	126.7	26.7	74.6	22.3	78.1	22.0	18.3	18.1	17.3	67.1	14.4	0.0	3.27	273.0
18-19 Jun	2.13	272.3	21.7	70.9	27.5	73.2	27.3	23.5	20.4	19.0	74.0	18.7	0.0	5.20	273.9
19-20 Jun	0.85	2.6	44.4	74.6	23.8	78.8	23.4	19.2	20.1	19.4	34.5	16.7	0.0	3.39	325.9
20-21 Jun	0.34	94.5	47.0	63.7	16.7	68.1	16.4	12.5	17.2	17.4	59.6	8.8	0.0	3.69	32.5
21-22 Jun	0.14	107.2	28.9	75.4	16.8	77.4	16.7	13.1	17.2	17.3	71.2	10.2	0.0	1.50	89.0
22-23 Jun	0.12	109.9	29.9	79.0	20.2	80.9	20.1	16.4	18.2	17.8	71.8	13.2	0.0	1.83	116.0
23-24 Jun	0.22	101.8	35.3	80.1	21.9	82.2	21.8	17.9	19.2	18.6	69.6	15.0	0.0	1.56	126.9
24-25 Jun	0.05	116.0	31.3	86.7	22.0	88.0	22.0	18.9	19.6	19.0	50.2	16.7	0.0	1.34	121.2
25-26 Jun	0.52	140.3	77.4	72.3	23.1	74.9	23.0	19.9	20.3	19.6	41.5	15.4	0.0	3.37	67.1
26-27 Jun	0.28	121.6	49.0	55.1	22.2	61.9	21.8	17.4	20.0	19.6	71.7	11.3	0.0	4.78	101.2
27-28 Jun	0.19	105.9	64.0	70.5	22.2	75.4	21.7	18.9	20.2	19.7	52.4	14.1	0.0	4.31	121.5
28-29 Jun	0.19	108.0	51.1	80.1	21.2	82.9	20.9	18.3	20.1	19.7	55.9	14.7	0.0	3.68	127.4
29-30 Jun	0.16	107.9	40.7	84.8	23.0	86.3	22.9	20.1	21.0	20.3	71.6	17.2	0.0	2.42	124.7
30 Jun-01 Jul	0.06	105.4	50.9	97.8	21.0	97.6	21.1	19.0	20.2	19.8	34.3	18.0	5.0	M	M
01-02 Jul	2.15	274.7	30.0	70.5	18.5	73.2	18.3	15.3	19.2	19.4	53.8	11.2	3.0	M	M
02-03 Jul	1.04	70.0	19.8	85.1	12.6	86.0	12.7	10.6	16.9	17.6	55.0	9.3	0.0	M	M
03-04 Jul	0.22	111.9	40.9	79.6	16.8	81.8	16.6	13.4	17.8	18.0	53.8	11.0	0.0	M	M
04-05 Jul	0.12	114.8	45.9	74.2	21.0	77.5	20.9	17.5	19.2	18.7	78.2	13.1	0.0	M	M
05-06 Jul	0.26	102.8	60.6	91.3	24.1	91.6	24.2	22.3	20.8	19.8	81.9	20.0	1.0	4.40	128.6
06-07 Jul	0.14	118.6	62.1	97.5	21.0	97.6	21.1	19.5	20.4	20.0	25.0	18.0	6.3	2.76	169.5
07-08 Jul	0.65	207.0	57.7	86.0	16.6	87.2	16.7	15.7	18.8	18.9	14.3	12.5	1.5	3.13	249.0

TABLE II–B.6. (CONTINUED)

Date	Wind Speed (m/s)	Wind Direction (true)	Standard Deviation in Wind Direction	1.5-m Relative Humidity (%)	1.5-m Air Temp. (C)	0.5-m Relative Humidity (%)	0.5-m Air Temp. (C)	Leaf Temp. (C)	2-cm Soil Temp. (C)	7-cm Soil Temp. (C)	Net Radiation (W/m2)	Absolute Humidity (g/m3)	Rain (mm)	61-m Wind Speed (m/s)	61-m Wind Direction (true)
08-09 Jul	1.07	80.6	28.8	91.2	12.7	91.9	12.8	11.7	16.8	17.3	44.4	10.2	0.0	2.46	295.3
09-10 Jul	0.61	344.4	54.5	96.8	14.4	96.5	14.6	13.7	16.7	16.8	40.0	12.1	7.9	2.53	294.9
10-11 Jul	0.06	110.5	32.0	92.0	15.6	92.4	15.8	14.7	17.4	17.4	35.9	12.3	0.0	1.43	116.1
11-12 Jul	0.68	315.4	41.6	84.0	18.8	85.6	19.0	16.7	18.5	18.2	60.3	13.5	0.2	3.04	303.0
12-13 Jul	0.10	108.2	41.4	85.0	21.2	86.8	21.3	19.2	19.6	19.0	60.5	15.7	0.0	1.62	154.7
13-14 Jul	0.76	216.8	43.8	82.1	26.9	84.4	26.8	23.2	21.7	20.7	65.3	21.0	0.0	3.82	259.6
14-15 Jul	1.05	351.3	48.6	80.7	25.8	82.6	25.8	22.8	22.5	21.6	86.8	19.2	6.0	3.89	322.9
15-16 Jul	0.53	113.0	42.6	75.1	18.8	78.8	18.7	15.5	20.0	20.2	72.9	12.1	0.0	3.39	21.0
16-17 Jul	0.11	130.5	75.2	99.8	14.8	99.0	15.0	15.1	17.8	18.1	4.2	12.7	12.5	3.60	95.3
17-18 Jul	0.13	104.3	62.5	99.3	18.4	99.0	18.6	18.0	18.3	18.1	17.8	15.8	0.0	1.74	143.3
18-19 Jul	1.36	280.6	39.8	91.8	17.7	92.3	17.9	16.4	18.7	18.6	41.4	13.9	2.0	4.45	283.8
19-20 Jul	0.29	126.5	42.3	84.4	19.4	86.0	19.7	17.7	19.5	19.2	47.3	14.1	6.6	1.94	209.3
20-21 Jul	0.68	86.2	26.0	94.3	17.1	94.3	17.4	15.1	18.1	18.1	M	13.9	0.0	2.18	276.7
21-22 Jul	0.42	95.9	30.9	85.3	18.2	86.3	18.4	M	18.8	18.8	M	13.0	0.0	1.60	346.8
22-23 Jul	0.11	107.3	43.9	85.3	21.8	87.6	21.8	M	20.0	19.5	53.5	16.3	0.0	3.26	150.6
23-24 Jul	0.30	138.1	35.1	96.7	19.3	96.6	19.6	M	19.0	18.8	39.7	16.3	0.0	1.77	285.8
24-25 Jul	0.09	105.9	35.5	90.5	20.1	91.4	20.2	M	19.5	19.3	65.0	15.7	0.0	2.05	168.8
25-26 Jul	0.15	108.0	35.1	89.3	22.9	90.0	23.1	M	20.7	20.1	79.0	18.2	0.0	2.54	158.2
26-27 Jul	0.21	85.1	41.3	93.3	19.4	94.1	19.5	M	20.1	20.1	61.1	11.3	0.0	2.51	331.3
27-28 Jul	0.22	108.5	31.7	81.0	20.0	82.8	20.2	M	19.8	19.7	74.2	13.6	0.0	2.85	112.3
28-29 Jul	0.34	114.7	61.2	95.4	22.0	96.2	22.1	M	20.7	20.3	30.6	18.6	15.4	3.66	163.1
29-30 Jul	1.27	291.3	32.2	76.3	20.8	79.7	20.5	M	20.2	20.3	57.7	13.4	0.0	4.67	289.3
30-31 Jul	0.34	102.2	26.3	83.5	19.6	85.0	19.8	M	19.8	19.9	68.0	13.8	0.0	2.04	186.5
31 Jul-01	0.17	102.6	47.1	83.7	24.1	86.0	24.1	M	21.2	20.6	77.7	18.0	0.0	2.55	192.3
01-02 Aug	0.41	16.2	84.4	87.6	15.1	89.0	15.0	M	18.8	19.4	-1.5	11.5	0.0	3.58	15.9
02-03 Aug	0.10	103.9	38.1	89.5	17.2	90.1	17.4	M	18.8	18.9	55.3	13.0	0.0	2.54	119.3
03-04 Aug	0.10	82.9	61.2	99.6	19.2	99.0	19.5	M	19.1	18.9	25.7	16.6	15.8	1.95	86.8
04-05 Aug	0.33	159.5	57.4	91.0	20.8	91.5	21.0	M	19.9	19.5	37.8	16.8	0.0	2.70	8.4
05-06 Aug	0.11	121.8	72.7	99.1	18.8	98.3	18.9	M	19.4	19.3	9.1	16.0	2.6	2.85	74.7
06-07 Aug	0.14	109.2	28.3	89.0	17.7	89.7	17.8	M	18.7	19.1	62.2	13.3	0.0	2.99	106.4
07-08 Aug	0.15	108.8	30.0	85.3	17.8	86.6	17.9	M	18.4	18.7	67.3	12.6	0.0	3.13	113.9
08-09 Aug	0.13	108.5	33.1	87.0	18.3	88.0	18.3	M	18.4	18.8	66.3	13.4	0.0	2.79	117.7
09-10 Aug	0.14	110.1	37.7	84.7	18.4	86.4	18.4	M	18.3	18.6	63.9	13.0	0.0	2.59	133.5
Average	**0.47**	**132.30**	**42.56**	**83.09**	**18.73**	**84.85**	**18.69**	**15.86**	**18.38**	**18.21**	**51.66**	**13.43**	**1.37**	**2.87**	**186.57**

TABLE II–B.7. METEOROLOGICAL DATA AVERAGED OVER THE 24-HOUR PERIOD (0900-0900)

Date	Wind Speed (m/s)	Wind Direction (true)	Standard Deviation in Wind Direction	1.5-m Relative Humidity (%)	1.5-m Air Temp. (C)	0.5-m Relative Humidity (%)	0.5-m Air Temp. (C)	Leaf Temp. (C)	2-cm Soil Temp. (C)	7-cm Soil Temp. (C)	Net Radiation (W/m2)	Absolute Humidity (g/m3)	Rain (mm)	61-m Wind Speed (m/s)	61-m Wind Direction (true)
03-04 Jun	0.42	93.9	51.7	87.3	14.8	88.6	14.6	13.1	14.9	14.7	51.7	11.2	0.0	2.23	319.6
04-05 Jun	0.52	142.7	27.6	71.4	16.2	73.5	16.1	14.1	15.6	14.9	133.8	9.5	0.0	1.82	249.5
05-06 Jun	0.93	138.2	39.9	71.3	20.2	73.9	20.1	17.9	16.9	15.7	149.2	12.2	0.0	2.97	152.3
06-07 Jun	0.29	149.0	52.0	68.7	22.3	71.3	22.3	20.0	18.3	16.9	155.6	13.2	0.0	2.25	171.4
07-08 Jun	0.84	324.8	72.3	81.4	12.8	82.2	12.7	13.1	15.3	15.4	49.3	9.9	5.9	4.41	258.7
08-09 Jun	0.93	142.8	42.2	62.5	12.2	65.5	12.3	12.0	14.9	14.7	166.8	6.7	0.0	3.17	342.7
09-10 Jun	0.28	133.6	48.7	65.0	13.8	67.0	14.0	13.5	15.3	14.7	160.7	7.4	0.0	1.84	112.5
10-11 Jun	0.27	115.1	67.4	68.6	17.9	71.3	18.0	17.8	16.3	15.2	106.4	10.5	4.0	3.20	90.4
11-12 Jun	2.34	260.2	34.5	80.2	15.4	80.7	15.4	15.3	15.5	15.2	66.6	10.8	1.0	4.13	260.1
12-13 Jun	1.47	138.6	20.5	71.3	12.3	73.5	12.4	12.8	15.3	14.9	166.7	6.5	0.0	2.90	277.2
13-14 Jun	1.06	76.7	35.9	62.4	17.7	66.5	17.6	15.7	16.1	15.2	123.6	9.8	0.0	3.12	326.2
14-15 Jun	0.86	140.0	39.2	59.1	15.2	62.3	15.3	13.4	15.6	15.1	146.7	7.5	0.0	3.25	332.8
15-16 Jun	0.64	145.4	26.1	62.8	16.1	65.9	16.2	14.0	15.7	15.0	158.4	8.2	0.0	2.10	288.0
16-17 Jun	0.28	157.8	42.0	66.1	20.7	69.8	20.7	18.2	17.2	15.9	147.3	11.8	0.0	2.34	247.2
17-18 Jun	0.69	165.4	28.8	68.9	23.4	72.0	23.4	20.4	18.7	17.2	145.7	14.3	0.0	3.13	271.3
18-19 Jun	2.03	271.4	28.0	66.7	27.9	68.9	27.9	24.8	20.7	18.7	151.6	18.2	0.0	5.00	268.9
19-20 Jun	1.14	73.8	39.0	71.8	25.6	75.3	25.4	22.1	21.0	19.6	111.4	17.9	0.0	3.41	319.0
20-21 Jun	0.43	154.5	53.7	61.2	17.6	65.0	17.5	14.8	17.8	17.6	120.2	9.2	0.0	3.43	24.8
21-22 Jun	0.28	143.9	43.2	66.7	18.5	68.8	18.7	16.3	18.1	17.4	166.6	10.0	0.0	1.44	96.9
22-23 Jun	0.23	141.4	39.9	70.8	21.6	72.7	21.8	19.1	19.0	17.8	165.4	12.9	0.0	1.79	118.6
23-24 Jun	0.30	148.7	46.6	73.4	23.3	75.4	23.5	20.6	19.9	18.6	157.5	15.1	0.0	1.46	124.0
24-25 Jun	0.16	159.9	38.9	80.1	23.4	81.3	23.6	21.2	20.1	18.9	126.7	16.8	0.0	1.17	155.9
25-26 Jun	0.49	174.0	72.2	69.5	24.5	71.6	24.6	22.1	20.8	19.5	121.9	16.1	0.0	2.67	106.1
26-27 Jun	0.43	116.7	57.7	51.2	23.8	56.9	23.6	20.1	20.9	19.8	166.5	11.5	0.0	4.75	95.2
27-28 Jun	0.34	112.3	68.7	65.3	23.1	69.3	23.0	21.0	20.9	19.7	148.5	13.9	0.0	4.68	123.0
28-29 Jun	0.30	111.0	58.9	74.7	22.1	77.0	22.1	20.5	20.6	19.7	145.1	14.6	0.0	3.88	126.3
29-30 Jun	0.29	116.6	52.4	80.0	23.9	81.0	24.1	22.3	21.6	20.3	163.0	17.2	0.0	2.99	127.3
30 Jun-01 Jul	0.14	117.5	58.9	93.4	22.0	93.0	22.2	20.7	20.6	19.9	78.3	18.2	11.0	M	M
01-02 Jul	1.79	275.8	41.7	74.0	19.8	75.9	19.9	17.7	19.9	19.6	103.6	13.1	3.0	M	M
02-03 Jul	1.55	123.8	20.6	80.0	13.9	80.8	14.1	12.6	17.7	17.9	119.6	9.6	0.0	M	M
03-04 Jul	0.29	136.7	50.2	74.3	18.1	76.1	18.3	16.0	18.4	17.9	141.7	11.3	0.0	M	M
04-05 Jul	0.24	114.4	55.7	68.5	22.0	71.5	22.2	19.7	19.7	18.6	171.6	13.1	0.0	M	M
05-06 Jul	0.33	107.3	65.4	88.9	24.0	88.7	24.3	23.1	20.7	19.5	136.7	19.5	1.0	4.54	129.6
06-07 Jul	0.26	119.9	67.4	91.5	22.6	91.6	22.8	21.4	20.9	20.1	76.7	18.5	7.0	3.37	171.9
07-08 Jul	0.63	189.3	64.0	82.1	18.3	83.5	18.4	17.4	19.4	19.1	50.2	13.3	1.5	3.58	238.5

TABLE II–B.7. (CONTINUED)

Date	Wind Speed (m/s)	Wind Direction (true)	Standard Deviation in Wind Direction	1.5-m Relative Humidity (%)	1.5-m Air Temp. (C)	0.5-m Relative Humidity (%)	0.5-m Air Temp. (C)	Leaf Temp. (C)	2-cm Soil Temp. (C)	7-cm Soil Temp. (C)	Net Radiation (W/m2)	Absolute Humidity (g/m3)	Rain (mm)	61-m Wind Speed (m/s)	61-m Wind Direction (true)
08-09 Jul	1.26	130.6	27.2	88.9	13.3	89.4	13.6	12.9	17.2	17.5	78.3	10.5	1.6	2.49	292.3
09-10 Jul	0.60	323.9	57.1	94.0	14.9	93.7	15.2	14.6	16.9	16.9	64.8	12.1	9.9	2.36	275.8
10-11 Jul	0.19	152.2	38.9	84.3	16.8	84.8	17.2	16.5	17.9	17.4	118.8	12.1	0.0	1.36	144.1
11-12 Jul	0.62	306.4	46.3	80.0	19.8	81.4	20.2	18.6	18.9	18.1	136.0	13.6	0.2	2.52	274.2
12-13 Jul	0.28	151.4	41.8	79.4	21.9	80.8	22.3	20.9	20.0	18.9	148.3	15.4	0.0	1.61	178.1
13-14 Jul	0.79	238.7	50.0	77.1	27.5	78.9	27.7	24.8	22.0	20.5	150.7	20.6	0.0	3.46	235.4
14-15 Jul	1.17	333.6	45.1	75.9	26.9	77.4	27.2	24.8	23.0	21.5	176.1	19.4	6.0	3.57	315.6
15-16 Jul	0.98	158.8	40.5	74.4	19.9	77.2	20.0	17.7	20.7	20.4	146.7	11.1	0.0	3.62	92.2
16-17 Jul	0.14	124.0	72.6	94.3	15.8	93.9	16.1	16.1	18.2	18.3	29.1	12.8	22.7	3.61	102.1
17-18 Jul	0.18	103.6	65.6	98.9	17.9	98.4	18.2	17.9	18.2	18.0	30.8	15.3	1.4	2.31	137.2
18-19 Jul	1.19	278.0	45.7	91.8	18.3	92.1	18.6	17.7	18.8	18.5	74.7	14.6	14.9	3.81	278.4
19-20 Jul	0.69	164.9	38.6	81.4	20.2	82.8	20.6	19.5	19.9	19.1	71.1	14.4	6.6	2.24	224.9
20-21 Jul	0.57	88.6	39.2	94.9	17.2	94.6	17.6	16.0	18.2	18.1	M	14.1	0.4	2.38	235.8
21-22 Jul	0.76	143.6	28.9	81.2	19.4	82.1	19.9	M	19.3	18.8	M	13.5	0.0	1.98	333.0
22-23 Jul	0.22	112.9	55.2	77.9	22.9	80.2	23.2	M	20.4	19.3	115.3	15.9	0.0	3.38	149.4
23-24 Jul	0.26	108.9	44.8	95.9	19.9	95.5	20.2	M	19.2	18.8	50.3	16.7	3.6	1.59	298.3
24-25 Jul	0.19	143.2	45.9	88.7	20.8	88.9	21.2	M	19.9	19.3	120.9	16.0	0.0	2.05	163.9
25-26 Jul	0.26	110.6	46.7	83.8	23.8	84.4	24.2	M	21.1	20.0	157.5	18.1	0.0	2.90	151.7
26-27 Jul	0.38	139.8	46.6	89.4	21.1	89.7	21.5	M	20.7	20.2	118.4	13.5	22.0	2.27	338.0
27-28 Jul	0.32	156.6	44.5	72.2	21.6	74.6	22.0	M	20.3	19.7	164.9	13.4	0.0	2.56	94.5
28-29 Jul	0.44	116.9	65.1	89.2	23.0	89.6	23.4	M	21.1	20.2	103.9	18.5	15.4	4.18	155.1
29-30 Jul	1.66	287.0	30.8	71.3	22.4	74.5	22.4	M	20.9	20.4	148.3	14.1	0.0	4.98	282.5
30-31 Jul	0.81	147.6	25.7	76.1	20.9	77.8	21.4	M	20.5	19.9	158.5	13.7	0.0	2.32	213.1
31 Jul-01	0.25	138.3	57.3	76.6	25.4	79.1	25.7	M	21.5	20.5	165.8	17.9	0.0	2.58	197.0
01-02 Aug	0.54	89.3	80.7	84.7	18.0	85.5	18.1	M	19.8	19.8	63.5	13.6	0.6	3.44	98.3
02-03 Aug	0.23	165.7	50.3	80.8	18.0	81.5	18.5	M	19.3	19.0	135.2	12.4	0.0	2.39	111.9
03-04 Aug	0.13	88.6	64.2	96.6	19.5	96.0	19.8	M	19.2	18.8	45.1	16.4	15.8	2.23	97.2
04-05 Aug	0.52	191.8	50.6	90.1	21.3	90.1	21.7	M	20.0	19.5	76.5	17.2	0.4	2.38	84.7
05-06 Aug	0.17	117.7	76.2	93.5	19.7	92.8	20.0	M	19.7	19.3	53.8	15.9	6.6	2.85	86.0
06-07 Aug	0.29	93.5	43.3	81.8	19.2	82.5	19.6	M	19.5	19.3	137.1	13.4	0.0	3.20	95.2
07-08 Aug	0.25	121.6	44.7	79.6	19.5	80.9	19.9	M	19.2	18.9	158.0	13.2	0.0	3.34	120.6
08-09 Aug	0.23	121.3	46.8	80.1	20.2	81.2	20.5	M	19.3	18.8	156.3	13.9	0.0	2.97	122.6
09-10 Aug	0.22	118.2	50.5	77.5	20.2	79.3	20.5	M	19.1	18.6	154.9	13.3	0.0	2.86	133.9
Average	**0.58**	**153.3**	**47.8**	**78.0**	**19.8**	**79.6**	**20.0**	**17.9**	**18.9**	**18.2**	**120.5**	**13.6**	**2.4**	**2.88**	**188.7**

TABLE II–B.8. SELECTED METEOROLOGICAL PARAMETERS AVERAGED OVER THE ENTIRE STUDY PERIOD

Parameter	Daytime (0900–1500)	Night-time (1500–0900)	24-h Average (0900–0900)
2.5-m Wind Speed (m/s)	0.93	0.47	0.58
61-m Wind Speed (m/s)	2.95	2.87	2.88
0.5-m Relative Humidity (%)	64.7	84.9	79.6
0.5-m Air Temperature (C)	24.3	18.7	20.0
0.5-m Absolute Humidity (g/m^3)	14.2	13.4	13.6
2-cm Soil Temperature (C)	20.6	18.4	18.9

TABLE II–B.9. FREQUENCY OF OCCURRENCE OF RAIN INTENSITY AS A FUNCTION OF WIND DIRECTION (%)

Wind Direction	Rainfall Intensity (mm/h)				Total
	0 -1	1–2	2–5	>5	
345–015	0.9	1.7	0	0	2.6
015–045	3.5	2.6	0	0	6.1
045–075	5.2	0.9	0.9	0.9	7.8
075–105	11.3	1.7	0.9	1.7	15.7
105–135	12.2	2.6	6.1	0.9	21.7
135–165	1.7	4.3	2.6	0	8.7
165–195	4.3	0	0	0	4.3
195–225	1.7	0	0	0	1.7
225–255	7.0	0	0	0	7.0
255–285	3.5	1.7	1.7	0	7.0
285–315	7.0	0	0.9	0	7.8
315–345	9.6	0	0	0	9.6
Total	67.9	15.5	13.1	3.5	100

II–B.6. SCENARIO CALCULATIONS

Using the meteorological data and tritium air concentrations provided, calculate:

(i) HTO concentrations in the free water of grass averaged over the study period for each of the 3 sampling sites (Bq/L). If possible, break the predictions down into a daytime (0900-1500) average and a night-time (1500-0900) average;

(ii) HTO concentrations in soil water averaged over the study period for each of the 3 sampling sites (Bq/L). If possible, break the predictions down into a daytime (0900-1500) average and a night-time (1500-0900) average;

(iii) the HTO concentration in precipitation averaged over the study period at the ARS site (Bq/L);

(iv) the non-exchangeable OBT concentration in grass at the 3 sampling sites on June 28, July 12 and August 9 (Bq/L water equivalent);

(v) HTO concentrations in soil water and in the free water of grass (Bq/L) at the ARS site at the following dates and times:

1500 h	June 15	0900 h	June 8
	June 28		June 29
	July 5		July 12
	July 19		

Wind directions were steady over the air sampling periods preceding these times so that grass and air concentrations should be in equilibrium. The plume was present over the ARS on June 28, June 29 and July 5 and absent on the other 4 dates.

95% confidence intervals on all predictions in (i)–(v).

CLARIFICATION OF SCENARIO 3

The following comments are offered to clarify the calculational endpoints for the CRL scenario in response to questions raised by one of the participants.

(1) Endpoints (i) and (ii): Participants are asked to provide HTO concentrations in vegetation and soil averaged over the daytime and night-time sampling periods. The observations (relative to the observed air concentrations) are significantly different for these two periods. Reproduction of these differences in the model predictions may provide insight into the physical processes operating during chronic releases and how best they can be simulated. But note that the terms “daytime” and “night-time” are not good descriptors for the vegetation samples. Vegetation concentrations depend on the air concentrations over the last couple of hours before sampling (which aren't known). Thus the “daytime” samples reflect air concentrations over (roughly) the period 1300-1500 whereas the “night-time” samples follow air concentrations over the period 0700-0900. Daytime and night-time results are not mandatory. Results averaged over the entire study period are also useful.

(2) Endpoint (iii): The precipitation concentration requested is the mean HTO concentration in all rain that fell during the period, whether the plume was present or not over the ARS site.

(3) Endpoint (v): The times specified are the times of soil and vegetation sampling, so the relevant air concentrations are those for the preceding sampling period. The presence or absence of the plume at a given location was deduced from observed wind directions, not from relative concentrations.

ADDENDUM TO SCENARIO 3: ADDITIONAL DATA AND INFORMATION

The following information is provided to answer questions that arose during discussion of the AECL scenario at the BIOMASS Tritium Working Group Meeting in Vienna, October 9 1998.

Source Term: Tritium release rates are measured continuously with a 2–3 day averaging time. Release rates for the study period were 9.8×10^5 Bq s^{-1} from the stack and 2.9×10^6 Bq s^{-1} from the NRU reactor, with a variability of a factor 2 from one sampling period to the next. The rates cannot be separated into day and night periods but there is no reason to believe there would be a systematic diurnal variation.

No detailed information is available on release rates from the Perch Lake Waste Management area.

Groundwater: The depth to the water table and tritium concentrations in groundwater at the 3 sampling sites are shown in Table II–B.a1. All of the values are estimates and have a large uncertainty.

TABLE II–B.a1. DEPTH TO THE WATER TABLE AND TRITIUM CONCENTRATIONS IN GROUNDWATER AT THE 3 SAMPLING LOCATIONS

Location	Depth to Water Table (m)	Tritium Groundwater Concentration (Bq/L)
Acid Rain Site	3	?
Perch Lake	1–1.5	40
Building 600	5	1000–5000

Buildings: A 1:2200 scale map of the CRL laboratory complex is attached. Releases from NRU (Building 150) occur through roof and side vents at a height of about 30 m. The buildings between NRU and B600 are all fairly low with elevations of 10 m or less. The terrain drops about 20 m from NRU to B600.

Stability Classes: Stability classes for each hour of the study period have been added to the meteorological spreadsheet HourMet.xls. These were determined from the 30-m standard deviation in wind direction and the temperature difference between 60 m and 30 m measured on the main Perch Lake tower. The frequency of occurrence of the stability classes and the mean wind speed in each class are shown in Table II–B.a2 for the 3 sampling sites. For ARS, the statistics are based on hours for which the wind direction lay in the range $115^o \pm 15^o$, the direction which carries the plume from the stack (the main contributor to concentrations at ARS) to the site. The statistics were calculated using data from the 61-m level of the Perch Lake tower. For the Perch Lake sampling site, the statistics were calculated for wind directions in the range $316^o \pm 15^o$ using information from the 30-m level of the Perch Lake tower. For Building 600, the statistics were based on wind directions in the range $330^o \pm 15^o$ and were calculated from data collected on a short mast about 30 m above ground on the roof of Building 456, which is located just south of Building 600.

TABLE II–B.a2. FREQUENCY OF OCCURRENCE OF STABILITY CLASSES AND MEAN WIND SPEEDS FOR THE 3 SAMPLING SITES

Stability Class	Acid Rain Site		Perch Lake		Building 600	
	Frequency (%)	Speed (m s^{-1})	Frequency (%)	Speed (m s^{-1})	Frequency (%)	Speed (m s^{-1})
A	5.8	1.4	11.8	0.9	23.8	1.9
B	3.7	1.4	10.6	1.0	6.1	2.3
C	6.8	2.2	15.9	1.5	16.4	1.5
D	25.1	3.1	17.8	2.0	20.9	1.8
E	35.2	3.1	24.0	1.9	17.9	1.9
F	23.4	2.7	19.9	1.0	14.9	0.9

Vegetation: Yield and leaf area indices were not measured during the study period and it is too late in the season to obtain representative values now. Grass yields measured at similar sites in 1992 lay between 0.75 and 1.3 kg m^{-2} wet weight. Inspection of soil cores from the sites indicates that root density is high down to about 5 cm and lower between 5 and 7 cm. A few roots are found to depths of 12–15 cm.

Tritium Measurements: Blank entries in Table II–B.a2 of the scenario description indicate that air concentrations were not measured, not that the concentrations were non-detectable.

OBT concentrations in grass at the beginning of the study period are not available.

All soil concentrations, including the initial ones, were made at 0900.

ANNEX II–C
SCENARIO 4 (SAROV) DESCRIPTION

History:

Scenario 4.2 drafted by L. Belovodskii (RFNC-VNIIEF, Russian Federation) and A. Golubev (RFNC-VNIIEF, Russian Federation), November 1999. Incorporates comments on Scenario 4.1.

Scenario 4.1 drafted by L. Belovodskii (RFNC-VNIIEF, Russian Federation) and A. Golubev (RFNC-VNIIEF, Russian Federation), April 1999. Incorporates comments on Scenario 4.0

Scenario 4.0 drafted by L. Belovodskii (RFNC-VNIIEF, Russian Federation) and A. Golubev (RFNC-VNIIEF, Russian Federation), January 1999.

II–C.1. GENERAL INFORMATION

Site: This is located in the forest-steppe natural-climatic zone.

Landscape: The area around the release points is a plain at an elevation 130m above sea level; the maximum variation of elevation within the site boundary is ± 25 m. The area to the South of the emission source is a forest. The area to the North of the emission source is a city with buildings of heights of ~10-30 m.

Climate: There is an Atlantic-continental European climate at the site. Each of the seasons during year is well defined. The annual average temperature is +3.8°C; the January average temperature is -11.3°C (minimum T = -40°C); the July average temperature is 19.5 °C (maximum T = +38°C). The average annual volume of precipitation is 560 mm of which about 70% occurs during the warm period of the year. The duration of the snow cover period is 140 days with an average thickness of snow cover of 55 cm. Average monthly volumes of precipitation and average monthly temperatures are shown on Figure II–C.1.

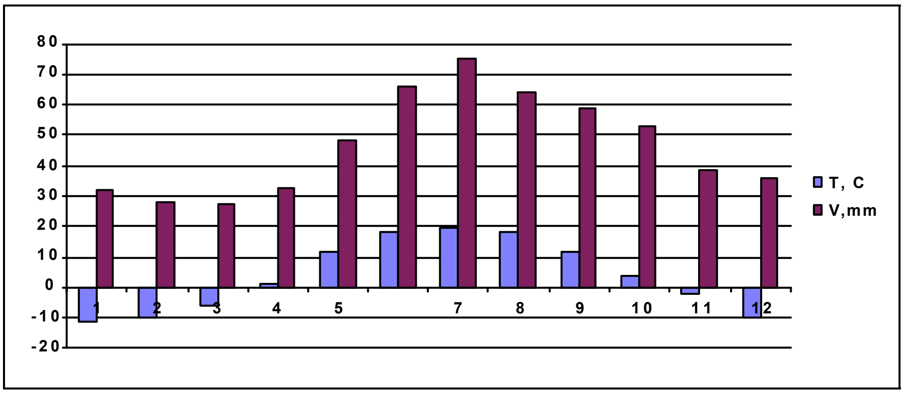

FIG. II–C.1. Monthly averaged temperature and volume of precipitation.

II–C.2. SOLAR RADIATION

Monthly and annual values of direct solar radiation, total solar radiation and radiation balance are presented in Table II–C.1.

Radiation balance (K) is:

$$K = (Q+q)*(1-b) - E,$$

where:

b is 0.15 – 0.2;
E is effective annual emission is 1460 MJ/m^2;
Q is direct solar radiation; and
q is scattered solar radiation.

TABLE II–C.1. MONTHLY AND ANNUAL DIRECT SOLAR RADIATION, TOTAL SOLAR RADIATION AND RADIATION BALANCE, MJ/M^2 (10^6 JOULE PER SQ. M)

Radiation	Month 1	Month 2	Month 3	Month 4	Month 5	Month 6	Month 7	Month 8	Month 9	Month 10	Month 11	Month 12	Annual
Net	22.8	50.9	152	240	361	394	356	283	157	74.5	30.3	20.3	2142
Total	83.3	161	334	467	607	650	618	504	315	175	88	63	4065
Balance	-29.7	-24.3	77	247	396	446	380	303	15.8	53.2	-22.6	-45.2	1796

II–C.3. OTHER RELEVANT DATA AND INFORMATION

Wind Roses: These are presented in Table II–C.2 for each month.

Data on wind speed and wind direction for 5 years of observation are presented in a meteorological data file in Excel format (the floppy disk has already been supplied to modellers, anyone else requiring the data should contact the Technical Secretariat).

Vegetation: The normal type of vegetation within the site boundary is a mixed forest. The common tree types growing at the site are: pine, birch, aspen, lime, oak, maple, and fir. Average tree height is 25±10 m, whilst the average age of the trees is about 100 years. The duration of the vegetation period is 147 days; the vegetation period begins at the first week of May and ends at the last week of September.

Soil properties: There are two types of sandy/sandy-loam soils that are present within the site boundary:

Grey forest soil.
Forest and meadow «podbel» (the Russian name of soil type like «podsol»).

Thickness of humus containing layer is 12 – 30 cm.

Value of pH is 5.5 – 6.0.

Approximate composition of top 30 cm of grey forest soil is:

Content of humus: 4-5%
Content of silt: 15%
Content of clay: 30 %
Content of sand: 50 %

Average depth of frozen soil in winter is 70 cm.

TABLE II–C.2. PERCENTAGE OF MONTHLY WIND ROSE

	Month 1	Month 2	Month 3	Month 4	Month 5	Month 6	Month 7	Month 8	Month 9	Month 10	Month 11	Month 12
N	1.5	4.7	4.6	3.7	5.5	5.1	5.9	5.0	2.4	3.9	5.1	3.7
NE	4.5	15.8	12.7	8.7	20.8	9.7	9.5	9.9	5.2	6.7	8.7	3.2
E	2.9	4.0	3.7	4.9	3.9	4.8	2.4	3.2	1.4	2.4	1.6	2.9
SE	34.5	24.7	26.7	28.6	19.7	23.8	14.3	16.5	19.9	18.5	14.4	21.5
S	11.8	7.5	16.3	9.7	7.2	8.2	5.4	5.6	7.7	7.4	12.6	9.5
SW	25.4	16.2	19.6	23.4	21.6	18.7	24.7	19.6	30.4	28.5	27.7	35.9
W	10.3	12.3	7.3	9.0	9.8	10.1	15.9	14.0	13.5	16.6	12.7	10.9
NW	9.2	14.7	9.2	12.0	11.6	19.4	21.8	26.3	19.6	16.0	17.2	12.4

TABLE II–C.3. WATER TABLE DEPTH AT DIFFERENT SAMPLING POINTS

Sampling point	1	2	3	4	5	6
Water table Depth, m	3	9	7	3	6	3

Groundwater: The approximate depth to the groundwater table is 1–20 m. Seasonal variation of the water table level does occur. The main volume of infiltration occurs in springtime, when snow melts, and in autumn, during a rainy period. Usually there is no surface water infiltration during summer time. Depth of water table for different sampling points is presented in Table II–C.3 (for location of sampling points see Table II–C.6).

Meteorological information: Meteorological information for 5 years of observation for the site under consideration is presented in file «MeteoBM.xls». The file contains the following information:

- date in a format «dd/mm/yy»;
- time in format «hh/mm»;
- relative humidity in %;
- wind direction in degrees (i.e. direction wind blowing from);
- air temperature in °C at height 1.5 m;
- wind speed in m/s at height 10 m;
- air pressure in torr; type of precipitation; and
- atmospheric stability classes evaluated in accordance with the Pasquill method with some improvements made by Institute of Experimental Meteorology (Russia).

A general view of the meteorological data is presented in Table II–C.4.

TABLE II–C.4. METEOROLOGICAL INFORMATION FOR TEST DATA SET

Date	Time	Rel. Humidity (%)	Wind Direction (°)	Air Temp. (°C)	Windspeed at 10m (m/s)	Air Pressure (Torr)	Type of Precipitation	Stability
03.11.86	7:30	96	150-210	1	1	757		D
03.11.86	15:30	93	150-200	1.5	0.5	756		D
03.11.86	16:30	94	140-160	1	1	756		D
03.11.86	17:30	95	100-150	1	1	756		D
03.11.86	18:30	95	120-160	1	1	756	Snow	D
03.11.86	19:30	96	100-140	1	1	756	Snow	D

TABLE II–C.5. DYNAMICS OF ANNUAL RELEASES TO THE ENVIRONMENT IN Bq/s

Year	1	2	3	4	5	6	7	8	9	10	11	12	13	14	15	16-20
Q	20	40	100	80	120	40	60	40	20	12	2	2	1	1	4	1

II–C.4. TRITIUM EMISSIONS AND RELATED INFORMATION

Tritium is released to the atmosphere during routine year-round facility operation. The linear velocity of release is 20 m/s, the temperature of released gases is +20°C, and the stack height is 30 m. Tritium is released to the atmosphere five days a week (Monday-Friday) from 8 a.m. to 10 p.m., excluding January 1,2, March 8, May 1,2,9, October 7, November 7,8. Average release rates of tritium during 20 years of observation in Bq/s are listed in Table II–C.5. Average ratio of HT and HTO in stack gases is about 1:1.

HTO deposition parameters by snow: The average amount of precipitation during winter is 160 mm of water equivalent; the average absolute humidity is 3 g/m^3.

HTO dry deposition velocity as determined by P A Davis (AECL) can be applied, i.e.:

$$V_g = 1.6*10^{-3}\ m/s$$

Average HTO snow-out coefficient Λ is:

$$\Lambda = 1.46*10^{-5} s^{-1}$$

Tritium on-site sampling and analysis: Tritium monitoring in environmental media includes:

- HT and HTO atmospheric monitoring - every 2 weeks;
- HTO monitoring in vegetation and soil - once a year at the end of the vegetation period;
- HTO monitoring in snow cover - once a year at the end of snow cover period.

Sampling technique: Air sampling is carried out by active and passive samplers, containing synthetic zeolites NaA with a catalyst for HT oxidation and without a catalyst. HT concentration is determined as a difference between HTO content in water extracted from zeolites with catalyst and without a catalyst. Water samples are collected in 2 litre glass bottles.

Snow samples: These are collected in plastic bags by an “envelop” scheme at a flat open plot of 10*10 m^2 size without bushes and trees. Snow samples are taken down as far as the underlying soil with care to exclude sampling of the surface soil. Volume of melted water is 3 litres.

TABLE II–C.6. SAMPLING LOCATIONS RELATIVE TO THE STACK

Sampling location	1	2	3	4	5	6
Distance, km	0.5	1.7	2.8	7.6	5	3
Direction, degrees	40	40	70	190	245	315

Note: N – 0°, E – 90°, S – 180°, W - 270°

Soil samples and vegetation: These are collected in plastic bags from an area of 10 × 10 cm^2 using a "triangle" scheme with sides of ~ 5 m and a depth of 1 cm. The water content of soil is 2 - 25%. Soil and vegetation sampling are performed at the same time. Vegetation is sampled from the same triangle. The amount of fresh vegetation in a sample is 1 kg. Vegetation with shallow roots (<20 cm) is used for sampling. The water content in grass vegetation is 10-15 %.

Samples processing: Water is extracted from zeolytes, vegetation and soil samples by a thermal vacuum desorption technique. Samples of drinking water are analysed without treatment; samples of sewage, snow and some types of water are filtered or distilled before analysis.

Measuring tritium content: Measurements of tritium activity in stack gases are carried out by an on-line ionization chamber. Measurements of tritium activity in environmental media are carried out by a liquid scintillation counter. The relative error of HTO measurement is 10%–100%.

II–C.5. ENDPOINTS TO BE CALCULATED

Modellers are requested to calculate the following:

A. Using average meteorological data:

Average annual tritium concentrations (Bq/l) of HTO in atmospheric moisture for 5, 10, 15 and 20 years after beginning of release at sampling points 1,2,3,4,5,6 (information about the location of the sampling points is provided in Table II–C.6);

Tritium concentrations (Bq/l) in plant tissue free water on 15 September, soil water on 15 of September and snow water on 31 March, each for 5, 10, 15 and 20 years after beginning of release at sampling points 2,4,6.

B. Using yearly averaged meteorological data:

(a) Average annual tritium concentrations (Bq/l) in atmospheric moisture for: 16th, 17th, 18th, 19th and 20th years after beginning of release at sampling points 1,2,3,4,5,6 (information about the location of the sampling points is provided in Table II–C.6);

(b) Tritium concentrations (Bq/l) in plant tissue free water on 15 September, soil water on 15 September and snow water on 31 March for: 16th, 17th, 18th, 19th and 20th years after beginning of release at sampling points 2,4,6.

ANNEX II–D
SCENARIO 5.0 (VALDUC) DESCRIPTION

History

Scenario 5.0 drafted by G. Guinois (CEA/DASE/RCE), July 1999.

II–D.1. GENERAL INFORMATION

The Valduc centre is located on a plateau about 500 meter high with valleys all around. The differences between the site and the valleys are 100 or 200 meters. The vegetation is composed of pine, maple and oak trees. The height of the trees in a 3 km area centred on the site is about 20–40 m. Further, the vegetation is essentially composed of agriculture fields and fallow land.

II–D.2. CLIMATE

Monthly temperature, precipitation, relative humidity and atmospheric pressure are given in Table II–D.1. They have been estimated from measurements taken during the 5-year period from 1992 to 1996. Over the 5-year period the mean temperature is 9.3°C, the lowest temperature is -10°C in January, the highest temperature is 28°C in July. Annual volume of precipitation is 871 mm; the rainfall is quite uniform each month.

II–D.3. METEOROLOGICAL INFORMATION

The wind rose has been established from sodar measurements. Figure II–D.1 shows the global wind rose and the rain wind rose. Stability classes have been calculated from the five last years of meteorological data (1993–1997) based on hourly sampling. The number of cases per 20 degree sectors and per wind velocity class with or without rain are given in Tables II–D.2 to II–D.7 and in the diskette of meteorological data previously distributed. The total number of cases for each stability class and the number of calm winds are given in each Table. Wind direction corresponds to the direction the wind is blowing from. Sodar measurements are made at 150 meters height above ground.

II–D.4. SOIL PROPERTIES

The uppermost part of the soil is composed of humus and clays with limestone fragments. Underneath are fractured limestone with red clay fracture fillings. The soil composition is:

Host rocks:	Fracture:
limestone 95%	limestone 85%
clay + oxides 5%	oxides 15%

TABLE II–D.1. MONTHLY AVERAGE VALUES OF METEOROLOGICAL PARAMETERS FROM 1992 TO 1996. (TEMPERATURE IS TAKEN AT 1 METER HEIGHT)

	January	February	March	April	May	June	July	August	September	October	November	December
Rain (mm)	75,52	60,4	51,05	46,3	74,08	67,76	73,66	64,44	91,04	85,14	99,4	82,2
Rain duration (mn)	2652	2174	2002	1482	1992	1150	1228	1398	2410	2622	3216	2774
Snow (cm)	8,5	8,4	0,125	0	0	0	0	0	0	0	4,4	4,6
Temperature (°C)	2,84	2,84	5,85	6,8	10,32	15,84	18,9	18,12	12,58	9,76	5,34	2,84
Relative humidity (%)	90,925	87,92	80,175	59,9	61,32	79,68	75,98	77,32	85,4	89,92	91,56	91,875
Atmospheric pressure (hPa)	964,04	964,5	964,025	961,925	962,675	964,7	964,64	964,22	962,26	962,62	963,24	961,1

TABLE II–D.2. STABILITY CLASSES A AND B

Stability class A

Velocity (m/s)	*20*	*40*	*60*	*80*	*100*	*120*	*140*	*160*	*180*	*200*	*220*	*240*	*260*	*280*	*300*	*320*	*340*	*360*	*total*
> 13	0	0	0	0	0	0	0	0	0	0	0	0	0	0	0	0	1	0	1
7 to 12	14	2	4	1	4	3	2	2	4	9	5	6	2	8	1	3	2	5	77
3 to 6	2	7	2	5	6	3	1	4	3	4	4	6	4	12	6	2	3	10	84
2	0	0	1	0	0	0	0	0	1	0	0	0	0	0	0	0	1	1	4
1	0	0	0	0	0	0	0	0	0	0	0	0	0	0	0	0	0	0	0
0,5 to 0,9	0	0	0	0	0	0	0	0	0	0	0	0	0	0	0	0	0	0	0
Vmean	8,1	5,8	6,7	5,3	5,8	6,1	6,7	5,6	6,5	7,9	6,4	6,4	5,8	6,3	5,5	7,3	7	5,7	

Wind < 0,5 m/s	1
Total number of values in class	167

Stability class B

Velocity (m/s)	*20*	*40*	*60*	*80*	*100*	*120*	*140*	*160*	*180*	*200*	*220*	*240*	*260*	*280*	*300*	*320*	*340*	*360*	*total*
> 13	1	0	0	0	0	0	0	0	0	1	1	1	0	0	0	0	0	0	4
7 to 12	13	6	3	4	4	1	3	9	12	16	14	8	22	13	10	7	4	13	162
3 to 6	26	14	9	18	13	17	12	9	18	16	12	15	23	28	23	15	9	28	305
2	2	0	2	1	2	0	0	1	0	2	1	1	1	2	2	0	0	0	17
1	0	0	1	0	0	1	1	0	1	0	2	0	0	2	0	0	0	0	8
0,5 to 0,9	0	0	0	0	0	0	0	0	0	0	0	0	1	0	0	0	0	0	1
Vmean	5,9	5,5	4,8	4,9	4,7	4,4	4,9	6,4	5,8	6,7	6,2	5,9	6,4	5,5	5,5	6,1	6,2	5,8	

Wind <0,5 m/s	2
Total number of values in class	499

TABLE II–D.3. STABILITY CLASSES C AND D

Stability class C

Velocity (m/s)	*20*	*40*	*60*	*80*	*100*	*120*	*140*	*160*	*180*	*200*	*220*	*240*	*260*	*280*	*300*	*320*	*340*	*360*	*total*
> 13	1	0	0	0	0	0	0	0	0	0	1	0	0	0	0	0	0	1	3
7 to 12	45	19	14	22	11	13	20	23	49	68	47	29	60	48	32	28	18	32	578
3 to 6	68	66	43	53	70	78	66	52	65	98	65	66	101	105	95	70	55	59	1275
2	5	7	9	8	8	5	4	2	4	3	9	4	7	2	8	4	8	6	103
1	2	1	0	2	2	0	4	0	2	3	1	3	2	0	2	2	3	3	32
0,5 to 0,9	0	0	1	0	0	0	0	1	2	0	1	0	0	0	0	0	0	1	6
Vmean	5,8	5,2	5	5,1	4,6	4,9	4,9	5,5	5,9	6	5,6	5,3	5,6	5,6	5,1	5,3	5,1	5,6	

Wind <0,5 m/s	4
Total number of values in class	2001

Stability class D

Velocity (m/s)	*20*	*40*	*60*	*80*	*100*	*120*	*140*	*160*	*180*	*200*	*220*	*240*	*260*	*280*	*300*	*320*	*340*	*360*	*total*
> 13	4	2	0	0	1	2	4	0	2	2	1	0	2	0	0	1	1	3	25
7 to 12	242	116	103	110	102	135	119	186	210	221	143	66	125	134	116	145	109	179	2561
3 to 6	414	267	207	222	336	392	398	403	478	494	373	292	547	600	591	412	332	393	7151
2	39	39	29	32	46	39	54	33	40	31	33	38	52	68	46	37	34	36	726
1	8	11	9	13	11	10	9	7	7	9	10	9	11	11	12	6	12	10	175
0,5 to 0,9	3	4	3	1	2	5	4	3	7	1	5	4	3	1	5	2	6	0	59
Vmean	5,7	5,1	5,3	5,2	4,7	5	4,8	5,3	5,5	5,4	5,1	4,5	4,8	4,7	4,7	5,1	5	5,5	

Wind <0,5 m/s	18
Total number of values in class	1071 5

TABLE II–D.4. STABILITY CLASSES E AND F

Stability class E

Velocity (m/s)	*20*	*40*	*60*	*80*	*100*	*120*	*140*	*160*	*180*	*200*	*220*	*240*	*260*	*280*	*300*	*320*	*340*	*360*	*total*
> 13	1	0	0	0	0	0	0	0	0	0	0	0	0	0	0	0	1	0	2
7 to 12	95	69	84	52	51	53	27	32	66	44	23	13	26	18	18	30	43	74	818
3 to 6	222	143	88	95	153	152	173	223	301	260	155	142	205	244	188	152	142	189	3227
2	23	11	14	9	12	17	34	28	23	16	27	34	29	23	19	28	24	21	392
1	7	4	7	4	4	8	4	5	8	9	9	5	6	4	6	4	8	3	105
0,5 to 0,9	2	4	0	0	2	2	5	2	4	2	6	2	2	0	3	1	2	2	41
Vmean	5,2	5,4	5,8	5,3	5,1	4,8	4,3	4,4	4,8	4,6	4,1	3,7	4,3	4,1	4,1	4,5	4,6	5,1	

Wind <0,5 m/s	13
Total number of values in class	4598

Stability class F

Velocity (m/s)	*20*	*40*	*60*	*80*	*100*	*120*	*140*	*160*	*180*	*200*	*220*	*240*	*260*	*280*	*300*	*320*	*340*	*360*	*total*
> 13	1	0	0	0	0	0	1	0	0	0	0	0	0	0	0	0	0	1	3
7 to 12	47	38	21	37	28	24	12	24	26	18	14	8	9	8	14	19	15	23	385
3 to 6	130	96	47	67	70	96	70	88	179	154	101	82	134	177	120	92	86	82	1871
2	11	11	6	8	13	13	10	18	17	12	17	15	22	20	21	13	10	15	252
1	8	1	5	3	4	2	6	2	5	6	3	6	5	8	9	3	3	9	88
0,5 to 0,9	1	1	1	0	0	0	1	1	1	0	2	2	0	3	1	2	2	0	18
Vmean	4,9	5,2	5,1	5,2	4,8	5	4,2	4,4	4,5	4,3	4	3,8	3,9	3,7	3,8	4,4	4,3	4,7	

Wind < 0,5 m/s	9
Total number of values in class	2626

TABLE II–D.5. STABILITY CLASSES A AND B WHEN IT RAINS

Stability class A during rain

Velocity (m/s)	*20*	*40*	*60*	*80*	*100*	*120*	*140*	*160*	*180*	*200*	*220*	*240*	*260*	*280*	*300*	*320*	*340*	*360*	*total*
> 13	0	0	0	0	0	0	0	0	0	0	0	0	0	0	0	0	0	0	0
7 to 12	0	0	0	0	0	0	0	0	0	0	0	0	0	0	0	0	0	0	0
3 to 6	0	0	0	1	0	0	0	0	1	0	0	0	0	0	0	0	0	1	3
2	0	0	0	0	0	0	0	0	0	0	0	0	0	0	0	0	0	0	0
1	0	0	0	0	0	0	0	0	0	0	0	0	0	0	0	0	0	0	0
0,5 to 0,9	0	0	0	0	0	0	0	0	0	0	0	0	0	0	0	0	0	0	0
Vmean	0	0	0	2,7	0	0	0	0	3,5	0	0	0	0	0	0	0	0	2,8	

wind <0,5 m/s	1
Total number of values in class	4

Stability class B during rain

Velocity (m/s)	*20*	*40*	*60*	*80*	*100*	*120*	*140*	*160*	*180*	*200*	*220*	*240*	*260*	*280*	*300*	*320*	*340*	*360*	*total*
> 13	0	0	0	0	0	0	0	0	0	0	0	0	0	0	0	0	0	0	0
7 to 12	0	0	0	0	0	0	0	0	0	0	0	0	0	0	0	0	0	0	0
3 to 6	1	0	0	0	0	0	1	1	1	0	4	2	4	2	1	1	6	0	24
2	0	0	0	0	0	0	0	0	0	0	0	0	0	0	0	0	0	0	0
1	0	0	0	0	0	0	0	0	0	0	0	0	0	0	0	0	0	0	0
0,5 to 0,9	0	0	0	0	0	0	0	0	0	0	0	0	0	0	0	0	0	0	0
Vmean	3,4	0	0	0	0	0	2,6	3,8	2,9	0	4,1	3,3	3,9	3	3,4	2,7	3,2	0	

Wind <0,5 m/s	5
Total number of values in class	29

TABLE II–D.6. STABILITY CLASSES C AND D WHEN IT RAINS

Stability class C during rain

Velocity (m/s)	*20*	*40*	*60*	*80*	*100*	*120*	*140*	*160*	*180*	*200*	*220*	*240*	*260*	*280*	*300*	*320*	*340*	*360*	*total*
> 13	0	0	0	0	0	0	0	0	0	0	0	0	0	0	0	0	0	0	0
7 to 12	0	0	0	0	0	0	0	0	0	0	1	0	0	0	0	0	1	1	3
3 to 6	12	2	7	3	6	4	8	6	5	10	28	29	34	26	25	18	10	6	239
2	2	0	1	0	0	2	1	0	0	0	0	1	0	1	1	0	0	0	9
1	0	0	0	0	0	0	0	0	0	0	0	0	0	0	0	0	0	0	0
0,5 to 0,9	0	0	0	0	0	0	0	0	0	0	0	0	0	0	0	0	0	0	0
Vmean	3,5	4	3,4	3,8	3,7	3,6	3,4	4,3	3,5	4,4	4,9	4,4	4,4	4,1	4,1	3,9	4,9	4,9	

Wind < 0,5 m/s	0
Total number of values in class	251

Stability class D during rain

Velocity (m/s)	*20*	*40*	*60*	*80*	*100*	*120*	*140*	*160*	*180*	*200*	*220*	*240*	*260*	*280*	*300*	*320*	*340*	*360*	*total*
> 13	0	0	0	0	0	0	0	0	0	0	0	0	0	1	0	0	0	0	1
7 to12	6	0	1	5	4	5	2	9	16	59	120	129	96	75	11	14	13	7	572
3 to 6	56	39	38	52	82	81	73	90	161	276	336	288	280	290	184	117	116	94	2653
2	2	1	0	6	3	7	12	9	10	6	13	13	7	8	4	5	6	4	116
1	0	0	0	0	0	0	0	0	0	0	0	0	0	0	0	0	0	0	0
0,5 to 0,9	0	0	0	0	0	0	0	0	0	0	0	0	0	0	0	0	0	0	0
Vmean	4,6	3,6	3,6	3,8	4	4,2	3,5	3,8	4,2	4,8	5,3	5,6	5,4	5,1	4,4	4,4	4,8	4,5	

Wind < 0,5 m/s	100
Total number of values in class	3442

TABLE II–D.7. STABILITY CLASSES E AND F WHEN IT RAINS

Stability class E during rain

Velocity (m/s)	*20*	*40*	*60*	*80*	*100*	*120*	*140*	*160*	*180*	*200*	*220*	*240*	*260*	*280*	*300*	*320*	*340*	*360*	*total*
> 13	0	0	0	0	0	0	0	0	0	0	0	0	0	0	0	0	0	0	0
7 to 12	0	0	0	0	0	0	0	0	0	0	0	0	0	0	0	0	0	0	0
3 to 6	8	5	8	10	9	5	6	16	14	27	47	40	41	41	27	26	14	11	355
2	1	0	1	3	1	1	3	3	2	3	7	1	5	4	0	2	1	0	38
1	0	0	0	0	0	0	0	0	0	0	0	0	0	0	0	0	0	0	0
0,5 to 0,9	0	0	0	0	0	0	0	0	0	0	0	0	0	0	0	0	0	0	0
Vmean	3,6	3,5	3	3,2	3,2	3	2,7	2,9	2,9	3	3,2	3,3	3,2	3,2	3,2	3,2	3,3	3,3	

Wind < 0,5 m/s	*0*
Total number of values in class	*393*

Stability class F during rain

Velocity (m/s)	*20*	*40*	*60*	*80*	*100*	*120*	*140*	*160*	*180*	*200*	*220*	*240*	*260*	*280*	*300*	*320*	*340*	*360*	*total*
> 13	0	0	0	0	0	0	0	0	0	0	0	0	0	0	0	0	0	0	0
7 to 12	0	0	0	0	0	0	0	0	0	0	0	0	0	0	0	0	0	0	0
3 to 6	3	3	5	4	1	4	6	1	2	2	2	2	6	4	2	1	7	4	59
2	1	1	1	2	1	1	0	0	1	2	2	0	0	0	2	0	0	0	14
1	0	0	0	0	0	0	0	0	0	0	0	0	0	0	0	0	0	0	0
0,5 to 0,9	0	0	0	0	0	0	0	0	0	0	0	0	0	0	0	0	0	0	0
Vmean	3,1	2,6	2,9	2,6	2,7	2,9	3,2	2,6	2,7	2,5	2,8	2,7	3,7	3,2	2,5	2,5	3,1	2,9	

Wind < 0,5 m/s	46
Total number of values in class	119

II–D.5. ATMOSPHERIC TRITIUM RELEASES

The tritium is released in the atmosphere from 3 sources. The location of each source is presented in Table II–D.8.

Coordinates: X axis West – East oriented, positive toward East
Y axis South – North oriented, positive toward North

TABLE II–D.8. SOURCES COORDINATES AND CHARACTERISTICS RELATIVE TO SOURCE 1. H IN METERS IS ABOVE GROUND LEVEL AT THE LOCATION, Z IS ABSOLUTE ELEVATION ABOVE SEA LEVEL

	X (m)	Y (m)	Z (m)	H (m)
Source 1	0	0	495	50
Source 2	-189	1400	482	20
Source 3	-161	1375	477	11.5
Sodar Station	238	819	430	150

The total amount of release for the 3 sources for each year from 1983 to 1988 is given in Table II–D.9.

TABLE II–D.9. TOTAL RELEASE (Bq)

Year	1983	1984	1985	1986	1987	1988
Total (E+15)	2.91	3.2	1.22	1.38	2.3	1.05

The amount of tritium released by each of the 3 sources since 1988 is given in Table II–D.10.

TABLE II–D.10: MEAN ANNUAL ACTIVITIES OF TRITIUM RELEASE FOR THE 3 SOURCES IN Bq

Year	1988	1989	1990	1991	1992	1993	1994	1995	1996	1997	1998
Source 1 (E+14)	8.7	9.69	8.7	9.25	5.76	7.49	10.5	7.13	4.53	2.24	2.34
Source 2 (E+13)	8.66	6.3	5.7	6.82	6.81	8.47	5.73	5.98	7.46	6.83	7.11
Source 3 (E+13)	8.52	8.38	10.6	10.9	7.07	4.34	5.82	3.59	2.6	1.99	1.96

The proportions of HTO and HT are 75% and 25%, respectively.

II–D.6. ENDPOINT CALCULATIONS

(1) For each year from 1988 to 1998 at the 4 stations whose coordinates are given in Table II–D.11 modellers are requested to calculate:

— annual average tritium concentration in air (Bq/m3),

— annual average tritium concentration in the grass tissue free TFWT water (Bq/l),

— annual average tritium concentration in rain water(Bq/l).

TABLE II–D.11. SAMPLING LOCATION COORDINATES OF STATION 1 TO 4 RELATIVE TO SOURCE 1 (SEE TABLE II–D.8)

Sampling location	Station 1	Station 2	Station 3	Station 4
X (m)	4372	3784	-3044	-2416
Y(m)	-3745	5138	3722	-2502
Z(m)	325	460	440	370

Note: Z is absolute elevation above sea level

(2) Modellers are requested to calculate:

- average tritium concentration in OBT from birch tree ring for the year 1988 only (use 3 separated sources given in Table II–D.10) at station 5 whose coordinates are given in Table II–D.12.
- annual average tritium concentration in OBT for birch tree for years 1983 to 1988 (use total release given in Table II–D.9) at station 5 whose coordinates are given in Table II–D.12.

TABLE II–D.12. SAMPLING LOCATION COORDINATES OF STATION 5 RELATIVE TO SOURCE 1 (SEE TABLE II–D.8)

Sampling location	Station 5
X (m)	9000.
Y(m)	-890.
Z(m)	370.

Note: Z is absolute elevation above sea level

(3) Modellers are requested to calculate at each sampling point given Table II–D.13, annual average tritium concentration in OBT for oak leaves sampled at 2 meters height for the year 1988. Results should be given in the form of a table with 3 columns (X,Y,OBT concentration) and 36 lines (samples S1 to S36).

TABLE II–D.13. SAMPLING LOCATION COORDINATES OF S1 TO S36 RELATIVE TO SOURCE 1 (SEE TABLE II–D.8)

Number of sampling	X (km)	Y (km)	Neighbourhood
S1	-9,75	10,25	I
S2	-5,3125	9,125	F
S3	-2,25	9	I
S4	2,875	8,6875	I
S5	6,5	9,3125	I
S6	10,5625	9,25	I
S7	-10	4,5	I
S8	-6,125	5,75	I
S9	-2,5	5,25	F
S10	2,75	5,75	I
S11	6,125	6,25	I
S12	11,4375	5,25	F
S13	-9,4375	2	I
S14	-5,5	1,3125	I
S15	-1,875	1,25	I
S16	1,875	1,125	F
S17	5	1,3125	F
S18	9,625	1,75	F
S19	-9,375	-2,6875	I
S20	-6,125	-1,625	I
S21	-1,75	-1,75	F
S22	2	-2,6875	F
S23	5,625	-3,125	F
S24	10,3125	-1,6875	I
S25	-9,0625	-6,4375	I
S26	-5,5	-5,9375	I
S27	-2,25	-6,125	F
S28	2,5	-5,5625	F
S29	5,8125	-6,375	I
S30	9,5	-6,0625	I
S31	-10,25	-9,875	I
S32	-6,875	-9,5625	F
S33	-0,875	-10,5625	I
S34	2,3125	-10,125	F
S35	5,6875	-9,4375	F
S36	9,375	-9,5625	F

Neighbourhood:
I = isolated tree (truly isolated tree or tree at the edge of a grove)
F = forest tree

ANNEX II–E
SCENARIO 1.4 DESCRIPTION

Modelling of the steady-state behaviour of tritium in the environment when atmospheric releases are assumed to be on average nearly constant and a steady-state equilibrium has been reached

History

Scenario 1.4 drafted by Y. Belot (Working Group Leader, Consultant, France) and B. Watkins TWG (Technical Secretariat, QuantiSci Limited, UK), October 1998. Incorporates comments on Scenario 1.3.

Scenario 1.3 drafted by Y. Belot (Working Group Leader, Consultant, France) and B. Watkins TWG (Technical Secretariat, QuantiSci Limited, UK), June 1998. Incorporates comments on Scenario 1.2.

Scenario 1.2 drafted by Y. Belot (Working Group Leader, Consultant, France) and B. Watkins TWG (Technical Secretariat, QuantiSci Limited, UK) to incorporate changes agreed by WG participants at Plenary meeting in Vienna, October 1997. Incorporates comments on Scenario 1.1.

Scenario 1.1 drafted by Y. Belot (Working Group Leader, Consultant, France) and B. Watkins TWG (Technical Secretariat, QuantiSci Limited, UK) to incorporate agreed revisions following Cadarache meeting. Incorporates comments on Scenario 1.0.

Working Group Meeting, Cadarache, France, 22–24 April 1997: Y. Belot (Working Group Leader, Consultant, France). Discussion of scenario description by WG participants. For information on meeting participants, see: IAEA (1997), Notes of BIOMASS Theme 3 Tritium Working Group Meeting, Cadarache, 22–24 April, 1997.

Scenario 1.0 drafted. See IAEA (1996). International Programme on Biosphere Modelling and Assessment Methods (BIOMASS). Theme 3: Biospheric Processes. Tritium Working Group Scope, Objectives and Approaches. 1996-12-20. IAEA, Vienna.

II–E.1. INTRODUCTION

Scenario 1.3 was established after the 1998 Spring Working Group meeting in Deep River and the corresponding results were discussed at the Autumn meeting in Vienna (see IAEA, 1998). It was considered that a reasonable convergence of results was obtained for the atmospheric part of the Scenario, and that differences still existing between the atmospheric approaches could not be reduced without collecting more information from the on-going observational field studies.

On the contrary, it was felt that the results obtained for the hydraulic part of the Scenario were quite unsatisfactory, because the results were varying by over an order of magnitude. The reason for that was not clear since it could be due either to the choice of the upper boundary condition (either constant-flux or constant concentration), or to the relatively high value of the transverse vertical dispersivity given as a starting point for the model calculations. In order to clarify the effects of the different factors, a number of changes to Scenario 1.3 were agreed, giving rise to the following Scenario 1.4 which now deals only with the dispersion of tritium in groundwaters as a consequence of infiltration of contaminated rain. (For any other details, see the original Scenario version 1.3 description.)

II–E.2. SCENARIO DESCRIPTION

II–E.2.1. Aquatic Pathway

The calculation of tritiated water in groundwaters starts from HTO concentrations in infiltration water defined as follows. Within a radius of 0.2 km around stack, HTO concentration is 500 Bq/l. From 0.2 km to 10 km upstream and downstream, the HTO concentrations are inversely proportional to the distance from the source, that is 100 Bq/l at 1 km and 10 Bq/l at 10 km. These rounded figures of concentrations will permit a straightforward comparison between concentrations in the aquifer and concentrations in the infiltration water.

The total infiltration rate (or recharge rate) is 150 mm per year. The horizontal extension of the unconfined aquifer is 10 km from the flow divide to the stream. The stack is placed at the midpoint between the divide and the stream (ie at 5 km from each) as shown in Figure II–E.1. The groundwater zone has a permeability of 1×10^{-4} m s^{-1}, and a porosity of 30%. The dispersivities can be high (A_x = 50 m, A_y = 5 m, A_z = 0.5 m), or low (A_x = 5m, A_y = 0.5 m, A_z = 0.05 m).

Calculations can be made using relatively complex finite element models that simulate the groundwater flow and tritium transport in the aquifer. In this case the data given above are sufficient to perform calculations of the water and tritium transport over the whole extension of the aquifer from the flow divide to the receiving stream.

Calculations can also be made in a more simple way by using analytical models of the Gaussian type for example. In this case, the water flow in the aquifer has to be approximated by assuming that the flow is nearly uniform within a zone of 3 km radius centred on the stack with a longitudinal pore water velocity of 42 m y^{-1} and a hydraulic head (aquifer thickness) of 59 m, which have been calculated at the vertical of the stack.

II–E.3. ENDPOINT CALCULATIONS

The requested calculational endpoints are expressed in Bq per litre of water.

Calculations are requested for aquifer vertical profile at 1 km downstream the stack. For the horizontal profile, results should be given at 2 m below water table, at 0.1 km intervals from 0.2 to 1 km and at 1 km intervals up to 3 km, both upstream and downstream from the source, at 20 years after the start of tritium flow through the watertable.

The above calculations should be made, if possible, first by using the constant-flux boundary condition, and as an alternative the constant-concentration boundary condition, with a calculation of the downward dispersive flux in the latter case. The objective is to determine if the use of alternative boundary condition is an acceptable modelling approach at least in some restricted cases, or if use of such a boundary condition can be totally excluded.

An additional request is to make the calculations not only for the previous set of high dispersivity coefficients, but also for a new set of low dispersivity coefficients (cf. the values given in the Section above). The need for these additional calculations arises from the fact that from the literature that low values seem to be more realistic than high values (see the review of Gelhar et al., 1992).

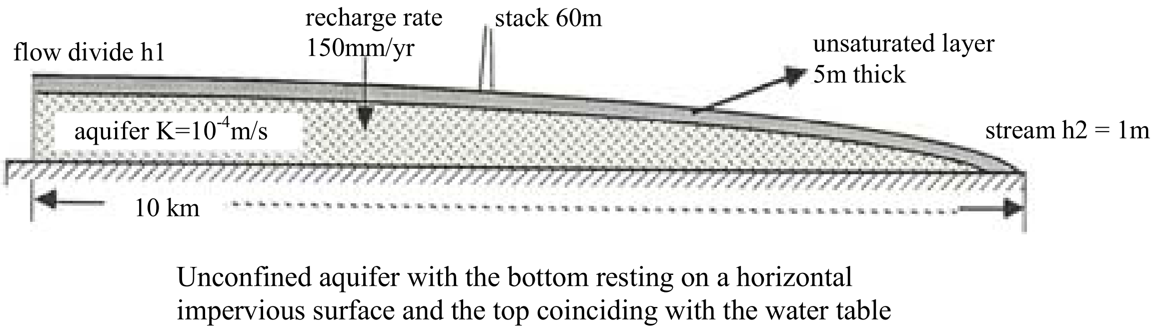

FIG. II–E.1. Diagrammatic representation of Scenario 1.4.

References

[1] GELHAR, L.W., et al., A Critical Review of Data on Field Scale Dispersion in Aquifers, Water Research **28** 1955-1974 (1992).

[2] INTERNATIONAL ATOMIC ENERGY AGENCY, Notes of BIOMASS Theme 3 Tritium Working Group Meeting, Vienna, 7–9 October 1998, IAEA, Vienna (1998).

ANNEX II–F
SCENARIO 2.4 DESCRIPTION

Modelling tritium transport above a near-surface watertable under realistic weather conditions

History

Scenario 2.4 drafted by Y. Belot (Working Group Leader, Consultant, France) and B. Watkins TWG Technical Secretariat (Enviros QuantiSci, UK), June 1999 incorporating amendments agreed by TWG participants at the Spring meeting, Sarov, 24–27 May 1999.

Scenario 2.3 drafted by Y. Belot (Working Group Leader, Consultant, France) and B. Watkins TWG Technical Secretariat (QuantiSci Limited, UK), November 1998 incorporating amendments agreed by TWG participants at the Plenary meeting, Vienna, 7–9 October 1998.

Scenario 2.2 drafted by Y. Belot (Working Group Leader, Consultant, France) and B. Watkins TWG Technical Secretariat (QuantiSci Limited, UK), June 1998 incorporating amendments agreed by TWG participants at the Spring meeting, Deep River 11–15 May 1998.

Scenario 2.1 drafted by Y. Belot (Working Group Leader, Consultant, France) and B. Watkins TWG Technical Secretariat (QuantiSci Limited, UK) incorporating amendments agreed by WG participants at the Plenary meeting, Vienna, 20–24 October 1997.

Scenario 2.01 drafted by Y. Belot (Working Group Leader, Consultant, France) and B. Watkins TWG Technical Secretariat (QuantiSci Limited, UK) following discussion at theSpring meeting, Cadarache, 22–24 April, 1997.

Scenario 2.0 drafted by Y. Belot (Working Group Leader, Consultant, France) and B. Watkins TWG Technical Secretariat (QuantiSci Limited, UK) following the initiation of the TWG in December 1996.

Scenario 2.0 Outline. See IAEA (1996). International Programme on Biosphere Modelling and Assessment Methods (BIOMASS). Theme 3: Biospheric Processes. Tritium Working Group Scope, Objectives and Approaches. 1996-12-20. IAEA, Vienna.

II–F.1. INTRODUCTION

Scenario 2.4, which is presented below, is an evolution of previous versions, without any fundamental modification of the situation to be modelled. It still considers a perched aquifer, which is situated at a 1-m depth beneath a non-vegetated soil, and contains tritium at a nearly constant concentration. The fluctuation of the watertable level is assumed to be negligible. Modellers are asked to calculate water and tritium profiles in the unsaturated soil column for specific months of the year, and tritium fluxes from the soil surface to the atmosphere for a twelve month period, starting from the assumption that the soil is devoid of any contamination. The fundamental issue is to investigate if dispersive and/or upward convective transport results in the movement of tritium to the upper layers of the soil so that it can then diffuse from the soil surface to the atmosphere. In other words, is a 1-m soil cover for instance sufficient to isolate a contaminated aquifer and prevent the movement of tritium to the surface? Can we find an answer to this question by standard modelling approaches or is a new method required?

Following lessons drawn from preliminary and intermediate results, and discussions during the 98 Plenary Meeting and 99 Spring Meeting, some modifications to the scenario input data and requested calculation endpoints have been introduced to the scenario description. At the Plenary Meeting in October 1998, it was decided to parameterise the soil water retention and movement in a more realistic way, with updated parameter values for some of the soil processes. At the Spring Meeting in May 1999, it was moreover agreed that a new approach to calculations, and modified endpoints, would be adopted. Changes include the following:

- Modellers will use the hourly meteorological data provided by W Raskob (FzK) if possible, otherwise daily or monthly averages will be used.
- Inclusion of hourly data of actual evaporation rate, in addition to the other meteorological data, provided by W Raskob (FzK).
- Modellers will undertake different calculations to assess the importance of different process by calculating tritium concentrations due to advection only, advection plus molecular diffusion, and advection plus molecular diffusion and dispersion.
- Endpoints have been modified so that results for the above conditions are to be provided for two specific dates during a year, namely 28 February and the 28 July at 12.00 h in each case.
- Modellers are also requested to provide cumulative fluxes of water (+ve or –ve) from the watertable to the above unsaturated soil, at the end of each month for a twelve month period, in order to check the balance of water in the unsaturated soil column.
- Modellers must also provide information on the number of soil layers in their model and the time steps used.

II–F.2. SCENARIO DESCRIPTION

II–F.2.1. Initial and boundary conditions

The scenario considers a near-surface aquifer (perched aquifer) contaminated at the constant level of 10^4 Bq per litre and situated at 1 metre depth. It is assumed that the surface soil is composed of homogeneous material as described in Table II–F.1 below. At this stage of modelling, no consideration is given to any vegetation growing in the soil. Figure II–F.1 shows a diagrammatic representation of the assumed scenario conditions.

TABLE II–F.1. CHARACTERISTICS OF THE SANDY LOAM SOIL

Soil Characteristic	Value
Sand	70%
Silt	20%
Clay	10%
Organic matter	0
Particles > 2 mm	0
Particle density (g/cm^3)	1.6
Porosity	*0.387*

At time zero, the overlying unsaturated soil and the atmosphere are uncontaminated. The initial distribution of water through this layer is assumed to correspond to the capillary rise of water. It is thus assumed at time zero that everywhere in the unsaturated layer the hydraulic head is equilibrated by the capillary pressure.

The meteorological conditions to be considered for the time of simulation are provided in two files that have been established by W. Raskob from FzK, Germany. The two files, given on two diskettes, each with 1 year of data as hourly records starting on the 1st of January at 0:00 universal time are:

- Hourly values of wind direction, Pasquill-Turner stability class, rain intensity, wind speed (at 10 m), air temperature (at 2 m), net radiation (at soil surface) and relative humidity (at 2 m) (this files has been distributed previously; it may be obtained on request from the Technical Secretariat).
- A new supplementary file that provides the corresponding hourly values of both the actual evaporation rate, and the actual evaporation rate minus condensation (supplied with this scenario description, or available from the Technical Secretariat).

II–F.2.2. Water retention in SL soil

The modelling of water movement in the unsaturated soil is usually based on the Richard’s equation and requires knowledge of the soil water retention and hydraulic conductivity curves that characterise the soil.

The soil water retention will be described by the Van Genuchten expression. The soil water content θ (in volume fraction) as a function of the negative capillary pressure h (in m) is:

$$\frac{\theta-\theta_r}{\phi-\theta_r}=\left[\frac{1}{1+(\alpha|h|)^n}\right]^m \tag{1}$$

where $\phi = 0.387$ is the total porosity; $\theta_r = 0.039$ the residual water content; $\alpha = 2.69\ \mathrm{m}^{-1}$, $m = 0.308$ and $n = 1.445$ for other parameters that depend on pore size distribution. The values of the soil parameters have been drawn from the average retention parameters given by Van Genuchten (personal communication) for a sandy loam type soil.

The companion relationship describing the unsaturated hydraulic properties of soils is the relation of hydraulic conductivity K(θ) to water content θ. The expression for this relation, also drawn from Van Genuchten, is the following:

$$\frac{K(\theta)}{K_s} = \left(\frac{\theta-\theta_r}{\phi-\theta_r}\right)^{1/2}\left[1-\left(1-\left(\frac{\theta-\theta_r}{\phi-\theta_r}\right)^{1/m}\right)^{m}\right]^{2} \tag{2}$$

where $K_s = 4.39 \times 10^{-6}$ m s^{-1} is the saturated hydraulic conductivity for the specified SL soil (Van Genuchten, same origin), and m, θ_r and ϕ have the same values as in the soil-water retention formula given above.

II–F.2.3. Movement of natural water and transport of tritiated water

The classical Richard's equation describing the water movement in unsaturated media will be solved in tandem with a transport equation describing the transport of tritiated water in liquid and vapour phases, with appropriate initial and boundary conditions. The transport and exchange phenomena will be assumed to be independent of the thermal profile in the soil. The computational time and spatial discretisation will be chosen to ensure calculation stability and minimize the computational error; these must be specified in the model description, which should be provided with the scenario endpoint calculations.

One of the main parameters in the tritium transport equation is the effective dispersion coefficient of tritiated water. This parameter includes contributions from both molecular diffusion and hydrodynamic (or convective) dispersion. The contribution from hydrodynamic dispersion is classically expressed as the product of an hydrodynamic dispersivity parameter by the pore water velocity. The hydrodynamic dispersivity parameter of the specified SL soil is assumed to be 0.05 m, the molecular diffusion coefficient of tritiated water in liquid water to be 2.3×10^{-9} m^2 s^{-1}, and the tortuosity factor to be 0.66.

II–F.3. ENDPOINT CALCULATIONS

Modellers will undertake, if possible, different calculations to assess the importance of different processes by calculating tritium concentrations due to advection only, advection plus molecular diffusion, and advection plus molecular diffusion and dispersion. In the three cases, modellers are requested to provide the following calculational endpoints concerning ordinary water and tritiated water transport in the soil:

- *H_2O and HTO profiles* should be given at 5, 15, 25, 35, 45, 55, 65, 75, 85, and 95 cm below the soil surface, each value being averaged over the 10 cm intervals centred on the specified depths. The results are to be provided for two specific dates during a year, namely the 28 February and the 28 July at 12.00 h in each case. H_2O should be expressed as dimensionless (v/v) soil water content, and HTO as tritium activity concentration in Bq kg^{-1} water.
- *HTO fluxes from the soil surface to the atmosphere* should be given each month for one year starting in January. The fluxes should be given as monthly averages and expressed in Bq m^{-2} month.

— *H_2O fluxes from the watertable to the above unsaturated soil* should also be given each month for one year starting in January. The fluxes should be given as monthly averages and expressed in kg m^{-2} $month^{-1}$ (ie mm $month^{-1}$). The flux should be positive for net upward flow and negative for net downward flow.

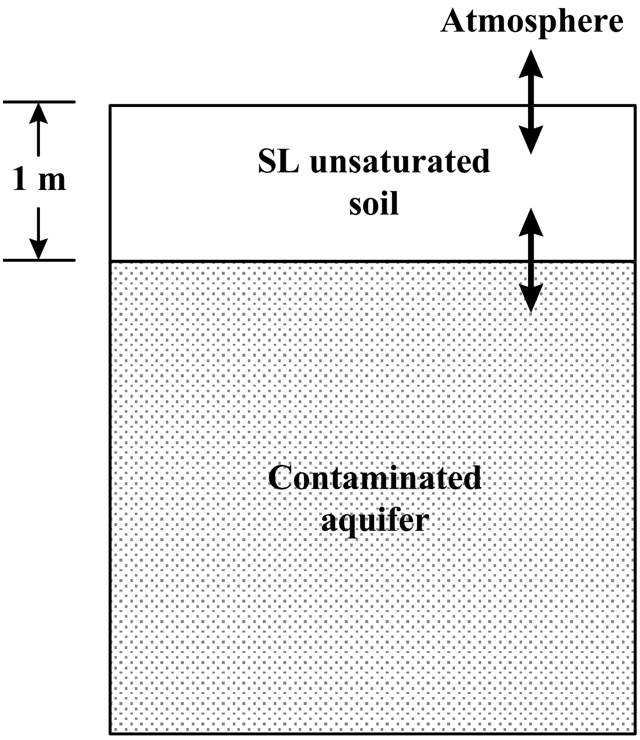

A sandy loan (SL) unsaturated soil above a
near-surface aquifer. Realistic meteorological conditions.

FIG. II–F.1. Diagrammatic representation of Scenario 2.4.

References

[1] INTERNATIONAL ATOMIC ENERGY AGENCY, International Programme on BIOsphere Modelling and ASSessment Methods (BIOMASS), Theme 3: Biospheric Processes, Tritium Working Group: Scope, Objectives and Approaches, IAEA, Vienna, 20 December (1996).
[2] INTERNATIONAL ATOMIC ENERGY AGENCY, Notes of BIOMASS Theme 3 Tritium Working Group Meeting, 20–24 October 1997, IAEA, Vienna. (1997).
[3] INTERNATIONAL ATOMIC ENERGY AGENCY, Notes of BIOMASS Theme 3 Tritium Working Group Meeting, Deep River, Canada, 13–15 May 1998, IAEA, Vienna (1998).

ANNEX II–G
SCENARIO 2.5 DESCRIPTION

Modelling tritium transport above a near-surface watertable under realistic weather conditions, with or without vegetation rooted in the soil

History

Scenario 2.5 drafted by Y. Belot (Working Group Leader, Consultant, France) and B. Watkins TWG (Technical Secretariat, Enviros QuantiSci, UK), November 1999 incorporating amendments agreed by TWG participants at the Plenary meeting, Vienna 4–8 October 1999.

Scenario 2.4 drafted by Y. Belot (Working Group Leader, Consultant, France) and B. Watkins TWG Technical Secretariat (Enviros QuantiSci, UK), June 1999 incorporating amendments agreed by TWG participants at the Spring Meeting, Sarov, 24–27 May 1999.

Scenario 2.3 drafted by Y. Belot (Working Group Leader, Consultant, France) and B. Watkins TWG Technical Secretariat (QuantiSci Limited, UK), November 1998 incorporating amendments agreed by TWG participants at the Plenary meeting, Vienna, 7–9 October 1998.

Scenario 2.2 drafted by Y. Belot (Working Group Leader, Consultant, France) and B. Watkins TWG Technical Secretariat (QuantiSci Limited, UK), June 1998 incorporating amendments agreed by TWG participants at the Spring meeting, Deep River 11–15 May 1998.

Scenario 2.1 drafted by Y. Belot (Working Group Leader, Consultant, France) and B. Watkins TWG Technical Secretariat (QuantiSci Limited, UK) incorporating amendments agreed by WG participants at the Plenary meeting, Vienna, 20–24 October 1997.

Scenario 2.01 drafted by Y. Belot (Working Group Leader, Consultant, France) and B. Watkins TWG Technical Secretariat (QuantiSci Limited, UK) following discussion at the Spring meeting, Cadarache, 22–24 April, 1997.

Scenario 2.0 drafted by Y. Belot (Working Group Leader, Consultant, France) and B. Watkins TWG Technical Secretariat (QuantiSci Limited, UK) following the initiation of the TWG in December 1996.

Scenario 2.0 Outline. See IAEA (1996). International Programme on Biosphere Modelling and Assessment Methods (BIOMASS). Theme 3: Biospheric Processes. Tritium Working Group Scope, Objectives and Approaches. 1996-12-20. IAEA, Vienna.

II–F.4. INTRODUCTION

Scenario 2.5, is based on the same sub-surface conditions as those considered in the previous versions of the scenario (see Annex II–F). A perched aquifer is situated at 1 m depth beneath the unsaturated zone soil surface, and contains tritium at a constant concentration. The soil is of a sandy-loam type and the fluctuation of the watertable level is assumed to be negligible throughout the year.

In this new version of the scenario, the modellers are asked to consider either a non-vegetated soil surface or a vegetated soil surface, in order to see the effect of vegetation on the tritium concentration in the soil profile and the resulting flux of tritium from the soil surface to the atmosphere. In both cases, the predictions will be undertaken by considering the ensemble of the processes that may contribute to the transport of tritium through the upper unsaturated soil layer (i.e. advection, molecular diffusion and hydrodynamic dispersion).

The input data to be used by modellers consists of three files of hourly meteorological conditions. Modellers are asked to calculate water and tritium profiles in the unsaturated soil column at specific dates of the year, and tritium fluxes from the soil surface to the atmosphere over each month of a twelve month period, starting from January.

II–F.5. SCENARIO DESCRIPTION

II–F.5.1. Initial and boundary conditions

The scenario considers a near-surface aquifer (perched aquifer) contaminated at the constant level of 10^4 Bq per litre and situated at 1 metre depth. The surface soil is assumed to consist of homogeneous material as described in Table II–G.1 below. Figure II–G.1 shows a diagrammatic representation of the assumed scenario conditions.

TABLE II–G.1. CHARACTERISTICS OF THE SANDY LOAM SOIL

Soil Characteristic	Value
Sand	70%
Silt	20%
Clay	10%
Organic matter	0
Particles > 2 mm	0
Particle density (g/cm^3)	1.6
Porosity	0.387

At time zero, the overlying unsaturated soil and the atmosphere are uncontaminated. The initial distribution of water through this layer is assumed to correspond to the capillary rise of water. It is thus assumed that at time zero everywhere in the unsaturated layer the hydraulic head is equilibrated by the capillary pressure.

The surface conditions to be considered for the time of simulation are provided in three files that have been provided by W. Raskob from FZK, Germany. The three files contain 1 year of data as hourly records starting on the 1st of January at 0:00 universal time.

The three files are the following:

- A first file, already distributed, provides hourly values of wind direction, Pasquill-Turner stability class, rain intensity, wind speed (at 10 m), air temperature (at 2 m), net radiation (at soil surface) and relative humidity (at 2 m).
- A second file, already distributed, provides data for two conditions: the first, the corresponding hourly values of the actual evaporation; and the second the actual evaporation/condensation rate for a non-vegetated soil. The values, given in mm per hour, are positive in case of evaporation and negative in case of condensation. Modellers can use either one of the two columns, according to the capability of their models.
- A third file, enclosed with this scenario, provides data for two conditions: the first, the actual evaporation/condensation rate at the soil surface itself; and the second for transpiration of a wheat crop rooted in that soil. The values of evaporation, condensation and transpiration flux, given in mm per hour, are negative in the case of condensation. Modellers can remove the negative values if they cannot handle them (this does not make a large difference).

The root system of the wheat plants is assumed to extend down to a 30-cm depth. 30% of the transpiration flux is considered to be extracted from the top 10 cm-layer, 35% from the middle 10cm-layer and 35% from the bottom 10-cm layer.

II–F.5.2. Water retention in SL soil

The modelling of water movement in the unsaturated soil is usually based on the Richard's equation and requires knowledge of the soil water retention and hydraulic conductivity curves that characterise the soil.

The soil water retention will be described by the Van Genuchten expression. The soil water content θ (in volume fraction) as a function of the negative capillary pressure h (in m) is:

$$\frac{\theta-\theta_r}{\phi-\theta_r}=\left[\frac{1}{1+\left(\alpha|h|\right)^n}\right]^m \qquad (1)$$

where $\phi = 0.387$ is the total porosity; $\theta_r = 0.039$ the residual water content; $\alpha = 2.69\ \text{m}^{-1}$, $m = 0.308$ and $n = 1.445$ other parameters that depend on pore size distribution. The values of the soil parameters have been drawn from the average retention parameters given by Van Genuchten (personal communication) for a sandy loam type soil.

The companion relationship describing the unsaturated hydraulic properties of soils is the relation of hydraulic conductivity K(θ) to water content θ. The expression for this relation, drawn also from Van Genuchten, is the following:

$$\frac{K(\theta)}{K_s}=\left(\frac{\theta-\theta_r}{\phi-\theta_r}\right)^{1/2}\left[1-\left(1-\left(\frac{\theta-\theta_r}{\phi-\theta_r}\right)^{1/m}\right)^m\right]^2 \qquad (2)$$

where $K_s = 4.39 \times 10^{-6}$ m s^{-1} is the saturated hydraulic conductivity for the specified SL soil (Van Genuchten, same origin), and m, θ_r and ϕ have the same values as in the soil-water retention formula given above.

II–F.5.3. Movement of natural water and transport of tritiated water

The classical Richard's equation with a sink term describing the water movement in unsaturated media will be solved in tandem with a transport equation describing the transport of tritiated water in liquid and vapour phases, with appropriate initial and boundary conditions. The transport and exchange phenomena will be assumed to be independent of the thermal profile in the soil. The computational time and space steps will be chosen to ensure calculation stability and to minimize the computational error.

One of the main parameters in the tritium transport equation is the effective dispersion coefficient of tritiated water. This parameter includes contributions from both molecular diffusion and hydrodynamic (or convective) dispersion. The contribution from hydrodynamic dispersion is classically expressed as the product of an hydrodynamic dispersivity parameter and the pore water velocity. The hydrodynamic dispersivity parameter of the specified SL soil is assumed to be 0.05 m; the molecular diffusion coefficient of tritiated water in liquid water is 2.3×10^{-9} m^2 s^{-1}; and the tortuosity factor is 0.66.

II–F.6. ENDPOINT CALCULATIONS

Modellers will undertake two sets of calculations, one for a non-vegetated soil, the other for a vegetated soil. In both cases, modellers are requested to provide the following calculational endpoints:

- *H_2O profiles* should be given at 5, 15, 25, 35, 45, 55, 65, 75, 85, and 95 cm below the soil surface, each value being averaged over the 10 cm intervals centred on the specified depths. The results are to be provided for two specific dates during a year, namely the 28 February and the 28 July at 12.00 h in each case. H_2O should be expressed as dimensionless (v/v) soil water content.
- *HTO profiles* should be given at 5, 15, 25, 35, 45, 55, 65, 75, 85, and 95 cm below the soil surface, each value being averaged over the 10 cm intervals centred on the specified depths. The results are to be provided for two specific dates during a year, namely the 28 February and the 28 July at 12.00 h in each case. HTO should be expressed as tritium activity concentration in Bq kg^{-1} of soil water (or equivalently Bq L^{-1}).
- *HTO fluxes from the soil surface to the atmosphere* should be given for each month for one year starting in January. The fluxes should be given as monthly averages and expressed in Bq m^{-2} $month^{-1}$.

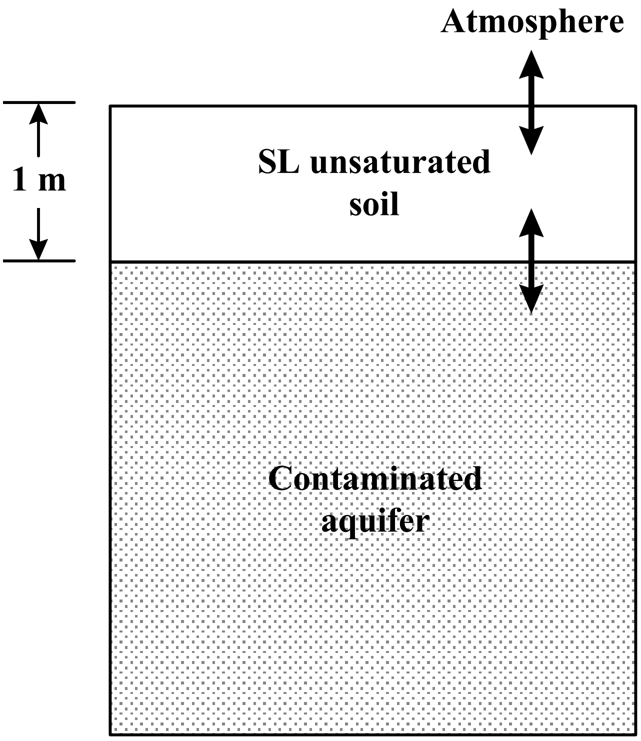

A sandy loan (SL) unsaturated soil above a
near-surface aquifer. Realistic meteorological conditions.

FIG. II–G.1. Diagrammatic representation of Scenario 2.4.

CONTRIBUTORS TO DRAFTING AND REVIEW

Contributors and Document History

Tritium WG TECDOC, Version 1.0: Final version produced by B.M. Watkins (Enviros QuantiSci, United Kingdom) following a Consultants' Meeting at CEA Headquarters, Paris, France, 15–17 January 2001, incorporating comments by Tritium WG participants during BIOMASS Plenary Meeting held 7–9 November 2000, subsequent comments on draft material and review comments by Y. Belot (Consultant, France) and P.A. Davis (AECL, Canada).

Part A:	Y. Belot	Consultant, France
Part B:	P. Davis	AECL, Canada
Part C:	A. Golubev	RFNC-VNIIEF, Russian Federation
Part D:	G. Guinois	CEA, France
Part E:	Y. Belot	Consultant, France
Part F:	Y. Belot	Consultant, France
Part G:	G. Guinois	CEA, France and M. Täschner, ZSR, Germany

Development of scenario descriptions, analysis of modelling and experimental results, and discussion of draft documents discussed by all participants at the following meetings:

BIOMASS Tritium WG Spring 1997 Meeting, Cadarache, France: 22–24 April 1997

BIOMASS Plenary and Working Group Meetings, Vienna, Austria: 20–24 October 1997

BIOMASS Tritium WG Spring 1998 Meeting, Deep River, Canada: 11–15 May 1998

BIOMASS Research Co-ordination, Plenary and Working Group Meetings,
Vienna, Austria: 5–9 October 1998

BIOMASS Tritium WG Spring 1999 Meeting, Sarov, Russian Federation: 24–27 May 1999

BIOMASS Research Co-ordination, Plenary and Working Group Meetings,
Vienna, Austria: 4–8 October 1999

BIOMASS Tritium WG Spring 2000, Toki, Japan: 8–12 May, 2000

BIOMASS Research Co-ordination, Plenary and Working Group Meetings,
Vienna, Austria: 6–10 November 2000

Consultants Meeting, CEA Headquarters, Paris, France: 15–17 January 2001

Main Tritium WG Participants:

H. Amano	Japan Atomic Energy Research Institute, Japan
M. Andoh	Japan Atomic Energy Research Institute, Japan
M. Balonov	International Atomic Energy Agency**
Y. Belot	Consultant, France*
L. Belovodsky	RFNC-VNIIEF, Russian Federation
G. Brachet	Commissariat á l'Energie Atomique, France
H. Camus	Permanent Mission of France, Vienna, Austria
P. Davis	Atomic Energy of Canada Limited, Canada

D. Delmont	Commissariat á l’Energie Atomique, France
O. Edlund	Studsvik EcoSafe AB, Sweden
D. Galeriu	Institute of Atomic Physics and Nuclear Engineering, Romania
A. Golubev	RFNC-VNIIEF, Russian Federation
G. Guinois	Commissariat á l’Energie Atomique, France
Y. Inoue	International Atomic Energy Agency**
D. Lush	Beak International Limited, Canada
S. Mavrin	RFNC-VNIIEF, Russian Federation
C. Meurville	Agence Nationale pour la Gestion des Déchets Radioactifs, France
R. Peterson	Lawrence Livermore National Laboratory, United States of America
W. Raskob	Forschungszentrum Karlsruhe – Technik und Umwelt, Germany
M. Täschner	Zentrum für Strahlenschutz und Radioökologie, University of Hannover, Germany
B. Watkins	Enviros QuantiSci, United Kingdom***
H. Yamazawa	Japan Atomic Energy Research Institute, Japan

Note:

* Tritium Working Group Leader
** IAEA Scientific Secretary
*** Technical Secretariat